1986

Trophodynamics of estuarine (salt marsh) heterotrophic nanoplankton (microbial ecology, salt marsh ecology, choanoflagellates, Virginia)

Alyce T. Fritz
College of William and Mary - Virginia Institute of Marine Science

Fritz, Alyce Thomson

TROPHODYNAMICS OF ESTUARINE (SALT MARSH) HETEROTROPHIC NANOPLANKTON

The College of William and Mary in Virginia PH.D. 1986

PLEASE NOTE:

In all cases this material has been filmed in the best possible way from the available copy. Problems encountered with this document have been identified here with a check mark ✓.

1. Glossy photographs or pages ✓
2. Colored illustrations, paper or print _____
3. Photographs with dark background ✓
4. Illustrations are poor copy _____
5. Pages with black marks, not original copy ✓
6. Print shows through as there is text on both sides of page _____
7. Indistinct, broken or small print on several pages ✓
8. Print exceeds margin requirements _____
9. Tightly bound copy with print lost in spine _____
10. Computer printout pages with indistinct print _____
11. Page(s) _____ lacking when material received, and not available from school or author.
12. Page(s) _____ seem to be missing in numbering only as text follows.
13. Two pages numbered _____. Text follows.
14. Curling and wrinkled pages _____
15. Dissertation contains pages with print at a slant, filmed as received ✓
16. Other _____

_____

_____

University
Microfilms
International

TROPHODYNAMICS OF ESTUARINE (SALT MARSH) HETEROTROPHIC NANOPLANKTON

A Dissertation

Presented to

The Faculty of the School of Marine Science

The College of William and Mary in Virginia

In Partial Fulfillment

Of the Requirements for the Degree of

Doctor of Philosophy

---

by

Alyce Thomson Fritz

1986

APPROVAL SHEET

This dissertation is submitted in partial fulfillment of

the requirements for the degree of

Doctor of Philosophy

Alyce Thomson Fritz

Alyce Thomson Fritz

Approved, July 1986

Kenneth L. Webb, Ph.D
Committee Chairman/Advisor

Leonard W. Haas, Ph.D.

Howard I. Kator, Ph.D.

Bruce J. Neilson, Ph.D.

Richard L. Wetzel, Ph.D.

William M. Dunstan, Ph.D.
Old Dominion University
NOrfolk, Virginia

DEDICATION

To my parents, Alice and Walter Thomson, in appreciation of their love and encouragement throughout my education and of their unflagging belief that I would successfully complete this work, and to my husband, Lowell Fritz, whose love and support made it possible for me to achieve this goal.

TABLE OF CONTENTS

Page

ACKNOWLEDGMENTS.....vi

LIST OF TABLES.....ix

LIST OF FIGURES.....x

ABSTRACT.....xvi

CHAPTER I. GENERAL INTRODUCTION.....2

CHAPTER II. VARIABILITY OF ESTUARINE NANOPLANKTON ABUNDANCES AND BACTERIAL PRODUCTION IN A MARSH-MUDFLAT SYSTEM

Introduction.....7

Methods and Materials.....12

Results and Discussion.....17

CHAPTER III. SEASONAL HETEROTROPHIC NANOPLANKTON TROPHODYNAMICS - IN SITU DETERMINATIONS OF GROWTH AND GRAZING RATES IN A MARSH-MUDFLAT SYSTEM

Introduction.....45

Methods and Materials.....50

Results.....63

Discussion.....110

CHAPTER IV. TROPHODYNAMICS OF ESTUARINE NANOPLANKTON DURING AUTUMN AND SPRING TRANSITIONAL PERIODS

Introduction.....122

Methods and Materials.....126

Results.....133

Discussion.....168

CHAPTER V. CHARACTERIZATION OF SPRING NANOPLANKTON ASSEMBLAGES USING ELECTRON AND EPIFLUORESCENCE MICROSCOPY

Introduction.....186

Methods and Materials.....189

Results.....198

Discussion.....259

CHAPTER VI. SUMMARY AND CONCLUSIONS.....264

REFERENCES.....274

VITA.....287

ACKNOWLEDGMENTS

This dissertation represents the culmination of the guidance, cooperative efforts and support of several individuals associated with the VIMS scientific community. I wish to express my sincere appreciation to all of those that have been involved in this study. Thanks are extended to my committee members, Dr. Leonard Haas, Dr. Richard Wetzel, Dr. Howard Kator, Dr. Bruce Neilson, and Dr. William Dunstan for their suggestions and criticism of this manuscript.

I owe a special debt of gratitiude to my major professor, Dr. Kenneth L. Webb, for his thoughtful counsel, enduring support and infinite patience. He was a source of remarkable insights, scientific and otherwise, during the many stages of my graduate career. I wish to thank him, too, for his critical review of the manuscripts. My deepest appreciation is extended to him for his advice, encouragement, and generous assistance in assembling the results of the research into a completed dissertation. It would not have been possible to have finished without his continued efforts.

The ideas for this project were inspired, nine years ago, by the innovative research of Dr. Larry Haas. At that time, he had developed several new scientific approaches and techniques for describing the nanoplankton dynamics of the Chesapeake system, many of which have been incorporated into this study. I wish to thank him for wholeheartedly sharing his knowledge and his enthusiasm in new

discoveries. I am much indebted to him for his invaluable quidance and continued interest and support throughout this research effort. It is appropriate that, in the end, I should thank him for providing valuable questions and comments for the manuscript and its conclusions.

At the mid-point of my research, I convinced a fellow graduate student, Helena Galvao, to collaborate in an investigation of the variability of nanoplankton dynamics. Her contributions to the success of the research projects were immeasurable. She was a constant source of stimulating ideas and conversations concerning marine science and the challenges associated with conducting research in a salt marsh system. Her dedication to the research and her sense of perspective and humor are deeply appreciated.

Special thanks are extended to Dr. Polly Penhale, for her time and effort expended in reviewing the first draft of this manuscript. Her critical comments and suggestions set me back on the right track and in addition, her continued encouragement was much appreciated.

I am owe a huge round of special thanks to many of the VIMS staff for their technical assistance and support, and for their professional excellence. I am indebted to Martha Rhodes for sharing her development of the diffusion chamber and her experience in microbial dynamics research. Thanks go to Ken Worrell for his innovation and dedication in building the chambers and the support structure. Patrice Mason provided invaluable assistance and advice in all phases of the electron microscopy technique and photomicroscopic analysis. Special thanks go to Mary Jo Shackelford, Kay Stubblefield, and Harold Burrell of the VIMS Art Department and William Jenkins of the Photography Lab for

preparing the figures and photography with such care and patience.

For the last four years of the work, I took the dissertation on the road from Virginia to New Jersey. I would like to offer many thanks to the members of the VIMS community, past and present, who provided me a home away from home and always, support and encouragement. Special thanks go to Janice Meadows and Mal Green of Dissertation Central; Colleen Becker and Jim Schwann, Susan Stevich and Ken Webb, Jane Ledwin and Bill Rizzo, Helena Galvao and Bill Weishar, and Ann Hayward Walker of Gloucester; Lee and Dave Benner, Karen and Fred Jacobs, and Bob Middleton of the I-95 Corridor; and Laura Murray and Michael Kemp, and Cathy Womack and Dave Ludwig of the Eastern Shore Bed and Breakfast Inns. Thank You All!

Finally, I am forever indebted to my husband, Lowell Fritz, for his innumerable contributions to this dissertation. In his words, he receives a well deserved "Assist". Above all, his love, patience, determination, sense of humor, and understanding through all the trials and tribulations made it possible for me to maintain my equilibrium and finish my tome.

LIST OF TABLES

Page

II.1. Ambient glucose concentration and heterotrophic uptake of ^{14}C-labelled glucose by free and attached bacteria and heterotrophic nanoplankton (HNANO) assemblages sampled from the marsh station.....35

III.1. Seasonal growth and grazing rates of heteroflagellates at the marsh station.....68

III.2. Seasonal growth and grazing rates of heteroflagellates at the mudflat station.....69

III.3. Correlation analyses of heteroflagellate growth and density versus bacteria density.....104

IV.1. Densities of cyanobacteria (cells ml^{-1}) at marsh and mudflat stations in fall 1982 diffusion chamber experiments.....146

IV.2. Growth and grazing rates of heteroflagellates at the marsh and mudflat stations for the autumn and spring transitional periods.....155

IV.3. Bacteria and heteroflagellate trophodynamics (growth, production and grazing parameters) and calculations for carbon flux in heteroflagellate-bacteria food web.....183

V.1. Dimensions of species described in text.....213-214

V.2. Growth and grazing rates of spring heteroflagellate assemblages at the marsh and mudflat stations.....255

LIST OF FIGURES

Page

II.1. Study site and station locations.....13

II.2. Seasonal variation in temperature (A), salinity (B), bacteria (C), and heteroflagellates (D) at the marsh station based on sampling at daily intervals within months from May 1981 to May 1982.....18

II.3. Seasonal variation in temperature (A), salinity (B), bacteria (C), and heteroflagellates (D) at the mudflat station based on sampling at daily intervals within months from May 1981 to May 1982.....20

II.4. Seasonal variation (weekly intervals from July to December 1982) of heteroflagellate and bacteria average densities from two hour sampling intervals during ebbing and flooding tides at the three stations (marsh, mudflat, and river).....22

II.5. Seasonal variation (July to December 1982) over weekly intervals of low water versus high water abundances of heteroflagellates and bacteria at three stations (marsh, mudflat, and river).....24

II.6. Daily and variation in temperature, salinity and ambient densities of heteroflagellates and bacteria during April 1983 at the marsh and mudflat stations.....26

II.7. Seasonal variation (weekly intervals from July to December 1982) of temperature and glucose concentration from two hour sampling intervals during ebbing and flooding tides at the three stations (marsh, mudflat, and river).....30

II.8. Seasonal variation (July to December 1982) over weekly intervals of low water versus high water abundances of temperature and glucose concentration at three stations (marsh, mudflat, and river).....32

II.9. Heterotrophic uptake of ^{14}C-labelled glucose based on kinetic model and ambient glucose concentrations for the 1 um fraction.....36

II.10. Heterotrophic uptake of ^{14}C-labelled glucose based on kinetic model and ambient glucose concentrations for the 15 um fraction.....38

II.11 Heterotrophic uptake of ^{14}C-labelled glucose. Curves are fitted to glucose uptake values in ug glucose l^{-1} h^{-1} versus added glucose (ug l^{-1}) for the 1 um fraction. The diffusion component (linear uptake) and kinetic (Michaelis-Menton) model curve are plotted.....40

II.12. Heterotrophic uptake of ^{14}C-labelled glucose. Curves are fitted to glucose uptake values in ug glucose l^{-1} h^{-1} versus added glucose (ug l^{-1}) for the 15 um fraction.....42

III.1 Study site and station location.....51

III.2. Diagram of diffusion chamber.....53

III.3. Diagram of support structure for diffusion chambers.....57

III.4. Marsh versus mudflat mean growth rates of bacteria (top) and of heteroflagellates (bottom) over a seasonal cycle.....65

III.5. Variability in monthly mean heteroflagellate growth rates (with standard error) from May 1981 to May 1982 and including October - November 1982 and April 1983 at the marsh and mudflat stations.....73

III.6. Seasonal variation in temperature and salinity at the marsh and mudflat stations.....75

III.7. Heteroflagellate growth rates versus temperature at marsh and mudflat stations.....77

III.8. Monthly mean heteroflagellate growth rates in comparison with two ranges of growth rates (1: slow - $u<0.057$ h^{-1}; 2: fast - $u>0.057$ h^{-1}) for marsh and mudflat over a seasonal cycle.....81

III.9. Temperature, salinity, and heteroflagellate versus bacteria densities for in situ diffusion chamber and for ambient populations during 27 May to 3 June 1981 at the marsh station.....84

III.10. Temperature, salinity, and heteroflagellate versus bacteria densities for in situ diffusion chamber and for ambient populations during 16-27 June 1981 at the marsh and mudflat stations.....86

III.11. Temperature, salinity, and heteroflagellate versus bacteria densities for in situ diffusion chamber and for ambient populations during 17-26 July 1981 at the marsh and mudflat stations.....88

III.12. Temperature, salinity, and heteroflagellate versus bacteria densities for in situ diffusion chamber and for ambient populations during 17-23 August 1981 at the marsh and mudflat stations.....90

III.13. Temperature, salinity, and heteroflagellate versus bacteria densities for in situ diffusion chamber and for ambient populations during 23-30 September 1981 at the marsh and mudflat stations and during 4-11 November 1981 at the marsh station.....92

III.14. Temperature, salinity, and heteroflagellate versus bacteria densities for in situ diffusion chamber and for ambient populations during 2-8 February 1982 at the marsh station and 17-28 March 1982 at the marsh and mudflat stations.....94

III.15. Temperature, salinity, and heteroflagellate versus bacteria densities for in situ diffusion chamber and for ambient populations during 17-28 April 1982 at the marsh station.....96

III.16. Temperature, salinity, and heteroflagellate versus bacteria densities for in situ diffusion chamber and for ambient populations during 17-28 April 1982 at the mudflat station.....98

III.17. Temperature, salinity, and heteroflagellate versus bacteria densities for in situ diffusion chamber and for ambient populations during 19-25 May 1982 at the marsh and mudflat stations.....100

III.18. Clearance rates (ul d^{-1} $bacteria^{-1}$) versus temperature at both marsh and mudflat stations.....106

III.19. Heteroflagellate grazing (ingestion) rates versus bacteria concentration over a seasonal cycle for marsh and mudflat stations.....108

IV.1. Study Site and Sample Locations.....127

IV.2. Diagram of the diffusion chamber and support structure.....131

IV.3. Daily means of nitrite concentration during July through December 1982; nitrite, nitrate, NH_4 combined means and individual means for the fall nitrite maxima at the three stations.....134

IV.4 Variation in temperature, salinity, autotrophic and heterotrophic nanoplankton and bacteria from July to December 1982 at the marsh and mudflat stations.....137

IV.5. Daily means in heteroflagellate density from July through December 1982 and inset for October through December.....139

IV.6. Tidal variation of heteroflagellates, bacteria, and autotrophs during the autumn and spring transitional periods.....142

IV.7. Temperature, salinity, autotrophs, and heteroflagellates versus bacteria densities for in situ diffusion chambers and for ambient populations during 27 October - 5 November 1982 at the marsh and mudflat stations.....148

IV.8. Temperature, salinity, autotrophs, and heteroflagellates versus bacteria densities for in situ diffusion chambers and for ambient populations during 13-23 April 1983 at the mudflat station.....158

IV.9. Temperature, salinity, autotrophs, and heteroflagellates versus bacteria densities for in situ diffusion chambers and for ambient populations during 13-23 April 1983 at the marsh station.....162

V.1 Study site and station locations.....190

V.2. Diagram of diffusion chamber and support structure.....192

V.3. Temperature, salinity, and heteroflagellate densities versus bacteria densities for in situ diffusion chamber experiment and ambient spring assemblages at the marsh station during 17-28 March 1982. SEM micrograph is of ambient assemblage including Diaphanoeca sp. in March 1982 at marsh station. Similar plots are presented for both the marsh and mudflat station during 17-28 April 1982...200

V.4. SEM micrograph of spring bloom assemblage of nanoplankton from the April 1982 in situ chamber experiment.....202

V.5. SEM micrograph of biflagellated heterotrophic monad from April 1982 chamber experiment.....202

V.6. SEM micrograph of a spring bloom assemblage of nanoplankton from the April 1982 in situ chamber experiment showing the direct attachment of Stephanoeca.....202

V.7. Temperature, salinity, and heteroflagellate abundance versus bacteria densities for in situ diffusion chamber experiments and ambient assemblages during 19-26 May 1982 at the marsh and mudflat stations.....205

V.8. Two naked heteroflagellates with long sinuous flagella from the May 1982 in situ chamber experiment.....205

V.9. Pedicellate Stephanoeca constricta in association with diatoms in the May 1982 in situ chamber experiment.....205

V.10. Temperature, salinity, and heteroflagellate densities versus bacteria abundances for in situ diffusion chamber experiments and ambient assemblages during 13-23 April 1983 at the marsh and mudflat stations.....207

V.11. SEM photomicrograph of small heteroflagellate from April 1983 diffusion chamber.....207

V.12 SEM micrograph of small bodonid form from April 1983 diffusion chamber 207

V.13 SEM micrograph of a loricate choanoflagellate and monad from April 1983 experiment.....207

V.14. Temperature, salinity, and heteroflagellate densities versus bacteria densities during 31 May - 5 June 1984 in situ chamber experiment at the mudflat station.....210

V.15. TEM photomicrograph of Acanthoecidae choanoflagellate from May-June 1984 in situ diffusion chamber experiment.....210

V.16. TEM photomicrograph of Paraphysomonas vestita from May-June 1984 in situ diffusion chamber experiment.....210

V.17. TEM photomicrograph of a haptophyte showing a hair-point flagella with mastigonemes from the May-June 1984.....210

V.18. Prototype of a choanoflagellate depicting diagnostic features of the lorica.....212

V.19. TEM photomicrograph of an Acanthoecopsis sp. from the May-June 1984 in situ diffusion chamber experiment.....215

V.20. TEM photomicrograph of a bodonid heteroflagellate from the May-June 1984 in situ diffusion chamber experiment.....215

V.21. TEM photomicrograph of a bicoecid heteroflagellate from the May-June 1984 in situ diffusion chamber experiment.....215

V.22. TEM photomicrograph of Paraphysomonas vestita from the May-June 1984 in situ diffusion chamber experiment.....215

V.23. Diaphanoeca grandis - Collapsed lorica with cell.....220

V.24. Stephanoeca diplocostata var. paucicostata. View of anterior end of lorica containing cell.....220

V.25. S. d. var. paucicostata. Two specimens among an assemblage of microplankton collected in April 1982.....220

V.26-27 Stephanoeca elegans. Specimens shown here were collected during April 1982 experiments.....225

V.28-33. Stephanoeca elegans. Specimens collected during April and May 1982 experiments each showing characteristic features.....229

V.34-36. Stephanoeca elegans (Stephanoeca constricta). Several specimens demonstrate constricted lorica and flared tubular opening and detail of fibrillar web.....232

V.37. Assemblages of Stephanoeca elegans (constricta) and S. urnula typical of those observed in April and May 1982.....235

V.38-40. Stephanoeca urnula. Organisms were abundant in April 1982 samples, and demonstrate different numbers of spiralled costae and resulting variations of the 'urn' shape.....235

V.41-43 Stephanoeca complexa. Specimens showing less organized arrangement and characteristic posterior chamber membrane (solid) which extends beyond the waist to the prominent anterior transverse costae.....239

V.44. Acanthoecopsis apoda with spherical protoplast and flagellum prominent.....243

V.45. Acanthoecopsis spiculifera. Two epibiont specimens attached to diatoms.....243

V.46. Acanthoecopsis unguiculata. Specimen shows diagonal costae which form complex, organized post chamber.....243

V.47-50. Savillea parva. Four specimens demonstrating characteristic tubular opening and small cell.....248

V.51-53. Saepicula pulchra. Three specimens demonstrate characteristic bell shape.....251

ABSTRACT

Seasonal occurrence and activity of heterotrophic nanoflagellates (HNANO or heteroflagellates) and bacteria were studied in a sheltered brackish water embayment of Chesapeake Bay wetlands (Virginia, USA) over a three year period (1981 - 1984). Epifluorescence direct counts and Scanning and Transmission Electron Microscopy (SEM and TEM) techniques were used for the description of organisms, enumeration, and biomass determinations. Seasonal bacterial growth rates and growth and grazing rates of bactivorous HNANO were estimated using diffusion chambers equipped with Nuclepore polycarbonate membrane filters (1.0 and 0.2 μm) in natural salt marsh tidal pools. Nanoplankton densities in both chambers and environment were monitored concurrently over several days to determine natural predator-prey interactions. Environmental monitoring of nanoplankton populations revealed a seasonal pattern of bacterial abundances with temperature while heteroflagellate abundances and growth rates showed no seasonal pattern nor correlation with fluctuations in bacterial densities. The large variability in abundances and in situ growth rates of heteroflagellates demonstrated the necessity of field experimentation based on short time scales in the dynamic estuarine (marsh-mudflat) system.

Heteroflagellate populations were dominated by 34 to 50 μm^3 sized monads, choanoflagellates, bodonids, and Paraphysomonas sp., all found in varying abundances throughout the year. Densities generally fluctuated between 1.0 - 5.0 x 10^3 cells ml^{-1} however, patchy, short-term blooms of HNANO of 0.5 to 2.5 x 10^4 cells ml^{-1} occurred periodically in sheltered marsh tidal pools. These blooms were concurrent with extended low tide or specific bacterial populations (i.e., cyanobacteria) typical of spring and autumn periods. Hetero-flagellate growth in diffusion chambers reflected the environmental blooms and increased diversity of low water assemblages. Mean growth and grazing rates ranged from u= 0.02 - 0.07 h^{-1} and I = 30 - 148 bacteria h^{-1}, respectively; values frequently indicated doubling times of 12 to 20 hours and ingestion rates of 1600 - 2850 d^{-1} during any season. The range in bacterial growth rates was similar with 1 or 2 doublings per day at densities of 4 - 8 x 10^6 cells ml^{-1}. Growth and grazing rates of heteroflagellates at ambient densities thus could account for 20 to 80% of daily bacterial carbon production. Although heteroflagellate ingestion rates did control seasonal fluctuations in bacteria densities, maximum growth in of bacteria and heteroflagellates chambers was closely coupled. Heteroflagellate grazing activity may regulate the rate of bacterial production by preventing substrate limitation and maintaining the bacterial population in an active growth phase.

The seasonal study demonstrated the dynamic nature of nanoplankton populations, particularly HNANO, during the autumn and

spring transition periods. The autumn experiments suggest that microaggreggregates (i.e., of cyanobacteria) activity in heteroflagellate trophodynamics. SEM photomicroscopy revealed that the dominant component of spring blooms may be composed of several members of the loricate choanoflagellate family, Acanthoecidae. Using modified EM techniques, eleven Acanthoecidae choanoflagellates species, identified from spring in situ chamber experiments, were described. In situ growth and grazing rates for these spring chamber populations ranged from 0.023 to 0.196 h^{-1} and 40 to 210 bacteria h^{-1} respectively. These high rates represent an opportunistic response to optimum conditions and an expression of maximum grazing potential.

The use of in situ diffusion chambers and combined epifluorescence and EM photomicroscopic analysis represents an ideal methodology for quantifying HNANO trophodynamics. The potential for high growth and grazing rates demonstrated by in situ chamber experiments under nearly all environmental conditions indicate heteroflagellates may serve as a relatively constant pathway of bacterial carbon into the estuarine food chain.

TROPHODYNAMICS OF ESTUARINE (SALT MARSH) HETEROTROPHIC NANOPLANKTON

CHAPTER I

GENERAL INTRODUCTION

This dissertation entitled "Trophodynamics of estuarine (salt marsh) heterotrophic nanoplankton" is comprised of six chapters which describe various components of a field survey and in situ growth and grazing experiments. Heterotrophic nanoplankton are defined as protozoans which fall in the size range of 2-20 μm and are commonly referred to in the literature by their abbreviation, HNANO. HNANO, are dominated by heterotrophic microflagellates. However, recent studies (Sherr et al. 1986) revealed that in some environments, the less than 20 μm fraction may include several types of small ciliates. The objectives of the research were to study the microbial food chain in a salt marsh-mudflat system with particular emphasis on the trophodynamics of heterotrophic flagellated nanoplankton, or heteroflagellates, ranging in size from 2 to 12 μm. Laboratory and field investigations in York River salt marshes were initiated in 1979. At this time, heteroflagellate importance in DOM cycling, nutrient regeneration, and trophodynamics in aquatic systems was generally accepted, but poorly documented. However, the role of heteroflagellates as bacteriovores remained controversial and little information existed for distribution and abundances of HNANO in estuarine systems. Quantitative information on growth and grazing rates of HNANO was not then available.

It was hypothesized that heteroflagellates, as bacteriovores, should be a significant component of highly productive salt marsh systems. The

hypothesis was based largely on the paradigm of dissolved organic matter (DOM) cycling (DOM---> bacteria---> HNANO) (Pomeroy 1974). The magnitude of DOM concentrations and fluxes, abundance of bacteria and possible diversity of food sources in marsh systems should provide an optimum environment for heteroflagellate growth and grazing activity. Shallow estuarine environments, such as salt marshes and associated mudflats, provide extremely transient conditions under which nanoplankton dynamics can be expected to reach a maximum variability. The recently developed epifluorescence direct count methodology (Watson et al. 1977, Haas 1982) provided a valuable tool for enumeration and identification to types of HNANO. The initial focus of the study was to monitor the abundance and seasonal distribution of HNANO in marsh system in order to describe major forms and the time scales of varability. At the beginning of the study (1978-1979) little information existed for either in vitro or in situ growth and grazing rates. Predictive models for predator-prey cycles based on environmental abundances and productivity rates were only available for oceanic and fjord environments (Sieburth 1979, Sorokin 1981, Fenchel 1982d). Preliminary laboratory investigations were designed to identify organisms cultured from the marsh and to measure growth and grazing at environmentally representative temperatures.

The environmental sampling (1978-1980) conducted in various salt marsh environments demonstrated the ubiquitous temporal and spatial distribution of heteroflagellates. During 1980, a field methodology was designed utilizing in situ incubations of diffusion chambers suspended in a tidal embayment to determine seasonal in situ growth and grazing rates of HNANO at marsh and mudflat stations. The diffusion chambers were a

modified McFeters and Stuart design developed by M. Rhodes and machinists of the VIMS staff (Rhodes et al. 1983). A support structure was constructed which allowed suspended chambers to move in the water column with tidal fluctuations. The methods for sampling and enumeration of HNANO and determination of other parameters, i.e. nutrients, glucose, heterotrophic uptake of ^{14}C-glucose at different tidal stages in a salt marsh-mudflat system, are described in Chapter II. Experiments were initiated in April 1981 and the use of in situ diffusion chambers combined with epifluorescence analysis was a valuable method of measuring rates under natural conditions. Results of the seasonal study demonstrated the potential for high growth rates though seldom as high as laboratory rates and, also the importance of short term sampling. Another graduate student (Galvao 1984) working in collaboration with this research effort conducted a concurrent study designed to determine minimal resolution or characterize temporal variability of the nanoplankton community in a salt marsh-mudflat ecosystem. Data from these combined seasonal studies revealed that considerable variation in nutrient conditions and in nanoplankton communities occurred during autumn and spring periods of temperature transition. HNANO during these transition periods were a dominant component of the nanoplankton.

Four years of in situ chamber experiments in the salt marsh-mudflat during spring confirmed the presence of spring bloom assemblages of choanoflagellate and concurrent blooms of cyanobacteria. A combination of methodologies, i.e. in situ chambers, epifluorescence and electron microscopy, was valuable for studying the spring bloom assemblages of choanoflagellates. Replicate samples from in situ diffusion chambers and

the water column, preserved in glutaraldehyde, were analyzed by both epifluorescence and electron microscopy (EM) analysis. A scanning electron microscopy (SEM) method was modified to preserve delicate flagellated protozoans (HNANO) and used in combination with epifluorescence in order to both identify HNANO and enumerate sequential samples for HNANO growth and grazing rates.

This dissertation then progresses from Chapter II which first describes the types and abundances of heterotrophic nanoplankton and seasonal variability in a salt marsh system. The three stations in the salt marsh-mudflat system represented three distinct environments at low tide. The study area was chosen because movement of the tide could be traced and sampled in various stages through the embayment. The area drained almost completely during low tide leaving discrete tidal pools. The environmental sampling at this site was the first documentation of large temporal variability for HNANO distributions over several seasonal cycles. The study involved four different time scales to measure the variability in temporal patterns.

Chapter III describes the in situ methodology developed to measure HNANO growth and grazing rates. This study utilized deployment of the chambers described above equipped with 0.20 and 1.0 μm polycarbonate Nuclepore membranes. The chapter demonstrates the ranges of growth and grazing rates and characteristic rates and variability in predator-prey cycles. Heteroflagellates ingest bacteria at rates which may influence bacteria growth phases.

Chapter IV focuses on the nutrient and nanoplankton dynamics of the autumn and spring transition periods. The chapter describes the results

of the collaborative research effort (Galvao, 1984) which was designed to monitor nutrients and nanoplankton variation on a tidal scale during the transition periods in conjunction with daily monitoring of environmental nanoplankton abundances and in situ growth and grazing experiments. The study was an attempt to improve resolution of field sampling and to monitor the various environmental parameters which may influence nanoplankton dynamics. The intensive sampling effort and growth and grazing rates of HNANO in diffusion chambers reveals unusual phenomenon on short time scales. Blooms in tidal pools were duplicated by similar events in chambers, i.e., heteroflagellate and cyanobacteria blooms (aggregrates). Results demonstrated opportunistic nature of HNANO and rapid dynamics, unusual nutrient dynamics of October, cyanobacterial blooms, and rapid response of HNANO to optimum conditions. Analysis of April conditions and extremes in physical conditions demonstrated the eurythermic and euryhaline capacities or nature of HNANO.

Chapter V presents the results of investigations of spring bloom assemblages through four successive years. The study describes nine choanoflagellate species new to the Chesapeake Bay. The combined use of: 1) in situ methods; 2) epifluorescence analysis for growth and grazing rates; and 3) SEM and TEM methodology for species identification and investigation of feeding mechanisms described in this chapter represents the culmination of the dissertation research. This combined in situ methodology and microscopy analysis holds great potential for identifying important HNANO species, and defining the time-frame of bloom formation, diel variations, and dynamics (including DOM release, nutrient regeneration, and trophic linkage).

CHAPTER II

VARIABILITY OF ESTUARINE NANOPLANKTON ABUNDANCES AND BACTERIAL PRODUCTION IN A MARSH-MUDFLAT SYSTEM

INTRODUCTION

Wetlands have long been recognized as productive and important components of estuarine ecosystems, and as sites of intensive DOM cycling Pomeroy 1974, Pomeroy et al. 1979). Microheterotrophs, particularly bacteria and heterotrophic nanoplankton (HNANO) or specifically, heterotrophic flagellates (heteroflagellates) have an essential role in regulating dynamics of carbon flux in aquatic systems (Gast 1985, Sherr et al. 1986). Nutrient and bacterial enriched water flushing salt marsh systems may be expected to demonstrate an active DOM bacteria-protozoan pathway (Lackey 1964, Newell et al. 1983, Wright and Coffin 1984, Pomeroy 1984). Heteroflagellates (HNANO) in the size range (2 - 20 μm) are ubiquitous in estuarine systems (Sherr et al. 1983) and frequently a dominant component of the estuarine (salt marsh) nanoplankton (Pomeroy and Johannes 1968, Sorokin 1979, 1981). Recent studies demonstrate that the HNANO are prolific grazers of bacteria and may indirectly impact dissolved carbon flux by regulating standing stocks, species composition, and metabolic activity of bacterioplankton (Haas and Webb 1979, Fenchel 1982d, Sherr et al. 1983, Azam et al. 1983, Sherr and Sherr 1983, Wright and Coffin 1984, Davis and Sieburth 1984, Davis et al. 1985, Fritz 1986b). A recent study of a bacteria and ciliate food web indicates suggests that bacteriovore grazing activity alters the DOM pool both

qualitatively and quantitatively (Taylor et al. 1985). HNANO may contribute directly to the DOM pool by cellular release. Researchers have calculated that 30 to 70% of estuarine bacterial productivity may be exploited by HNANO (Linley et al. 1983, Fenchel 1982d, Sherr et al. 1983, Landry et al. 1984, Wright and Coffin 1984).

Although the potential importance of bacterial and bacteriovore activity to DOM cycling in estuarine systems is recognized, little quantitative data exists for the spatial and temporal HNANO distributions, for the interrelationships of the different components of estuarine nanoplankton over annual cycles, or for the rates of bacterial productivity specific to systems where the HNANO growth and grazing potential has been determined (Fenchel 1982d, Sherr and Sherr 1983). These types of data have been reported recently for nearshore environments and Narrangansett Bay (Davis et al. 1985), although bacterial productivity data are still lacking.

The possibility of gradients in DOC flux and in the abundances and activities of heterotrophic microbes between marsh habitats and less enriched river waters has been investigated (Bent and Goulder 1981, Ferguson and Palumbo 1982, Newell and Christian 1981, Rublee et al. 1983, Wright and Coffin 1983). However most of these studies used larger spatial scales (whole estuaries). Investigations using small time scales provide data only for bacteria fluctuations, whereas studies which present data for both HNANO and bacteria are generally conducted in non-tidal systems and use larger time scale sampling, on the order of days rather than hours.

Tracing DOM pathways and resolution of DOM--->bacteria---> HNANO

interactions in an estuarine system should involve investigation of spatial and temporal distributions of various components microbial community and bacteria production, e.g. heterotrophic uptake rates of glucose or ^{3}H-thymidine, over small time scales. This requires using several different time scales to account for the inherent variability of an estuarine tidal system and spatial scales to account for tidal advection of nanoplankton within estuarine environments. Factors influencing presence or abundance of bacteria include dormancy, temperature, substrate supply, and grazing. Previous studies have shown no clear pattern in distribution of bacteria in estuarine systems other than lowering of numbers during colder months and the presence of a mid-estuarine peak (Wright and Coffin 1983, Rublee et al. 1983).

Recent literature indicates planktobacteria are more numerous and uniform in distribution (Ferguson and Palumbo 1979, Sieburth 1979) and are not as influenced by short-term tidal effects as are epibacteria. Although the nature of bacterial populations changes over tidal cycle, with an increase of epibacteria at low tide, total numbers of bacteria do not vary (Wilson and Stevenson 1981). Studies have reported seasonal depression in bacteria numbers correlated with decreases in temperatures or substrate supply, but most indicate that numbers vary less than an order of magnitude ($3 - 9 \times 10^{6}$ cells ml^{-1}) over an annual cycle, in contrast to the large seasonal range for other components of nanoplankton. Temperature had been suggested as a regulating mechanism, but Wright and Coffin (1984a) suggest that temperature merely influences the other factors which determine fluctuation in planktonic/bacterial populations. In planktonic environments, the actual density reached by

the bacteria can be determined by the way in which substrate supply and grazing interact. Taylor et al. (1985) takes the hypothesis of regulation of bacteria through HNANO grazer control one step further and has shown that bacteriovore grazing activity releases DOM which in turn supports bacterial production.

Description of seasonal and spatial variations in bacteria and HNANO abundances may be obtained concurrently through the use of epifluorescence direct count analysis. This chapter investigates the seasonal abundances and trophodynamics of estuarine bacteria and nanoplankton in a shallow salt marsh-mudflat ecosystem where maximum variation in environmental conditions may be expected. The seasonal fluctuations in abundances of bacteria and HNANO and the spatial and temporal scales necessary to resolve any patterns or interrelationships of bacteria, HNANO, temperature, DOM and bacterial productivity or activity were investigated. The marsh-mudflat system provided the opportunity to observe differences along a spatial scale ranging from marsh tidal pool, creek, mudflat, and river. At ebbing and flooding tides the flow of water could be traced through the system and at low tide separate tide pools frequently formed in the marsh-mudflat environments. A major objective was to determine differences between high tide, river influenced, and low tide, marsh influenced, nanoplankton assemblages. The second major objective was to determine the degree of variability in bacteria and HNANO populations and bacterial productivity (heterotrophic uptake) by comparing data based on different temporal (weekly, daily, tidal (hourly) scales. It is necessary the determine the degree of variability on several time scales before the inter-

relationships between bacteria and HNANO abundances and the influence of seasonal factors, such as temperature and substrate supply, can be established.

METHODS AND MATERIALS

The study site is a small well-defined tidal embayment (300 m x 100m) located at Carmines Islands (37°17'N, 76°32'W) in the Chesapeake Bay estuary. The embayment opens directly into the York River. Three stations were established which represented a longitudinal gradient between marsh and river: Station 1, Marsh; Station 2, Mudflat; and Station 3, River (Fig. 1). The sampling strategy was designed to investigate temporal and spatial aspects of nanoplankton dynamics ranging from a a short-term basis (hourly intervals within a tidal cycle or daily within a week) to a long-term basis (weekly intervals). The spatial scale was provided by three stations along the tidal embayment. Samples were collected at low tide during a 7 to 8 day cycle each month from May 1981 to May 1982, except during December and January, when ice cover prevented sampling. The second series of environmental data was obtained by sampling weekly or biweekly during one tidal cycle each week from 21 July to 21 December 1982, except during October when two tidal cycles were sampled weekly (Galvao, 1984). Additional tidal cycles were sampled in the last week of January and in mid-April 1983. Sampling was carried out at the same time of day to minimize photoperiod effects. Sampling intervals bracket alternatively one high tide or one low tide on successive weeks. The stations were sampled in sequence (1,2,3 or 3,2,1) following the direction of ebb and flood, respectively. During low tide, shallow tidal pools formed at Stations 1 and 2. All three stations were sampled for each low tide cycle and whenever possible, for high tide cycles. Sampling during the autumn and spring was intensified. Two

Figure 1. Study site and station locations.

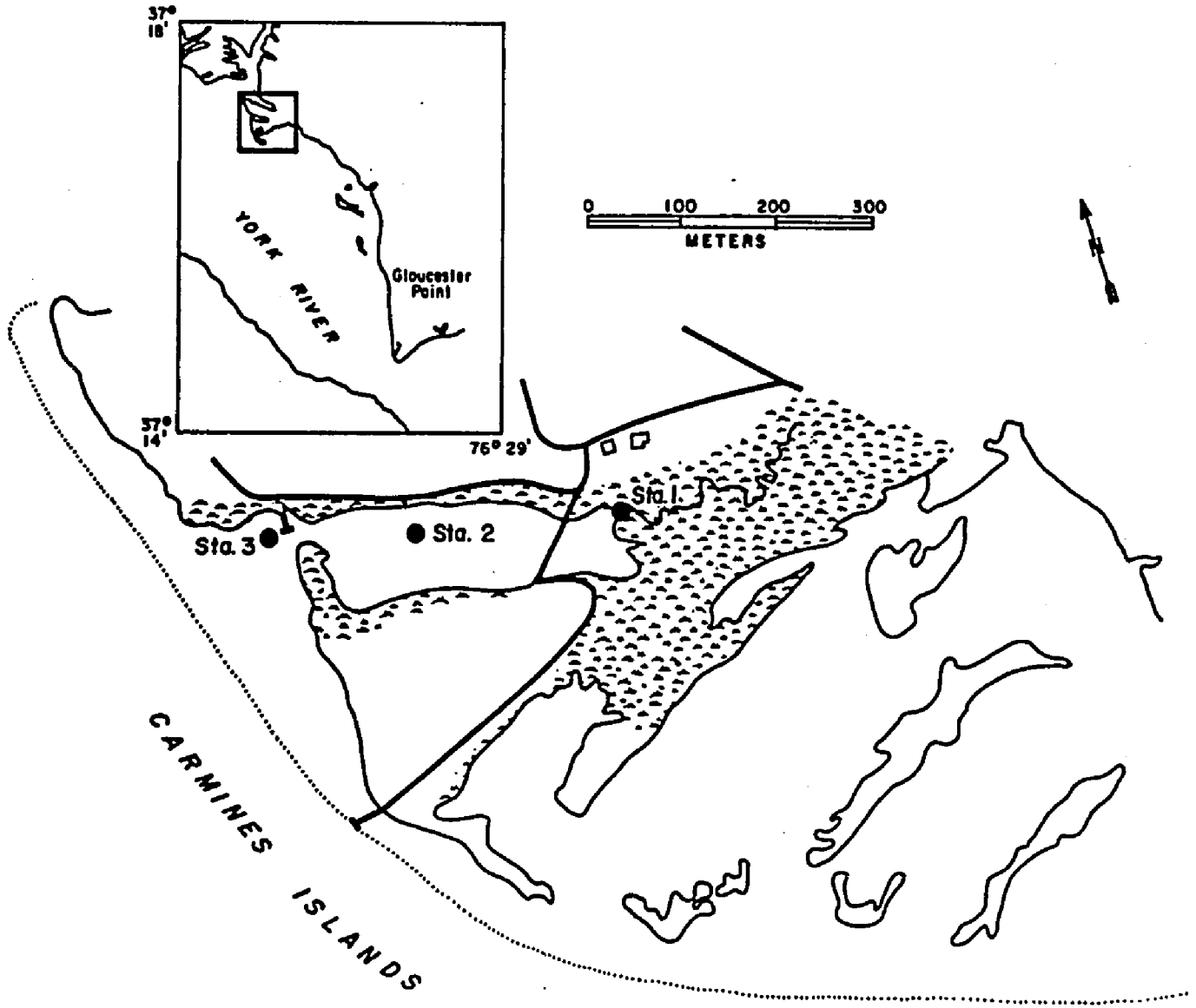
37° 18'
37° 14'
76° 29'
YORK RIVER
Gloucester Point
0 100 200 300
METERS
Sta. 1
Sta. 2
Sta. 3
CARMINES ISLANDS

tidal cycles during October were sampled weekly and two cycles (one each, high and low) were sampled during mid-April. In addition sampling during these periods was carried out at daily intervals during the week between tidal cycles.

The sub-surface water samples (2 ml) taken for direct cell counts were fixed in 0.3% glutaraldehyde in the field. All heterotrophic microorganisms were enumerated with epifluorescence microscopy (Haas 1982) with the modification of increased length of glutaraldehyde fixation (1 to 24 hours). Sub-surface water samples (20 ml) were filtered in the field through precombusted (2 h at 480°C) Whatman GF/F filters and and the filtrate frozen for dissolved glucose analysis. Glucose analyses were performed using a sensitive fluorometric technique developed by Hicks and Carey (1968) for saline waters. The solutions were read in a Turner 111 Fluorometer equipped with a F4T5-green phosphor lamp, a Wratten No. 58 excitation filter overlaid by a polaroid filter to reduce polarized light and a Wratten No. 25 emission filter. The cuvette door contained a flow-through temperature stabilizing cell to minimize temperature increases during readings.

Microbial activity was quantitated as the uptake of ^{14}C-labeled glucose (Crawford et al. 1973). Water was sampled from Station 1 at either a high or low tide and brought to the laboratory for fractionation and incubation at environmentally representative temperatures for approximately 2 to 3 hours (duration depending on the temperature). Two series of 10 ml samples, one of the 1 µm and the other of the 15 µm fractionated marsh water, were run for ^{14}C uptake and another corresponding replicate series were run for CO_2 respired. The 15 µm

fraction contained attached bacteria and marsh heteroflagellates in addition to the predominantly heterotrophic bacteria of the 1 μm fraction. Filters were placed in toluene-based scintillation counting cocktail to determine the CPM. Calculations of uptake kinetics (V_{max}) were performed according to Caperon et al. (1972).

Correlation analysis were conducted with data for daily samples from May 1981 through May 1982 in order to determine if any statistically significant relationships existed between HNANO and bacteria abundances, HNANO and temperature, and bacteria and temperature. For statistical analyses of July through December 1982 samples, data was separated into two water level periods: periods of high water levels (HW) represent conditions when the water column measured >40 cm at station 1, >55 cm at station 2 and >65 cm at station 3, whereas periods of low water (LW) represent <40 cm at station 1, <55 cm at station 2 and <65 cm at station 3. In addition, low versus high water concentrations of HNANO, bacteria, glucose, and temperature were compared through plotting concentrations at lowest and highest water heights. The low water concentrations most often represent tidal pool assemblages. Ebb versus flood comparisons were obtained by averaging concentrations sampled before and after low water or high water.

RESULTS AND DISCUSSION

Daily temperature, salinity and concentrations of bacteria and heteroflagellates measured over a season at the marsh and mudflat stations are shown in Figures 2A,B,C,D and 3A,B,C,D respectively. Temperature varied seasonally at both stations from a high of 35° to a low of 2°C; while the seasonal salinity ranged between 13 and 23 ppt. Bacteria concentrations varied seasonally from 2.0×10^6 to 2.0×10^7 cells ml^{-1}; while seasonal heteroflagellates abundances ranged between 0.5 to 24 x 10^3 cells ml^{-1}. For temperature, salinity, and HNANO and bacteria abundances, variation between days was as great as between months and in all cases the magnitude of the daily variation was as much as 50% of the seasonal range. Figures 4 and 5 also demonstrate the large variability of bacteria and heteroflagellate abundances on a weekly basis over a season range. Differences in abundances at these shorter temporal (Figs. 2, 3, 4, 5) scales are as great as difference in seasonal variation between summer and winter. The April 1983 data (Fig. 6) for bacteria and nanoplankton at marsh and mudflat stations for low water demonstrates more clearly the large daily variation possible even at the same tide stage. The insets for two of the days show hourly fluctuations during tidal cycles bracketing either low (April 13 - 1500) or high tide (April 18 - 1300). Figure 6 indicates that the variations in concentrations of both bacteria and heteroflagellates, due in part to tidal advection, may be nearly equal to daily or even weekly differences in bacteria and HNANO abundances. Bacteria in the tidal environment vary independently of heteroflagellates on a hourly and daily basis. Daily

Figure 2. Seasonal variation in temperature (A), salinity (B), bacteria (C), and heteroflagellates (D) at the marsh station based on sampling at daily intervals within months from May 1981 to May 1982.

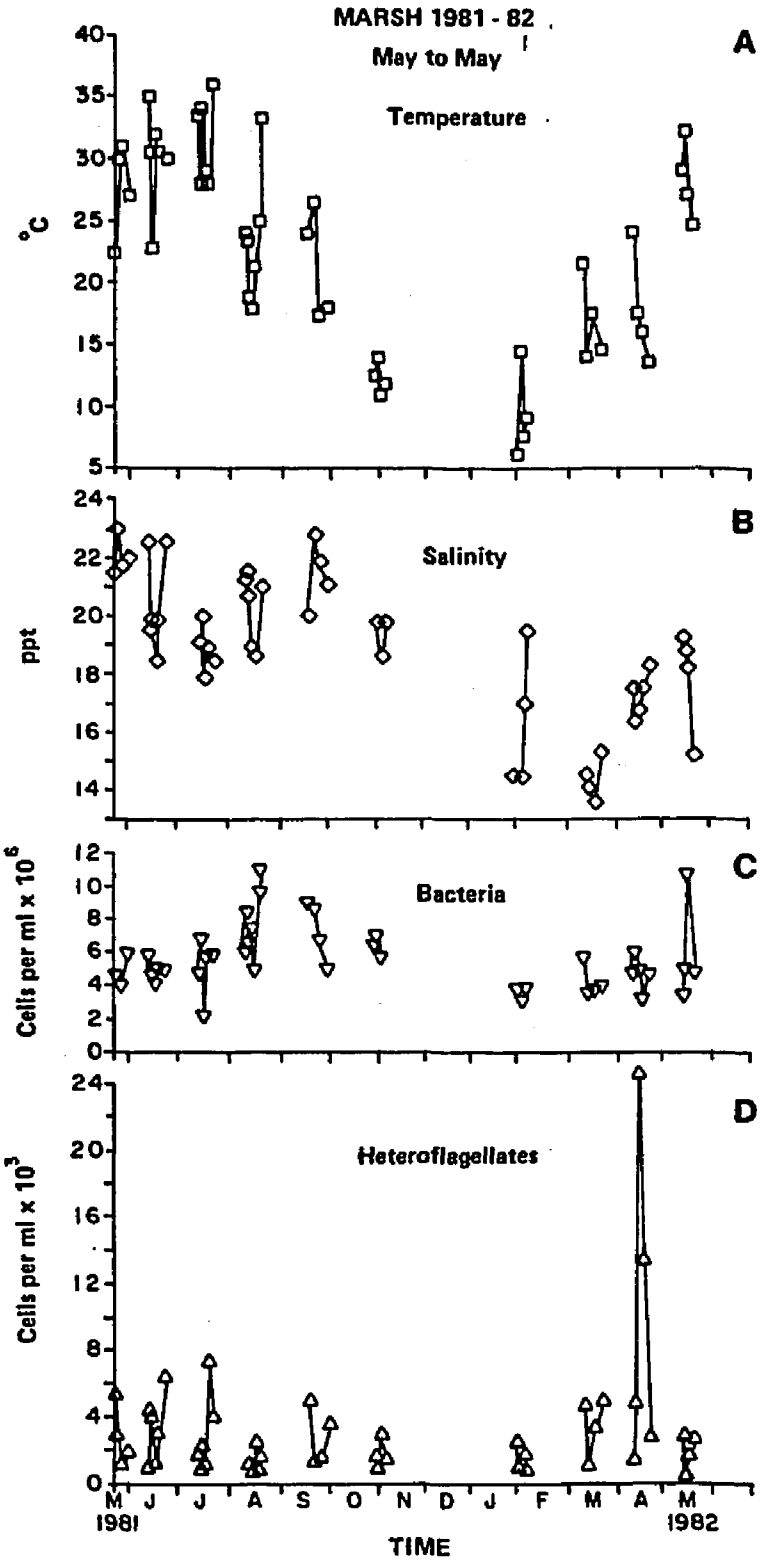
MARSH 1981 - 82
May to May
A
Temperature
°C
40
35
30
25
20
15
10
5
B
Salinity
ppt
24
22
20
18
16
14
C
Bacteria
Cells per ml x 10⁶
12
10
8
6
4
2
0
D
Heteroflagellates
Cells per ml x 10³
24
20
16
12
8
4
0
M J J A S O N D J F M A M
1981
1982
TIME

Figure 3. Seasonal variation in temperature (A), salinity (B), bacteria (C), and heteroflagellates (D) at the mudflat station based on sampling at daily intervals within months from May 1981 to May 1982.

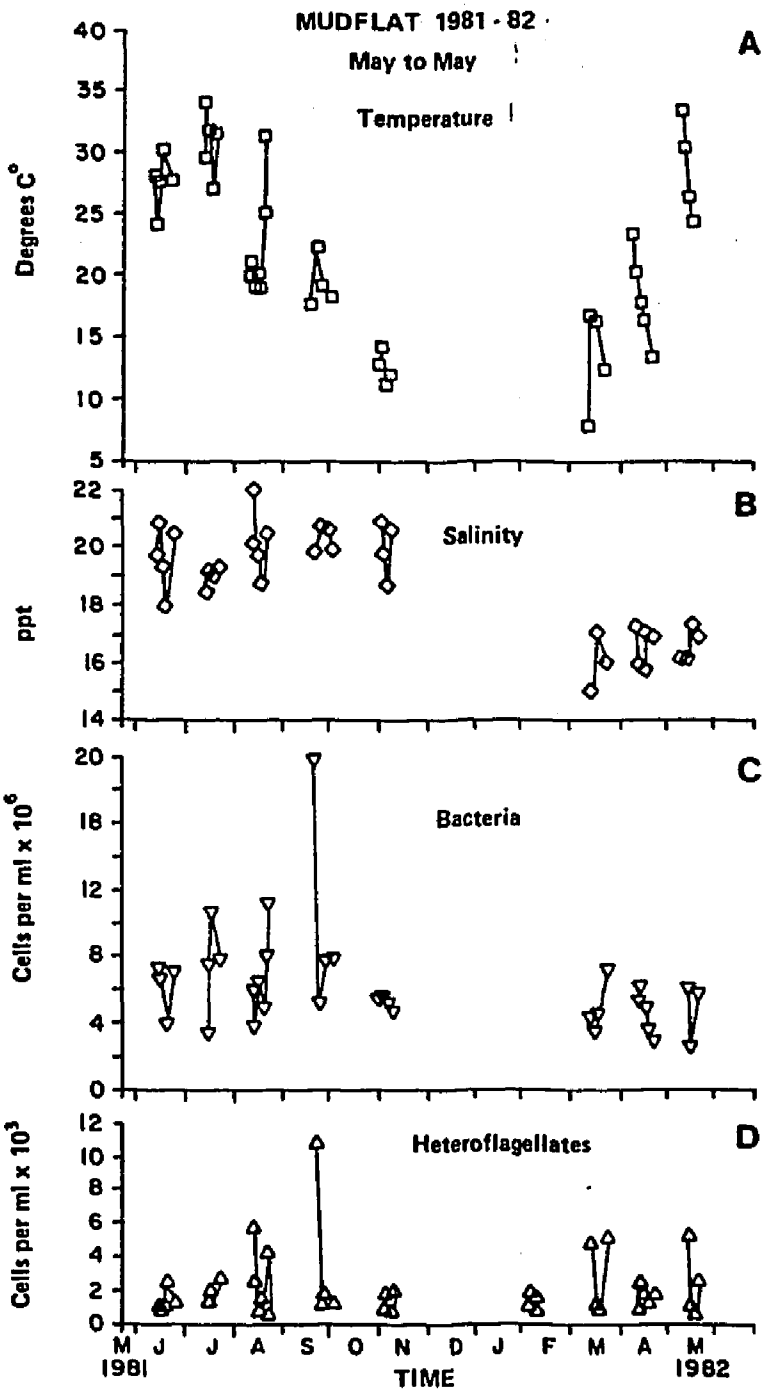
MUDFLAT 1981 - 82
May to May
A
Temperature
Degrees C°
40
35
30
25
20
15
10
5
B
Salinity
ppt
22
20
18
16
14
C
Bacteria
Cells per ml x 10⁶
20
18
12
8
4
0
D
Heteroflagellates
Cells per ml x 10³
12
10
8
6
4
2
0
M J J A S O N D J F M A M
1981
TIME
1982

Figure 4. Seasonal variation (weekly intervals from July to December 1982) of heteroflagellate and bacteria average densities from two hour sampling intervals during ebbing and flooding tides at the three stations (marsh, mudflat, and river).

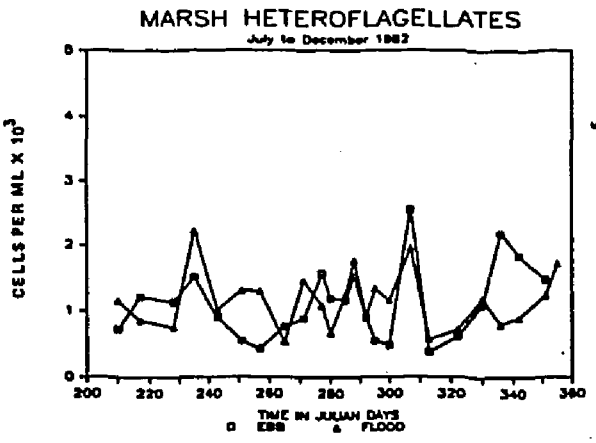
MARSH HETEROFLAGELLATES
July to December 1982
CELLS PER ML X 10³
TIME IN JULIAN DAYS
□ EBB ▲ FLOOD

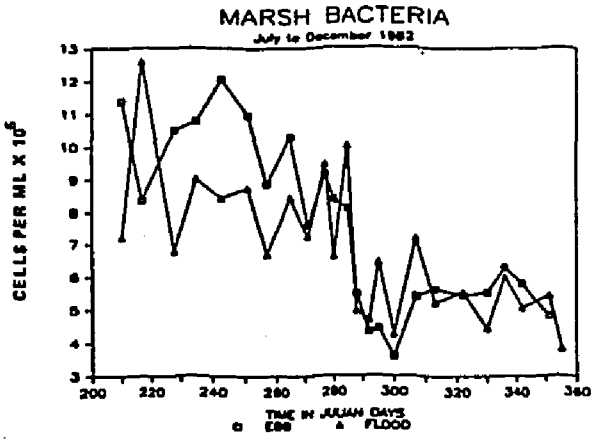
MARSH BACTERIA
July to December 1982
CELLS PER ML X 10⁶
TIME IN JULIAN DAYS
□ EBB ▲ FLOOD

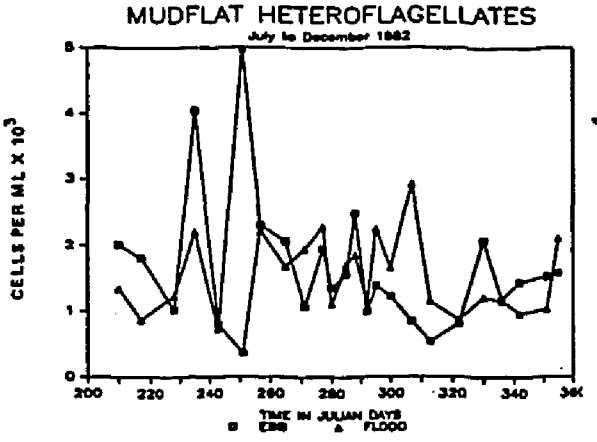
MUDFLAT HETEROFLAGELLATES
July to December 1982
CELLS PER ML X 10³
TIME IN JULIAN DAYS
□ EBB ▲ FLOOD

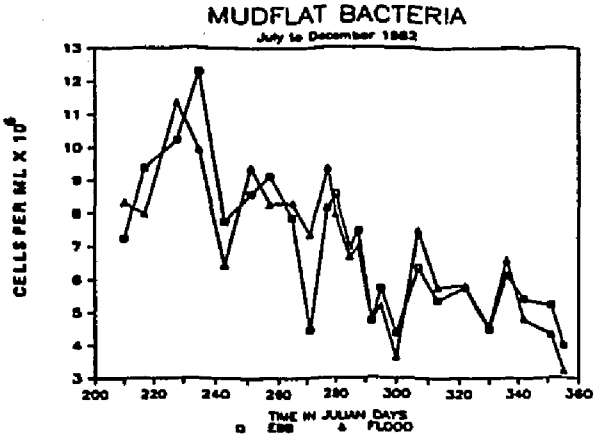
MUDFLAT BACTERIA
July to December 1982
CELLS PER ML X 10⁶
TIME IN JULIAN DAYS
□ EBB ▲ FLOOD

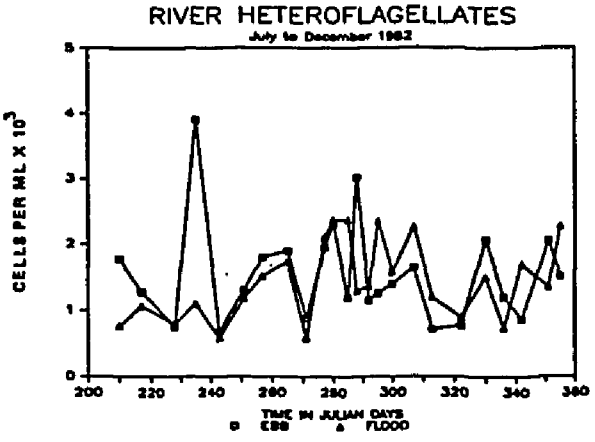
RIVER HETEROFLAGELLATES
July to December 1982
CELLS PER ML X 10³
TIME IN JULIAN DAYS
□ EBB ▲ FLOOD

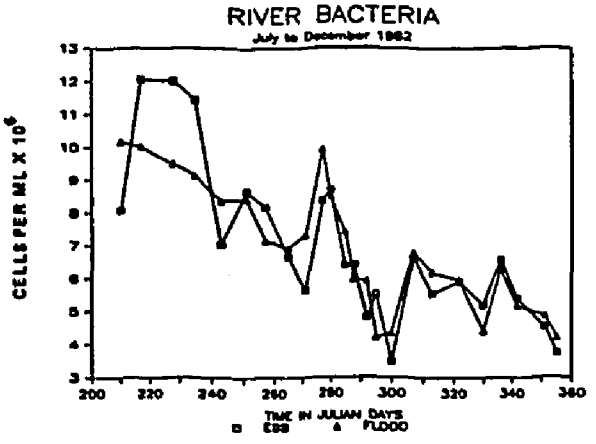
RIVER BACTERIA
July to December 1982
CELLS PER ML X 10⁶
TIME IN JULIAN DAYS
□ EBB ▲ FLOOD

Figure 5. Seasonal variation (July to December 1982) over weekly intervals of low water versus high water abundances of heteroflagellates and bacteria at three stations (marsh, mudflat, and river). Low water values represent concentrations from tidal pools at marsh and mudflat stations.

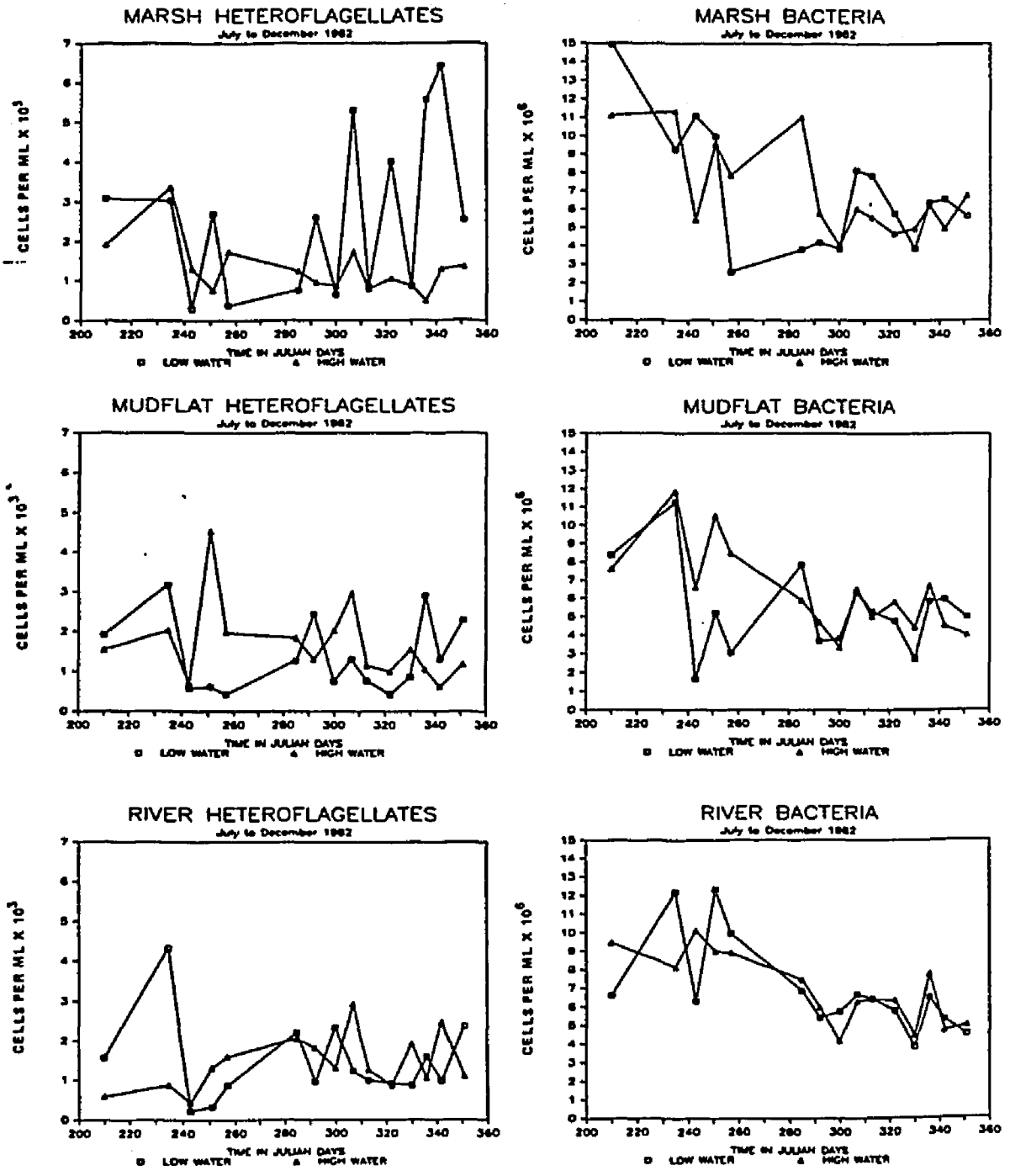
MARSH HETEROFLAGELLATES
July to December 1982
CELLS PER ML X 10³
TIME IN JULIAN DAYS
o LOW WATER
Δ HIGH WATER
MARSH BACTERIA
July to December 1982
CELLS PER ML X 10⁶
TIME IN JULIAN DAYS
o LOW WATER
Δ HIGH WATER
MUDFLAT HETEROFLAGELLATES
July to December 1982
CELLS PER ML X 10³
TIME IN JULIAN DAYS
o LOW WATER
Δ HIGH WATER
MUDFLAT BACTERIA
July to December 1982
CELLS PER ML X 10⁶
TIME IN JULIAN DAYS
o LOW WATER
Δ HIGH WATER
RIVER HETEROFLAGELLATES
July to December 1982
CELLS PER ML X 10³
TIME IN JULIAN DAYS
o LOW WATER
Δ HIGH WATER
RIVER BACTERIA
July to December 1982
CELLS PER ML X 10⁶
TIME IN JULIAN DAYS
o LOW WATER
Δ HIGH WATER

Figure 6. Daily variation in temperature, salinity and ambient densities of heteroflagellates and bacteria during April 1983 at the marsh and mudflat stations. Insets show hourly variation over a low (13 April - 1500 h) and high (18 April - 1300 h) tidal cycle of ambient heteroflagellate, bacteria, and autotroph densities.

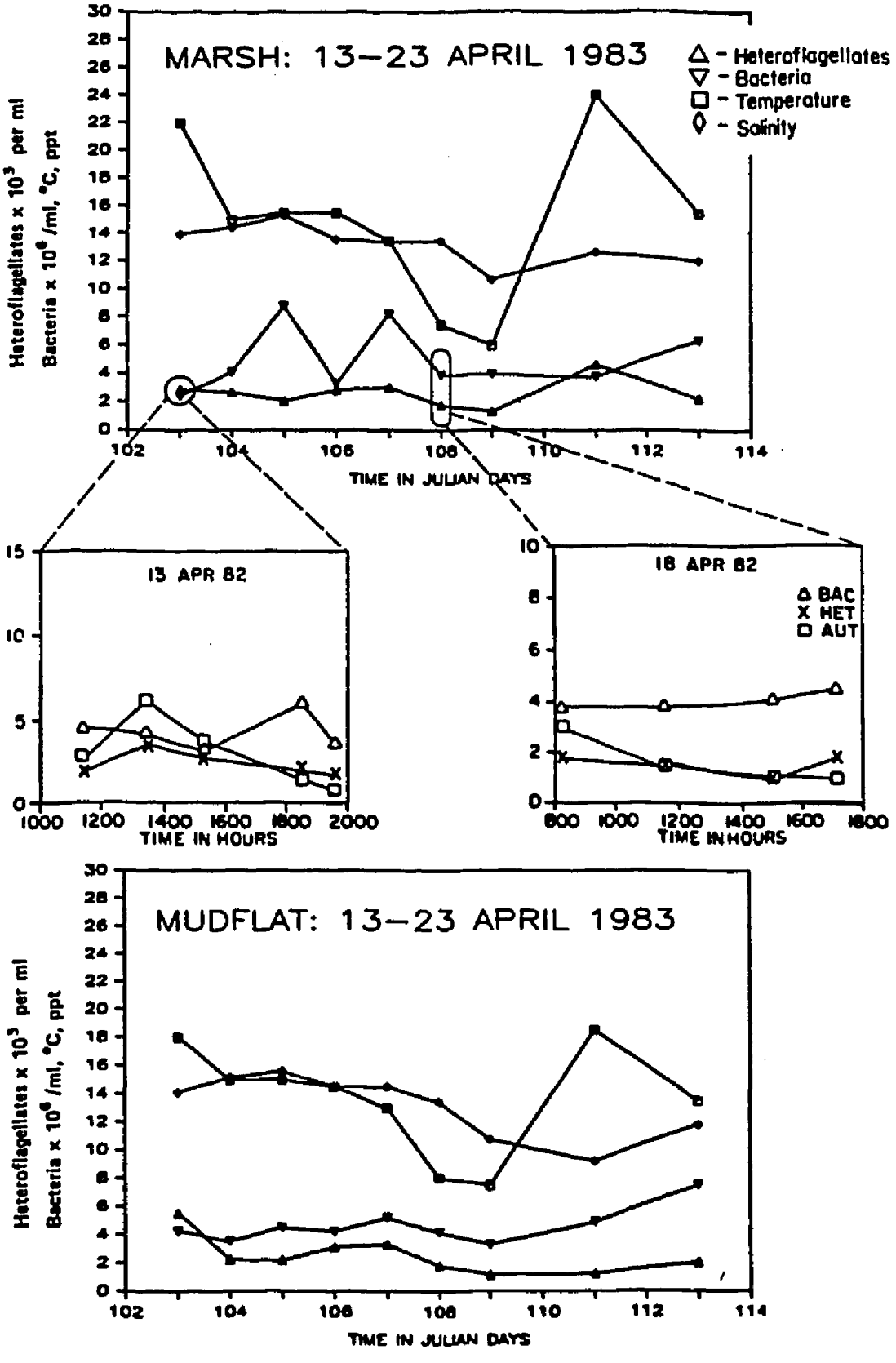
MARSH: 13–23 APRIL 1983
Δ - Heteroflagellates
▽ - Bacteria
□ - Temperature
◊ - Salinity
Heteroflagellates x 10³ per ml
Bacteria x 10⁶ /ml, °C, ppt
TIME IN JULIAN DAYS
13 APR 82
TIME IN HOURS
18 APR 82
Δ BAC
X HET
□ AUT
TIME IN HOURS
MUDFLAT: 13–23 APRIL 1983
Heteroflagellates x 10³ per ml
Bacteria x 10⁶ /ml, °C, ppt
TIME IN JULIAN DAYS

sampling at low water no correlation between HNANO and bacteria concentrations; nor between temperature and either HNANO or bacteria. However Figures 2 and 3 do indicate lower bacteria concentrations at temperatures below 15°C.

Data obtained in a second seasonal study designed to resolve temporal variability on a tidal scale (Galvao 1984) again indicated that short term variability was greater than seasonal (July to December 1982) variability. Statistical analysis using daily means of tidal scale sampling confirmed the lack of correlation of HNANO with bacteria concentrations, of HNANO with temperature, and indicated a significant positive correlation of bacteria with temperature.

Graphs of the averages of two to three samples of HNANO and bacteria abundances on ebbing and flooding tide are shown in Figure 4 with concentrations at ebb plotted versus flood over a seasonal cycle. Figure 4 exhibits the lack of seasonal pattern in heteroflagellates abundances and a decrease in bacteria concentrations beginning on 12 October to the seasonal low of 27 October. Peaks of HNANO abundance, particularly at the mudflat station during ebbing tide may reflect patchiness of HNANO assemblages in tidal waters, pehaps due to aggregates forming in the mudflat environment. The low water versus high water graphs (Fig. 5), plot the concentration of bacteria and HNANO at low water and high water. Specifically, the low water concentration represents a sample from the tidal pools at the marsh and mudflat stations. The graphs show the extremes in ambient variability between tidal stages and reveal peaks of HNANO at the marsh station which correspond to low water assemblages of heteroflagellates forming in

tidal pools. The HNANO bloom concentrations (>4.0 a 10^3 cells ml^{-1}) in November and December confirm the lack of temperature correlation but indicate the importance of the periods of extended low water typical of these particular tidal cycles. Intensive sampling during April 1983 (Fig. 6) resolved the variability of nanoplankton abundances at a shorter or smaller time scale. The daily sampling at maximum low water also revealed HNANO peaks or formation of tidal pool assemblages during tidal cycles with periods of extended low water, but these peaks are quickly diluted by flooding tides. It is evident that on a short time scale, absolute concentrations of bacteria vary independently of HNANO concentrations; it is impossible to discern predator-prey cycles from the marsh-mudflat environmental sampling.

Glucose peak concentrations also were much higher from the marsh station both on ebb and flood from marsh station (Figs. 7, 8) indicating perhaps release of DOM from marsh soils, Spartina, and algal mats (Chalmers et al. 1985, Taylor et al. 1985). Glucose concentrations were consistently greater at low water than high water at all three stations, and also were significantly higher at low tide at the marsh station than at either mudflat or river stations (Galvao 1984). One could speculate that these differences may be reflected in the levels of bacterial activity at the marsh station, particularly at low water.

The glucose uptake heterotrophy experiments were conducted using 1 μm and 15 μm fractions of the ambient bacteria and HNANO sampled over different tidal stages at the marsh station. The 15 μm fraction contained attached bacteria and HNANO which through grazing pressure may

Figure 7. Seasonal variation (weekly intervals from July to December 1982) of temperature and glucose concentration from two hour sampling intervals during ebbing and flooding tides at the three stations (marsh, mudflat, and river).

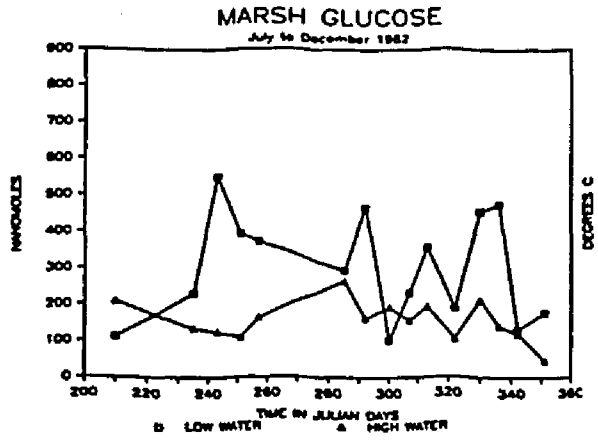
MARSH GLUCOSE
July to December 1982
MICROMOLES
DEGREES C
TIME IN JULIAN DAYS
o LOW WATER
Δ HIGH WATER

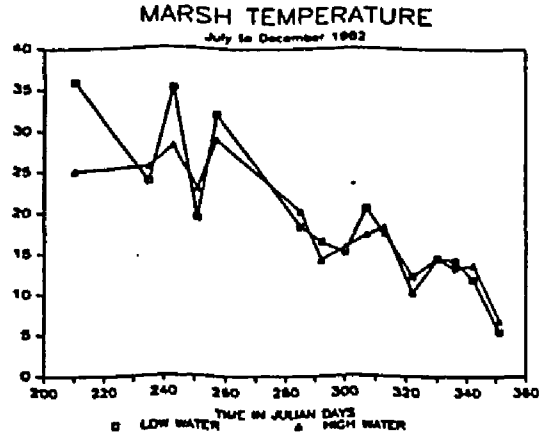
MARSH TEMPERATURE
July to December 1982
DEGREES C
TIME IN JULIAN DAYS
o LOW WATER
Δ HIGH WATER

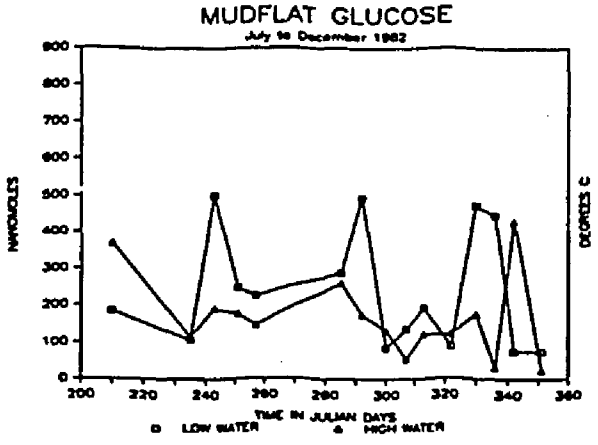
MUDFLAT GLUCOSE
July to December 1982
MICROMOLES
DEGREES C
TIME IN JULIAN DAYS
o LOW WATER
Δ HIGH WATER

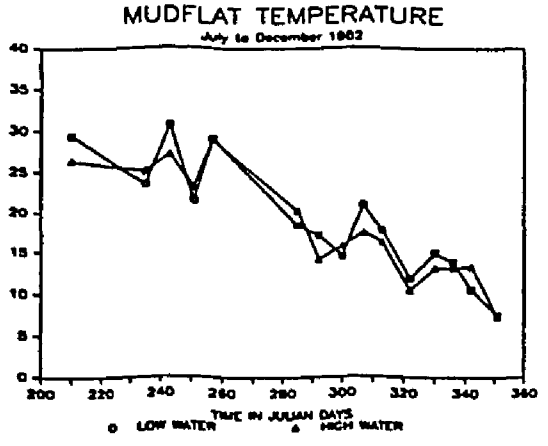
MUDFLAT TEMPERATURE
July to December 1982
DEGREES C
TIME IN JULIAN DAYS
o LOW WATER
Δ HIGH WATER

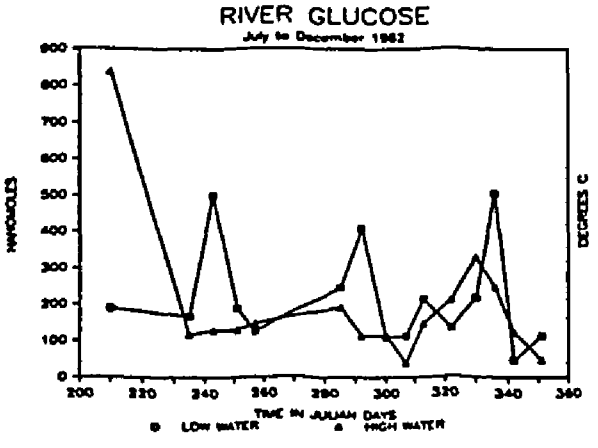
RIVER GLUCOSE
July to December 1982
MICROMOLES
DEGREES C
TIME IN JULIAN DAYS
o LOW WATER
Δ HIGH WATER

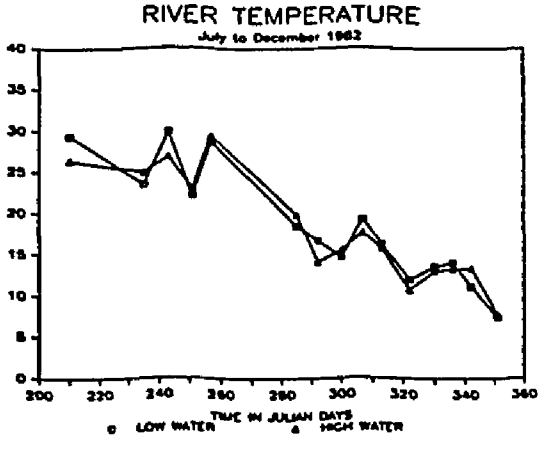
RIVER TEMPERATURE
July to December 1982
DEGREES C
TIME IN JULIAN DAYS
o LOW WATER
Δ HIGH WATER

Figure 8. Seasonal variation (July to December 1982) over weekly intervals of low water versus high water temperature and glucose concentration at three stations (marsh, mudflat, and river). Low water values represent measurements from tidal pools at marsh and mudflat stations.

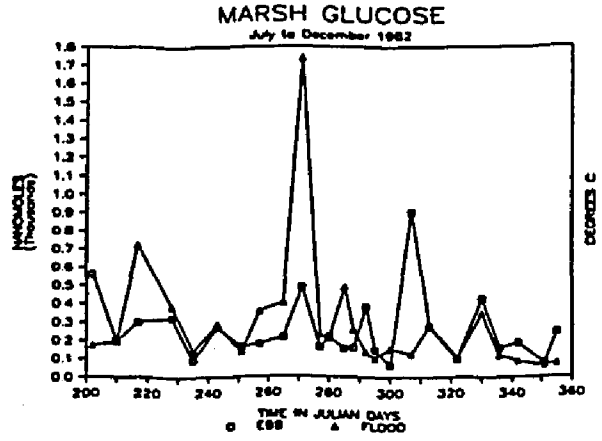
MARSH GLUCOSE
July to December 1982
NANOMOLES (Thousands)
DEGREES C
TIME IN JULIAN DAYS
o EBB
▲ FLOOD

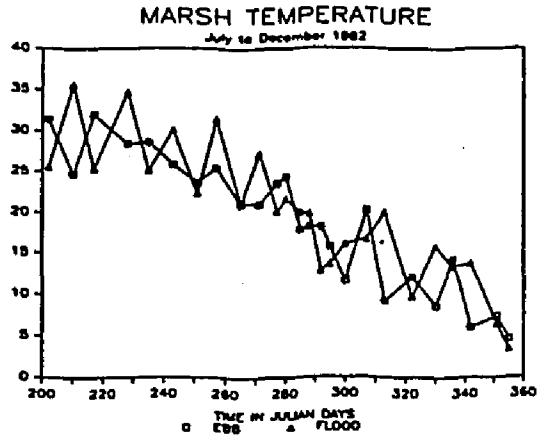
MARSH TEMPERATURE
July to December 1982
TIME IN JULIAN DAYS
o EBB
▲ FLOOD

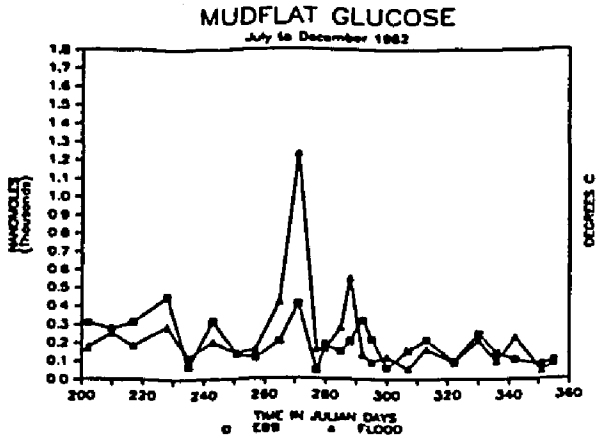
MUDFLAT GLUCOSE
July to December 1982
NANOMOLES (Thousands)
DEGREES C
TIME IN JULIAN DAYS
o EBB
▲ FLOOD

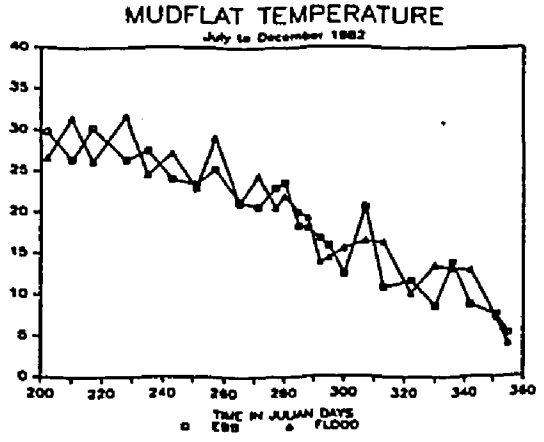
MUDFLAT TEMPERATURE
July to December 1982
TIME IN JULIAN DAYS
o EBB
▲ FLOOD

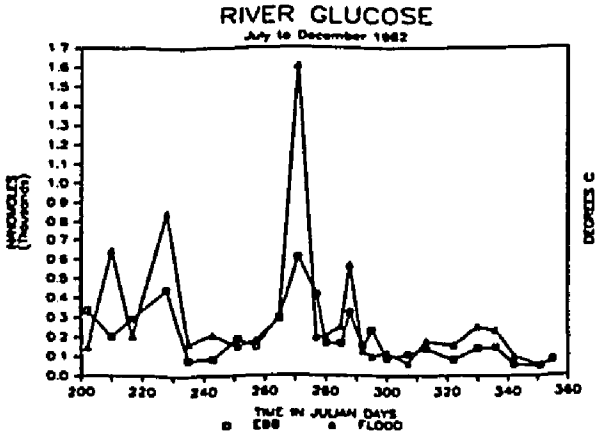
RIVER GLUCOSE
July to December 1982
NANOMOLES (Thousands)
DEGREES C
TIME IN JULIAN DAYS
o EBB
▲ FLOOD

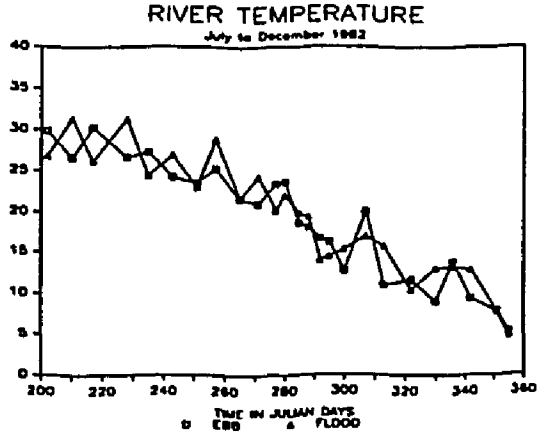
RIVER TEMPERATURE
July to December 1982
TIME IN JULIAN DAYS
o EBB
▲ FLOOD

stimulate bacterial activity thus resulting in higher rates of growth and uptake. The ^{14}C glucose uptake and CO_2 respiration data indicate high rates of uptake for both the 1 μm and 15 μm fractions with a range of 0.03 - 1.66 mgC $l^{-1}h^{-1}$ and respective means of 287 μgC $l^{-1}h^{-1}$ and 641 μgC $l^{-1}h^{-1}$ (Table 1). The uptake data was fitted to a series of curves (Figs. 9-12) to calculate the maximum uptake velocity (V_{max}) and indicated multiphasic uptake kinetics of both kinetic and diffusion components (Figs. 11, 12). Multiphasic uptake systems may be an adaptation to microenvironments where nutrient concentrations fluctuate in both space and time (Azam and Hodson 1981, Nissen et al. 1984). The data fitted using a Michaelis-Menten kinetic model and the measured concentration of ambient glucose (Caperon and Meyer, 1972, Webb pers. comm.) (Figs. 9, 10) resulted in anomalous curves perhaps due to inaccurate (too high) glucose measurements. V_{max} was calculated from the second series of curves (Figs. 11, 12) fitted to the data points. Included in several of the graphs are the plots of the simplified Michaelis-Menten kinetic model curve and the linear diffusion component which demonstrates that the fitted curve represents multiphasic kinetics. The 1 μm and 15 μm fractions demonstrate similar curves for each of the dates and, based on limited data, the higher concentrations of attached bacteria in the 15 μm fraction may contribute to higher uptake values.

Variation in heterotrophic uptake rates (V_{max}) or bacterial production also may be correlated to tidal stage, i.e. higher rates at low tide (Newell and Christian 1981), and differences in temperatures and glucose concentrations. Bacterial heterotrophic activity appears to

Table 1. Ambient glucose concentration (μg l^{-1}) and heterotrophic uptake of ^{14}C-labelled glucose by free and attached bacteria and heterotrophic nanoplankton (HNANO) assemblages sampled from the marsh station at low or high tide. Both the 1 μm and 15 μm fractions contained bacteria, while the 15 μm fraction also contained HNANO. Values of maximum uptake velocities (Vmax) are in the units of ng glucose l^{-1} min^{-1} total bacteria population^{-1}. Values of Vmax C are as μg C l^{-1} hr^{-1} $bacteria^{-1}$ "corrected". All data are sorted from low to high temperatures over the October 1982 to April 1983 sampling period.

DATE	FRACTION μM	TIDE TIME STAGE	TEMP	MEASURED GLUCOSE μG/L	BACTERIA FREE X 10 6TH	BACTERIA ATTACHED X 10 6TH	HNANO X 10 3RD	% CO2	VMAX	KS	DIFFUSION CONSTANT	VMAX C
04/18/83	<1	HIGH	11.00	36.00	2.12		0.14	50.90	0.56	4.36	1.01	25.30
11/18/82	<1	HIGH	13.00	18.00	4.30	-	0.16	32.50	3.42	19.00		352.80
12/02/82	<1	HIGH	13.00	27.00	4.56	-	0.19	27.40	2.24	7.50		244.80
10/27/82	<1	LOW	14.50	18.00	3.34			23.00	6.02	24.20		482.40
11/03/82	<1	HIGH	18.00	18.00	3.69	0.21	0.38	35.00	1.73	1.60	0.07	161.50
04/13/83	<1	LOW	19.00	63.00	2.64		0.29	62.90	4.70	47.40	0.02	297.60
08/10/82	<1	HIGH	26.50	100.00	8.98			60.20	2.05	12.20		441.60
MEAN								41.70	3.36	16.61		287.00
04/18/83	<15	1500	11.00	36.00	3.59	0.42	1.19	55.40	0.91	25.43		87.10
11/18/82	<15	0930	13.00	18.00	6.09	0.88	1.36	7.20	1.09	2.65		181.70
12/02/82	<15	1000	13.00	27.00	6.88	1.30	1.73	42.80	2.37	12.80		465.60
10/27/82	<15	1030	14.50	18.00	4.37	0.46	1.31	18.80	7.25	13.00	0.22	840.00
11/03/82	<15	1000	18.00	18.00	6.73	1.76	2.56	27.70	5.39	9.15	0.28	1099.20
04/13/83	<15	1400	19.00	63.00	3.89	0.52	1.95	37.30	1.48	15.90	0.04	50.50
08/10/82	<15	11-1200	26.50	100.00	15.50	2.30		46.70	3.88	7.40		1656.00
MEAN						1.09	1.68	33.70	3.58	12.33		640.90

Figure 9. Heterotrophic uptake of ^{14}C-labelled glucose based on kinetic model and ambient glucose concentrations for the 1 μm fraction. Glucose uptake (μg glucose l^{-1} h^{-1}) is plotted versus glucose concentration (added plus ambient in μg l^{-1}).

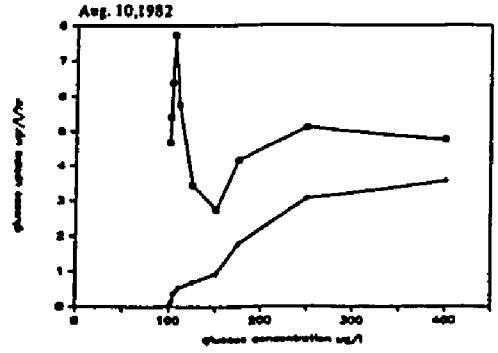
Aug. 10,1982

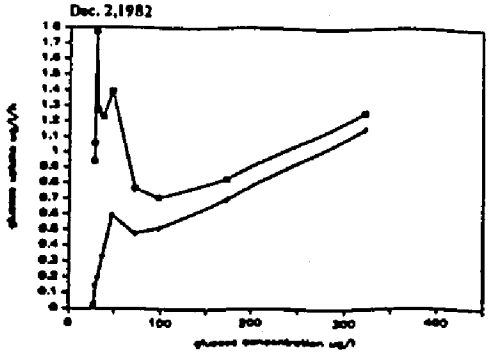
Dec. 2,1982


Oct. 27,1982

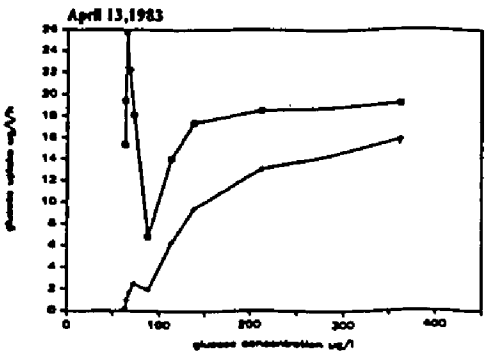
April 13,1983

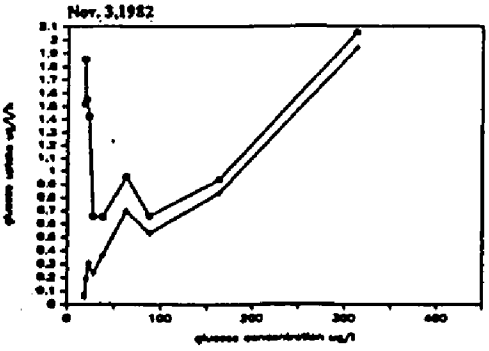
Nov. 3,1982

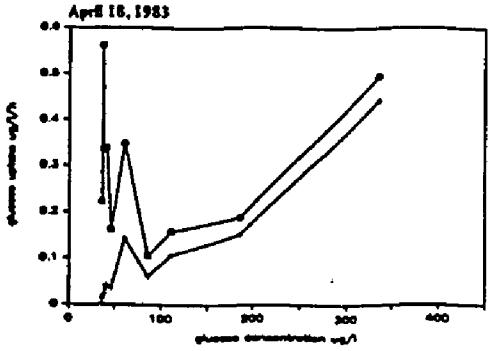
April 18, 1983

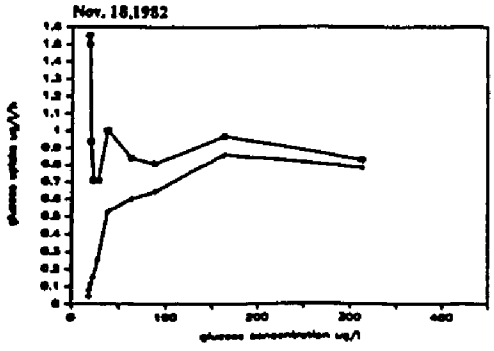
Nov. 18,1982

Figure 10. Heterotrophic uptake of ^{14}C-labelled glucose based on kinetic model and ambient glucose concentrations for the 15 µm fraction. Glucose uptake (µg glucose l^{-1} h^{-1}) is plotted versus glucose concentration (added plus ambient in µg l^{-1}).

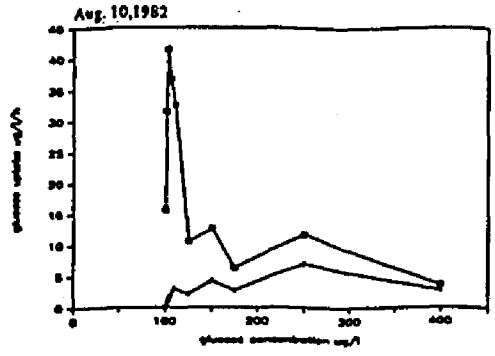
Aug. 10,1982

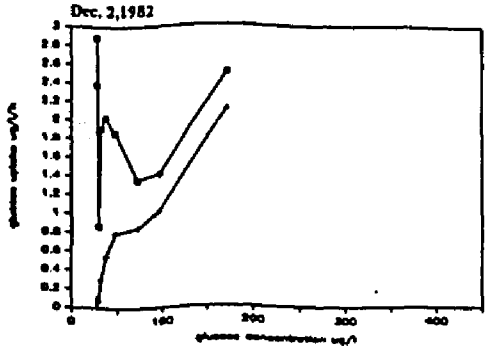
Dec. 2,1982

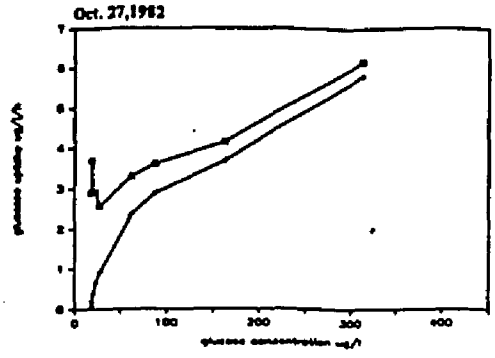
Oct. 27,1982

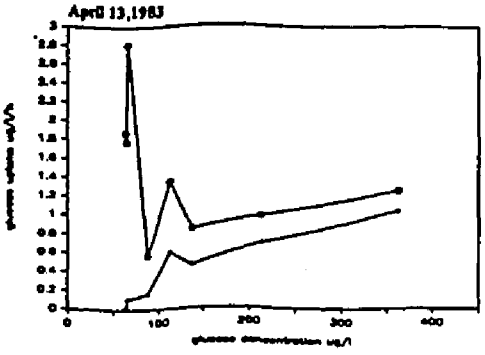
April 13,1983


Nov. 3,1982

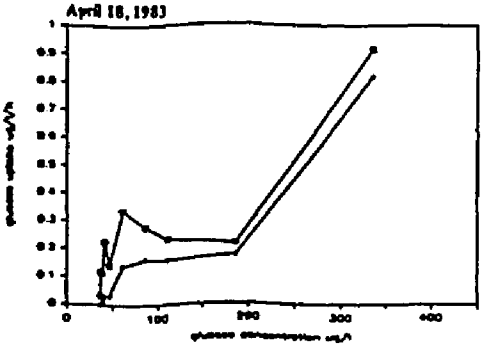
April 18, 1983

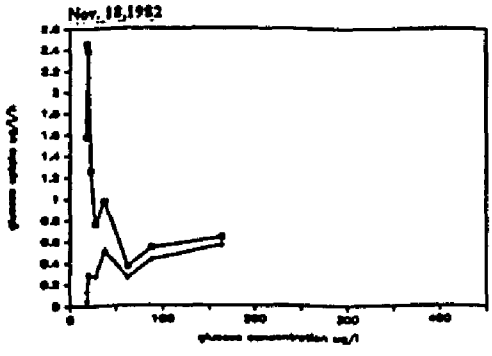
Nov. 18,1982

Figure 11. Heterotrophic uptake of ^{14}C-labelled glucose. Curves are fitted to glucose uptake values in ug glucose l^{-1} h^{-1} versus added glucose (μg l^{-1}) for the 1 μm fraction. The diffusion component (linear uptake) and kinetic (Michaelis-Menton) model curve are plotted in several dates to demonstrate multiphasic uptake.

Aug. 10,1982

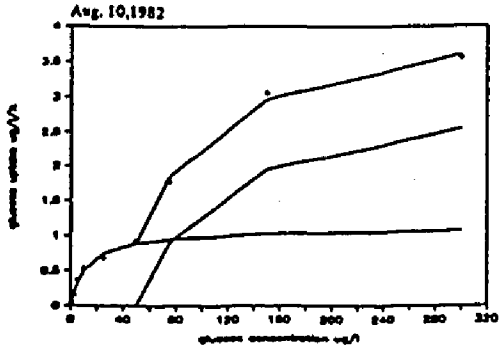

Dec. 2,1982

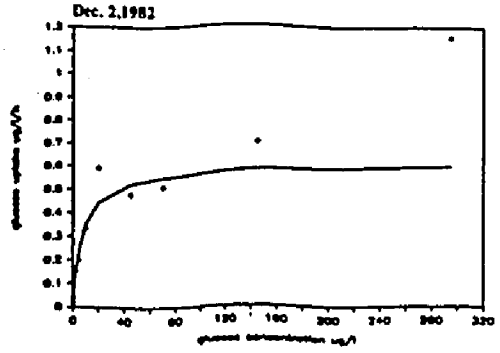

Oct. 27,1982

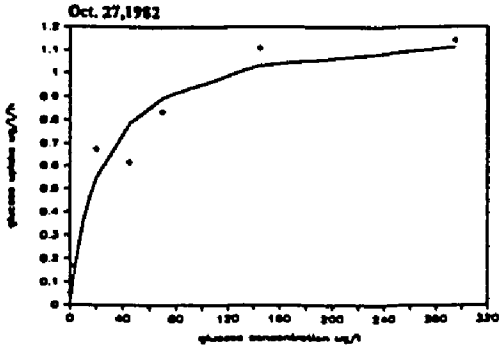

April 13,1983

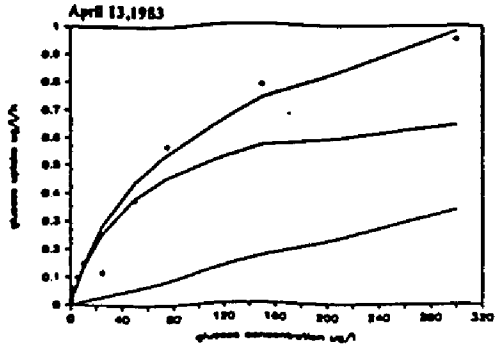

Nov. 3,1982

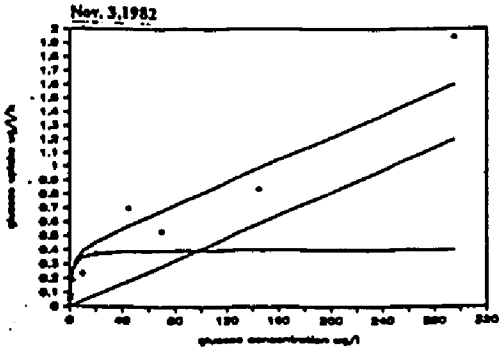

April 18, 1983

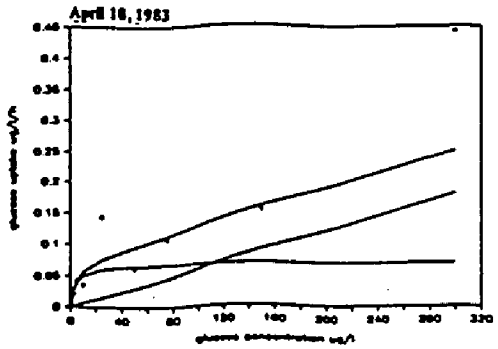

Nov. 16,1982

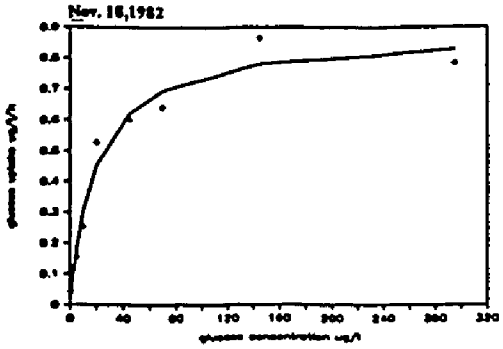

Figure 12. Heterotrophic uptake of ^{14}C-labelled glucose. Curves are fitted to glucose uptake values in ug glucose l^{-1} h^{-1} versus added glucose (ug l^{-1}) for the 15 um fraction. The diffusion component (linear uptake) and kinetic (Michaelis-Menton) model curve are plotted in several dates to demonstrate multiphasic uptake.

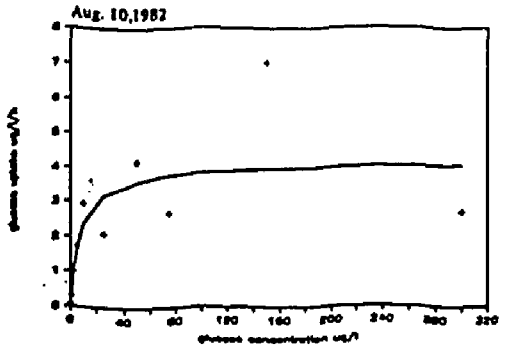
Aug. 10,1982

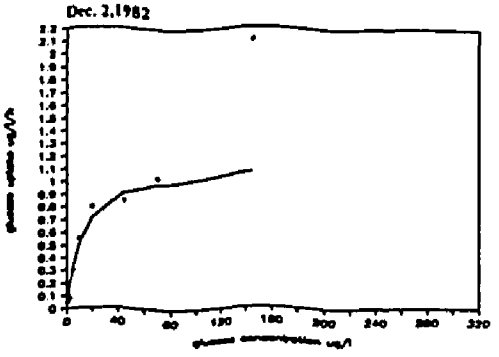
Dec. 2,1982

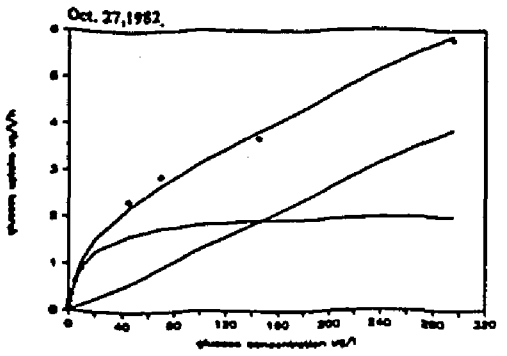
Oct. 27,1982

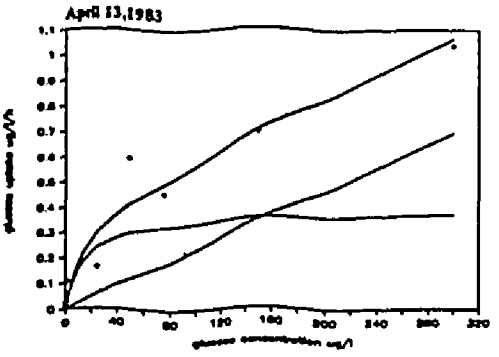
April 13,1983

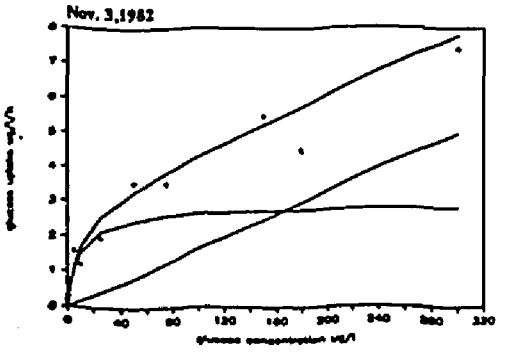
Nov. 3,1982

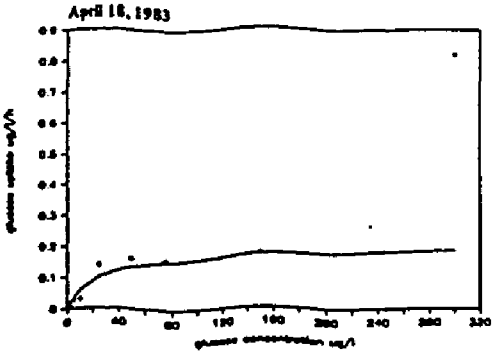
April 18, 1983

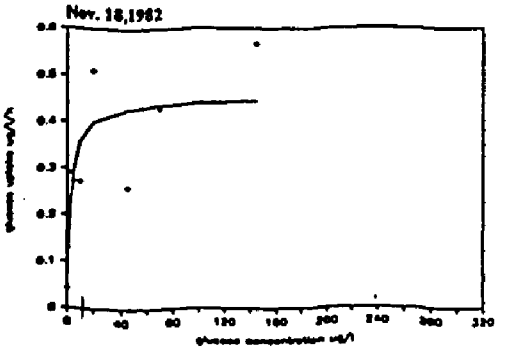
Nov. 18,1982

be correlated to temperature. CO_2 respired for both fractions was positively correlated with temperature and although there was no significant correlation for V_{max} the lowest rate and highest rates were measured at the lowest and highest temperatures, respectively. There was insufficient data to establish a low versus high tide correlation, although V_{max} for low tide of spring and fall were generally higher than for high tide assemblages. The limited data does show that the range of variability in bacterial production during short temporal scales (including time scales based on tidal stage) can be as great as seasonal variation. Further heterotrophic uptake studies (or determinations of bacterial specific activity) should be conducted on short time scales (i.e., successive tidal stages) in order to determine the full range of bacterial production in a marsh-mudflat system. Better estimates of bacterial production for tidal environments are necessary before the transfer of secondary production to higher trophic levels via HNANO ingestion of bacteria can be evaluated quantitatively.

CHAPTER III

SEASONAL HETEROTROPHIC NANOPLANKTON TROPHODYNAMICS - IN SITU DETERMINATIONS OF GROWTH AND GRAZING RATES IN A MARSH-MUDFLAT SYSTEM

INTRODUCTION

The aquatic microbial food chain paradigm of a pathway from dissolved organic matter (DOM) to phagotrophic nanozooplankton via ingestion of bacteria (Pomeroy 1974) has been confirmed using recently developed epifluorescence microscopic and staining techniques (Azam et al. 1983, Pomeroy 1984, and Sieburth 1984). Recent research indicates that heterotrophic protozoans may regulate stocks, species composition, and metabolic activity of bacterioplankton in environments ranging from estuarine (Wright and Coffin 1984a,b) to oceanic (Sieburth 1984, Davis et al. 1985). Bacteriovores may indirectly impact DOM flux through regulation of bacterial activity and in addition, may directly influence carbon cycling by releasing or stimulating release of DOM (Stoecker et al. 1983, Taylor et al. 1985). The phagotrophic nanoplankton (HNANO), primarily the heterotrophic microflagellates (heteroflagellates) ranging from 2 to 12 μm in size, are numerically and, as bacteriovores, functionally important component of coastal estuarine systems (Sherr and Sherr 1983, Sherr et al. 1984, Davis et al. 1985). The high productivity, high substrate and bacteria concentrations of salt marsh-mudflat systems represent an environment where the role of microheterotrophs in the microbial trophodynamics may be quantitated. Although much speculation exists concerning the role of HNANO in marine

ecosystems based on recent enumeration techniques using epifluorescence direct count and laboratory growth rate determinations, little quantitative information is available for in situ growth and grazing dynamics of HNANO under natural conditions.

Laboratory experiments on growth and grazing rates demonstrate that microheterotrophs are characterized by high rates and responsiveness to changing conditions (Fenchel 1982a, b, c, d, Newell et al. 1983, Sherr et al. 1983, Davis and Sieburth 1984, Sherr and Sherr 1984, Taylor et al. 1985). These same characteristics indicate that cultures isolated from the environment or microbial systems studied in defined, uniform laboratory environments would change quickly in vitro and no longer be representative of microbial communities in the nature (Pomeroy 1985). Most methods for determining marine bacterioplankton growth and production rates use bottle incubations. They also require several assumptions that can produce different estimates of specific growth rates for the same sample (Christian et al. 1982). The estimation of growth using frequency of dividing cells (FDC) does not require in vitro incubations but the regression of growth rates of FDC may be influenced by nutrient concentrations and temperature (Newell and Christian 1981) which often can not be duplicated in vitro.

Bacterial populations confined in vitro for as little as 3-4 hrs may no longer resemble the original population after (Ferguson et al. 1984). Heterotrophic nanoplankton grown in laboratory incubations inevitably consume much larger or different types (e.g., culturable) bacteria than encountered in the environment which in turn may affect growth and grazing response (Fenchel 1982a). The dynamics of natural

heterotrophic nanoplankton can not be duplicated under conditions where the natural environmental variability, bacterial populations and microhabitats have been changed, replaced, or removed. Environmental monitoring and in situ incubation techniques should provide the best means of understanding the trophodynamics of heterotrophic nanoplankton in variable estuarine systems.

Direct in situ measures of bacterial and microbial community growth have been employed only recently. These involve either enclosing a water sample in dialyis bags or diffusion chambers equipped with porous polycarbonate membranes. The enclosed nanoplankton populations remain under the same physical-chemical conditions as the natural environment. The predominant use of diffusion chambers was to test the survival of indicator organisms such as Escherichia coli under relatively natural conditions for public health considerations (McFeters and Stuart 1972, Anderson et al. 1983, Rhodes et al. 1983). Chambers only recently have been used for determinations of in situ growth of natural bacterial communities or for observations of nanozooplankton community dynamics (Furnas 1982a,b, Landry et al. 1984). Dialysis bags have been used frequently to monitor community phytoplankton and nutrient dynamics in coastal ecosystems (Sieburth 1973), however, dynamics may be affected by lack of exchange and mixing.

Furnas (1982a) conducted comparative experiments of phytoplankton growth in dialysis bags and diffusion chambers constructed with polycarbonate membranes. The higher permeability and exchange rates of the polycarbonate filter membranes offset the lower surface area to volume ratio as compared to dialysis bags. The diffusion chambers,

essentially a modified McFeters and Stuart (1972) design, permitted rapid growth of microplankton species at low ambient nutrient levels. Microflagellates and non-motile ultraplankton assemblages grew under all conditions tested including an estuarine environment and wet table incubations (Furnas 1982b). Furnas also observed growth of colorless flagellated nanoplankton, although rates were much slower than those of autotrotrophic forms. Landry et al. (1984) and Turley and Lochte (1985) also were successful in measuring growth rates in replicate experiments without sustaining chamber effects, e.g., bacterial growth on walls or decrease in diffusion or change in the chemical continuum with ambient. Results of experiments (Landry et al. 1984; Turley and Lochte 1985) in oligotrophic oceanic and nearshore environments have demonstrated the value of the diffusion chambers for in situ studies of nanoplankton dynamics.

This chapter is the second of a series which investigates the nanoplankton trophodynamics of a small shallow salt marsh-mudflat system located in a subestuary of the Chesapeake Bay. The previous chapter (II) discussed the high degree of spatial and temporal variability of the different components of salt marsh, estuarine nanoplankton (and the necessity for sampling over short time scales). Variation in abundance on a daily basis can be as great as the seasonal variation. Relationships or predator-prey cycles are difficult to establish based on the variation in abundances of the different components of the environmental nanoplankton populations. Patterns in variability in populations or different components, i.e., predator-prey cycles, were not discerned.

The environmental monitoring study conducted from May 1981 through April 1983 (Chapter II) demonstrated that shallow tidal pools are important environments for heteroflagellates assemblages and glucose accumulation. One of the major objectives of the field experimentation presented in this chapter and others that follow is the development of an in situ methodology for quantifying growth and grazing rates of heteroflagellates and for quantifying the predator-prey interactions. Use of diffusion chambers equipped with Nuclepore polycarbonate membranes of two different pore sizes allowed for the estimation of in situ heteroflagellate growth and grazing rates on varying assemblages of bacteria under various environmental conditions. A tidal float and pool support structure simulated a tidal pool environment of extended low tide and high surface area (sediment, water, and air interfaces) conducive for formation of high nanoplankton concentrations. The major goals of this field research were to define the role of heterotrophic nanoplankton (HNANO or heteroflagellates) in marsh systems quantitatively; to determine the seasonal range of growth and grazing rates for salt marsh system heteroflagellates; and to describe patterns or time scales of predator-prey interactions of the microbial trophodynamic paradigm.

METHODS AND MATERIALS

Field Stations

The marsh-mudflat site of the HNANO community dynamics study was located in a small, brackish (10-22 ppt) tidal embayment (300 x 100 m) at Carmines Island, Virginia (37° 17'N, 76°32'W; Fig. 1). The embayment is connected to the York River by a narrow channel at one end, is bordered on both sides by a fringing Spartina alterniflora marsh and is fed by a tidal creek at the other end. Sampling station 1 (marsh) was located where the tidal creek enters the embayment forming a small marsh tidal pool at low water. Station 2 (mudflat) was located in the middle of a large shallow tidal pool formed in the embayment during low water. Diffusion chambers were suspended at the respective marsh and mudflat stations in shallow water reservoirs sunk in the substrate; this arrangement simulated protected tidal pools typical of this cove marsh.

Field Methods

A field experimental methodology was developed to obtain in situ growth rates of bacterioplankton and heterotrophic nanoflagellates (HNANO) interacting in a marsh-mudflat plankton community using in situ diffusion chambers. Diffusion chambers were identical to the modified McFeters-Stuart (1972) design employed by Rhodes et al. (1983) and were constructed of autoclavable Lexan, a polycarbonate material. A detailed illustration of the chamber is given Figure 2. Chambers held a 40 ml volume and were modified by addition of BUNA-N O-rings in grooved retainer plates and two threaded sampling ports inserted or attached to

Figure 1. Study site and station locations.

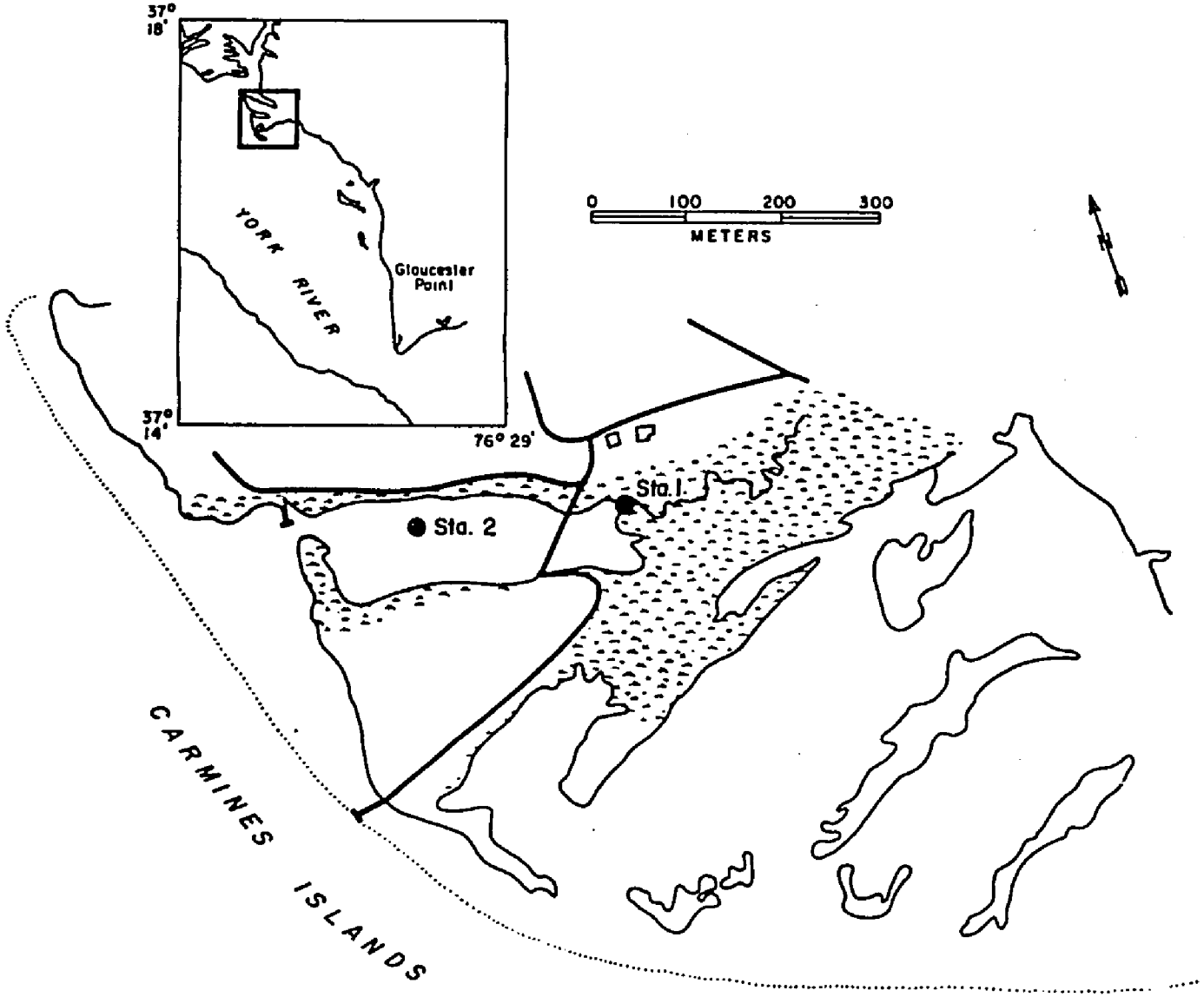
37° 18'
37° 14'
76° 29'
YORK RIVER
Gloucester Point
0 100 200 300
METERS
N
Sta. 1
Sta. 2
CARMINES ISLANDS

Figure 2. Diagram of diffusion chamber.

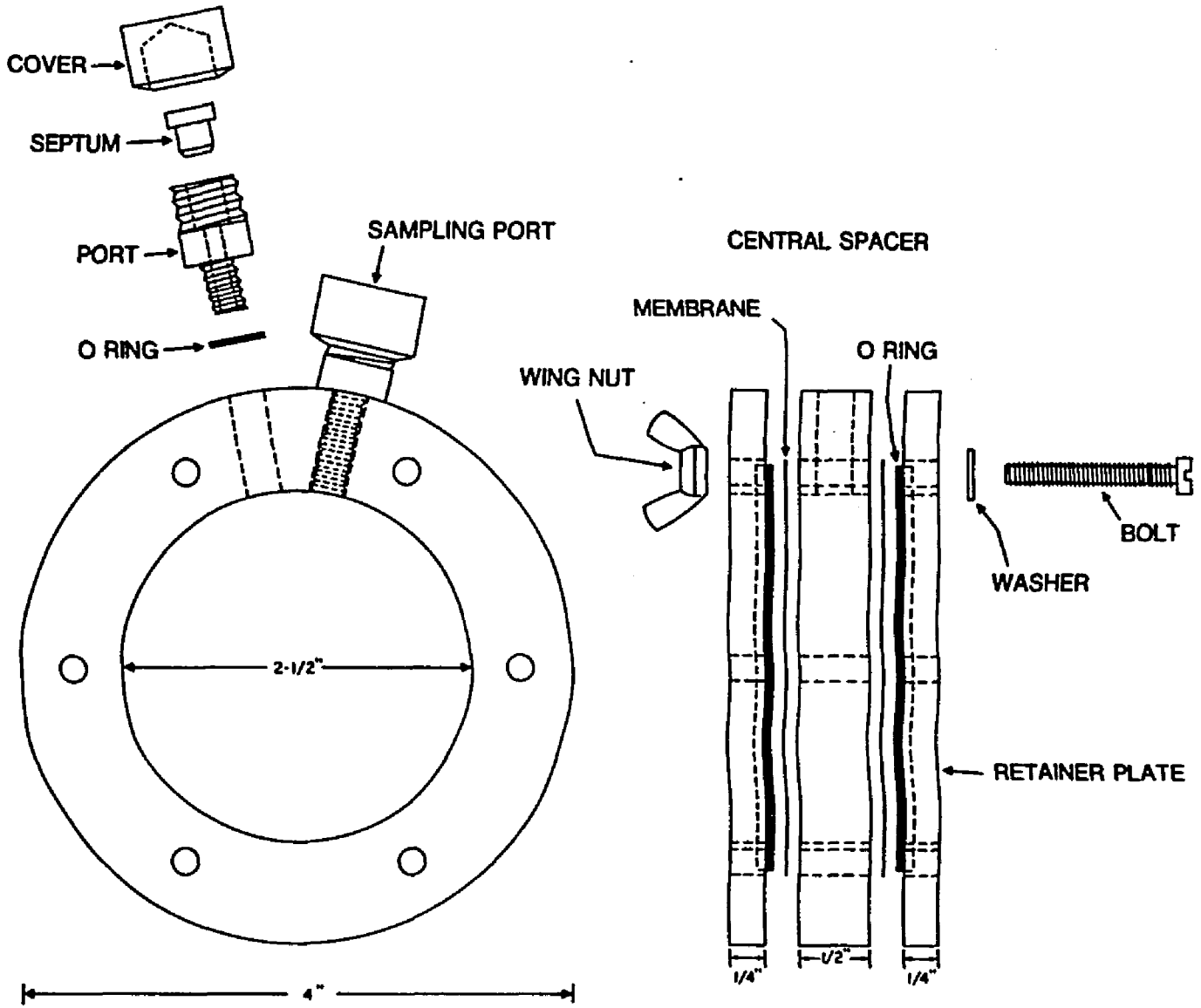
COVER
SEPTUM
PORT
O RING
SAMPLING PORT
2-1/2"
4"
CENTRAL SPACER
MEMBRANE
O RING
WING NUT
BOLT
WASHER
RETAINER PLATE
1/4"
1/2"
1/4"

central spacer, sealed with BUNA-B O rings, and fitted with serum bottle stoppers (Bittner Corp., Norcross, GA) and threaded caps to prevent fouling. Chambers deployed in this study were fabricated using Nuclepore polycarbonate permeable membranes of two different pore sizes, 0.20 and 1.0μm. A saffranin dye study similar to Anderson et al. (1983) demonstrated that the 0.20 μm membrane chambers allowed exchange of dissolved substances with relatively rapid replacement time of 2 to 5 hours and 1.0 μm chambers which allowed an even more rapid replacement time of 2 to 3 hours and exchange half-life of less than 1 hour (Furnas 1982a). The 0.20 um chambers retained HNANO and bacteria allowing chemical continuum with ambient and the 1.0 μm chambers retained HNANO but allowed the interchange and maintenance of ambient bacteria populations.

The chambers were assembled by securing the retainer plates to the sterilized central spacer with stainless steel wing nuts and bolts) and then were transported to the field. The innocula, consisting of freshly collected low tide water from mudflat and marsh stations gently gravity-filtered through Nitex membranes (<40 μm) was added to chambers. Previous seasonal experiments (Fritz, unpubl. man.) using various size fractions (<15 μm, <40 μm, and total) and ambient sampling revealed low densities (0 - 40 cells ml^{-1}) and extremely patchy distribution of ciliates in the marsh-mudflat system. Because marsh-mudflat tidal waters frequently contained large benthic diatoms and flocculent detrital material, the <40 μm fractionation was used to eliminate interference in nanoplankton enumeration from resuspended material while maintaining ambient patchy distribution of ciliates. Innoculum of ambient bacteria

concentrations for 0.20 μm chambers were obtained by either gentle vacuum filtration of water through a 1.0 μm polycarbonate membrane or from a 1.0 μm chamber submerged in the water column and allowed to fill. The chamber fills in approximately 5 minutes with ambient bacterial concentrations while effectively eliminating predators without filtering stress.

Chambers were immediately suspended in ambient water at low tide in shallow water reservoirs sunk into the substrate. Samples were taken within the first 24 hours and thereafter, at 24 to 48 hour intervals over a 5 to 7 day period. The support structure consisted of a float that housed the chambers in open cages equipped with flow-through plexiglass baffles and allowed chambers to move through the water column with tidal fluctuations, yet remain submerged during spring low tide (Fig. 3). Samples (2 ml) were collected from sampling ports in the chambers using syringes with 22 guage needles and preserved immediately in the field with 6% glutaraldehyde for epifluorescence enumeration (Haas 1982). Epifluorescence microscopy direct count analysis of different autotrophic and heterotrophic components of the chamber microbial community was used to determine change in densities, types, and sizes of organisms.

Duplicate larger volume, 10 - 20 ml samples for ciliate enumeration, were taken at the initiation and termination of chamber experiments. Both chamber and concurrent environmental samples for ambient nanoplankton community and various physical parameters were taken at low tide over a 10 day period. During this incubation period, water at stations frequently formed protected tidal pools at low tide during which time a quiescent system of multiple interfaces (air-water-sediment) and

Figure 3. Diagram of support structure for diffusion chambers.

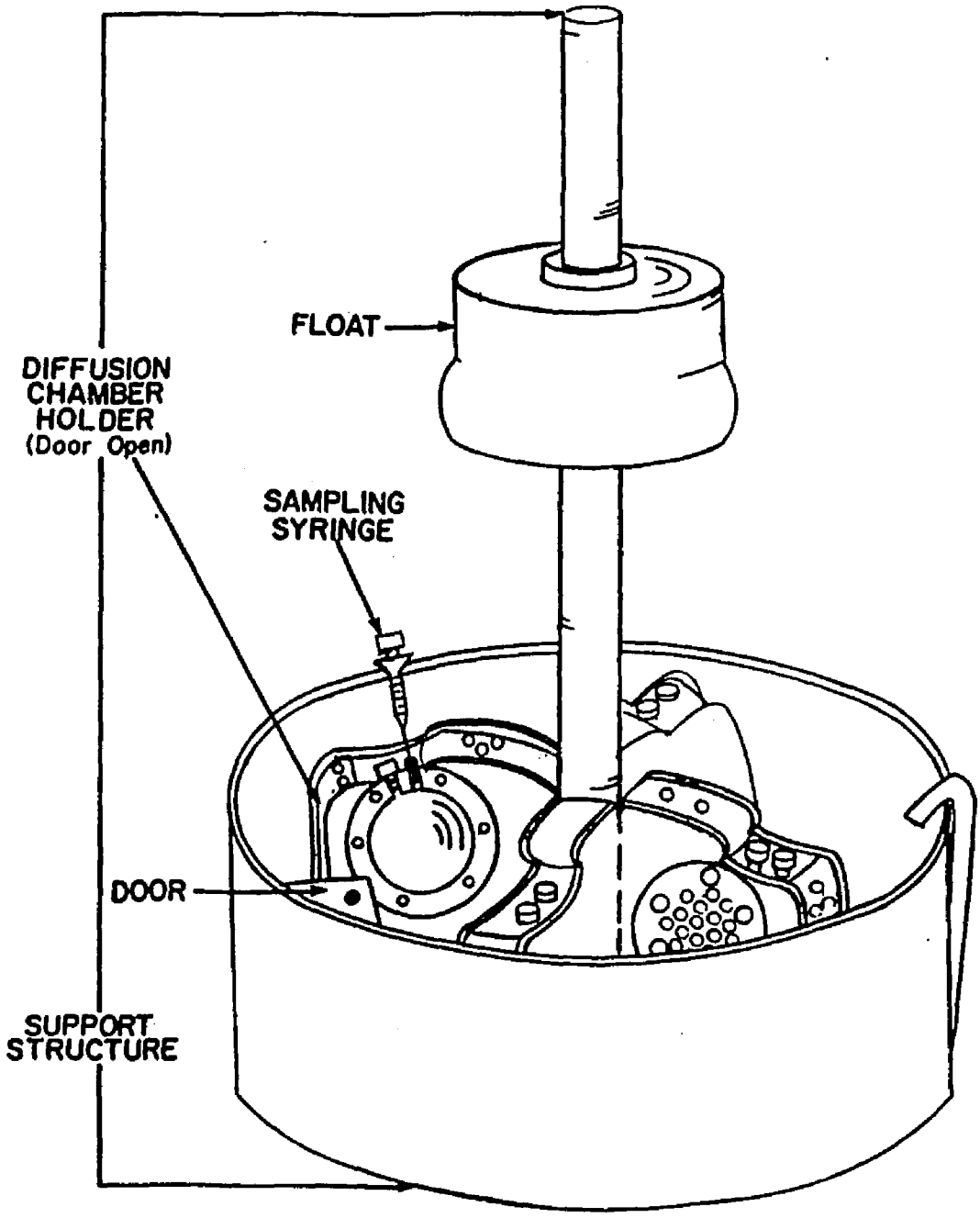
FLOAT
DIFFUSION
CHAMBER
HOLDER
(Door Open)
SAMPLING
SYRINGE
DOOR
SUPPORT
STRUCTURE

microniches developed. Quiescent conditions created in the chambers most closely correspond to this type of environment where there is less turbulence. Fluctuations in nanoplankton populations affected by environmental variability inherent in marsh-mudflat tidal pool system, can thus be monitored without advection effects. In situ diffusion chamber data and environmental sampling for nanoplankton at low tide to minimize advection affects makes possible the evaluation of short term cycles in predator-prey interactions.

Bacteria and Heteroflagellate (HNANO) Growth Rate Determinations

Growth rates were based on changes in densities of organisms, assuming exponential growth throughout a sampling interval which may be defined as

$$N_t = {}_oe^{(\mu-d)t} \qquad (1)$$

and calculated as

$$\mu = (\ln N_t - \ln N_o)/t \qquad (2)$$

where N_o and N_t are cell numbers per ml at the beginning and end of a sampling interval (t). The specific growth growth rate was used to calculate the population doubling time, Dt(in hours), as

$$Dt = \ln 2/\mu \qquad (3)$$

and divisions per day, $K(day^{-1})$ as

$$K = \mu/\ln 2 \times 24 \qquad (4).$$

Growth rates of bacteria (μ_b) were calculated from changes in numerical density of bacteria incubated in 0.20 μm chambers. Relative distribution of sizes and types were monitored by frequent sampling (3 to 12 hour intervals) over a 2 day period or until populations reached a stationary phase where bacterial assemblages began to deviate from

environmental. The 1.0 μm bacteria chambers contained environmental assemblages of actively growing bacteria which were maintained throughout the sampling period due to exchange of ambient bacteria and substrates. Comparison of bacteria densities in these 1.0 μm control chambers with fluctuations in ambient densities gave an indication of when bacterial growth was occurring during the 1.0 μm HNANO growth experiments.

Heteroflagellate growth rates (μ_h) for each monthly experiment were determined from increases in heteroflagellate density in both 0.20 and 1.0 μm chambers containing HNANO assemblages. The μ_h, D_t, and K were calculated using equations 2 - 4 and by using the increase in density during approximately 24 hour intervals of growth when bacteria assemblages either increased or followed ambient fluctuations.

Grazing Impact and Grazing Rate Determinations

Grazing impact or decrease in bacteria due to HNANO grazing pressure was evaluated in 0.20 μm chambers by direct comparison of bacteria density in chambers with the fluctuations in ambient bacteria density. The comparison of plots of 1.0 μm HNANO and 1.0 μm bacteria chambers reveal potential grazing impact by HNANO under conditions more closely mimicking ambient, i.e., varying bacterial assemblages. For example, grazing impact in 1.0 μm chambers is indicated when bacteria decrease in HNANO chambers relative to ambient concentrations or to concentrations in 1.0 μm bacteria chambers.

Grazing rates were calculated using two difeerent approaches or two different set of equations. The first, as described by Landry et al. (1984), involves the derivation of maximum clearance and ingestion rates

from estimates of bacteria growth and mortality. First the mortality coefficient is derived from the difference between the bacterial population growth rates (μ_b) determined in the 0.20 μm bacteria chamber and the observed rate of change of the bacterial population (r) determined in HNANO chambers. The observed rate of change of bacterial populations in chambers due to grazing (r) can then be defined as

$$r = (\ln N_t - \ln N_o)/t = \mu - d, \qquad (5)$$

where μ = bacterial population growth rate and d = mortality rate, both in units per hour. The mortality rate, assumed due to heteroflagellate predation, then can be calculated as

$$d = \mu - r. \qquad (6)$$

The clearance rate (F = volume cleared of prey predator^{-1} h^{-1} or d^{-1}) can then be calculated as

$$F = d/P \qquad (7)$$

by dividing the prey's or bacteria mortality rate by the mean density of predators or heteroflagellates present during the sampling interval. This assumes an exponential rate of growth of the predator population and P is calculated as

$$P = (X_t - X_o)/\ln X_t - \ln X_o) \qquad (8)$$

Ingestion rate expressed as average number of bacteria (prey) consumed per heteroflagellate (predator)$^{-1}$ h^{-1} or d^{-1}) is calculated as the mean bacteria density (B) times the heteroflagellate clearance rate (F)

$$B = (X_t - X_o)/\ln X_t - \ln X_o) \qquad (9)$$

$$I = F \times B \qquad (10)$$

The second approach for calculating maximum ingestion rate (U_m) is from Fenchel (1982b) which assumes the exponential growth rates of

heteroflagellate and the eventual yield are functions of bacteria density. The maximum ingestion rate U_m or bacteria consumed per hour is calculated as the heteroflagellate specific growth rate (μ) from diffusion chambers divided by Y, the yield constant,

$$U_m = \mu/Y \qquad (11)$$

Y, the yield constant is expressed as the numbers of flagellates produced per bacterium and is calculated as

$$Y = (N_t - N_o)/B \qquad (12)$$

B is the initial bacterial concentration or average density of bacteria when populations are not changing in the diffusion chambers. Maximum ingestion rate or U_m are determined in 0.20 μm chambers at initial stages of growth when bacteria concentration and growth rates were fairly stable (e.g., ~Dt=24h) and in 1.0 μm chambers when bacterial densities followed ambient patterns.

RESULTS

Heteroflagellate assemblages growing in chambers were characterized by four basic types at both the marsh and mudflat stations. These included rounded forms (monads and Paraphysomonas) in two different size ranges (~2 μm and 3-5 μm), choanoflagellates (2-3 μm), small bodonids (2-4 μm); and ellipsoid bodonid 3-5 (w) x 7-10 μm (l). The most numerous biflagellated forms were bodonids and Paraphysomonas sp. (vestita) which demonstrated a greater range in size from 3-4 μm (most common) to 5-7 μm. An apochlorotic cryptomonad (pointed body), although not abundant, appeared throughout the year. Small monads and collared choanoflagellates (1-3 μm, 15 - 35 μm^3) also were dominant components of seasonal assemblages. Low tide assemblages of increased heteroflagellate numbers usually occurred in association with larger bacteria (epibacteria) in the marsh tidal pool. Mudflat bacterial assemblages were more variable both in types and density than in the marsh. Mudflat ambient heteroflagellate populations also more frequently reflected nanoplankton assemblages imported from the river, particularly when they were dominated by large achlorotic cryptomonads (pointed bodies) and large Paraphysomonas.

The autotrotrophic component was dominated by prasinophytes (Pyramimonas), chlorophytes (Micromonas, Apedinella), haptophytes, small dinoflagellates (Katodinium, Prorocentrum, and Gymnodinium), large and small cryptomonads, and centric, chain, and very abundant pennate diatoms, particularly Nitzchia. The ambient mixed assemblage of

autotrophs (10^3 or 10^4 cells ml^{-1}) usually outnumbered the heteroflagellates (10^3 cells ml^{-1}) and were generally much larger (>10 μm) in size. Chambers reflected these ambient assemblages, however the fractionated chamber innoculum contained reduced numbers of larger phytoplankton (i.e., Nitzchia). Total numbers of autotrophs were within the same order of magnitude (10^3 cells ml^{-1}). The seasonal pattern was the same in both fractionated water used in chambers and ambient water. The seasonal pattern of ciliates showed low abundances during the colder months to increasing numbers in late May and June (1.0×10^2 cells ml^{-1}) to maximum abundance in July and August (8×10^2 cells ml^{-1}). This pattern occurred in both the chambers and the environment.

Small (<2μm) autotrophic flagellates were not an important component of the natural (marsh-mudflat system) assemblage, present sporadically in numbers at least an order of magnitude less than heteroflagellates. Occasional cyanobacteria blooms occurred concurrently with heteroflagellate blooms. These events were generally replicated or magnified in chamber populations. Heteroflagellate assemblages growing in both marsh and mudflat chambers increased in diversity from two to four or five types and sizes. Paraphysomonas, monad and small bodonid types increased in size range (i.e., 2-4 μm to 4-5 μm) after one or two doublings.

Both bacteria and heteroflagellate growth rates, determined during each monthly experiment, were quite variable. Coefficients of variation (CV) for the monthly means ranged from 10 - 70%. The seasonal variation of bacteria and of HNANO mean growth rates of the marsh and mudflat are plotted for comparison in Figure 4. Degree or types of variability of

Figure 4. Marsh versus mudflat mean growth rates of bacteria (top) and of heteroflagellates (bottom) over a seasonal cycle (May 1981 to May 1982, October - November 1982, and April 1983.

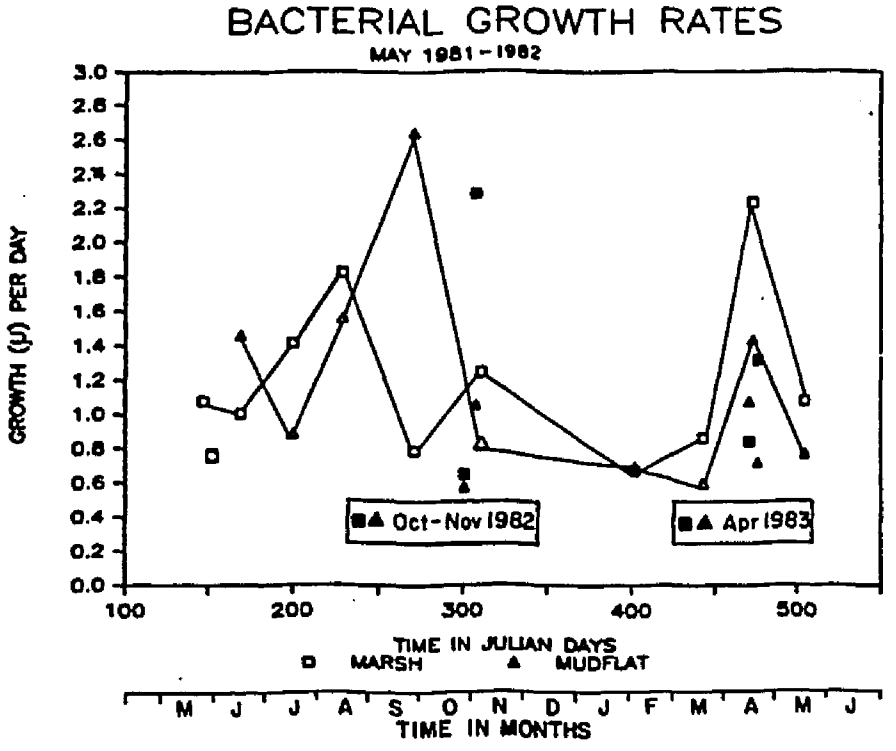
BACTERIAL GROWTH RATES
MAY 1981-1982
GROWTH (μ) PER DAY
3.0
2.8
2.6
2.4
2.2
2.0
1.8
1.6
1.4
1.2
1.0
0.8
0.6
0.4
0.2
0.0
Oct-Nov 1982
Apr 1983
100
200
300
400
500
TIME IN JULIAN DAYS
MARSH
MUDFLAT
M J J A S O N D J F M A M J
TIME IN MONTHS

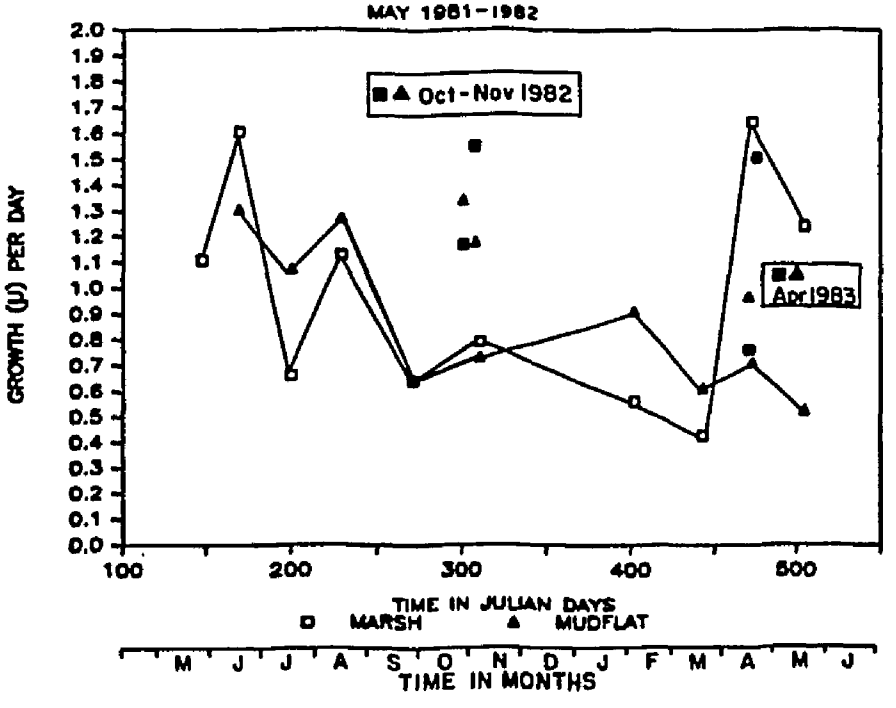
HETEROFLAGELLATE GROWTH RATES
MAY 1981-1982
GROWTH (μ) PER DAY
2.0
1.9
1.8
1.7
1.6
1.5
1.4
1.3
1.2
1.1
1.0
0.9
0.8
0.7
0.6
0.5
0.4
0.3
0.2
0.1
0.0
Oct-Nov 1982
Apr 1983
100
200
300
400
500
TIME IN JULIAN DAYS
MARSH
MUDFLAT
M J J A S O N D J F M A M J
TIME IN MONTHS

monthly growth rates are demonstrated in Figures 5 and 8. Representative patterns of predator-prey interactions (daily variation) for each month are shown in Figures 9 through 16. The full range of growth and grazing rates and CVs are given in Tables 1 and 2.

Bacteria growth rates exhibited a sequence of different phases resulting in fairly large CV for rates determined at 4 hour intervals during the 24 hour growth period. After 24 to 48 hours of incubation, bacterial assemblages entered a stationary phase in growth changed in species composition and size distribution from the ambient population. The seasonal pattern of bacterial growth rates at both stations reflects the large variability possible and the general trend for increased summer rates (Fig. 4).

Heteroflagellate growth rates determined during monthly chamber experiments were extremely variable even between replicate chambers. Heteroflagellate assemblages and bacteria in each chamber demonstrated a variety of initial growth responses including immediate growth, a lag phase, or decrease in numbers before growth. Plots of estimated growth rate for June 1981 (Fig. 10), demonstrate the variability of in situ growth reponse even under replicated environmental conditions. Although growth in chambers did not always begin concurrently, monthly means were frequently similar. Initial growth usually occurred within the first 24 hours or at least within 48 hours. Growth rates and patterns in both 1.0 and 0.20 μm chambers were not significantly different ($p > 0.05$). Growth rates of the two pore size chambers were pooled for monthly averages for evaluation of seasonal patterns and marsh versus mudflat comparisons. Bacterial populations in the larger pore size chambers most frequently

Table 1. Seasonal growth and grazing rates of heteroflagellates (predators - P) at the MARSH station. Growth, clearance and ingestion rates are mean values of monthly in situ diffusion chamber experiments

	HETEROFLAGELLATE GROWTH										CLEARANCE	INGESTION		
Date	μh^{-1}	μd^{-1}	SD	SE	CV(%)	Range μh^{-1}	Dt (h)	P	Amb B	B	$\mu l\ d^{-1}$	Bh^{-1}	Bd^{-1}	PERCENT GRAZED
1981														
27 May	0.046	1.11	0.38	0.22	34.3	0.028-0.057	15.1	58.70	4.52	4.43	—	—	—	
18 Jun	0.067	1.61	0.75	0.30	46.4	0.043-0.128	10.4	4.08	4.57	5.52	0.70	148	3552	>100%
19 Jul	0.028	0.66	0.49	0.25	74.3	0.016-0.058	24.8	6.35	4.43	6.44	0.10	41	984	52
18 Aug	0.047	1.13	0.42	0.19	37.3	0.026-0.075	14.8	21.82	6.52	8.12	0.31	123	2952	50
27 Sep	0.027	0.64	—	—	—	0.027	25.7	17.31	8.50	—	—	80	1920	28
6 Nov	0.033	0.79	—	—	—	0.033	21.0	7.63	6.83	6.67	0.19	54	1296	16
1982														
6 Feb	0.023	0.56	—	—	—	0.023	30.1	2.79	3.59	3.60	0.41	55	1320	64
19 Mar	0.018	0.43	0.05	0.03	11.3	0.016-0.020	38.5	8.61	3.41	5.28	0.11	33	792	24
18 Apr	0.068	1.64	1.36	0.48	81.7	0.025-0.196	10.2	29.13	4.79	7.87	0.42	120	2880	>100
20 May	0.052	1.24	0.59	0.34	34.6	0.027-0.074	13.3	11.86	4.81	8.01	0.42	115	2760	29
28 Oct	0.049	1.17	0.40	0.18	34.2	0.040-0.079	14.1	3.70	3.87	3.50	0.45	74	1776	55
4 Nov	0.065	1.55	0.63	0.26	40.7	0.031-0.102	10.7	19.90	5.38	3.88	0.32	70	1680	99
1983														
16 Apr	0.032	0.76	0.03	0.01	3.3	0.014-0.064	21.7	—	4.53	5.27	0.26	57	1344	36
21 Apr	0.063	1.51	0.03	0.01	1.7	0.031-0.095	11.0	30.50	4.19	5.65	0.29	95	2280	58

μ - heteroflagellate growth rate (hour - h; day - d)
SD - standard deviation; SE - standard error; CV - coefficient of variation; Dt - doubling time (h - hours)
P - maximum density (x 10^3 cells ml^{-1}) of predator or heteroflagellate during growth in diffusion chambers
Amb B - ambient bacteria (x 10^6 cells ml^{-1})
B - bacteria density (x 10^6 cells ml^{-1}) during heteroflagellate growth
Clearance - volume of water cleared per flagellate per day
Ingestion - bacteria (B) consumed per hour (h) or per day (d) per flagellate
Percent grazed - percent standing crop or bacteria turnover (assuming 24 h generation time) consumed by heteroflagellates

Table 2. Seasonal growth and grazing rates of heteroflagellates (predators - P) at the MUDFLAT station. Growth, clearance and ingestion rates are mean values of monthly in situ diffusion chamber experiments. (See Table 1 for explanation of column headings.)

	HETERDFLAGELLATE GROWTH										CLEARANCE	INGESTION		
Date	μh^{-1}	μd^{-1}	SD	SE	CV(%)	Range μh^{-1}	Dt (h)	P	Amb B	B	$\mu l\ d^{-1}$	Bh^{-1}	Bd^{-1}	PERCENT GRAZED
1981														
18 Jun	0.054	1.30	0.55	0.31	41.8	0.030-0.075	12.8	5.66	6.73	5.40	0.43	97	2335	32%
19 Jul	0.045	1.07	0.73	0.30	68.1	0.021-0.104	15.5	16.65	7.56	20.00	--	55	1318	38
18 Aug	0.053	1.27	0.03	0.19	25.9	0.043-0.063	13.1	12.29	5.92	7.76	0.31	44	1056	48
27 Sep	0.027	0.65	--	--	--	0.027	25.7	39.99	5.20	5.92	--	--	--	
6 Nov	0.031	0.73	0.05	0.04	69.0	0.029-0.032	22.7	3.96	5.82	5.45	0.46	76	1829	62
1982														
6 Feb	0.038	0.91	0.32	0.16	35.2	0.029-0.058	18.3	2.70	3.49	2.50	1.13	117	2808	>100
19 Mar	0.026	0.61	0.19	0.10	30.3	0.020-0.037	27.1	7.82	3.52	5.23	--	32	768	29
18 Apr	0.030	0.71	0.13	0.05	18.8	0.019-0.036	23.4	10.19	6.17	5.99	0.43	123	2952	>100
20 May	0.020	0.53	0.07	0.05	13.6	0.020	31.4	1.48	2.50	4.57	0.58	112	2688	74
28 Oct	0.055	1.34	0.37	0.17	27.1	0.031-0.069	12.7	3.30	3.79	3.93	0.61	92	2218	94
4 Nov	0.049	1.18	0.33	0.13	28.0	0.032-0.070	14.1	8.49	6.50	4.53	0.48	74	1776	44
1983														
16 Apr	0.040	0.97	0.45	0.17	46.5	0.021-0.068	17.3	17.26	4.04	7.72	0.27	80	1920	>100
1984														
1 Jun	0.041	0.99	0.37	0.17	37.7		16.8	--	6.94	9.07	0.29	96	2304	>100

corresponded to ambient low tide assemblages and abudances.

Monthly averages of seasonal growth and grazing parameters along with corresponding ambient and chamber heteroflagellates and bacteria concentrations during maximum periods of growth for each station are presented in Tables 1 and 2. There were no significant differences between marsh and mudflat rates nor range in monthly means and annual averages for diffusion chambers at marsh and mudflat stations. CVs for monthly means ranged from 2 to 82% and 14 - 69% for marsh and mudflat respectively. Total ranges of rates including those of May 1981 through May 1982, Oct/Nov 1982, and April 1983 were large with a minimum rate of 0.014 and $0.016h^{-1}$ determined in both marsh and mudflat and a maximum rate of $0.12h^{-1}$ in the mudflat and $0.196h^{-1}$ in the marsh. These rates indicate potential generation times of 43 hours to a division possible in just 3.5 hours during periods of rapid growth.

Despite large ranges and variability in growth rates, the range of monthly means (Figs. 4 and 5) and annual averages for marsh ($1.15\ d^{-1}$) and mudflat ($0.98\ d^{-1}$), were very similar (Tables 1 and 2). Averages indicate generation times of approximately 14 to 17 hours, respectively. Generally most initial growth rate determinations corresponded to generation times of greater than 12 hours, usually ranging between 20 to 28 hours, i.e., about one doubling per day. Chambers, which demonstrated rapid change in numbers or size or types of heteroflagellate in nanoplankton assemblages resulting in high densities of heteroflagellates, usually yielded growth rates of greater than two doublings per day. The upper range or "accelerated rates" are defined here to include rates of greater than two doublings per day or $\mu = <0.057$

h^{-1} or <1.37 d^{-1}. The accelerated rates usually occurred when more diverse assemblages and larger sized heteroflagellates and prey predominated. Marsh station growth rates demonstrated a slightly greater percentage (32%) of accelerated rates than the mudflat station (28%). Overall, growth rate determinations in the marsh-mudflat system indicate that approximately 72% of ambient heteroflagellate rates fall between 0.016 and 0.056 h^{-1}.

Heteroflagellate growth occurred at all ambient bacteria densities encountered at initiation of in situ experiments. These concentrations ranged from 3.5×10^6 cells ml^{-1} measured in February to 8.0×10^6 cells ml^{-1} typical of summer months. As a result, it was not possible to determine the threshold level of bacterial concentrations necessary for heteroflagellate growth. The lag in heteroflagellate growth did not correspond to lower bacterial concentrations nor was there any correlation between initiation of growth rates (μ) and initial bacterial density [B] or average bacterial density (B) of a growing population. Maximum growth occurred when bacteria concentrations ranged between 3.6 - 8.12×10^6 cells ml^{-1} and 2.5 - 12.5×10^6 cells ml^{-1} for marsh and mudflat respectively, but concentrations most commonly ranged between 4.5 through 8.0×10^6 cells ml^{-1}. Neither magnitude of growth rates nor density of predators achieved (sustained) were density-dependent on initial bacteria concentration as predicted (Fenchel 1982b).

Concentrations of heteroflagellates growing in diffusion chambers were frequently three to twenty times greater than corresponding ambient populations (Figs. 8-17). Maximum heteroflagellate concentrations were observed in diffusion chambers at both marsh and mudflat stations during

April, May (1981 and 1982), summer months, and November 1982 (Figs. 9-17). Peak concentrations, of greater than 20.0 x 10^3 cells/ml, observed in marsh and mudflat chambers were most often dominated by blooms of choanoflagellates and Paraphysomonas sp. One exception occurred during the fall, November 1982, chambers dominated by cyanobacteria and large bodonid and apochlorotic cryptomonad "pointed body" blooms. Presence of high heteroflagellate concentrations in chambers corresponded to periods of high rates, except during a September 1981 choanoflagellate bloom observed in two chambers which immediately followed a prasinophyte bloom. This bloom occurred at the end of the incubation when the sampling interval may not have been frequent enough to register a number of synchronous divisions. Also maximum average monthly growth rates did not always correspond to peak heteroflagellate density; high growth rates, as in June 1981 (Fig. 10) did not consistently result in high (i.e., greater than the ambient maximum density) heteroflagellate densities.

Annual Patterns

Average monthly growth rates and standard errors are plotted along with temperature/salinity (Figs. 5 and 6) to illustrate seasonal growth patterns and the lack of significant correlation ($p > 0.05$) of growth rates with temperature (Fig. 7). Annual patterns of mean growth rates (Fig. 4) are similar at both stations. The mean and range of May 1981 rates of 1.11 d^{-1} (Range 0.028 $\pm$ 0.057 h^{-1}) are very similar not only to May, 1982 (1.24 d^{-1}; 0.027 $\pm$ 0.074h^{-1}) but to those of August 1981 (1.13d^{-1}; 0.027 $\pm$ 0.074h^{-1}). Mean rates after August fluctuated between μ= 0.40 and 0.80 d^{-1}, indicating average generation times of

Figure 5. Variability in monthly mean heteroflagellate growth rates (with standard error) from May 1981 to May 1982 and including October - November 1982 and April 1983 at the marsh (top) and mudflat (bottom) stations.

MARSH HETEROFLAGELLATE GROWTH RATES

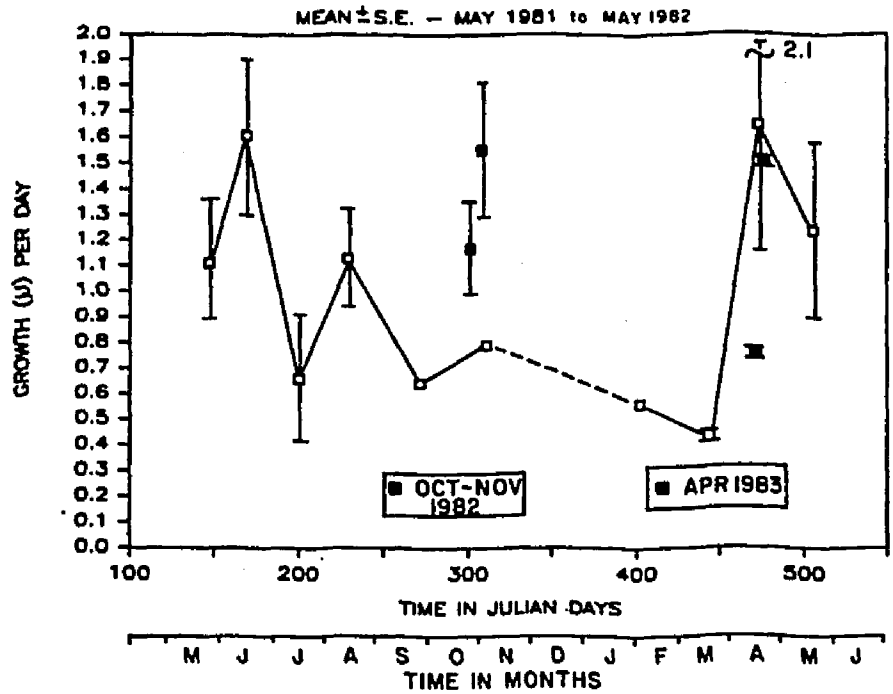

MUDFLAT HETEROFLAGELLATE GROWTH RATES

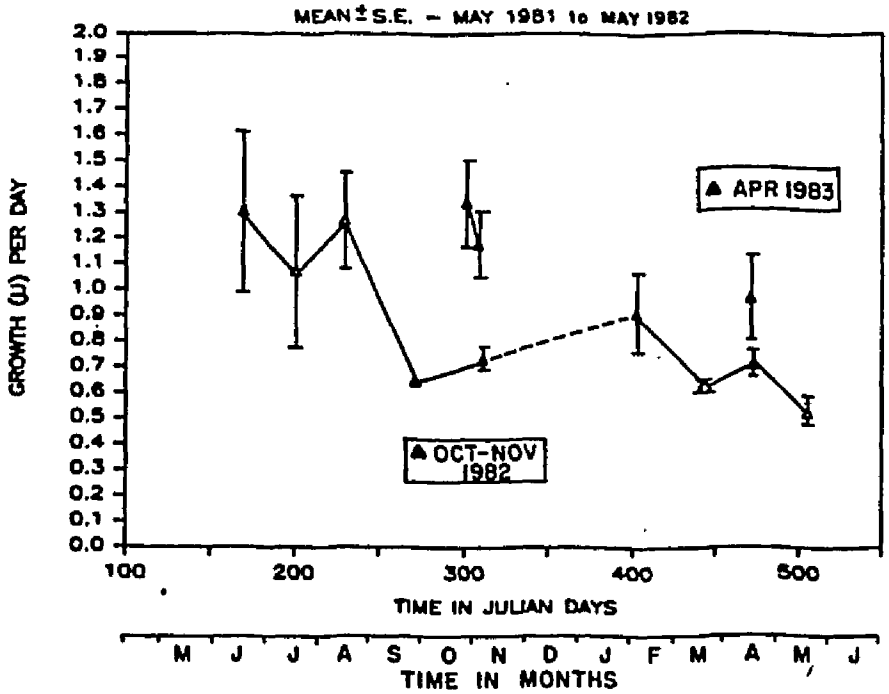

Figure 6. Seasonal variation in temperature and salinity at the marsh (top) and mudflat (bottom) stations for comparison with seasonal growth rate curve (see Figure 5).

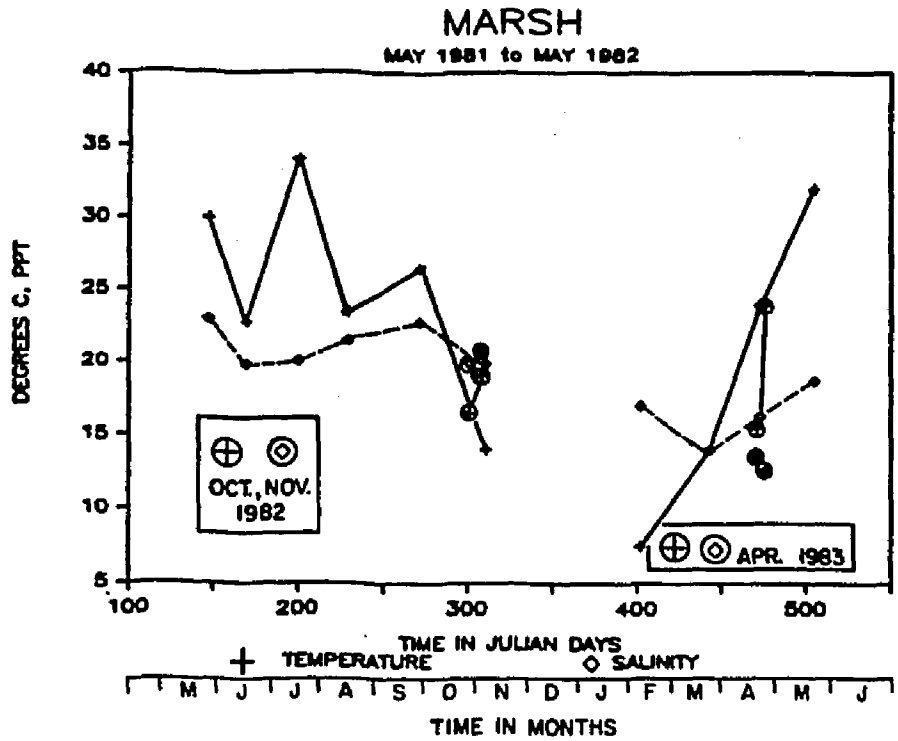
MARSH
MAY 1981 to MAY 1982
DEGREES C, PPT
40
35
30
25
20
15
10
5
100
200
300
400
500
OCT., NOV. 1982
APR. 1983
TIME IN JULIAN DAYS
+ TEMPERATURE
◇ SALINITY
M J J A S O N D J F M A M J
TIME IN MONTHS

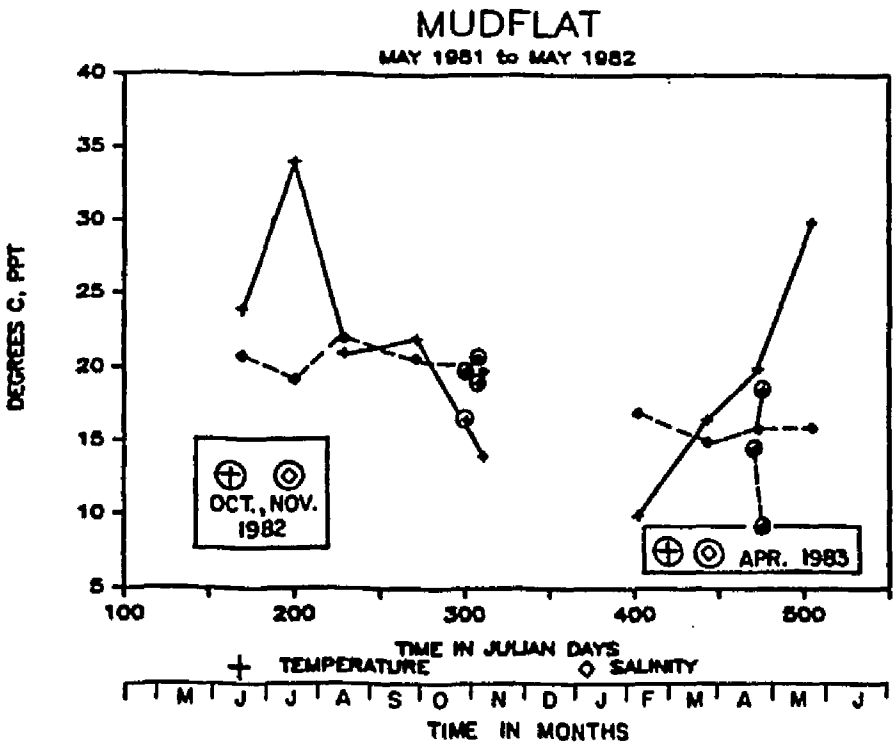
MUDFLAT
MAY 1981 to MAY 1982
DEGREES C, PPT
40
35
30
25
20
15
10
5
100
200
300
400
500
OCT., NOV. 1982
APR. 1983
TIME IN JULIAN DAYS
+ TEMPERATURE
◇ SALINITY
M J J A S O N D J F M A M J
TIME IN MONTHS

Figure 7. Heteroflagellate growth rates versus temperature at marsh and mudflat stations.

MARSH HETEROFLAGELLATES

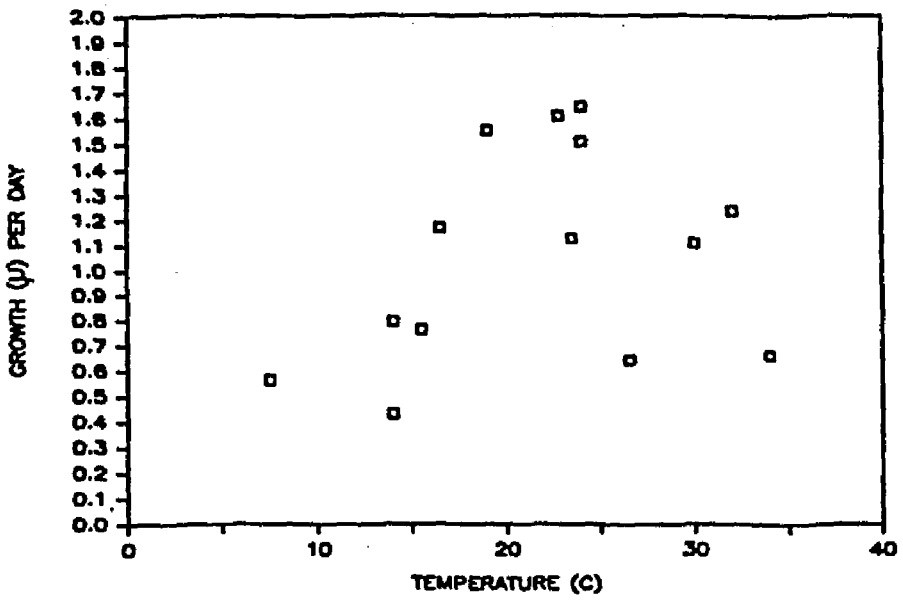

MUDFLAT HETEROFLAGELLATES

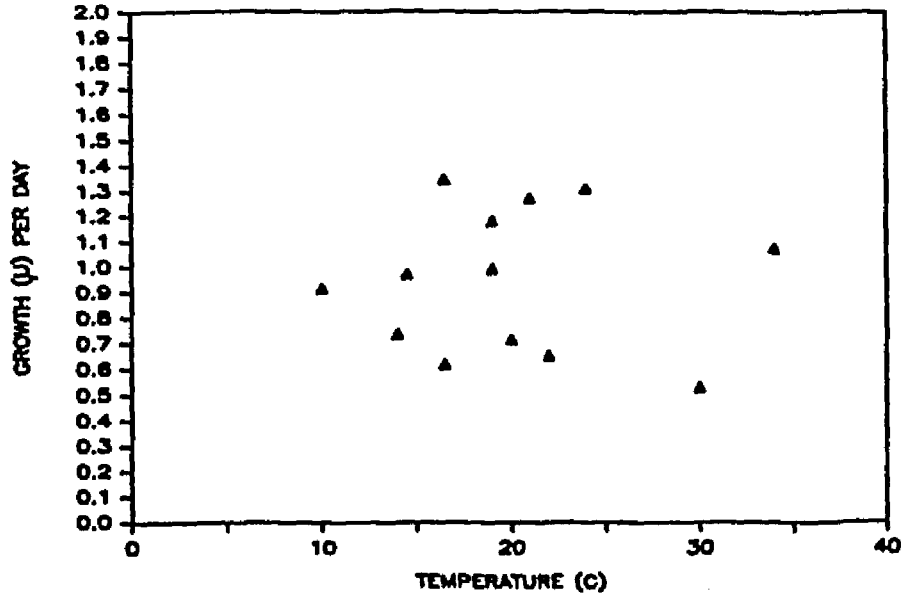

approximately 24 hours for the colder months. Although rates for February and March were similar, a single accelerated rate measured in February at the mudflat indicated potential for high rates even at colder temperatures (e.g., <10°C). The pattern of increased rates in April 1982 with increasing temperatures was followed by a decrease in May growth rates (concurrent with a further increase in temperature) at both stations. Temperatures increased during the May 1982 experiment but growth rates did not increase correspondingly. Growth rates of May 1982, although similar to those of the previous May decreased in comparison with the April 1982 peaks rates.

The April 1982 and 1983 experiments were carried out during the same period of lunar month in consecutive years and rates were similar at both marsh and mudflat stations. During April 1983 two series of experiments were carried out from 13-22 April and 18-23 April. Environmental conditions during the first series of experiments were similar to April 1982 although salinities were depressed by late winter-spring rainfall. The first series of April 1983 growth rates were lower than the marsh and somewhat higher than the mudflat rates determined in the previous year (1982). The second chamber experiment was begun when temperatures decreased below normal and produced increased rates which were comparable to those measured in April 1982 when the temperature range was approximately 10°C greater. Temperatures were in fact lower than those recorded in March but in contrast, growth rates were some of the highest measured in this study. These series of spring experiments, conducted when temperatures frequently fluctuate around the temperatures (10-15°C) normally considered biologically limiting, further demonstrates the lack

of positive correlation ($p > 0.05$) of annual heteroflagellate growth pattern with temperature (Fig. 7).

Monthly average growth rates and the corresponding averages for two representative ranges (defined earlier) of rates observed during in situ experiments are shown in Figure 8. These plots show the large variability in seasonal growth pattern and indicate the potential for rapid growth throughout the year. The accelerated (higher than average) rates occur during each season except during winter months when bacteria concentrations fall to the lower seasonal range of $3.0 - 4.5 \times 10^6$ cells ml^{-1} and bacterial generation times are generally 24 hours. Although heteroflagellate growth rates are correspondingly lower during the winter range of lower temperatures, overall there was no significant correlation of the rates with bacterial growth rates. Marsh plots (Figure 8) indicate that the two growth ranges follow a similar annual pattern while mudflat growth ranges for heteroflagellates demonstrate more variability particularly in June and July. The most obvious deviation from the monthly mean curve of mudflat rates occurs in July when the peak can be attributed to a choanoflagellate bloom in one chamber. The potential for accelerated rates in the first 24 hours of incubation is demonstrated in April 1982 marsh station figure (Fig. 15). Episodic blooms in individual chambers occurred frequently in summer months and contributed to two different rate curves.

Data also demonstrate great differences and variations in the seasonal pattern from year to year. The 1981 pattern would indicate a decrease in activity with the onset of fall with lower temperatures and decreased bacteria abundances. However values for the autumn 1982

Figure 8. Monthly mean heteroflagellate growth rates in comparison with two ranges of growth rates (1: slow - $\mu<0.057\ h^{-1}$; 2: fast - $\mu>0.057\ h^{-1}$) for marsh (top) and mudflat (bottom) over a seasonal cycle (May 1981 to May 1982, with data from October - November 1982 and April 1983 included).

MARSH HETEROFLAGELLATE GROWTH RATES

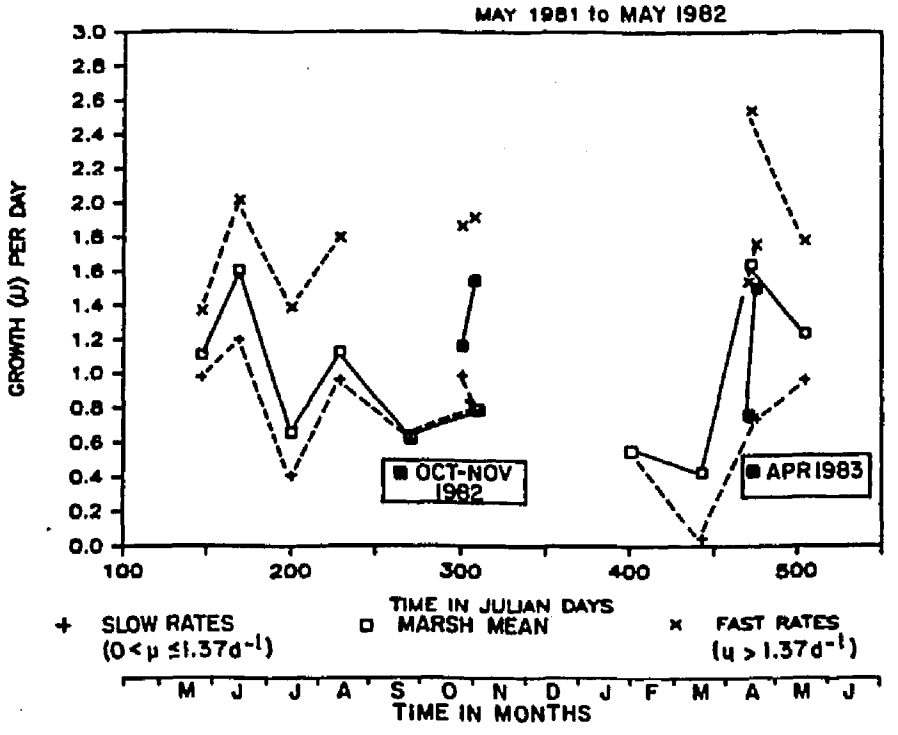

MUDFLAT HETEROFLAGELLATE GROWTH RATES

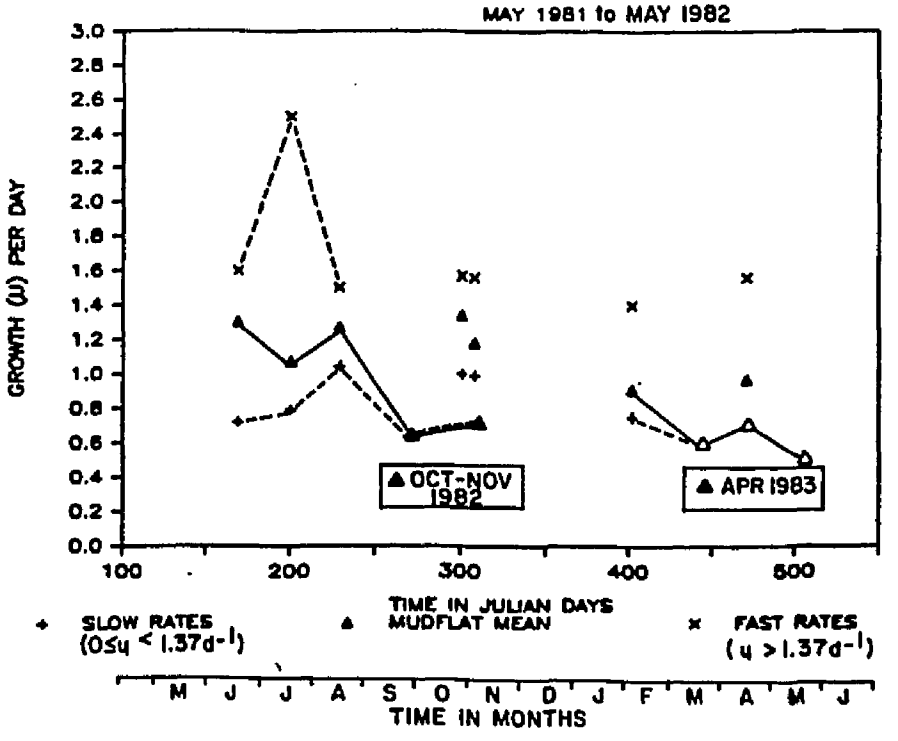

transitional period experiment, demonstrate very different results or response. Temperatures and bacterial populations had already declined to levels considerably lower than September, yet chambers yielded much greater rates than in 1981 including several accelerated rates. Temperature, which increased during the 1982 experiment remained considerably lower than summer ranges. Rates during this fall period were comparable to or greater than summer rates of the previous year. Growth rates of various heteroflagellate communities may be quite variable from year to year. Differences among monthly mean rates can not be attributed to a seasonal pattern but to individual variability or patchiness. Differences in pattern of mean rates from monthly experiments can not be related to a seasonal variation in temperature.

Different predator-prey interactions were observed through comparisons of graphs of ambient populations with the graphs showing the cycles of increase and decrease of bacteria and heteroflagellates in experimental chambers (Figs. 9-17). The fluctuation in heteroflagellate and bacteria abundances over the 5 to 8 day diffusion chamber experiments illustrate dynamics and variability in predator-prey interaction. Growth curves from each monthly experiment at both stations demonstrate the different patterns possible during the identical time period and environmental conditions. Differences in predator-prey interactions were not related to the station location.

Figures 9-17 not only reveal the sequence of increase and the concentration of bacteria during heteroflagellate growth but indicate the heteroflagellate concentration at which bacteria abundances decline. Bacteria densities generally continued to increase during the lag period

Figure 9. Temperature, salinity, and heteroflagellate versus bacteria densities for in situ diffusion chamber and for ambient populations during 27 May to 3 June 1981 at the marsh station.

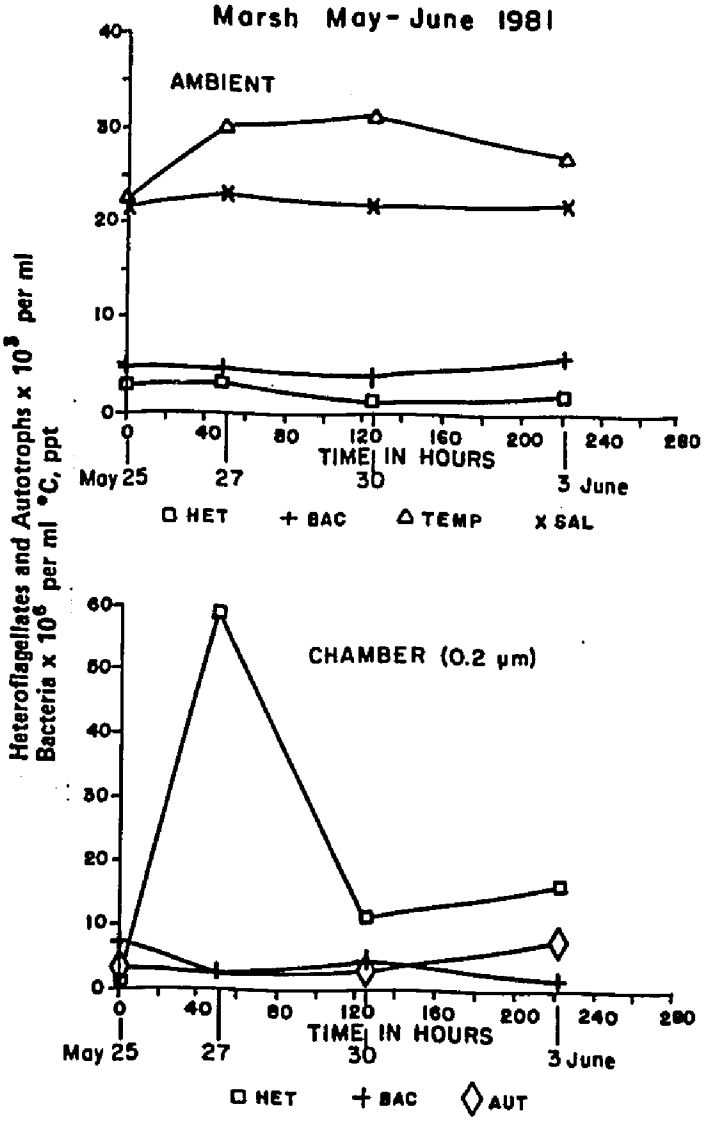
Marsh May-June 1981
AMBIENT
Heteroflagellates and Autotrophs x 10³ per ml
Bacteria x 10⁶ per ml °C, ppt
TIME IN HOURS
May 25
27
30
3 June
HET
BAC
TEMP
SAL
CHAMBER (0.2 µm)
AUT

Figure 10. Temperature, salinity, and heteroflagellate versus bacteria densities for in situ diffusion chamber and for ambient populations during 16-27 June 1981 at the marsh and mudflat stations.

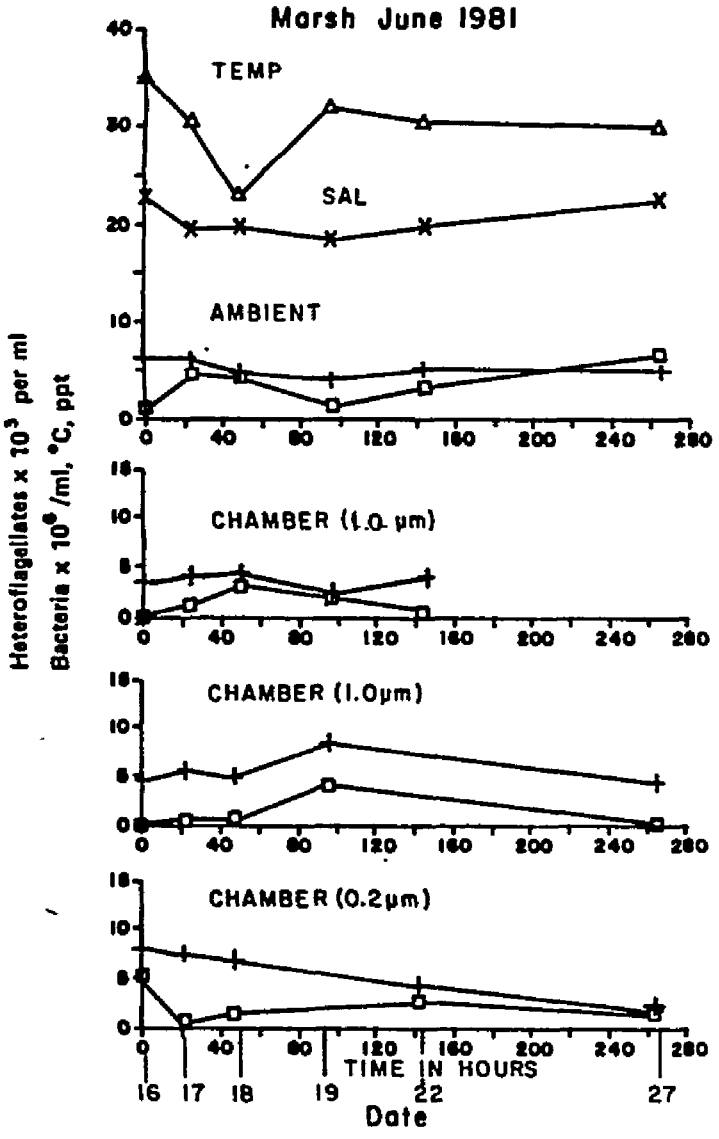

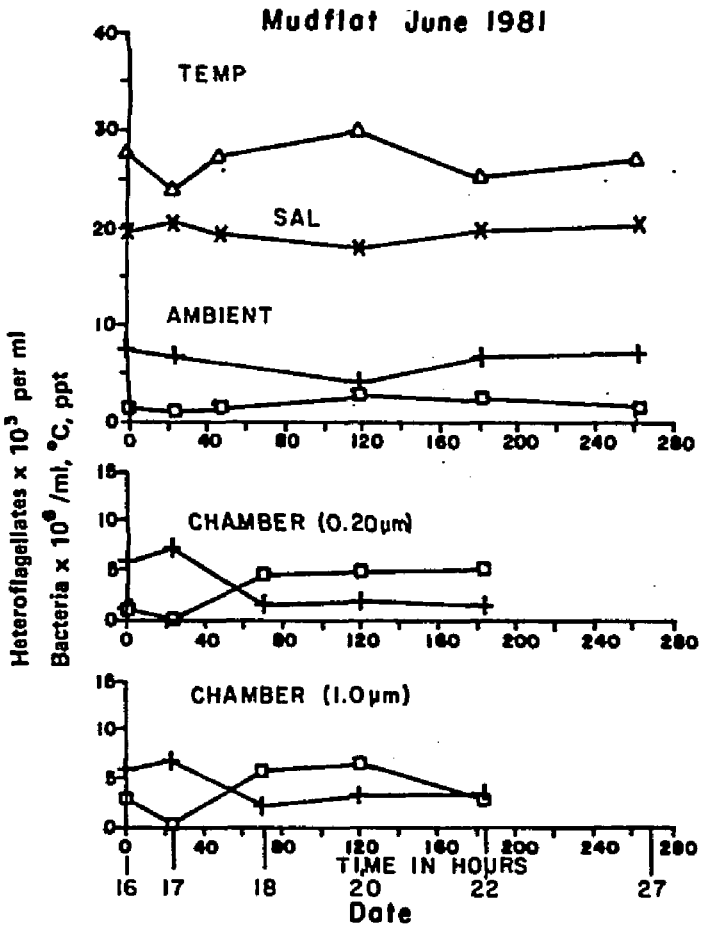

□ HETEROFLAGELLATES
\+ BACTERIA
△ TEMPERATURE
X SALINITY

Figure 11. Temperature, salinity, and heteroflagellate versus bacteria densities for in situ diffusion chamber and for ambient populations during 17-26 July 1981 at the marsh and mudflat stations.

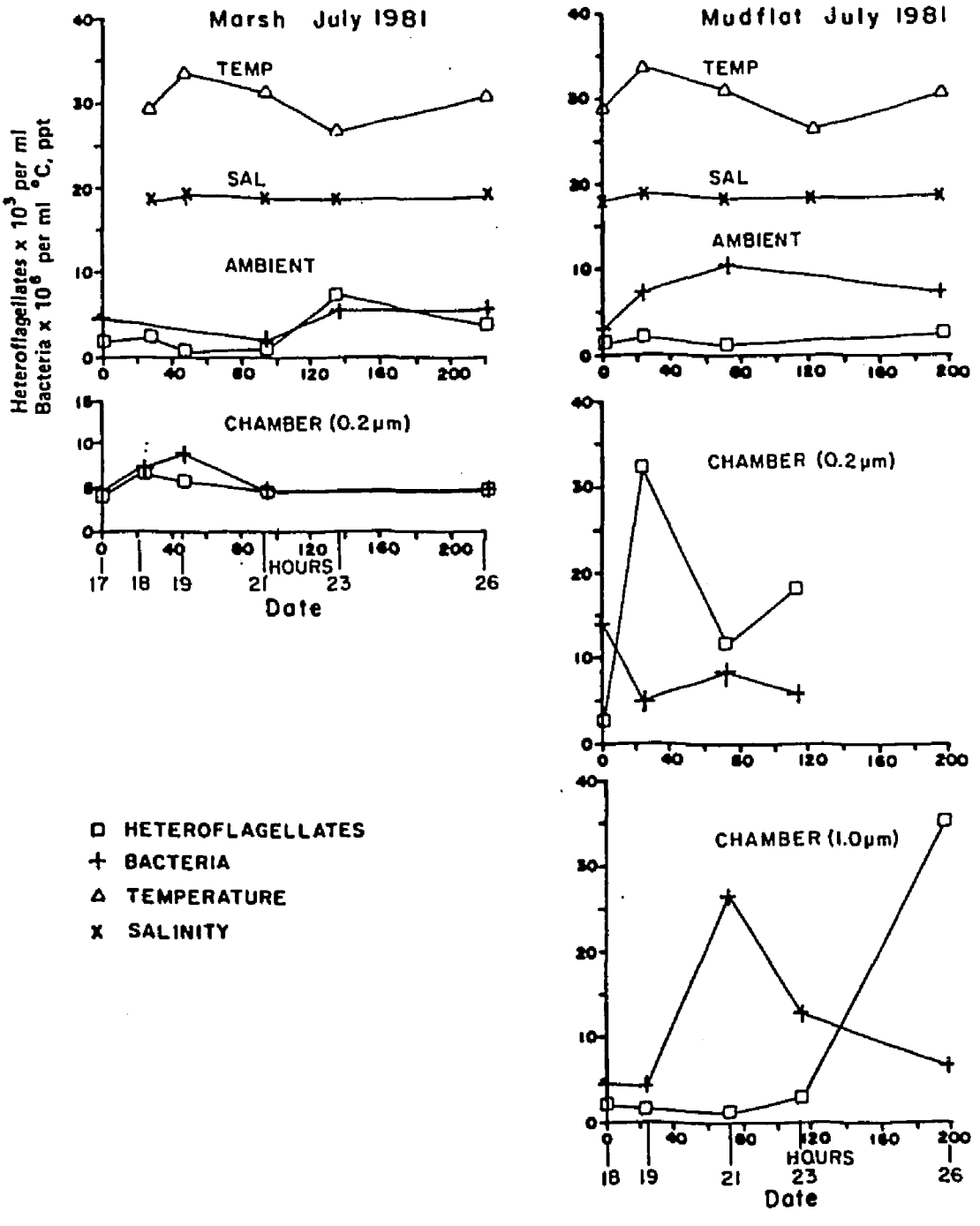
Marsh July 1981
Mudflat July 1981
TEMP
SAL
AMBIENT
CHAMBER (0.2µm)
CHAMBER (1.0µm)
Heteroflagellates x 10³ per ml
Bacteria x 10⁶ per ml
°C, ppt
HOURS
Date
17
18
19
21
23
26
HETEROFLAGELLATES
BACTERIA
TEMPERATURE
SALINITY

Figure 12. Temperature, salinity, and heteroflagellate versus bacteria densities for in situ diffusion chamber and for ambient populations during 17-23 August 1981 at the marsh and mudflat stations.

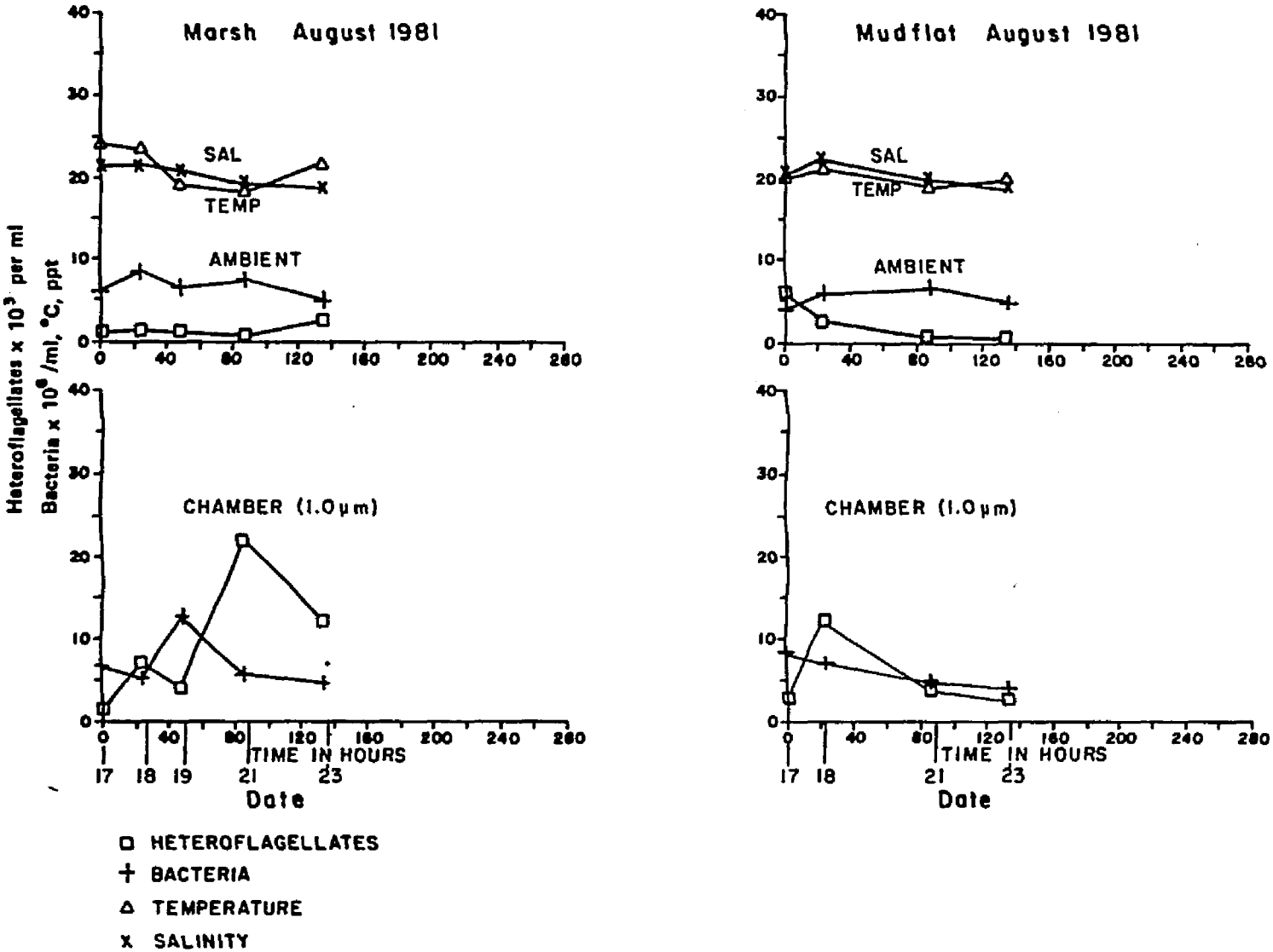
Marsh August 1981
Mudflat August 1981
SAL
TEMP
AMBIENT
CHAMBER (1.0µm)
Heteroflagellates x 10³ per ml
Bacteria x 10⁶ /ml, °C, ppt
TIME IN HOURS
Date
17 18 19 21 23
HETEROFLAGELLATES
BACTERIA
TEMPERATURE
SALINITY

Figure 13. Temperature, salinity, and heteroflagellate versus bacteria densities for in situ diffusion chamber and for ambient populations during 23-30 September 1981 at the marsh and mudflat stations and during 4-11 November 1981 at the marsh station.

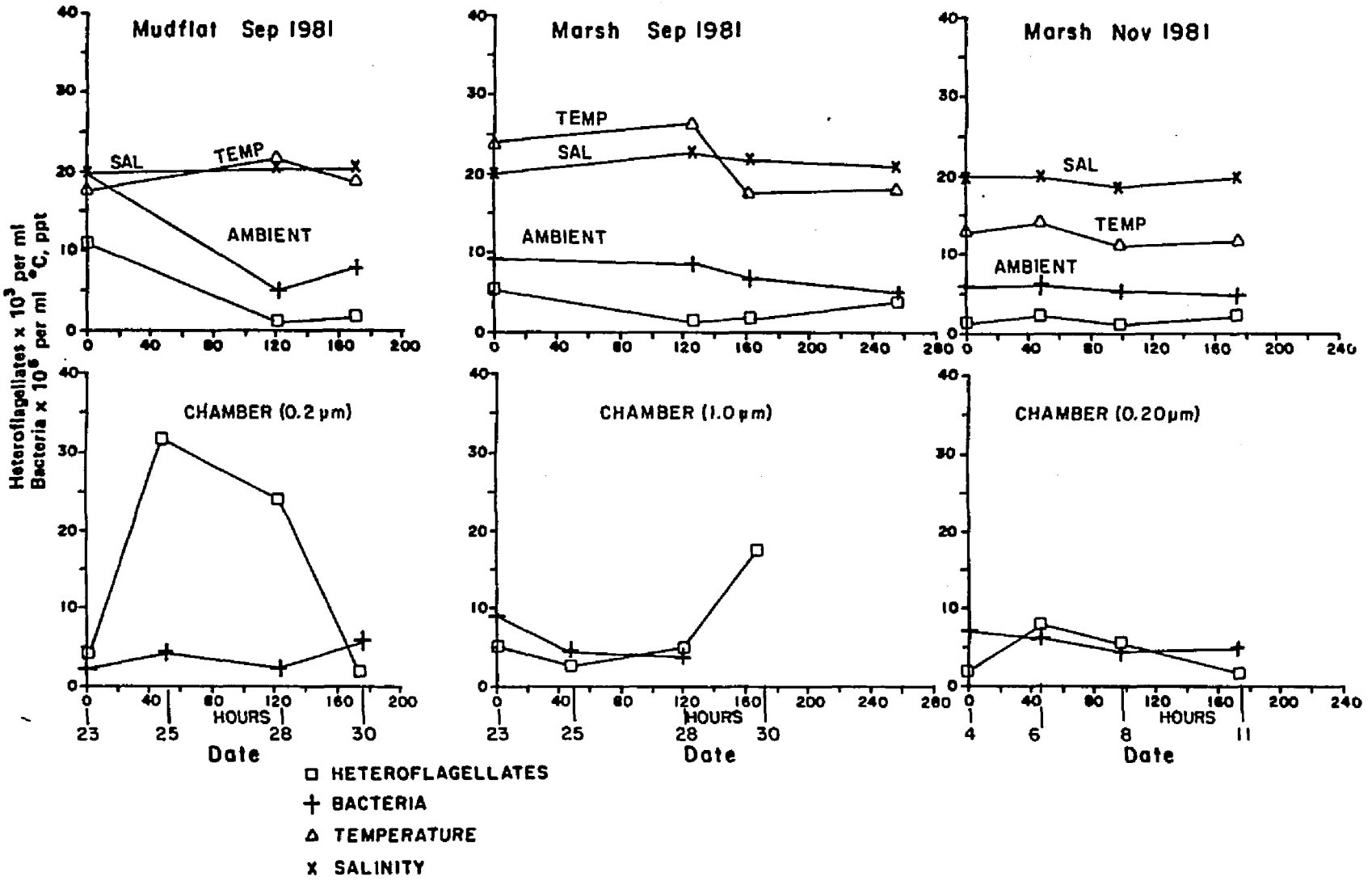
Mudflat Sep 1981
Marsh Sep 1981
Marsh Nov 1981
SAL
TEMP
AMBIENT
CHAMBER (0.2 µm)
CHAMBER (1.0 µm)
CHAMBER (0.20µm)
Heteroflagellates x 10³ per ml
Bacteria x 10⁶ per ml
°C, ppt
HOURS
Date
HETEROFLAGELLATES
BACTERIA
TEMPERATURE
SALINITY

Figure 14. Temperature, salinity, and heteroflagellate versus bacteria densities for in situ diffusion chamber and for ambient populations during 2-8 February 1982 at the marsh station and 17-28 March 1982 at the marsh and mudflat stations.

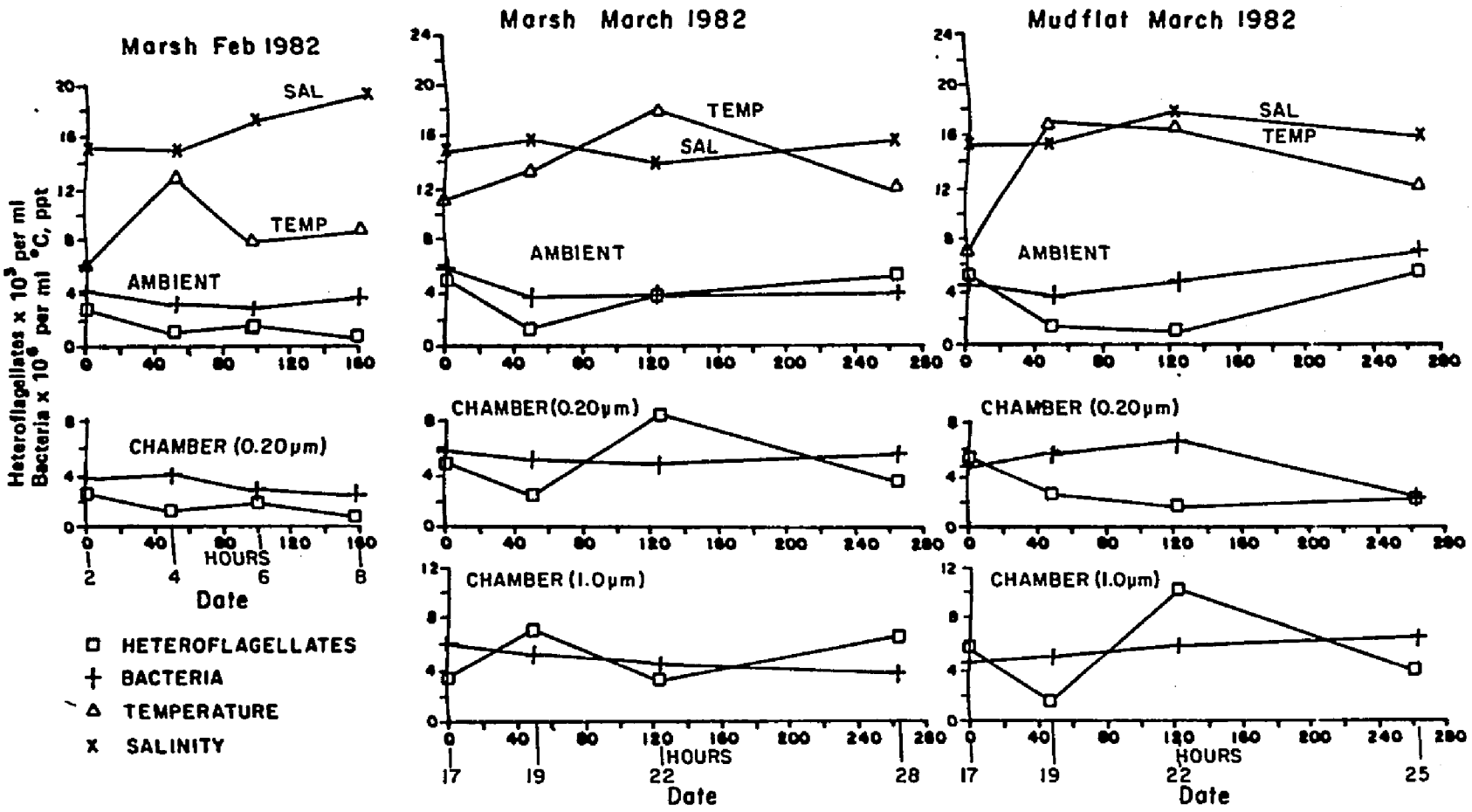
Marsh Feb 1982
Marsh March 1982
Mudflat March 1982
SAL
TEMP
AMBIENT
CHAMBER (0.20µm)
CHAMBER (1.0µm)
Heteroflagellates x 10³ per ml
Bacteria x 10⁶ per ml
°C, ppt
HOURS
Date
HETEROFLAGELLATES
BACTERIA
TEMPERATURE
SALINITY

Figure 15. Temperature, salinity, and heteroflagellate versus bacteria densities for in situ diffusion chamber and for ambient populations during 17-28 April 1982 at the marsh station.

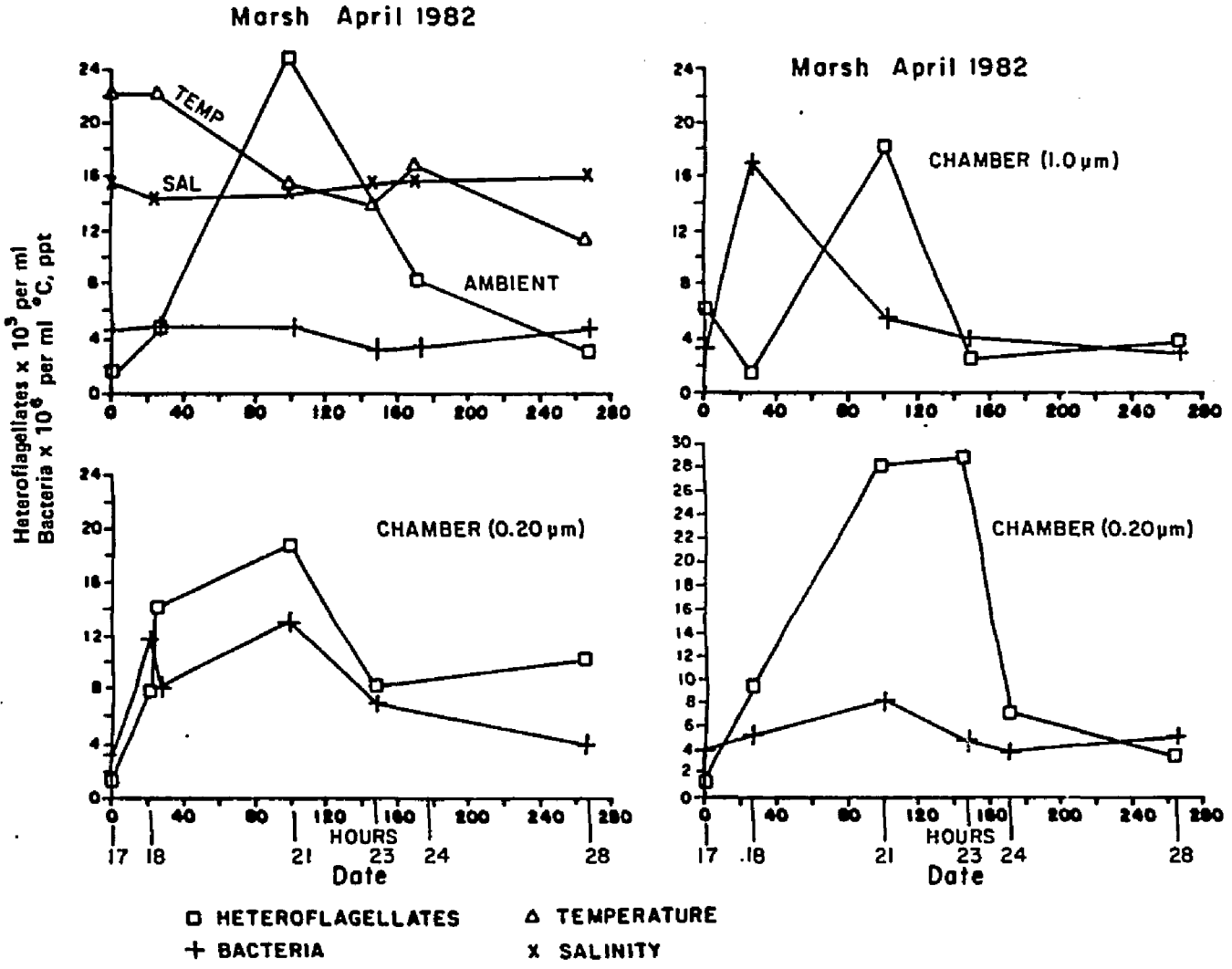
Marsh April 1982
TEMP
SAL
AMBIENT
CHAMBER (0.20 µm)
Heterotlagellates x 10³ per ml
Bacteria x 10⁶ per ml °C, ppt
HOURS
17 18 21 23 24 28
Date
Marsh April 1982
CHAMBER (1.0 µm)
CHAMBER (0.20µm)
HOURS
17 .18 21 23 24 28
Date
HETEROFLAGELLATES
BACTERIA
TEMPERATURE
SALINITY

Figure 16. Temperature, salinity, and heteroflagellate versus bacteria densities for in situ diffusion chamber and for ambient populations during 17-28 April 1982 at the mudflat station.

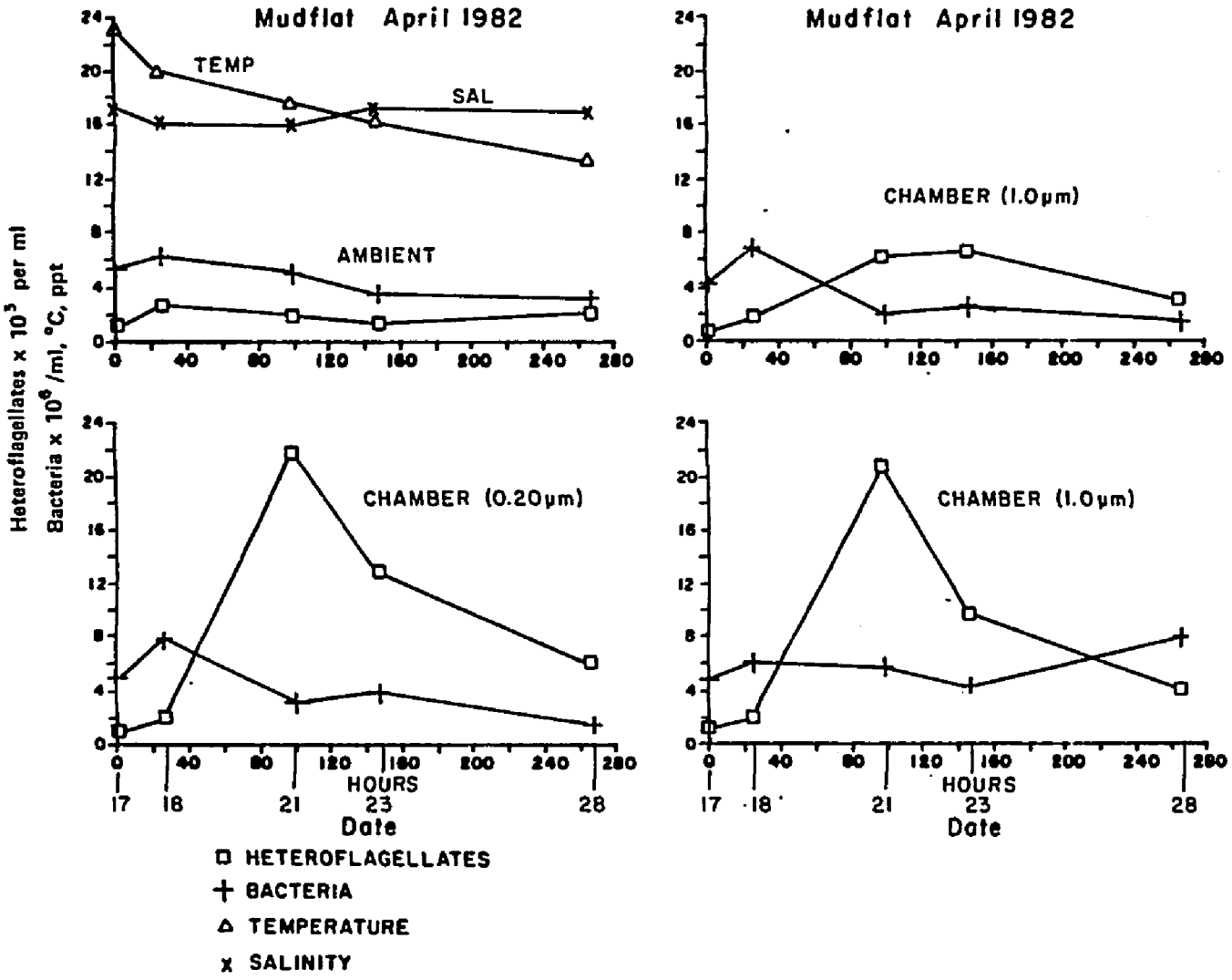
Mudflat April 1982
TEMP
SAL
AMBIENT
Heteroflagellates x 10³ per ml
Bacteria x 10⁶ /ml, °C, ppt
Mudflat April 1982
CHAMBER (1.0µm)
CHAMBER (0.20µm)
CHAMBER (1.0µm)
HOURS
Date
17
18
21
23
28
HETEROFLAGELLATES
BACTERIA
TEMPERATURE
SALINITY

Figure 17. Temperature, salinity, and heteroflagellate versus bacteria densities for in situ diffusion chamber and for ambient populations during 19-25 May 1982 at the marsh and mudflat stations.

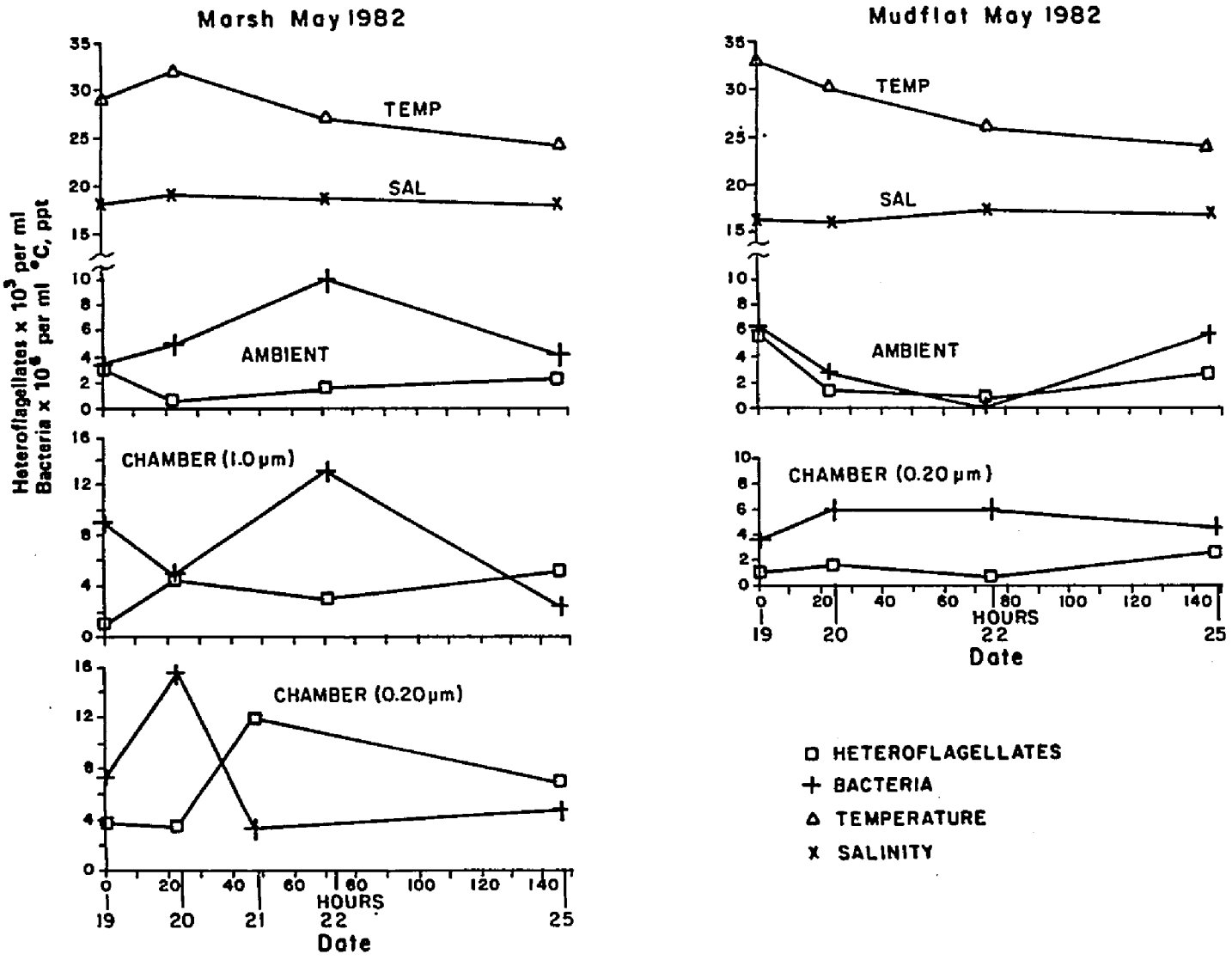
Marsh May 1982
Mudflat May 1982
TEMP
SAL
AMBIENT
CHAMBER (1.0 µm)
CHAMBER (0.20 µm)
Heteroflagellates x 10³ per ml
Bacteria x 10⁶ per ml
°C, ppt
HOURS
Date
19
20
21
22
25
HETEROFLAGELLATES
BACTERIA
TEMPERATURE
SALINITY

of heteroflagellate growth, or during the initial 24 -48 hour period when heteroflagellate abundances remained close to the range found in the water column during the tidal cycle, i.e., 0.5 - 3.0 x 10^3 cells ml^{-1}. Chamber bacteria concentrations generally followed ambient patterns, particularly evident in the larger pore size (1.0 μm) chamber where greater exchange was possible. Chamber bacteria concentrations differed markedly from the ambient range of fluctuations only when heteroflagellate concentrations were considerably above ambient bloom levels of 4.0 x 10^3 cells ml^{-1}. Bacteria concentrations, decreased by grazing activity of HNANO blooms, also quickly recovered within 24 hours and heteroflagellate numbers returned to ambient levels. A decrease in bacteria after an increase in heteroflagellate concentrations above ambient levels, ie. > 6 x 10^3 cells ml^{-1}, may indicate either a grazing effect or simply a decrease reflecting the environmental variability.

Comparisons of fluctuations of bacteria in chamber and ambient made it possible to evaluate the influence of environmental variability. The in situ diffusion chamber growth patterns indicate predator-prey dynamics are more closely coupled in terms of time scales than the previous predictive models (Fenchel 1982d, Laake et al. 1983). These growth curves (Figs. 9-17) show smaller amplitutes in fluctuations of bacteria than the extreme fluctuations of the previously reported sinusoidal (bloom and crash) growth curves or cycles (Fenchel 1982d, Linley et al. 1983, Newell et al. 1983, Laake et al. 1984, Sieburth 1984). The patterns of increase and decline of in situ chamber predator-prey concentrations were variable. The series of bacteria and subsequent heteroflagellate peaks, if offset, were generally out of phase by a day

rather than by the predicted 2 or 3 days. A series of correlation analyses for various heteroflagellate growth rates versus densities of bacterial prey (B and $\bar{B}$), and heteroflagellate predators (P and $\bar{P}$) versus bacterial densities (B and $\bar{B}$) during heteroflagellate growth were conducted (Table 3). The only positive correlation existed between mean heteroflagellate concentrations ($\bar{P}$), determined at the 50% point in growth curve (halfway during growth) and mean bacteria ($\bar{B}$) concentration determined in the same manner. Positive correlation here indicates possible coupling of heteroflagellates and bacteria during maximum periods of growth. Heteroflagellate growth frequently coincided with increasing bacterial densities and the correlation of P-predators (determined before densities greatly exceeded ambient) and B-bacteria supports this coupling of active growth.

Grazing

Grazing rates were variable during individual chamber incubations and demonstrated high degree of variability among station replicates, with a total annual range of chamber monthly means of 32-148 bacteria P^{-1} h^{-1} (770-3550 bacteria P^{-1} d^{-1}). The range of clearance and grazing rates for any experiment varied at nearly the same magnitude of the range of monthly means observed throughout the year (0.12 to 0.5 ul d^{-1}). The most common range of clearance rates was 0.012 to 0.018 ul h^{-1} and grazing rates generally fell between 50 and 150 bacteria P^{-1} h^{-1}, respectively at both stations throughout the year. Clearance rates measured at the marsh station are somewhat higher than mudflat monthly means rates. However when the full range of rates is

Table 3. Correlation analysis of heteroflagellate growth versus bacteria density and predator (heteroflagellate) concentration versus bacteria density.

Y1	Y2	N	r	p
μ	B_I	69	0.12	$p > .05$
μ	$\bar{B}$	62	0.20	$p > .05$
B_I	P	66	0.21	$p > .05$
$\bar{B}$	$\bar{P}$	52	0.62	$p < .01$ *
$\bar{B}$	P	60	0.17	$p > .05$

N = number of Y1 and Y2 data pairs

r = Pearson product-moment correlation coefficient

μ = heteroflagellate growth rate

B_I = initial bacteria concentration

$\bar{B}$ = mean density of bacteria during measured heteroflagellate growth

P = predator or heteroflagellate concentration after measured heteroflagellate growth

$\bar{P}$ = mean density of predators or heteroflagellates during measured growth

considered, differences between stations are insignificant.

There was no significant correlation with temperature although the seasonal fluctuation in rates was similar for both stations (Fig. 18). High rates, greater than 100 bacteria P^{-1} h^{-1}, were measured at each station throughout the year except winter when rates were generally lower. There also was no significant correlation ($p > 0.05$) between heterotrophic growth and clearance rates nor any correlation between bacteria concentration and clearance or grazing rates (Figs. 18 and 19). Summer grazing rates were quite variable, however chambers containing larger forms of bacteria generally yielded higher rates. Observation of chamber populations using epifluorescence did reveal that larger forms of bacteria were preferentially grazed.

Heteroflagellate concentrations measured after growth in chambers were always higher than ambient, while bacteria more frequently remained within the ambient range. Calculations of total bacteria consumed by chamber HNANO population accounted for a large percentage of bacterial population or for one to two doublings of bacteria. Monthly grazing rates were used to calculate the range of ambient bacteria population potentially consumed by ambient concentration of flagellate present at stations during monitored growth periods (Tables 1 and 2). These calculations indicated that ambient concentrations of heteroflagellates could consume, in a 24 hour period, 29% to >100% of the bacteria present in tidal pools. Thus, because average bacterial generation times were less than 24 hours, or $k > 1$ d^{-1}, HNANO bacteriovores could account for at least 50% of marsh-mudflat bacterial production or turnover.

Figure 18. Clearance rates ($\mu l\ d^{-1}$ bacteria^{-1}) versus temperature at both marsh and mudflat stations.

MARSH

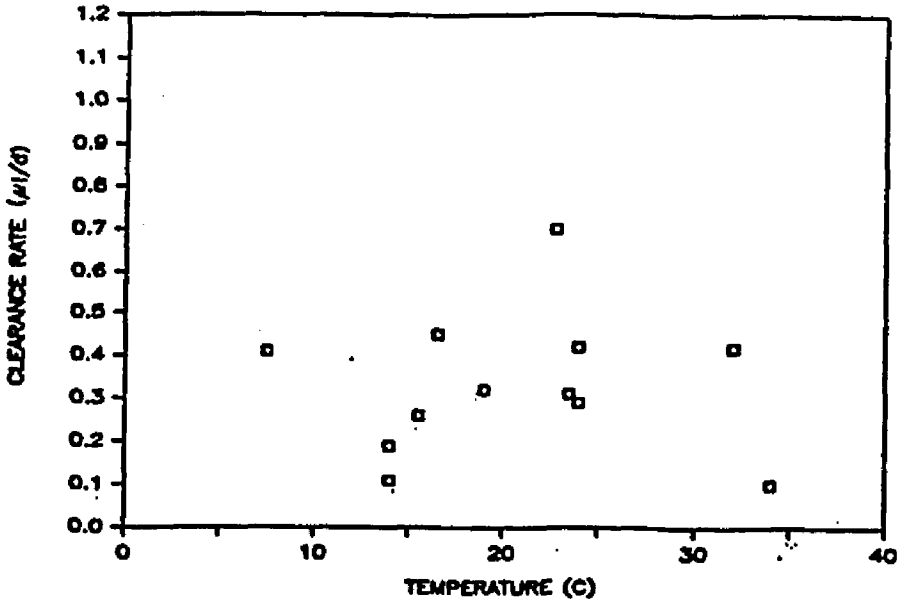

MUDFLAT

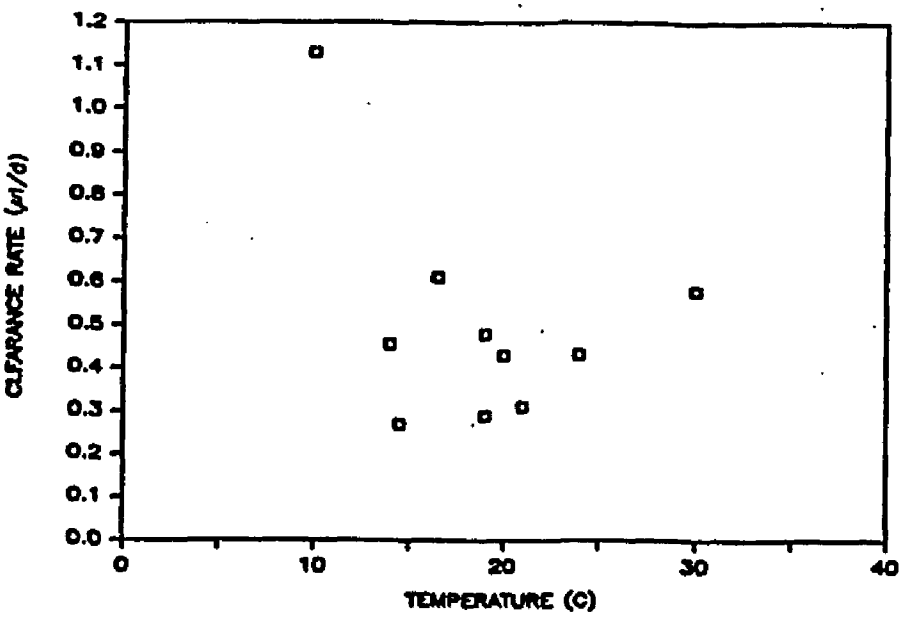

Figure 19. Heteroflagellate grazing (ingestion) rates versus bacteria concentration over a seasonal cycle for marsh and mudflat stations.

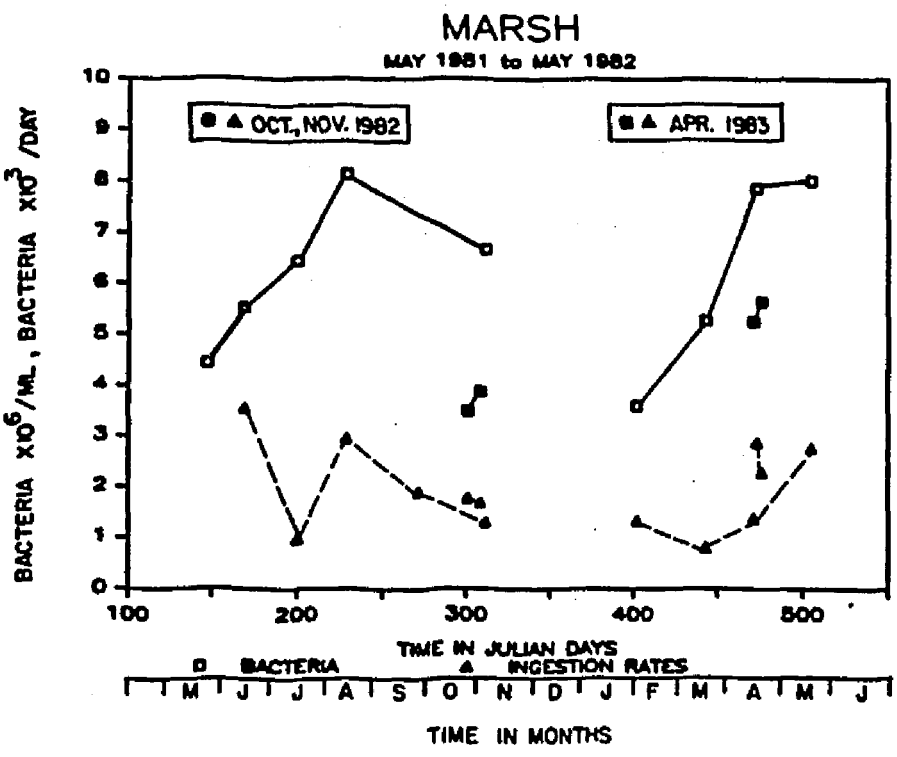
MARSH
MAY 1981 to MAY 1982
OCT., NOV. 1982
APR. 1983
BACTERIA X10⁶/ML, BACTERIA X10³/DAY
TIME IN JULIAN DAYS
BACTERIA
INGESTION RATES
M J J A S O N D J F M A M J
TIME IN MONTHS

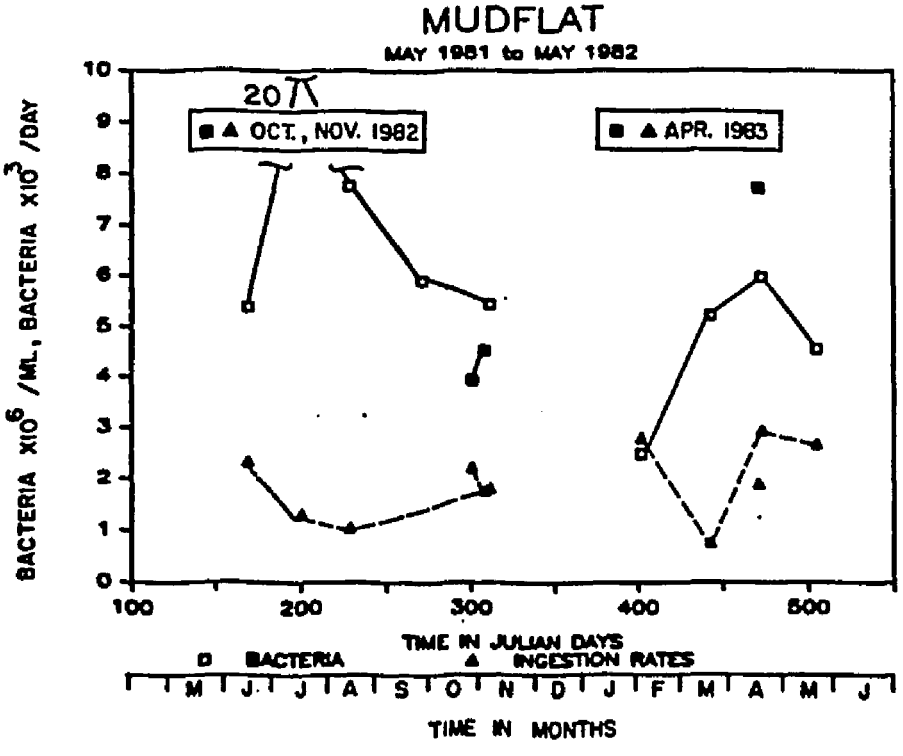
MUDFLAT
MAY 1981 to MAY 1982
20
OCT., NOV. 1982
APR. 1983
BACTERIA X10⁶/ML, BACTERIA X10³/DAY
TIME IN JULIAN DAYS
BACTERIA
INGESTION RATES
M J J A S O N D J F M A M J
TIME IN MONTHS

DISCUSSION

Diffusion chambers incubated at tidal pool sites simulated the quiescent environment of tidal pools formed on mudflats or in tidal creeks during extended low tides. Field design and epifluorescence methodology made possible examinations of in situ growth and grazing rate for natural nanoplankton assemblages which experience short time scale environmental variability induced by fluctuating tides. Several factors affect rates of growth and grazing including the physical environment, interaction with other nanoplankton, nutritional state of heteroflagellates, and type, size, and abundance of bacterial prey. Most previous investigations (Fenchel 1982a,b,c,d; Sherr and Sherr 1983; Sherr et al. 1983, 1984, Davis and Sieburth 1984, Taylor et al. 1985) have utilized cultured populations of heteroflagellates and cultured bacteria unlike those normally encountered in the environment. Experiments using cultured heteroflagellates also eliminate variability introduced by interactions of mixed populations at different stages of growth and different nutritional states. This may result in an overestimate of in situ growth and grazing rates. Laboratory experiments also demonstrated that ambient bacterial populations quickly adapt to higher substrates and within three hours shift to fast growing culturable types (Ammerman et al. 1984, Ferguson 1984, and Fritz, unpubl. man.). Such an increase in bacterial size and uniform growth patterns of in vitro populations results in more efficient heteroflagellate growth and grazing (Fenchel 1982a,b, Anderson and Fenchel 1985; Sherr et al. 1983) than ambient

populations exhibited.

Variability in heteroflagellate and bacteria growth rates at both the marsh and mudflat stations indicates the wide range of growth response and growth potential for marsh-mudflat system nanoplankton possible throughout the year. Tidal exchange on the marsh-mudflat system results in a high degree of physical disturbance and environmental variability which may account for the variable initial growth response and higher proportion of slower growing heteroflagellates in the first few hours of incubation. The lag in growth observed in some chambers may be due to starved nutritional and low energy state indicated by pale fluorescence and high porportion of smaller cells, often characteristic of the ambient populations used for chamber innoculum. During active growth, heteroflagellate assemblages increase in size and diversity (usually from 2 recognizable types to 3-6 types) after 48 to 72 hours of incubation. Because of the great variability in growth rates and physical changes (individuals increase in size) of heteroflagellate populations, it seems possible that the populations undergo synchronous divisions once the optimum nutritional state is achieved. Sampling intervals of greater than one or two hours may miss a synchronous division. This could account for the high numbers of heteroflagellates in chambers where the growth rate determination did not yield a high rate. Growth rates determined at short (2-4 hour intervals) with Paraphysomonas demonstrated growth occurs in short intervals followed by stationary phases during which heteroflagellates may continue feeding. This again may reflect synchronous divisions and also diel variations in growth patterns which

may be accounted for in future experiments by using a series of diffusion chambers sampled (alternately) at one or two hour intervals.

Several recent studies have examined the relationship between heteroflagellate growth and absolute bacteria concentration (Fenchel 1982b, Davis and Sieburth 1984). Davis and Sieburth (1984) asserted that bacteria concentration rather than types was the factor controlling growth and grazing. This was based on the assumption that the previous experiments conducted in other geographic areas used different environmental heteroflagellates incubated with correspondingly different bacterial populations. However none of the experiments cited were conducted in situ and most likely regional variability or differences in bacterial types has been eliminated by development of large rapidly growing bacterial populations typical of cultured steady-state populations. Consequently the heteroflagellate growth response to different environmental bacterial populations may not be adequately represented by previously cited results. The heteroflagellate growth experiments of these studies may not have used the true range of bacteria endemic to each environment. In addition arguments for density-dependent growth (Fenchel 1982b and Davis and Sieburth 1984) were based on experiments involving bacterial abundance in a range much higher (10^7-10^9 cells ml^{-1}) than environmental concentrations and thus may not reflect environmental dynamics. Bacteria types, then can not be discounted as a controlling factor influencing HNANO growth and grazing.

Threshold levels of bacteria necessary for heteroflagellate growth were experimentally determined by Davis and Sieburth (1984) and Anderson and Fenchel (1985). Bacteria densities of the marsh-mudflat system

exceeded the experimentally determined threshold levels of 2.5×10^6 cells ml^{-1} (Davis and Sieburth 1984) and of 1.5×10^6 cells ml^{-1} (Anderson and Fenchel 1985). Because heteroflagellate growth was observed over the entire range of fluctuating bacteria densities, it was not possible to establish a threshold level for marsh-mudflat heteroflagellates. Neither magnitude of growth rates nor density of heteroflagellate predators achieved during chamber incubations were density-dependent on initial bacteria concentration as predicted by Fenchel (1982b, c). The lack of direct correlation between either ambient and chamber bacteria abundances with heteroflagellate concentrations in the estuarine marsh-mudflat system suggests that factors other than bacteria density affect growth or grazing response of ambient populations. Heteroflagellates growing in chambers frequently increased concurrently with bacterial growth in the environmental control chambers indicating coupling of growth rates. The positive correlation of bacteria prey and predator heteroflagellate mean concentrations in diffusion chambers during growth (at the 50% growth point) indicates that heteroflagellate growth may be more closely linked as a short term response to growth rates of bacterial populations.

Seasonal patterns of mean HNANO growth rates in diffusion chambers are not correlated with seasonal ambient bacterial concentrations nor with temperature ranges. Variation in average monthly rates observed over an annual cycle also may not represent seasonal variation. The maximum numbers of heteroflagellates ($1.0 - 3.0 \times 10^4$ cells ml^{-1}) generally occurred in chambers when temperatures ranged between 15 and 25°C. During winter months the frequency or percentages of accelerated

growth rates was lower and average heteroflagellate densities in chambers rarely exceeded 1.0 x10^4 cells ml^{-1}. However greatest growth and activity do not always occur during the warmest months, as previously indicated by laboratory experiments at ambient temperatures (Sherr et al. 1984; Davis et al. 1985). Growth rates at temperatures below 15°C in either the marsh and mudflat stations were variable and not significantly lower than the range of monthly or average annual growth rates. Heteroflagellate blooms, which dominated microbial communities for short periods, were observed during both spring and fall transitional periods (see Chapter 4) when populations experienced the widest temperature ranges. Temperature then, was not a limiting factor for heteroflagellate growth, either in laboratory experiments (Fritz, unpubl. man.) or during the marsh-mudflat in situ chamber experiments.

Both ambient and diffusion chamber results indicate that factors influencing heteroflagellate growth rates include variable bacterial growth rates and microplankton grazing pressure. Heteroflagellate growth rates often were similar to high bacteria growth rates during blooms or periods of high growth (i.e., more than two doublings per day). In turn, the lower heteroflagellate growth rates during winter months may reflect the coupling of heteroflagellates with lower bacteria growth, rather than a direct temperature effect. Although the correlation between temperature and bacterial growth in the marsh-mudflat system was not significant, lower bacterial growth rates typical of winter have been correlated to decreased temperatures in other aquatic environments (Ferguson and Rublee 1976, Wright and Coffin 1983).

High concentrations of ambient heteroflagellates occur in colder

months even though growth rates are moderate (less than two doublings per day); concentrations observed during winter months frequently were greater than during months when temperatures ranged between 15-25°C. This may be attributed to the considerable reduction in levels of nanoplankton predators, e.g., ciliates and molluscan larvae, during the cooler months (winter and spring) and reduced grazing pressure. During the summer, growth rates are high but grazing pressure by numerous microplankton predators may increase, thus potentially causing greater fluctuations in densities of summer heteroflagellate populations. Further investigations of grazing effects by microplankton predators on heteroflagellates should use smaller size fractions (<5 or 8 μm) to ensure ciliate free fractions. Experiments with different known concentrations of ciliates or other microplankton should be conducted to establish rates in this apparently tightly coupled trophic linkage.

Seasonal observations, particularly during cyanobacterial blooms, indicated that growth of heteroflagellates also may be strongly influenced by bacterial type or stability of an environment, i.e., microaggregates or other stagnant high surface area niches, and type of bacteria available for ingestion. There was no statistical difference in mean growth rates between marsh and mudflat chambers over the annual cycle, although occasionally during the annual cycle, different populations or assemblages were present at each station. Occasionally, individual chambers at each station developed a choanoflagellate bloom (i.e., July 1981 at the mudflat station and August 1981 and April 1982 at the marsh station) which was not replicated at the other station. The most prominent difference occurred in April 1982 when

choanoflagellate blooms occurred in the marsh tide pool and were transported from the marsh tidal creek into the mudflat tide pool. The slightly elevated annual ambient mean for HNANO at low tide may be the result of HNANO assemblages (increased abundances) developing in small shallow pools on marsh surface or on the mudflat during extended periods of low water. Microaggregates of large bacteria such as those found in low tide assemblages or in quiescent tidal pools in marsh also may provide optimum conditions and suitable food for growth.

Increased heteroflagellate densities and growth rates at both stations were most frequently associated with large-sized bacteria or cyanobacteria, perhaps indicating an opportunistic response to availability of optimal prey. Observations of individual chamber population associations formed in individual chambers and timing of growth pulses with changes in type of bacteria indicate the importance of the type of bacteria in marsh-mudflat nanoplankton trophodynamics. Range of growth rates observed in chambers indicated heteroflagellates may be able to respond quickly within hours to quiescent conditions and optimum prey to form blooms of actively grazing heteroflagellates, particularly in association with cyanobacteria.

Predator-Prey Cycles

Many laboratory experiments and simulations of predator-prey interactions demonstrate a sinusoidal cycles of growth, crash, growth. These experiments are based on reaching threshold concentrations of bacteria and exceeding carrying capacity when heteroflagellates reach high densities (Fenchel 1982d, Linley et al. 1983, Laake et al. 1984, Anderson and Fenchel 1985, Davis et al. 1985). In contrast to the

predicted models or reported predator-prey cycles consisting of two to four peaks offset by several days, no long term (5 to 8 day) cycle was evident in the ambient sampling, nor was there any consistent oscillatory cycle evident in chamber experiments from the marsh-mudflat system. Cycles reported in the literature were developed from either: 1) laboratory data involving both heteroflagellate and bacteria at concentrations much greater than ambient; or 2) observations of more static aquatic environments, i.e., the semi-enclosed, non-tidal, or stratified estuaries (Sorokin 1981, Fenchel 1982d, Laake et al. 1984, Anderson and Fenchel 1985) or nearshore environments (Davis et al. 1985). Variability in these systems is less influenced by tidal variability and they usually contain less bacteria ($<3 \times 10^6$ cells ml^{-1}) than the tidal Virginia marsh-mudflat system. The high predator-prey densities of laboratory experiments may be conducive to the crash/bloom cycle not normally observed in the marsh-mudflat system. During the in situ chamber incubations, heteroflagellates reached densities comparable to laboratory experiments, but bacteria concentrations never decreased below either the ambient minimum in the marsh-mudflat or to levels predicted by a predator-prey model. Bacteria abundances investigated in other aquatic systems fluctuated more closely to threshold levels over a 5 to 7 day period resulting in tighter coupling of predator-prey threshold densities or greater density-dependence for initiation of heteroflagellate growth. However, no consistent weekly cycle was established in the marsh-mudflat system where the variability of the non-limiting concentrations of bacteria is more likely induced by tidal advection and a 5 to 8 day classic predator-prey cycle was observed

infrequently.

No positive correlation of heteroflagellates and bacteria concentrations existed either with ambient bacteria concentrations or with concentrations at initiation of growth in diffusion chambers. Growth rates were not positively correlated with either the ambient or initial chamber bacterial density, Data from this marsh-mudflat system does suggest, as Davis et al. (1985) indicated for Narrangansett Bay populations, that heteroflagellates rapidly alter their growth rates with changing bacterial production. Diffusion chambers demonstrate the short-term opportunistic response of heteroflagellates to stable conditions. Frequently bacteria and heteroflagellates increased concurrently rather than out of phase, again confirming a close coupling of growth patterns.

Grazing rates are variable in part because they are based on variable bacterial growth rates; different types of bacteria within the assemblage grow at different rates. Diel variation, which was not measured, also may contribute to the variability in rates. Epifluorescence microscopy analysis confirmed the opportunistic nature of heteroflagellates. They will respond quickly to optimum prey under stable conditions which result in a rapid 1 to 3 day cycle and efficient grazing in aggregates. Grazing in the marsh-mudflat system did not vary with temperature but may have been influenced by bacteria concentrations. The marsh station clearance rates did decrease with increasing bacteria densities however mudflat clearance rates did not follow the same pattern. The decrease in marsh station clearance rates may be related in part to larger sizes of bacteria. Results of Fenchel

(1982b,c), Davis and Sieburth (1984) and Sherr et al. (1983) suggest that clearance rates decrease with increasing bacteria concentrations. However Davis and Sieburth's (1984) and Anderson and Fenchel's (1985) data for estuarine species grazing on bacteria in the range of concentrations typical of the Chesapeake Bay marsh-mudflat did not conform to the overall trend. Davis and Sieburth's (1984) linear regression of ingestion and bacteria demonstrates that grazing approaches saturation near concentrations found in the marsh-mudflat system which is supported by the lack of correlation between clearance rates and bacteria concentrations and clearance rates determined from the in situ marsh-mudflat experiments.

During any season, heteroflagellate grazing activity accounts for nearly half the bacterial production with estimates ranging from 20 to 100% of daily bacterial turnover based on bacterial growth rates determined for in situ diffusion experiments. Both environmental patterns and in situ experiments demonstrated that heteroflagellates do not control the major fluctuations in bacteria concentrations nor do estuarine bacterial concentrations regulate or control the number of heteroflagellates found in estuarine environment. Growth rates did indicate that generation times of bacteria and heteroflagellates were frequently similar and peak growth was closely coupled. Bacteria growing without grazing pressure or in the absence of heteroflagellates enter a stationary phase after 48 hours which may be due to in part to substrate limitation. Heteroflagellate grazing activity may regulate the standing stocks of bacteria to the extent that it prevents substrate limitation. Heteroflagellate grazing pressure may maintain bacteria in

a youthful phase so bacteria may flourish when optimum conditions for growth occur such as in the summer when substrate and temperatures are not limiting.

Heteroflagellates may affect microbial productivity through increased grazing and remineralization activities as short-term responses to increased bacterial populations, thus sustaining both bacterial growth and cycling of bacterial carbon in estuarine trophodynamics. The potential for high growth and grazing rates demonstrated by in situ chamber experiments under nearly all environmental conditions and the lack of seasonal pattern in fluctuating densities indicate heteroflagellates may serve as a relatively constant pathway of bacterial carbon into estuarine food chain or play an important role in estuarine trophodynamics by serving as a relatively stable link from bacteria to microzooplankton.

Diffusion chambers proved to be an ideal field methodology for obtaining environmentally representative estimates or at least potential rates of heteroflagellate growth and grazing on short time scales. Closer (more accurate) estimates of growth and grazing rates and possibly nutrient regeneration rates may be obtained though the use of a series of in situ chambers sampled at even shorter intervals (<2 hours) than used in previous in situ experiments. Estimates of grazing rates by different classes or species of nanoplankton may be improved by using epifluorescence analysis with the DAPI stain for nucleotides of bacteria (Sherr and Sherr 1983) or more specific activation and emission wavelength filters for cyanobacteria fluorescence. Ultimately, heteroflagellates (HNANO), at the high range of environmental

concentrations and growth rates, may serve as an important food source (prey) for larger nano- and microplankton predators. This trophic linkage also may be confirmed using in situ diffusion chamber experimentation and known concentrations of ciliates or larval molluscs to establish grazing rates. Various refinements of the in situ diffusion chamber techniques presented here may provide a valuable tool for determining the temporal and spatial scales necessary for a quantitative evaluation of nanoplankton dynamics.

CHAPTER IV

TROPHODYNAMICS OF ESTUARINE NANOPLANKTON DURING AUTUMN AND SPRING TRANSITIONAL PERIODS

INTRODUCTION

The complexity and trophic interactions (close coupling) of the microbial food web are well known (Pomeroy 1974, 1975, 1984; Sieburth et al. 1978, Haas and Webb 1979, Fuhrman 1981, Sorokin 1981, Fenchel 1982a,b,c,d, Azam et al. 1983, Sherr et al. 1984). Yet studies of nanoplankton trophodynamics, including heterotrophic bacteria and flagellated mastigophorans, frequently neglect the smaller or finer temporal and spatial scales (Meyer-Reil at al. 1979, Goldman 1984, Pomeroy 1984). Shallow estuarine environments such as salt marshes and associated mudflats provide extremely transient conditions under which nanoplankton dynamics can be expected to reach a maximum in terms of variability. The potential role of heterotrophic flagellates (HNANO or heteroflagellates), an important component of estuarine salt marsh nanoplankton (Newell et al. 1983, Sherr and Sherr 1983, Galvao 1984, Chapter 1) as dominant predators is universally accepted. However little quantitative data exists documenting the scale and magnitude of trophic interactions and predator-prey cycles in estuarine environments. Short-term investigations are necessary to determine adequate time scales in field sampling of microbial processes and trophodynamics in productive marsh-mudflat systems typical of Virginia estuaries.

Seasonal occurrence and activity of HNANO was studied in a sheltered

brackish water embayment of Chesapeake Bay from April 1981 through May 1982 (Chapter 3). Seasonal bacterial and heteroflagellate growth and grazing rates were investigated using differential filtration and diffusion chambers in natural salt marsh tidal pool conditions. This sampling program, using epifluorescence direct counts, revealed that heteroflagellates vary little seasonally and usually fluctuate between $1.0 - 5.0 \times 10^3$ cells ml^{-1}. Patchy short term pulses or blooms, i.e., increased HNANO concentrations to 0.45 to 2.5×10^4 cells ml^{-1}, occurred periodically throughout the year concurrent either with short periods of increased temperatures or specific bacterial populations in sheltered marsh tidal pools. These 1-3 day episodes of increased HNANO concentration were frequently observed during the transitional periods of spring and fall. These transition periods are characterized by seasonal change in temperatures, nutrients, bacteria abundances, and autotroph populations. The seasonal study of HNANO predator-prey cycles, during 5 to 8 day periods of each month, revealed that the transitional periods of both autumn and spring, were possibly the most dynamic in terms of heteroflagellate species diversity, abundances, and growth. Bacteria and autotroph abundances corresponded to the general seasonal trends in temperature by decreasing in October and increasing in April; however heteroflagellate abundances fluctuated widely during autumn and spring.

A second seasonal study was conducted in the marsh-mudflat system from July 1982 through January 1983 (Galvao 1984) which provided background information for further in situ growth and grazing HNANO experiments. The sampling strategy of this second study was designed to characterize the temporal variability of the nanoplankton community and

interrelations of its components as well as to measure dissolved substances indicative of estuarine microbial processes. Additional temporal scales were selected to improve the resolution of sampling required to fit the time scale of microbiological processes. The analysis of short-term variability within a tidal cycle on a long-term basis provided information necessary to distinguish true seasonal trends (i.e., of transition periods) from short-term variability inherent in the estuarine marsh-mudflat system.

Investigations of the role of heteroflagellates in the microbial food web in a productive marsh system must examine the complete range of environmental variability and factors regulating nanoplankton dynamics before the impact of heteroflagellate grazing on microbial communities can be evaluated. This paper is the result of a collaboration of the two research efforts described above designed to assess interactions within the nanoplankton community (Galvao 1984, Chapter 1). Of particular interest were trophic interactions of heteroflagellates and bacteria with respect to the different conditions of the autumn and spring periods. The transitional period research used an intensified sampling effort on 3 different temporal scales and identical spatial scales to describe the magnitude of events typical to the transitional periods. The evaluation of nanoplankton dynamics were focused at the marsh and mudflat tidal pools. In situ diffusion chamber experiments were carried out concurrently during the intensified survey to monitor bacteria and heteroflagellate growth rates and estimate grazing impacts on environmental assemblages developing in the tidal pools during the transition periods.

Current hypotheses of trophic interaction and the microbial loop (Azam et al. 1983) of carbon flux through bacteria to HNANO now include the importance of microaggregates (Goldman 1984) and microzones (Ammerman et al. 1985) consisting of bacterial and nutrient rich material. Cyanobacteria aggregates, which were not normally observed in the marsh-mudflat system, were an important component of nanoplankton of both autumn and spring transitional periods (Chapter 3). Diffusion chambers provided an ideal quiescent environment to study the dynamics of aggregate formation and potential for stimulated HNANO growth and grazing activities.

MATERIALS AND METHODS

The study site is a small well-defined tidal embayment (300 m x 100 m) located at Carmines Islands ($37^{o}17'N$, $76^{o}32'W$) in the Chesapeake Bay estuarine system. The embayment opens directly into the York River. Three stations were established which represented a longitudinal gradient between marsh and river: Station 1, Marsh; Station 2, Mudflat; and Station 3, River (Fig. 1). The sampling strategy was designed to investigate temporal and spatial aspects of nanoplankton dynamics. Temporal scales were defined on a short-term basis (hourly intervals within a tidal cycle) and a long-term basis (daily and weekly intervals). The spatial scale was provided by the three stations along the tidal embayment. One tidal cycle was sampled each week from 21 July to 21 December 1982, except during October when two tidal cycles were sampled weekly. Additional tidal cycles were sampled in the last week of January and in mid-April 1983. Sampling was carried out at 2 hour intervals and at the same time of day to minimize photoperiodicity effects. The sampling intervals bracket alternatively one high tide or one low tide each successive week. The stations were sampled in sequence (1,2,3 or 3,2,1) following the direction of ebb and flood, respectively. During low tide, shallow tidal pools formed at Stations 1 and 2. All three stations were sampled for each low tide cycle and whenever possible, for high tide cycles. Sampling during the autumn and spring transition periods was intensified. Two tidal cycles during October were sampled weekly and two cycles (one each, high and low) were sampled during mid-April. In addition sampling was carried out at daily intervals during

Figure 1. Study site and station locations.

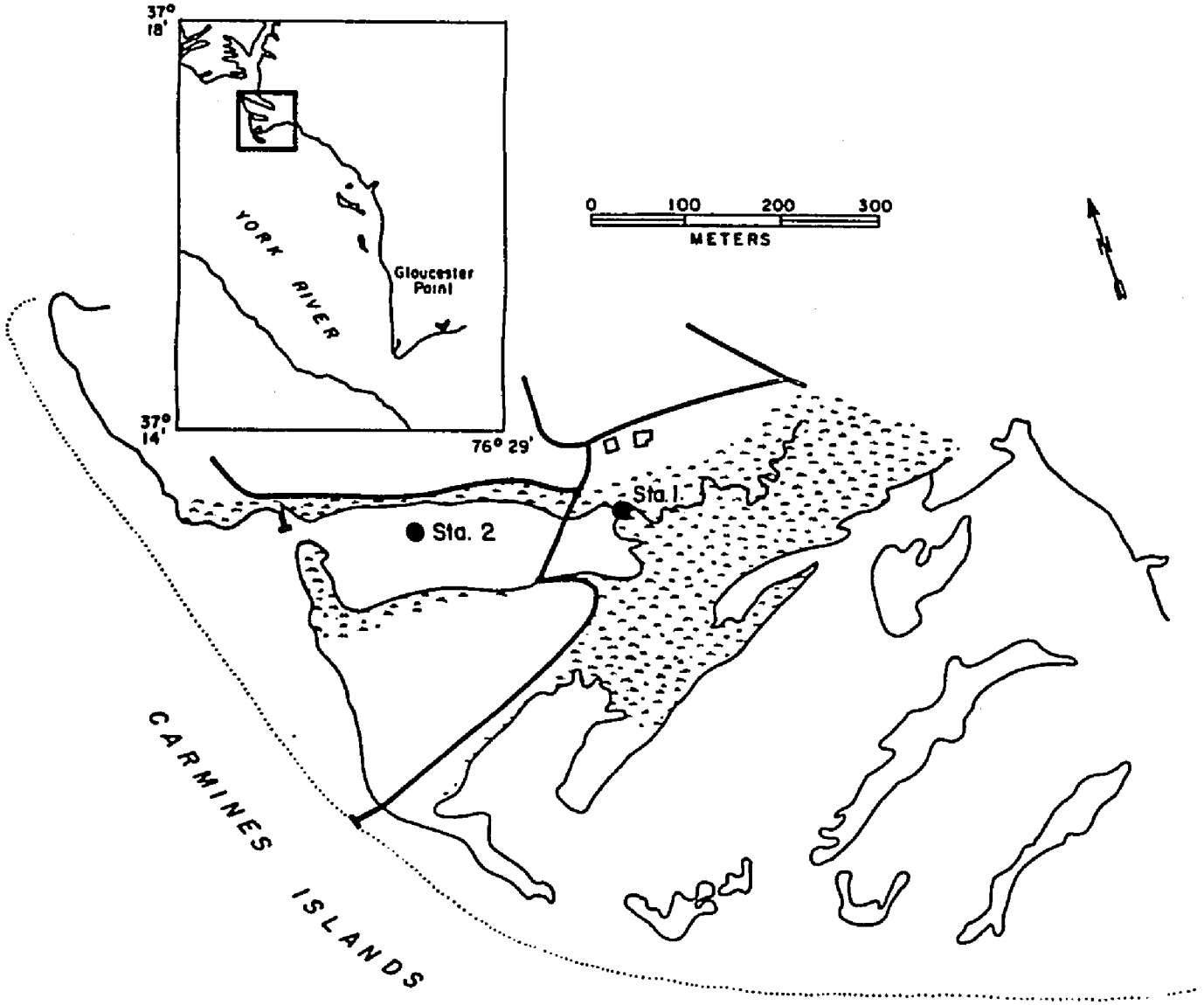
37° 18'
37° 14'
76° 29'
YORK RIVER
Gloucester Point
0 100 200 300
METERS
N
Sta. 1
Sta. 2
CARMINES ISLANDS

the week between tidal cycles to correspond with in situ diffusion chamber experiments.

For nutrient analyses, sub-surface water samples (20 ml) were filtered in the field through precombusted (2 h at 480°C) Whatman GF/F filters. Laboratory analyses for NH_4^+, NO_2^-, NO_3^-, and PO_4^{-3} in water were carried out using a Technicon AutoAnalyzer following standard EPA methodologies (Kopp and McGee 1979). For direct cell counts, sub-surface water samples (2 ml) were fixed in 0.3% glutaraldehyde in the field. All autotrophic and heterotrophic microorganisms were enumerated with epifluorescence microscopy (Haas 1982). Five ml sub-surface water samples were analyzed for chlorophyll _a_ using a simplified DMSO (dimethyl sulfoxide) extraction technique (Webb and Hayward, unpubl. man).

Growth and grazing rates of heteroflagellates (HNANO) were estimated following the protocol of Chapter 3. Activity of environmental populations of bacteria and HNANO (both total and size-fractioned through <36 μm mesh) were determined at the marsh and mudflat tidal pools using in situ diffusion chambers equipped with polycarbonate permeable membranes of 0.2 and 1.0 μm pore sizes. The size-fractioned community represented ambient populations of heteroflagellates, autoflagellates, diatoms, small organic aggregates, and occasionally included small non-loricate ciliates (<15 μm) and amoebas typical of patchy distribution in whole water. Diffusion chambers were suspended in marsh and mudflat stations in shallow water reservoirs sunk into substrate. This simulated protected tidal pools typical of the marsh fringing the tidal embayment. The support structure allowed chambers to move through the water column of both the reservoir and tidal pool with tidal fluctuations, yet remain

submerged in the reservoir during spring low tide (Fig. 2).

Nanoplankton concentrations in both the diffusion chambers and water column environment were monitored concurrently over several days at daily intervals. Epifluorescence microscopy direct counts were used to determine natural growth rates (μ = instantaneous h^{-1} or d^{-1}; Dt = doubling (generation) time (h)) in diffusion chambers over a 24 hour period. Predator-prey interactions were determined by comparing abundances of bacteria and HNANO determined at daily intervals in the environment at low water with changes in abundances determined in diffusion chambers at the same intervals. Grazing rates and/or maximum ingestion rates for heteroflagellates phagocytizing growing bacteria were estimated using two different experimental approaches based on growth rates of bacteria and heteroflagellates dtermined in both 0.20 μm and 1.0 μm chambers (Chapter 3). Various parameters (mortality rates, clearance F, μl d^{-1}, and ingestion rates) of heteroflagellates were calculated using rate determinations similar to those of Landry et al. (1984). Maximum ingestion rates also were determined using prey density-dependent yield (Y) of heteroflagellates (predator) and growth rate (μ) as defined by Fenchel (1982b). Diffusion chamber data and environmental data from epifluorescence direct counts at low water made possible the evaluation of short term cycles (2 - 7 days) in predator-prey interactions and correlation between bacteria and heteroflagellate abundances.

Figure 2. Diagram of diffusion chamber and support structure.

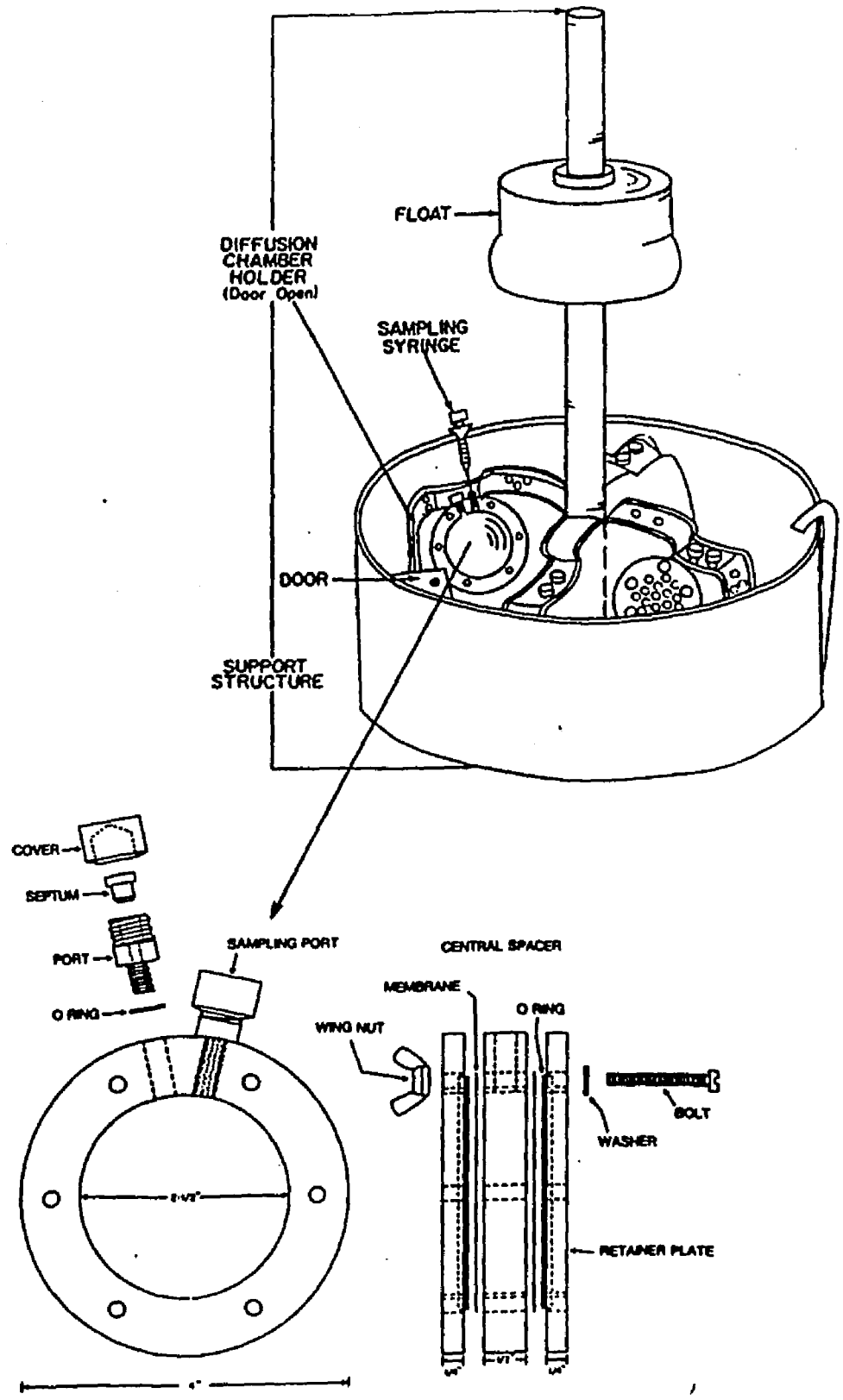

DIFFUSION CHAMBER

RESULTS

Nutrients were monitored from July 1982 through January 1983 and during a short period in spring 1983 for both long-term (seasonal) trends and short-term (weekly and tidal) trends (Galvao 1984), particularly during the autumn and spring transition periods. Ammonium daily mean values demonstrated no seasonal trends while nitrate and phosphate daily mean values increased and decreased, respectively, from summer to winter (Galvao 1984). Dissolved inorganic nitrogen (DIN) concentrations during both transition periods (autumn and spring) were generally higher than during summer and winter. The most conspicuous trend in DIN in the tidal embayment at all three stations was the fall maxima in NH_4^-, NO_3^- , and NO_2^- extending over a three week period between 7 October and 3 November 1982 (Fig. 3). Daily mean DIN concentrations reached 20 µg-at N/l and nitrate daily means reached concentrations (6 µg-at N/l) 20 times higher than summer values (0.2-0.4 µg-atN/l) during this period (Fig. 3). Tidal and longitudinal differences among stations during the autumn period indicated a river origin. Nitrate daily means also exhibited a maximum in spring 1983 (9 µg-at N/l), apparently again derived from a river source origin. The increased concentrations of phosphate corresponded to an ebb tide phenomenon, when concentrations at the marsh station reached values 2-4 times those during flood tide. The autumn nitrate and nitrite peaks far exceeded any other seasonal peak in magnitude and length. Short-term sampling (use of closer sampling intervals, i.e., sampling hourly intervals biweekly, rather than on a weekly or monthly basis) made it possible to define this nitrogen event during the autumn transition

Figure 3. Daily means of nitrite concentration during July through December 1982; nitrite, nitrate, NH_4 combined means and individual means for the fall nitrite maxima at the three stations.

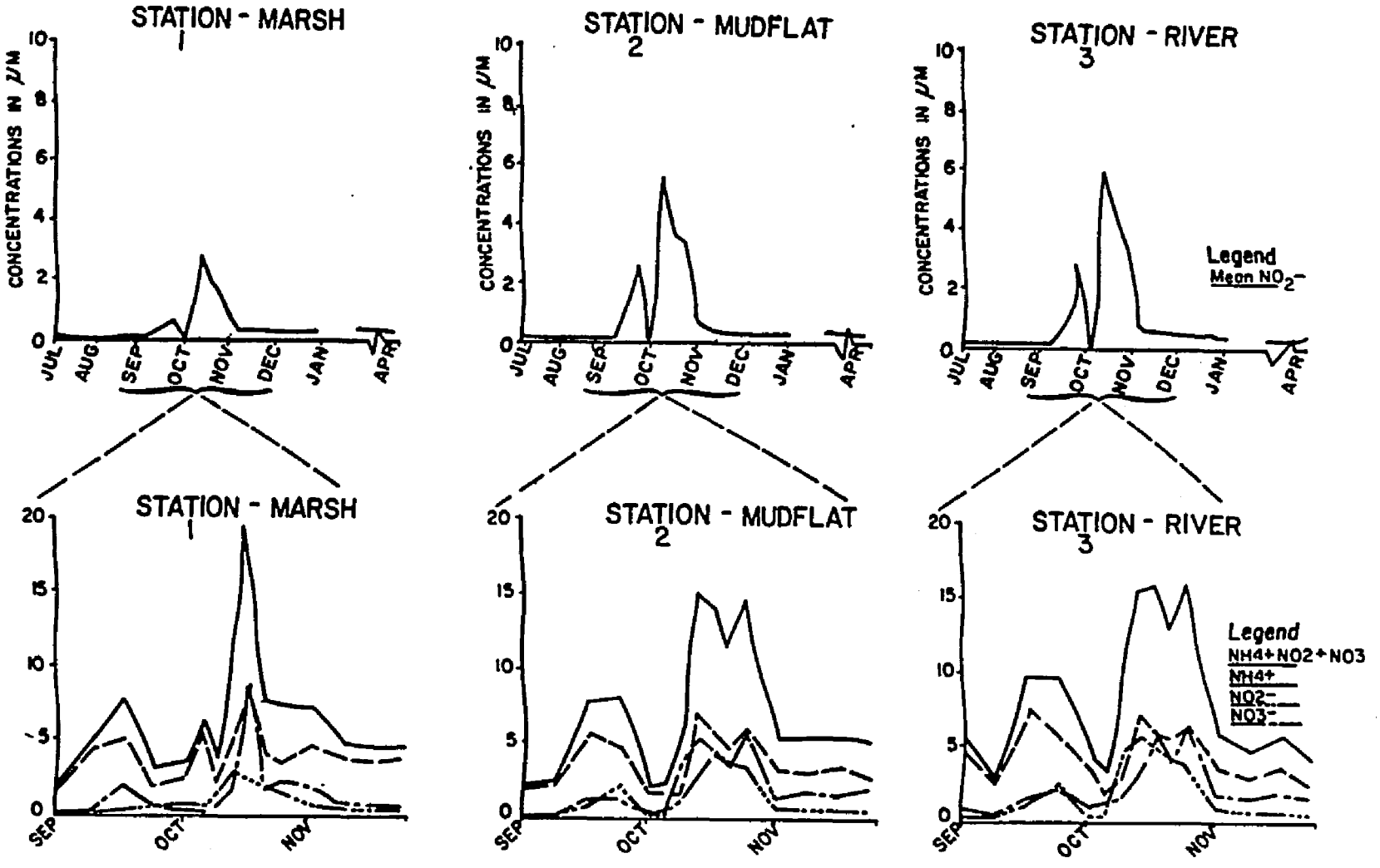
STATION - MARSH
1
STATION - MUDFLAT
2
STATION - RIVER
3
CONCENTRATIONS IN µM
0
2
4
6
8
10
JUL
AUG
SEP
OCT
NOV
DEC
JAN
APR
Legend
Mean NO2-
STATION - MARSH
1
STATION - MUDFLAT
2
STATION - RIVER
3
0
5
10
15
20
SEP
OCT
NOV
Legend
NH4+NO2+NO3
NH4+
NO2-
NO3-

period.

An evaluation of annual trends in abundances of the various components of nanoplankton based on Pearson correlation coefficients between different components ($r = 0.7-0.8$, $P=0.00$) showed that temperature was the dominant factor regulating variations in bacterioplankton standing stocks. No significant correlations ($r > 0.5$, $P=0.00$) were found between heterotrophic bacteria and heteroflagellate abundances. Bacteria concentrations followed seasonal trends similar to water temperatures in the tidal embayment at all three stations (Fig. 4). Regression analyses revealed a positive linear relationship between temperature and bacteria. Daily means of eukaryotic flagellates, both heterotrophic and autototrophic, did not exhibit any seasonal trends (Fig. 4) nor did regression analysis ($p > 0.05$) reveal any relationship between temperature and flagellate abundances.

Seasonal patterns exhibited evidence of a possible concurrent trend during the autumn transitional period of high nutrient levels and senescence of nanoplankton populations. Both phytoplankton and bacterioplankton standing stocks decreased to a minimum during the period of fall nitrite maxima in October (Figs. 3, 4). Chlorophyll _a_ analyses during this period also revealed the presence of larger amounts of degraded pigment. Heterotrophic microflagellate cell counts did not exhibit any significant change during high nitrate period (Oct-Nov 1982) (Fig. 5). Both heterotrophic and autotrophic nanoplankton (Figs. 3, 4) exhibited a short-term increase at the end of nitrite event in early November 1982. Overall, an increase in heteroflagellate abundance relative to total nanoplankton occurred during fall and winter, the

Figure 4. Variation in temperature, salinity, autotrophic and heterotrophic nanoplankton and bacteria from July to December 1982 at the marsh and mudflat stations.

SALINITY AND TEMPERATURE

STATION 1 – MARSH

STATION 2 – MUDFLAT

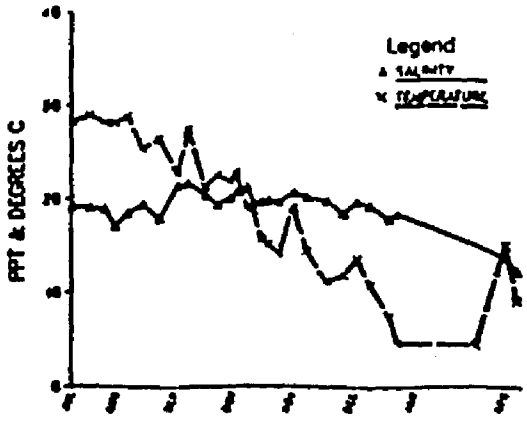

NANOPLANKTON

STATION 1 – MARSH

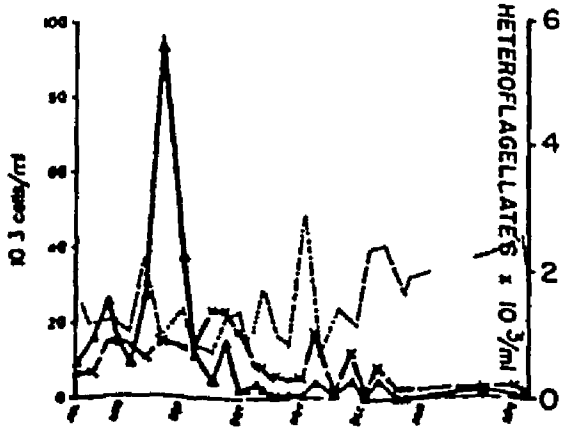

STATION 2 – MUDFLAT

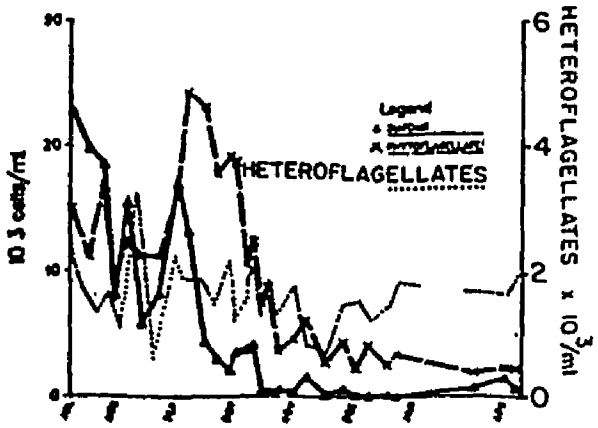

BACTERIA

STATION 1 – MARSH

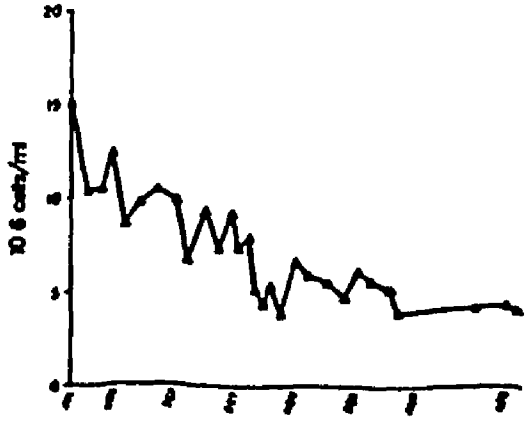

STATION 2 – MUDFLAT

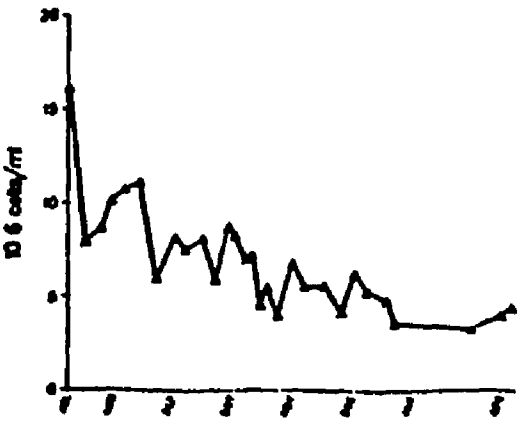

Figure 5. Daily means in heteroflagellate density from July through December 1982 and inset for October through December.

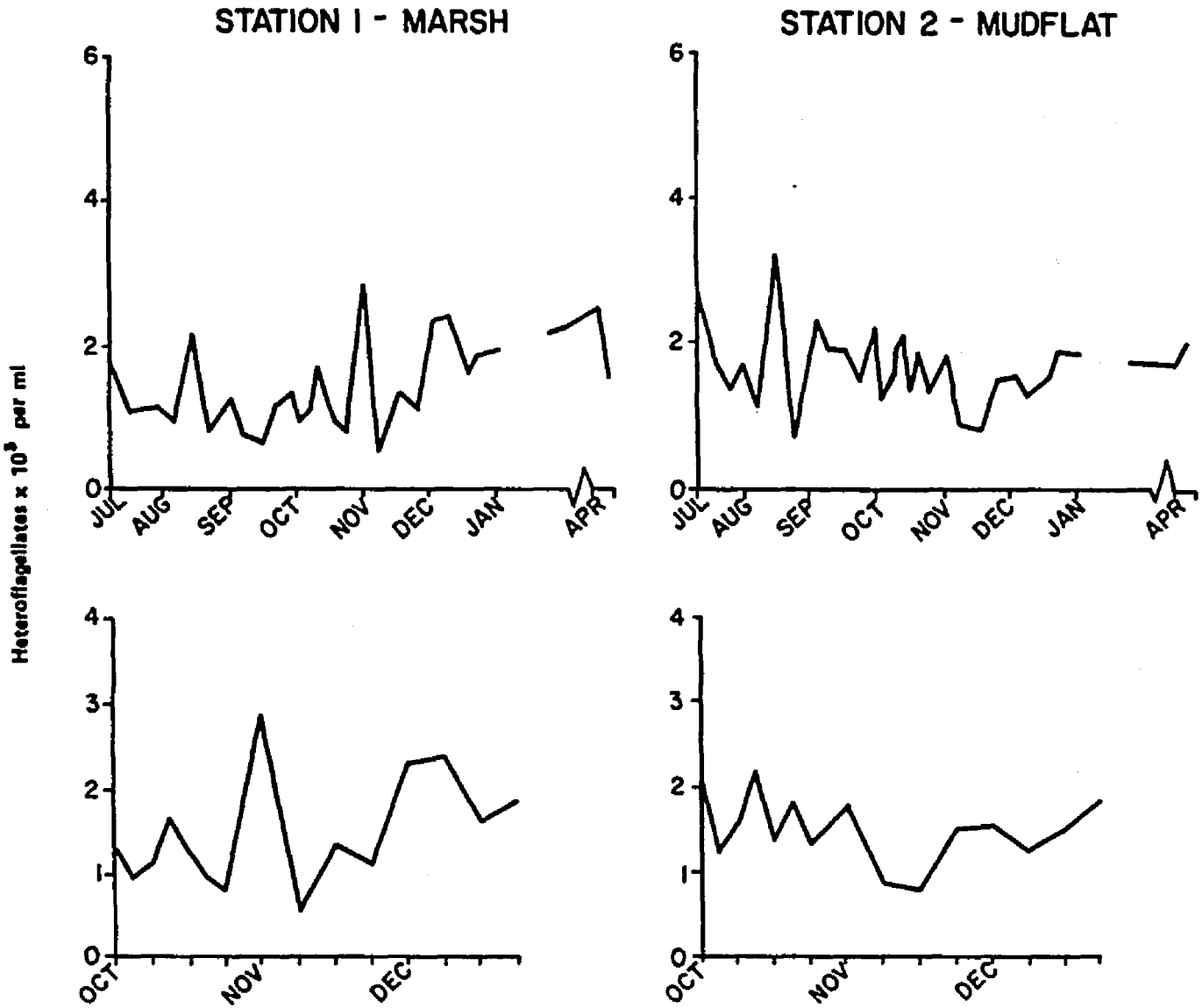
STATION 1 - MARSH
STATION 2 - MUDFLAT
Heteroflagellates x 10³ per ml
6
4
2
0
JUL
AUG
SEP
OCT
NOV
DEC
JAN
APR
4
3
2
1
0
OCT
NOV
DEC

maximum was evident in April (Figs. 4, 5). The overall comparison of nanoplankton populations did reveal that heteroflagellates are a significant component of nanoplankton during early autumn and spring, with concentrations averaging between 2.2 - 2.7 x 10^3 cells ml^{-1}, slightly above the 1982 annual average (1.7 x 10^3 cells ml^{-1}).

The finer (small) time scale sampling was designed to show tidal and daily variation in nanoplankton abundances. Both transition periods demonstrate some large fluctuations in autotrophs, heteroflagellates, and bacteria densities with no obvious cyclical or interrelated predator-prey cycles. Instead each nanoplankton component appeared to fluctuate independently. Intensive tidal cycle sampling did not reveal a diurnal pattern but rather, variability induced by tidal movement (Fig. 6). Hourly or daily variations of bacteria (4.0-8.0 x 10^6 cells ml^{-1}) and heteroflagellates (1.0-5.7 x 10^3 cells ml^{-1}) exhibited in Figures 6, 7, 8, and 9 are in part a reflection of patchy distributions typical of marsh-mudflat system (Galvao 1984, Chapter 2). However, epifluorescence microscopy analysis of samples from tidal pools formed at the marsh station during both transition periods at low tide did reveal the phenomena of distinct microheterotrophic assemblages characterized by elevated densities and increased diversity. This was consistent with previous long-term seasonal sampling programs (Galvao 1984, Chapter 2). The formation of "low tide assemblages," demonstrated by peaks in Figure 6, were composed of greater than seasonal average concentrations of polymorphic flagellates (2-6 x 10^3 cells ml^{-1}) and very large polymorphic bacteria (1 μm wide; 3-5 μm long), which constituted, in some cases 20-40%, of total bacterioplankton. Composition and activity of these

Figure 6. Tidal variation of heteroflagellates, bacteria, and autotrophs during the autumn and spring transitional periods.

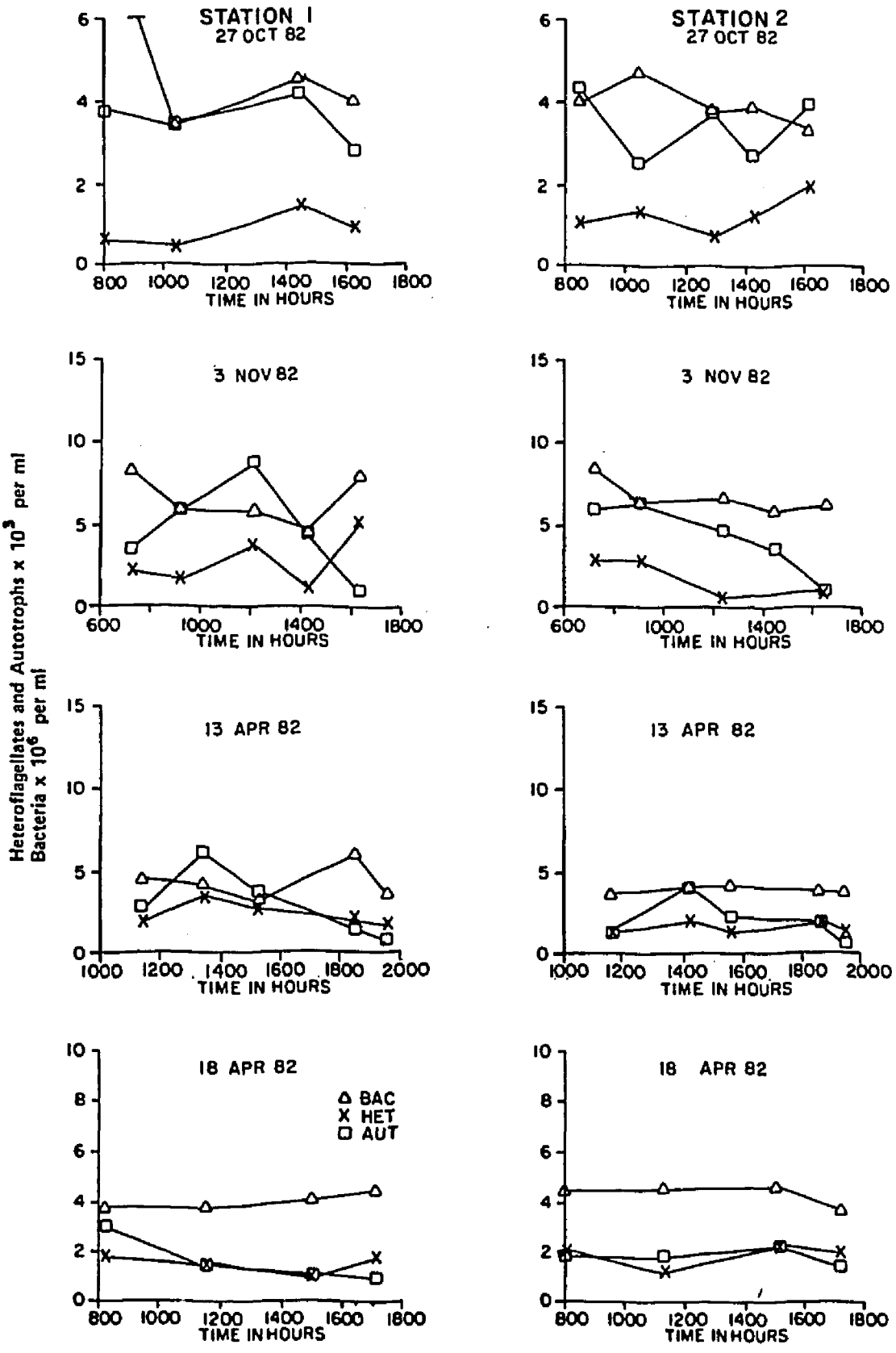
STATION 1
27 OCT 82
STATION 2
27 OCT 82
3 NOV 82
3 NOV 82
13 APR 82
13 APR 82
18 APR 82
18 APR 82
Δ BAC
X HET
□ AUT
TIME IN HOURS
Heteroflagellates and Autotrophs x 10³ per ml
Bacteria x 10⁶ per ml

assemblages though of short duration (2 to 6 hours), may contribute significantly to marsh system trophodynamics or DOM cycling through grazing and nutrient generation activities or as prey. In situ diffusion chamber experiments detailed below represent an attempt to evaluate heteroflagellate growth and grazing activities over a short time scale during these variable and dynamic autumn and spring transition periods.

October, November 1982 Growth and Grazing Experiments

Environmental monitoring in the marsh-mudflat system during 1982 confirmed the trends in bacteria and nanoplankto abundances observed in 1981. In addition, the sampling documented peaks in NO_2^- and NO_3^- concentration due to river input and marked fluctuations in heterotrophic nanoplankton (HNANO) populations. Intensive sampling during October and November 1982 also revealed a relative increase in cyanobacteria abundances (x 10^2 to 10^5 cells ml^{-1}) and diversity beginning 26 October, and continuing through 4 November 1982. Growth and grazing of HNANO and bacteria populations monitored in diffusion chambers experiments reflect the dynamics of cyanobacteria populations observed through environmental monitoring.

Chamber incubations initiated 27 October (Fig.7) contained bacterial populations ranging from 4.0 to 6.0 x 10^6 cells ml^{-1} which included a large percentage of medium size rods (1.0 x 0.50 μm) and 10^3 to 10^4 cells ml^{-1} cyanobacteria. Synechococcus doublets and clusters numbered in the 10^3 cells ml^{-1} at both marsh and mudflat stations. Patchily distributed cluster-forming types of large cyanobacteria increased from 10^3 to 10^6 cells ml^{-1} within the low water films found in

the marsh pool. These clusters were composed of large rod-shaped cells resembling Anacystis nidulans and Agmenellum or Micropopedia. Both 0.20 μm and 1.0 μm chambers at each station contained an assemblage of heteroflagellates dominated by a small (2.0 - 3.0 μm (1) and 15 to 35 μm^3 volume) monad type and a relatively large percentage (10 to 20%) of large forms (Paraphysomonas and achlorotic cryptomonad or "pointed body" with a volume of approximately 75 to 100 μm^3).

Bacteria Growth

Bacteria growth rates were quite variable ranging from growth rates (μ) and doubling times (Dt) of μ=0.015h^{-1}; Dt 45.3h (stationary phase) to growth pulses of μ=0.081; Dt 8.6h with an average of μ=0.027h^{-1}; Dt25.4h during the slower growth period and μ=0.057h^{-1}; Dt 12.2h for faster growing assemblages. The concentrations of bacteria in 0.20 μm chambers did not differ from 29 October ambient, chambers at both stations contained a more diverse variety of bacteria and a slightly greater biomass, due to dense clusters of very small rod-shaped bright green bacteria, and cyanobacteria (easily recognized by intermittent orange fluorescence). Clusters of cyanobacteria were comprised of elongated rods of various sizes ranging from 0.2 x 1.0 μm to 1.5 x 2.0 μm) arranged in round irregular clusters (Anacystis-like) or in regular geometric patterns (Agmenellum-like). Bacterial concentrations in 1.0 μm chambers at both stations increased relative to 0.20 μm chambers and ambient on 29 October (Table 1). This increase, can be attributed to the larger pore size (1.0 μm) which allows for greater diffusion or invasion of small ambient cyanobacteria into the chamber, in addition to proliferation of cyanobacteria surviving from the 27 October innoculum. Bacterial growth

Table 1. Densities of cyanobacteria (cells ml^{-1}) at marsh and mudflat stations in fall 1982 diffusion chamber experiment

	Marsh		Mudflat	
Date	Ambient	Chamber	Ambient	Chamber
27 Oct	0.14×10^3		2.47×10^3	
28 Oct	0.00		1.22×10^3	
29 Oct	0.67×10^3		6.06×10^3	0.14×10^3
2 Nov	0.00	4.81×10^4	0.24×10^3	0.14×10^4
3 Nov	0.12×10^3	2.88×10^6	0.60×10^3	3.42×10^5
4 Nov	6.28×10^6			
5 Nov	0.07×10^3			

rates measured for 2-5 November also accounted for rapidly growing cyanobacteria (μ=0.08 to 0.1 h^{-1}) which appeared to bloom and crash in chambers.

Heteroflagellate Growth

Heteroflagellate growth patterns in diffusion chambers were similar at both marsh and mudflat stations. Fluctuations in heteroflagellate activity was observed within two growth periods accompanied by cyanobacteria blooms, a phenomenon not observed in previous environmental monitoring. Growth rates corresponding to the first peak averaged μ=0.049 h^{-1} within first 20 to 23 hours for all chambers at both stations. Marsh chamber growth rates within the first 24 hours averaged μ=0.042 h^{-1} (Dt=16.4h, K=1.47 d^{-1}) and mudflat rates averaged μ=0.054 h^{-1} (Dt=12.8h, K=1.87 d^{-1}) but were much more variable. The distribution of growth rates within the range of μ=0.032 to 0.069 h^{-1} indicates that heteroflagellates may have divided at two different rates, either at one (Dt~24h) or two (Dt~11h) divisions d^{-1}. The variability in response and increase in densities of heteroflagellates during the first 24 hours shown in Figure 7 is typical of in situ growth rate determinations and reflects environmental variability and patchy distributions of heteroflagellates. The decrease in bacteria concentrations both in situ and in chambers at the mudflat station may be explained in part by longer exposure to adverse effects of high NO_3^- and NO_2^- (27-28 Oct, last day of increased values before decline) input from river. Exposure to nitrite may have exerted a greater influence in the larger pore size (1.0 μm) chambers, where exchange with ambient occurs more rapidly, and

Figure 7. Temperature, salinity, autotrophs, and heteroflagellates versus bacteria densities for in situ diffusion chambers and for ambient populations during 27 October - 5 November 1982 at the marsh and mudflat stations.

OCTOBER-NOVEMBER 1982

NANOPLANKTON, SALINITY, AND TEMPERATURE

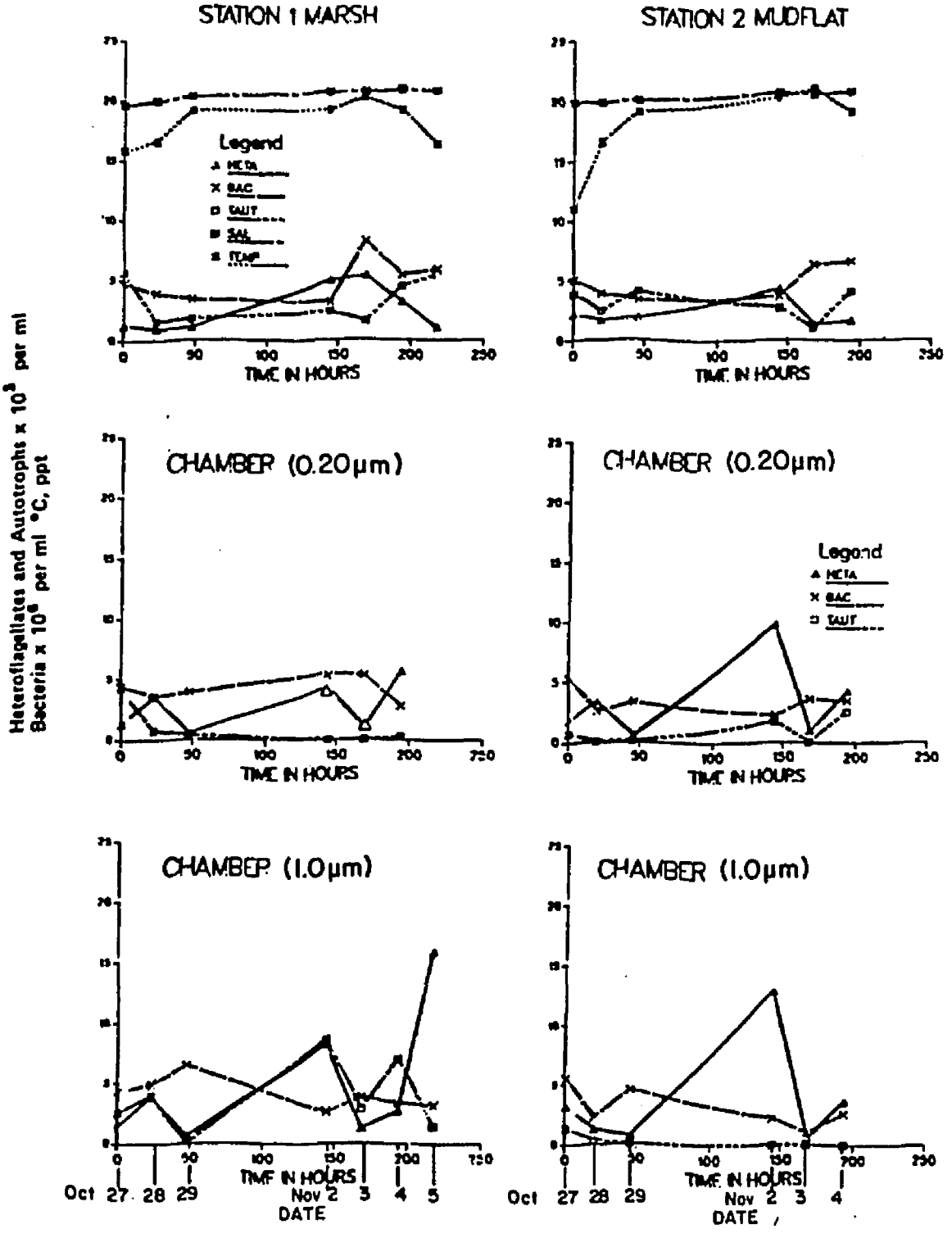

populations may have responded more quickly. Populations in both mudflat and marsh chambers during 28-29 October, paralleled the environmental trend of decrease in heteroflagellate size and numbers (Fig. 7). Diversity of HNANO assemblage was reduced and consisted of smaller forms (monads and bodonids) in both ambient and chambers.

Ambient heteroflagellate concentrations (~4 - 5 x 10^3 cells ml^{-1}) measured in both stations at low water on 2 November were significantly higher than seasonal average (1.7 x 10^3 cells ml^{-1}, July 1982 - April 1983; 2.4 x 10^3 cells ml^{-1}, May 1981 - May 1982). Concurrently, a second more pronounced growth period resulting in high HNANO cell densities occurred in chambers at both stations. The sampling period of 2-5 November (Fig. 7) was characterized by unseasonally warm temperatures and extended periods of low water which formed quiescent tidal pools. Diversity, numbers, and sizes of heteroflagellates increased particularly at the marsh tidal pool, where surface films of cyanobacteria were easily established. Protected quiescent waters also resulted in greater relative abundances of large epibacteria and unusual blooms of a diverse cyanobacterial assemblage not frequently observed in the Carmine Island marsh-mudflat system. The assemblage, similar to marsh pool surface film bloom observed 27 October, occurred 2 November at protected mudflat and marsh pools in approximate concentrations of x 10^3 and x 10^2 cells ml^{-1} respectively. Patches of surface film clusters (x10^6 cells ml^{-1}) appeared in both protected mudflat and marsh pools by 3 November. Diffusion chambers, which also provided optimum quiescent (high nutrient) conditions, duplicated this unusual bloom phenomenon; concentrations of cyanobacteria clusters (mats) and filaments increased from 2 November

concentrations of $x10^3$ to 3 November levels of $x10^5$ to 10^6 cells ml^{-1}. Although the decline in bacterial numbers on 3 November is evident in Figure 7, biomass increased 10 to 50 fold with cyanobacteria proliferation. The chamber assemblage of 2 November consisted of dense clusters of cells, some with enlarged cell volume of 1 - 2 μm^3 versus the normal range of 0.1 - 0.6 μm^3. By 3 November most cyanobacteria were enlarged forms and some appeared vacuolated (Anacystis - like).

All heteroflagellate growth chambers in the marsh demonstrated similar growth pulses concurrently with increases in environmental HNANO during 2-5 November. Chambers yielded rapid growth in cell densities of up to 3.8×10^4 cells ml^{-1} (from 3 to 5 Nov) and increased HNANO species size and diversity. The diversified species assemblage which developed in chambers resembled low tide pool assemblage and was dominated by five types, two of which, the pointed body and bodonid forms, were relatively large (5 - 10 um diameter or length). Ambient pointed body abundances (150 - 250 cells ml^{-1}) were relatively high and in chambers where they were ingesting cyanobacteria, concentrations were as great as ($2 - 6 \times 10^3$ cells ml^{-1}). After cyanobacteria decreased in (from 10^6 to 10^3 cells ml^{-1}) in chambers, pointed bodies (phagotrotrophic cryptomonads) decreased markedly, although other large Paraphysomonas forms remained at high concentrations. Heteroflagellate concentrations in the chambers were much greater than peaks encountered in ambient pools (Fig. 7) on 2 November (mudflat) and 3 November (marsh).

The data for 2-5 November shows the short time scale of nanoplankton interactions, in particular HNANO growth and decline (Fig. 7). The high growth and densities of heteroflagellates (cells ml^{-1}) is followed by a

decline in numbers to ambient levels within range of tidal variation during a 3 November cyanobacteria bloom, and then by rapid recovery of heteroflagellate and heterotrophic bacteria numbers. Growth rates in mudflat chambers during second growth period ranged from μ=0.032h^{-1}; Dt 21.8h to 0.07h^{-1}; Dt 9.9h with an average μ=0.049 h^{-1}; Dt 14.1h and were similar to those of previous growth period. HNANO growth rates at the marsh station were similar to mudflat but some were considerably higher (range μ= 0.031 to 0.102 h^{-1}). Growth rates also are grouped at the either end of the range; doubling times are either approximately 20 hours or 9 hours. Chamber growth curves (Fig. 7) indicate that high growth (2 to 4 divisions per day) and high HNANO yield was possible with relatively low bacteria concentrations (3.0 - 5.0 x 10^6 cell ml^{-1}).

Environmental HNANO abundances during the experiment were variable and high densities were not sustained as long as in chamber populations (Fig. 7). Environmental sampling during the intensive sampling period (Oct 26 - Nov 5) also revealed that ambient HNANO vary independently of bacteria abundances; the peak in HNANO (i.e., Nov 2) did not occur simultaneously with increased bacteria concentrations. For example, on 3 November bacteria densities increased concurrently with temperature increase and remained relatively high for several days while environmental heteroflagellates decreased and autoflagellates increased. This pattern or lack of defined environmental predator-prey cycles where the heteroflagellate density (sinusoidal) curve lags that of bacteria by 3 to 5 days, was confirmed by comparison of fluctuations of HNANO and bacteria abundances from 4 October through 9 November.

Grazing

Both mudflat and marsh chamber HNANO populations were dominated by large forms, some containing ingested cyanobacteria. Grazing rate determinations reveal similar trends at both stations. Ingestion and clearance rates were variable but all occurred within the high end of the seasonal range for ambient salt marsh populations (Chapter 3). Ingestion ranged between 50 to 130 bact h^{-1} (1200 - 3120 bact d^{-1}) (ave. = 86 bact h^{-1} or 2064 bact d^{-1}) and clearance rates ranged between 0.39 to 0.76 µl d^{-1} (ave. = 0.54 µl d^{-1}). Clearance rates with cyanobacteria as prey were variable (0.24 - 0.70 µl d^{-1}) and ingestion rates ranged between 6 to 20 bact h^{-1}. Grazing rates in chambers where the large forms and aggregates were most abundant produced the highest range of rates ranging between 70 - 130 bact h^{-1}. Variability in ingestion rates did not appear closely correlated to growth rates, but may be explained by differences in assemblages of heteroflagellates and bacteria.

The marked decrease in abundances of larger rod-shaped bacteria (1.0 x 3.0 µm) and cyanobacteria (size range 0.5 x 0.3 µm to 1.0 x 3.0 µm) in all chambers after 24 hours indicated preferential grazing of larger bacteria. In contrast, marsh chamber heterotrophic bacterial abundances and species composition, fluctuated independently of the heteroflagellate population. Plots of marsh chambers indicate no apparent significant grazing impact on the total bacteria population due in part to increasing clusters of very small cyanobacteria also flourishing in the marsh pool and increase in heterotrophic bacterial growth with decrease in NO_2^- and NO_3^-. Ambient and chamber heteroflagellate populations declined in numbers, species diversity and

sizes in all chambers by 29 October and clearance and grazing rates also decreased in most chambers to a range of F= 0.12 to 0.30 $\mu l\ d^{-1}$ and ingestion rate I= 50 to 68 bacteria h^{-1} or 1200 - 1680 bacteria d^{-1}. The second growth period of 2-5 November was characterized by increased diversity and size of heteroflagellate species. Grazing and clearance rates at both stations increased from 80 to 100 (ave. 92 $\pm$14; F= 0.44 $\mu l\ d^{-1}$) in those chambers dominated by pointed bodies and large bodonid forms (100 - 200 μm^3). Rates in chambers containing smaller forms ranged between 40 to 60 bacteria h^{-1}; F= 0.28 $\mu l\ d^{-1}$. Medium and large-sized bacteria, particularly cyanobacteria, decreased considerably in all chambers during 3-5 November after a 24 hour period of active growth and grazing in all chambers during 3-5 November (Fig. 7 and Table 2). Bacterial biomass also decreased but total numbers during this interval remained at ambient levels; perhaps because of actively growing smaller to medium-sized bacteria.

April 1983 Growth and Grazing Experiment

Initial environmental conditions of April 1983 were typical of spring warming trend with daily average temperatures of approximately 15°C. Temperatures were similar to the autumn period, but salinities were considerably lower due to increased rainfall of previous months. Salinity regime of Virginia estuaries indicated a greater than average intrusion or extension of freshwater downstream. Spring nutrient concentrations were slightly higher than summer values though not as elevated as those measured during the autumn period. Bacteria concentrations increased above the winter low of 2-4 x 10^6 to 4-8 x 10^6 cells ml^{-1} range during April sampling.

Table 2. Growth and grazing rates of heteroflagellates (predators - P) at the marsh and mudflat stations during autumn and spring transitional periods. Growth, clearance and ingestion rates are mean values of in situ diffusion chamber experiments.

	HETEROFLAGELLATE GROWTH										CLEARANCE	INGESTION	
Date	μh^{-1}	μd^{-1}	SD	SE	CV(%)	Range μh^{-1}	Dt (h)	P	Amb B	B	$\mu l\ d^{-1}$	Bh^{-1}	Bd^{-1}
AUTUMN 1982													
28 October													
Marsh	0.049	1.17	0.40	0.18	34.2	0.040-0.079	14.1	3.70	3.87	3.50	0.45	74	1776
Mudflat	0.055	1.34	0.37	0.17	27.1	0.031-0.069	12.7	3.30	3.79	3.93	0.61	92	2218
4 November													
Marsh	0.065	1.55	0.63	0.26	40.7	0.031-0.102	10.7	19.90	5.38	3.88	0.32	70	1680
Mudflat	0.049	1.18	0.33	0.13	28.0	0.032-0.070	14.1	8.49	6.50	4.53	0.48	74	1776
SPRING 1983													
16 April													
Marsh	0.032	0.76	0.03	0.01	3.3	0.014-0.064	21.7	--	4.53	5.27	0.26	57	1344
Mudflat	0.040	0.97	0.45	0.17	46.5	0.021-0.068	17.3	17.26	4.04	7.72	0.27	80	1920
21 April													
Marsh	0.063	1.51	0.03	0.01	1.7	0.031-0.095	11.0	30.50	4.19	5.65	0.29	95	2280

μ - heteroflagellate growth rate (h - hour; d - day)
SD - standard deviation; SE - standard error; CV - coefficient of variation
Dt- doubling time (hours)
P - maximum density (x 10^3 cells ml^{-1}) of heteroflagellate during growth in diffusion chambers
Amb B - ambient bacteria (x 10^6 cells ml^{-1})
B - chamber bacteria density (x 10^6 cells ml^{-1}) during heteroflagellate growth
Clearance - volume of water cleared per flagellate per day
Ingestion - bacteria consumed per hour (h) or per day (d) per flagellate

Intensive sampling bracketing mid-day (April 13) low tide cycle revealed a large daily temperature range (12 - 22°C), a pulse of hetero- and phytoflagellates (including high numbers of cryptomonads), chlorophyll a, unattached bacteria, gametes, and a peak in glucose. These peaks were particularly evident (Fig. 9) during period of afternoon low water and warmer temperatures at marsh tidal pool site. During April 18 (bracketing both low and high tide) most nutrient parameters were low (except for NO_3^-) as temperatures and salinities fell markedly with evening snowfall. Anomalous weather conditions represent transition period variability. Within 48 to 60 hours warming trend and periods of low extended tides resumed with a recurrence of low tide nanoplankton assemblage. Nanoplankton populations and chamber growth dynamics reflected ambient patterns.

Bacteria Growth

Daily sampling indicated bacteria decreased during periods of low temperature and higher water (tides) but demonstrated rapid recovery with increasing temperature. Growth rates varied between 0.024 and 0.081 h^{-1} but most rates fell between 0.027 and 0.055 h^{-1}, averaging μ= 0.032 h^{-1}. During the 13 - 17 April period medium and large size (0.22 to 0.7 μm^3) bacteria were abundant. Growth rates ($\sim$<0.03 h^{-1}), size distribution, and abundances in 1.0 μm control chambers decreased with decreased temperatures and salinities of 18 - 20 April. Bacteria populations shifted again with an increase in both medium and large size component including cyanobacteria (>0.3 μm^3) and abundant fine dust (very small bacteria VSB, <0.1 μm^3). Growth rates increased slightly ($\sim$<0.06 h^{-1}) as

temperatures and salinities returned to normal during periods of extended low water.

Heteroflagellate Growth

The initial heteroflagellate assemblage of the mudflat growth and grazing chambers was composed of an assemblage of three different types and sizes of monads and bodonids, abundant in ambient at low tide. Growth patterns demonstrate variability in time course and magnitude of growth response (Fig. 8). Initial growth at the mudflat began either at a slow rate $\mu = 0.021 h^{-1}$ or at relatively high rates (range $\mu = 0.036\ h^{-1}$ to $0.062\ h^{-1}$) following a 24 to 48 hour lag phase. Growth coincided with increased numbers of mixed sizes of bacteria in chambers. Mudflat chambers demonstrate two periods of growth (Fig. 8). The second period of growth was characterized by relatively rapid growth of more than one division per day and high yield in heteroflagellate cell numbers and biomass. The levels exceeded the annual ambient range. The increase of relative sizes and species diversity of HNANO in mudflat chambers (mimicked) increases observed in isolated tidal pools during low tides of the spring transition period. Sizes ranged from 15 μm^3 of small monads and bodonids to 75 μm^3 of larger bodonid and Paraphysomonas-like forms, but was dominated by 30 μm^3 choanoflagellate and monad-like forms.

The high HNANO growth rates and cell yield in mudflat chambers also occurred during a period of decreasing temperatures (16-21 April). Low temperatures apparently had little adverse affect on heteroflagellate growth rates although ambient bacteria abundances and growth rates decreased during 18-20 April (Fig. 8). Peak heteroflagellate growth coincided with greater ambient HNANO abundances. The decrease of

Figure 8. Temperature, salinity, autotrophs, and heteroflagellates versus bacteria densities for in situ diffusion chambers and for ambient populations during 13-23 April 1983 at the mudflat station.

APRIL 1983

HETEROFLAGELLATES, AUTOTROPHS AND BACTERIA

MUDFLAT STATION 2

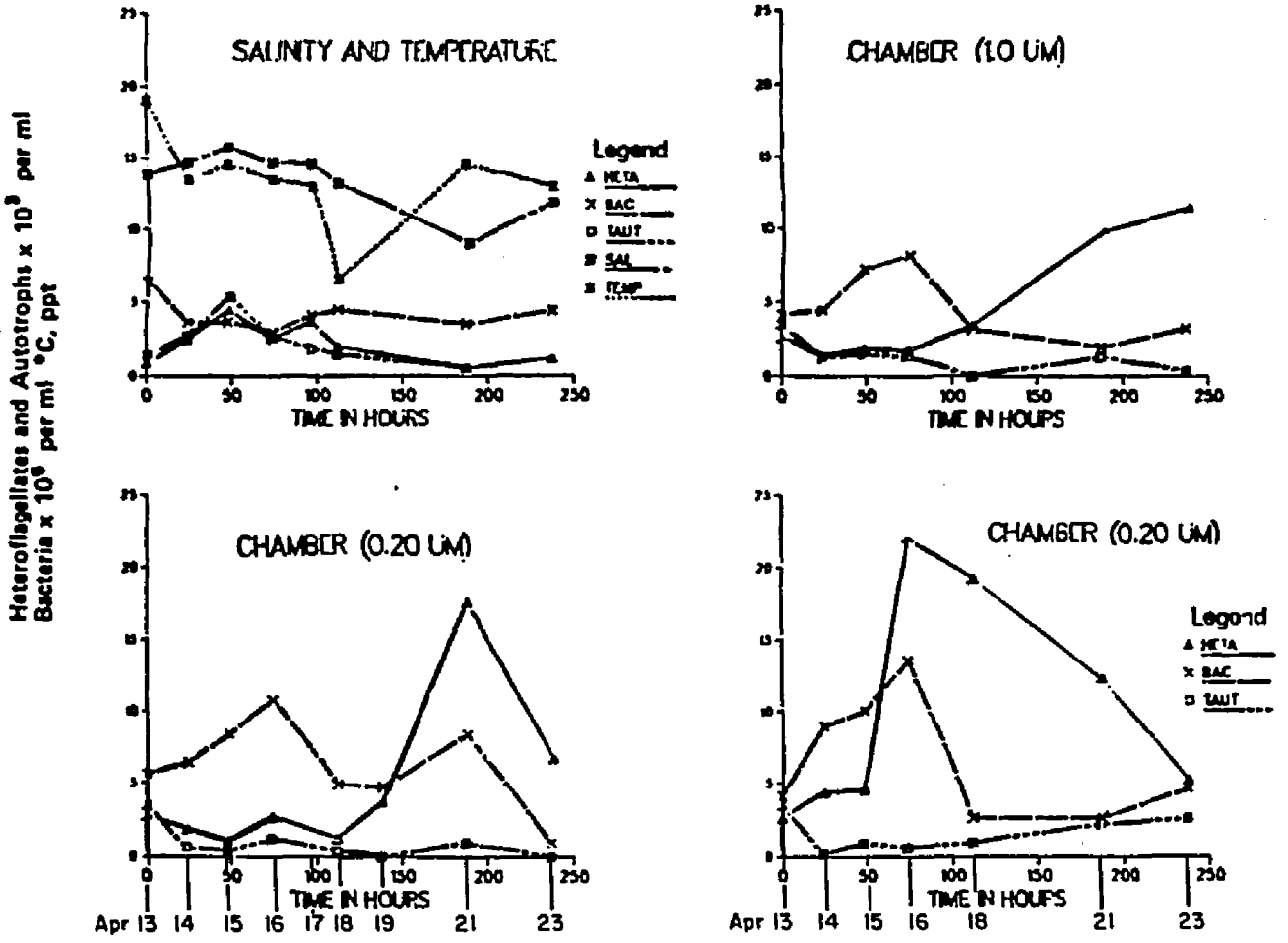

bacteria in chambers relative to ambient indicated possible grazing effect (Fig. 8). However, as in the autumn experiments, the high heteroflagellate densities and increasing biomass remained elevated even at relatively low bacterial concentrations. Figures 9 and 10 show that that heteroflagellates eventually decrease in 0.20 µm chambers but rather the 'crash' in the classic predator-prey cycle, return to concentrations typical of the ambient range. concentrations typical of ambient range. Reduced bacteria levels quickly recovered to levels typical of the upper ambient range within 24 hours of HNANO decrease.

The 1.0 µm chamber incubated at the mudflat station (Fig. 8) reflected ambient fluctuations in HNANO until 16 April when increased densities indicated slow growth (μ= 0.025h^{-1}). The 1.0 µm growth curve shows continued growth throughout the period of maximum environmental HNANO concentrations. HNANO densities achieved during the incubation, although slightly less than 0.20 µm chambers, were much higher than in the ambient. Species composition increased to include larger species. Choanoflagellates densities increased concurrently, during the maximum growth period (18 - 21 April), with increases in ambient (tidal pool, 21 April) and 0.20 µm chamber populations. Bacteria decreased slightly in comparison with ambient perhaps indicating grazing impact. However unlike 0.20 µm chambers where HNANO numbers decreased significantly after 21 April, growth in 1.0 µm chamber continued through 23 April.

Growth curves from the first series of marsh chamber incubations begun 13 April 1983 reveal growth patterns similar to mudflat chambers (Fig. 9). These included lag periods and two periods of growth with an overall average for 13 - 21 April of μ= 0.032h^{-1}, Dt 22h; and maximum

heteroflagellate densities of 2 - 4 x 10^4 cells ml^{-1}. The marsh chambers contained a relatively large distribution of medium and larger sized bacteria typical of marsh pool at low tide. Increases in chamber bacteria concentrations to 6 to 8 x 10^6 cells ml^{-1} corresponded to increasing environmental concentrations. Initial heteroflagellate growth in chambers, ocurring without a lag phase, was relatively slow (ave. μ=0.02, Dt 33h, k=0.67d^{-1}) and perhaps was most representative of ambient HNANO rates. Increased growth (range μ= 0.027 to 0.068 h^{-1}) occurred in 0.20 µm and 1.0 µm chambers between 15 and 18 April. This second growth period, characterized by increased densities,size, and diversity of heteroflagellate assemblage (1.2 to 2.5 x 10^4 cells ml^{-1} - Table 2), occurred in synchrony with growth in mudflat chambers and increasing ambient concentrations. HNANO concentrations were much greater (5 to 10 times) than ambient after 3 to 5 days of growth (16 April, Fig. 10). Heteroflagellate grazing impact, as in mudflat chambers, is evident in marsh curves (Fig . 9) where 0.20 µm chamber bacteria populations remain considerably below ambient levels. Flagellate densities also decreased following the decrease in bacteria densities but continued to fluctuate slightly above ambient levels.

The environmentally representative populations and conditions of 1.0 µm chambers are particularly evident through comparison with marsh ambient graphs (Fig. 9). Bacteria concentrations in 1.0 µm chambers reflect fluctuations in ambient daily pattern. Changes in growth rates correspond to temperature and salinity changes during the incubation period. The first series of 1.0 µm chambers initiated 13 April demonstrated either a lag phase to slow growth (μ= 0.014 to 0.018 h^{-1}) in

Figure 9. Temperature, salinity, autotrophs, and heteroflagellates versus bacteria densities for in situ diffusion chambers and for ambient populations during 13-23 April 1983 at the marsh station.

APRIL 1983

HETEROFLAGELLATES, AUTOTROPHS AND BACTERIA

STATION 1 MARSH

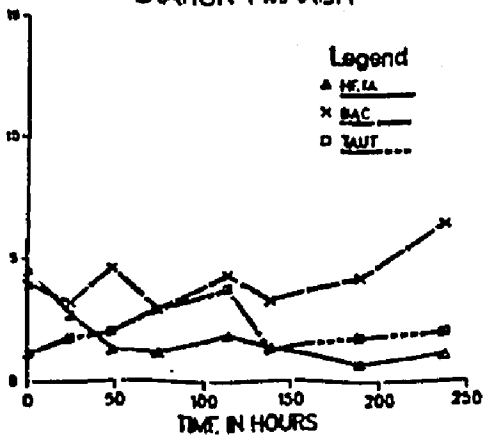

STATION 1 MARSH

SALINITY AND TEMPERATURE

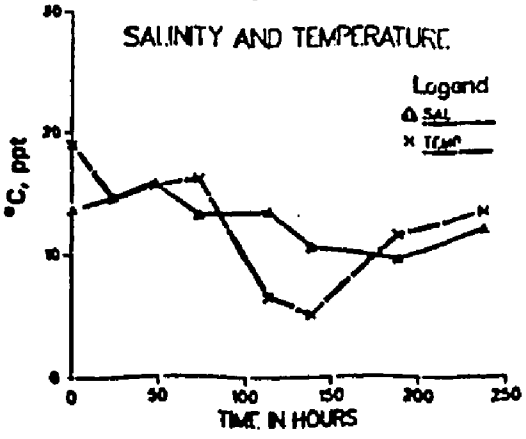

Heteroflagellates and Autotrophs x 10^3 per ml
Bacteria x 10^6 per ml

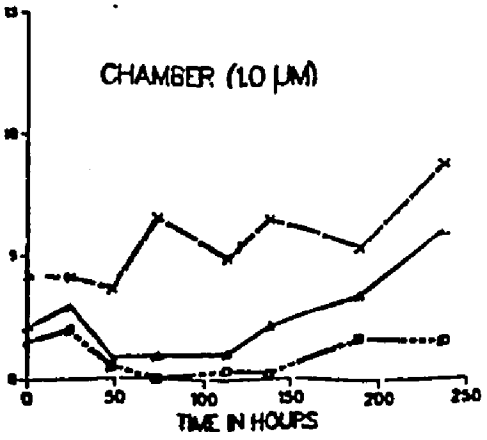

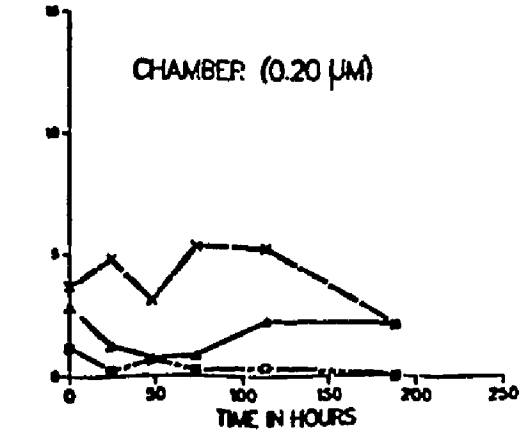

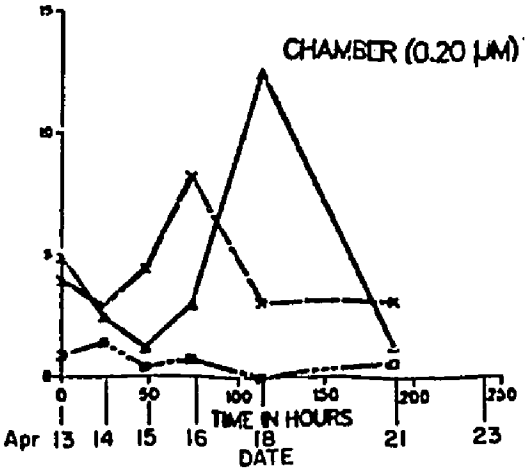

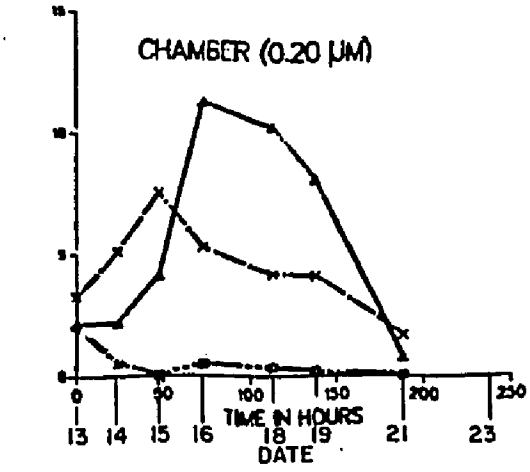

the first 48 hours. The decrease in HNANO numbers in reflected the ambient decrease in marsh populations at low water. Growth rates of at least one division per day (μ= 0.028 h^{-1}, Dt ~24h) were coincident with an increase in marsh pool HNANO numbers during 16 - 19 April period. In contrast to 0.20 µm chambers the increase of bacteria in marsh 1.0 µm chambers continued to mimic ambient patterns and supported continued heteroflagellate growth through the entire incubation.

The second series of chambers (1.0 µm) was initiated on 18 April during a period of low temperature. Growth began without a lag phase at relatively high rates (μ= 0.031 and 0.063 h^{-1}), and was synchronous with the second growth period of the first series of 0.20 and 1.0 µm chambers. HNANO in the second series 1.0 µm chambers were dominated by two forms typical of early growth stages in chambers. Sizes (cell volumes - 15 to 50 μm^3) increased slightly as HNANO numbers increased above ambient levels. The subsequent decrease in marsh HNANO populations was due perhaps to stress of reduced salinities and large temperature ranges) and change in ambient bacteria assemblages. Accelerated growth (μ= 0.062 and 0.105 h^{-1}) in these chambers corresponded to an increase in environmental HNANO and increase in numbers and diversity of bacteria at the marsh pool during a period (21 - 23 April) of increasing temperatures, salinities, and duration of low water. Rapid heteroflagellate growth in 1.0 µm chambers also occurred in synchrony with ambient bacteria growth and with an increase in abundance of larger rod-shaped bacteria and cyanobacteria and increase in abundance of fine dust (VSB <0.10 μm^3) bacteria.

Ciliates and amoebas appeared in only one chamber (Fig. 9, 1.0 µm chamber); concentrations of 20 to 40 cells ml^{-1} were detected late in the

incubation. Initial growth under predation pressure by ciliates and/or amoebas at concentrations of less than 20 per ml was relatively slow (μ= 0.014 to 0.028 h^{-1}). HNANO concentrations in this 1.0 µm chamber reached levels several times greater than ambient although the increase was more gradual than in other first series chambers. The HNANO concentrations continued to increase steadily to the end of the sampling period (23 April) (even with concentrations of 20 - 40 ciliates ml^{-1}) while bacteria reflected ambient pattern of increase. This may be contrasted with other chambers (Figs. 8, 9) where bacteria decrease (significantly) and heteroflagellates return to ambient levels. Thus the 1.0 µm chamber containing ciliates (which graze both bacteria and heteroflagellates), appears most representative of environmental populations.

Grazing

Grazing and clearance rates measured in mudflat chambers were similar to marsh rates although more variable during initial stages of growth. Rates could be divided into two different ranges. The lower range of approximately 33 - 65 bacteria h^{-1} may be typical of ambient populations. A significantly higher range of grazing rates of 90 - 120 bacteria h^{-1} may be typical of in situ grazing experiments. Clearance rates were also variable, ranging between 0.126 - 0.35 µl d^{-1}, with an overall average of 0.2 µl h^{-1}. Grazing rates did not vary with change in growth rates but frequently corresponded with change in heteroflagellate species composition and types of bacterial prey. During slow growth phases, the average grazing and clearance rates varied from I= 43 h^{-1} and F= 0.20 µl h^{-1} to I= 107 h^{-} and F= 0.325 µl h^{-1}. As growth accelerated,

grazing rates did not always increase porportionately; for example, a chamber with the highest growth rate demonstrated low to medium grazing rates.

The range of clearance rates (F= 0.13 to 0.33 µl d^{-1}, ave. 0.27 µl d^{-1}) and grazing (35 - 85 bacteria h^{-1}, ave. 56 bacteria h^{-1}) rates for marsh chambers were similar to mudflat chambers though less variable. High grazing rates (90 to 100 bacteria h^{-1}) occurred in later stages of growth. Grazing activity also corresponded more closely with changes in species composition and available prey (types and sizes of bacteria) than with varying growth rates. As heteroflagellate diversity and biomass increased to include larger forms (particularly large bodonids), grazing rates increased in some chambers. One chamber containing a large percentage of a small form resembling Pleuromonas jaculans produced a lower grazing rate (30 -36 bacteria h^{-1}; F=0.137µld^{-1}) which is consistent with the predicted low species-specific clearance rate for P. jaculans (Fenchel 1982b). Grazing rates increased considerably (average 95 bacteria h^{-1}) during a period of rapid growth from 21 - 23 April, reflecting the increased abundances of bacteria and availability of different types of bacterial prey including cyanobacteria.

Grazing impact on bacteria or decrease in bacteria below ambient levels as a result of heteroflagellate grazing pressure can be assessed easily from comparison of chamber and ambient plots. Epifluorescence direct counts of bacteria in 0.20 µm chambers at both stations revealed similar pattern of decrease of larger and medium sized bacteria during periods of growth and grazing. However chamber plots show no grazing impact until heteroflagellates reach densities of 3 to 10 times that of

ambient. Bacteria concentrations seldom dropped below the lowest range of environmental abundances and quickly recovered to ambient levels when heteroflagellate abundances returned to normal (ambient ranges). Levels of bacteria in 1.0 μm chambers continued to reflect ambient fluctuations in growth even when actively growing and grazing heteroflagellate populations reached densities greater than ambient concentrations. Epifluorescence analysis showed no evidence of heteroflagellate ingestion of autotrophs. The graphs did not reveal any pattern of decrease of chamber autotrophs (Figs. 8, 9) which could be related to heteroflagellate abundances or grazing activity. Autotrophs (species and numbers) fluctuations corresponded to ambient patterns (Figs. 8, 9) and occasionally increased concurrently with heteroflagellates. The plots of bacteria densities and grazing rates indicate heteroflagellates in the marsh-mudflat system potentially consume large numbers of bacteria, however with little grazing impact (or grazer control) on the total bacterial population.

DISCUSSION

A seasonal survey of short term variability, both daily and hourly, of nutrient concentrations, nanoplankton populations and in situ predator-prey interactions in an estuarine marsh-mudflat system revealed the dynamic nature of nanoplankton populations during early autumn and spring periods. Overall, both periods exhibited similar ranges in temperature (10 - 25°C), and nanoplankton abundances (HNANO range of approx. 0.5 - 5.0 x 10^3 cells ml^{-1}). Although bacteria abundances were intermediate to low, heteroflagellates relative abundances were greatest during the autumn, spring transition periods. Frequent sampling was necessary to reveal short-term patterns of autumn NO_2 maxima and large variability in nanoplankton population and dynamics. Fluctuations in heteroflagellate abundances over a daily tidal cycle were frequently of greater magnitude than those observed over weekly or monthly time scales. Intensive sampling during both autumn and spring supported previously observed phenomena of nanoplankton assemblages in tide pools during low water. Short-term peaks of diverse heteroflagellate and bacteria populations were observed in tide pool environments.

In situ diffusion chamber experiments during autumn and spring periods indicated that high growth rates and high densities of heteroflagellates corresponded to periods of increased ambient heteroflagellate populations. Periods of chamber growth were concurrent with increased bacterial growth or change in species composition. Both chamber and ambient heteroflagellate abundances and activity during

autumn and spring transition were as great as those measured in the summer when temperatures and bacterial numbers were greater. Mass occurrence of cells and accelerated growth occur as frequently as in the summer. Clearly, annual heteroflagellate population patterns in shallow water environments can not be attributed simply to seasonal patterns in bacterial abundance or temperature variation.

Bacteria Growth

Bacteria growth rates were similar for both fall and spring (0.032 h^{-1}; Dt ~24 h) with pulses of more rapid growth of μ= 0.05 - 0.09h^{-1} during cyanobacterial blooms of October and warming trends of April. The bacteria growth patterns suggest substrate limitation because, without grazing pressure, experimental chamber populations did not continue to increase after the first one or two doublings nor exceed maximum environmental maximum of 1.3 x 10^7cells ml^{-1}. The lack of grazing pressure may account for frequent stationary phases in the chambers (Iturriaga 1981, Christian et al. 1982, Ferguson et al. 1984, Taylor et al. 1985). Without grazer control of bacterial abundances, environmental (DOM) substrate concentrations can be depleted quickly at normal growth rates or after two doublings (Ammerman et al. 1984, Haagstrom et al. 1984). Weekly or daily sampling during both autumn and spring transition periods also confirmed seasonal trends of lower growth rates with either decreased temperature and/or increased concentration of nutrients. During October decreased bacteria concentrations in the mudflat may result from a combination of decreasing temperatures and increase of NO_2^- to toxic levels. A decrease in autotroph population during October may be another factor contributing to the decline in bacteria. Increased

bacterial substrate limitation may result from decreased release of dissolved organic matter (DOM) by autotrophs (Wiebe et al. 1978, Davis and Sieburth 1984). However elevated nutrient and temperature conditions of marsh mudflat tidal pools may have promoted patchy distribution of cyanobacterial blooms (Paerl and Ustach 1982, Paerl 1985). Relatively high nitrogen (NO_2^-, NO_3^-) imported from the river (Galvao 1984), and extended periods of low water in tidal pools with associated elevated temperatures provided optimum conditions for cyanobacteria growth. This phenomenon was reflected in chambers which also provide an optimum (high nutrient, quiescent) environment; cyanobacteria flourished in aggregates with heteroflagellates.

Heteroflagellate Growth

Growth in chambers (Figs. 7-9) during each fall and spring transition period was variable at the start of incubations, typical of previous diffusion chamber experiments (Chapter 3). This is largely due to variability induced by tide and patchy distribution of nanoplankton populations at the initiation of incubation. During April the abnormal rapid decrease in temperature and subsequent decrease in salinity and autotroph populations may have contributed to the static populations of heteroflagellates in some chambers. Environmental variability, rapidly shifting ambient nanoplankton populations, and variation in chamber population growth suggest in situ rates may change quickly over a short period. Growth rates during both periods ranged from an average of one doubling per day to accelerated rates of 2 to 3 doublings per day. Growth may start at a fairly rapid rate, 1.5 to 2 doublings or divisions

per day, if optimum conditions such as food resources exist at the beginning of the incubation.

Heteroflagellate populations in chambers often demonstrate two phases of growth as evident in April chamber plots (Figs. 8, 9). The initial lag phase or slower rates ranging from μ= 0.02 to 0.035 h^{-1}, and average doubling times of 24 hours or greater is perhaps characteristic of ambient unstable conditions (Fenchel 1982d, 1985, Furnas 1982b, Sherr et al. 1984, Davis et al. 1985, Chapter 3). Heteroflagellates in both the environment and initially, in diffusion chambers are characteristically smaller and less robust in appearance (Fenchel 1982a,c; Fritz unpubl. man.) than well-fed laboratory cultures grown with an abundance of cultured bacteria (Ammerman et al. 1984, Ferguson et al. 1984). A lag phase in growth may result from handling disturbance of innoculation or may indicate food-limitation. Divisions may not occur until after several hours after active grazing. Ensuing rapid divisions may indicate adaptation to a more favorable environment where food-limitation is no longer a factor.

A second phase of increased growth, observed in chambers during both transition periods, suggest that heteroflagellates have acclimated to chamber conditions. Chambers represent specialized conditions of the tidal pools at low water where advection effects are removed and microniches are more stable. A second phase of chamber growth is also characterized by increased diversity and size of heteroflagellates similar to that observed in situ during periods of extended low water. Autumn and spring low water periods also were characterized by diversity of food sources including cyanobacteria and, in April, gametes of molluscs. However

heteroflagellate densities achieved in the chambers were much greater and were sustained longer than those of ambient tidal pools where blooms are disrupted by advection effects.

The higher growth rates and densities observed during the transition periods in the marsh-mudflat diffusion chambers were similar to those determined by Sherr and Sherr (1983) in laboratory incubations at environmentally representative temperatures. Rates were not as high as those reported by Fenchel (1982a,b) however Fenchel's cultured organisms were fed larger bacteria (0.66 μm^3) and at densities much higher (10^7 to 10^9 cells ml^{-1}) than occur in the Virginia marsh. The full range of in situ rates for different growth phases in both spring and autumn coincided instead with Fenchel's (1982d) estimated range of growth rates derived from environmental observations.

Variability

Observations of growth and grazing activity (Figs. 7-9; Tables 1 and 3) for both spring and fall incubations demonstrate great variability in rates in the marsh-mudflat system. During October, variability in growth response may be attributed to a combination of unusual nutrient conditions relative to previous months and the presence of dense cyanobacteria assemblages. The autumn ambient and chamber nanoplankton assemblages initially contained large heteroflagellates forms (Paraphysomonas) which, from microscopic observations, were actively digesting cyanobacteria. Cyanobacteria aggregates provide an optimum food source because their large size, mucoid sheaths, including bacterial associations, and clumped distribution facilitate efficient feeding (Fenchel 1982a, Paerl 1983, Landry et al. 1984, Gast 1985). Their

presence may have promoted the initial pulse of growth by the large heteroflagellates in chambers. The unusually high and potentially toxic levels of NO_2 and decreased bacteria populations particularly in mudflat chambers, may have contributed to the subsequent decline of heteroflagellates during the last days of October.

The optimum growth period for chamber populations occurred during the second interval (2-5 November) when heteroflagellates also reached maximum environmental concentrations during periods of extended low tide. Nanoplankton abundances in tidal pools and chambers may reflect the decreased NO_2 levels and increased temperatures and bacteria assemblages, particularly cyanobacteria blooms, surface films and quiescent tide pool environments. Autumn chambers were characterized by proliferation of aggregates composed of very large cyanobacteria (Anacystis, Microcystis, Agmenellum), and many larger heteroflagellate (75 - 125 μm^3) forms. Chamber heteroflagellate rapid growth and increase in size and diversity indicated an opportunistic response or rapid selection for larger forms dependent on available types of prey. Heteroflagellate growth curves during rapid cyanobacterial growth indicated the possible suppression of heteroflagellate growth for a short period; however, a diverse assemblage of large heteroflagellates capable of ingesting cyanobacteria subsequently developed within less than 24 hours. Rapid development of this assemblage demonstrated the great potential for rapid recovery and growth and the opportunistic grazing response of heteroflagellates.

Data from April revealed even greater variability between chambers from marsh and mudflat stations than evident in autumn. Maximum growth occurred within the 2nd through the 4th day of the April incubation. The

presence of heteroflagellate predators, e.g., ciliates and amoebas, may account in part for variability in estimated growth rates, however predators (amoebas) were detected in only one chamber at the initiation of the experiment and bactiverous ciliates appeared only towards the end of one out of eight chamber incubations. The role of predators in contributing to irregular population abundances or actual decrease of heteroflagellate populations was limited due to low concentrations (<40 predators per chamber or <10 cells ml^{-1}) during April chamber experiments.

Anomalous weather conditions occurring mid-incubation, from April 18-20, introduced additional variability into an already variable and complex time scale (tidal, diel, and daily); this affected nanoplankton dynamics. The normal warming trend of spring was interrupted by a snowstorm. The severe decrease in temperatures and salinities (Fig. 14) appeared to decrease activity and abundances of phytoplankton and limit growth of bacterial populations. However, as in previous experiments, HNANO were both euryhaline and eurythermic. The HNANO grew at relatively high rates while maintaining relatively high concentrations throughout the April period.

Predator-Prey Interactions

Environmental monitoring of HNANO in the shallow estuarine tidal system on a weekly basis did not reveal any seasonal cycles in heteroflagellates or bacteria concentrations (Chapter 2). Sinusoidal or lagged oscillatory prey-predator cycles were not observed during the finer time scale sampling (tidal- 2 hour intervals and weekly - daily

intervals). Tidal cycle sampling also revealed that the bacteria fluctuated independently of heteroflagellate abundances at all stations. During a tidal cycle, peaks in heteroflagellate densities corresponded most closely to formation of low water tidal pools rather than to peak concentrations of bacteria; heteroflagellate concentrations decreased quickly with flooding tides. Daily fluctuations of nanoplankton populations demonstrate that bacteria and heteroflagellate densities vary independently of each other over a 7 to 10 day period. However bacteria responded to varying nutrient and temperature conditions were observed on a time scale of days. The decrease, observed in autumn, of heterotrophic bacteria component and increase in cyanobacteria, corresponded to an increase in the level of nitrogen. These conditions are similar to those associated with the cyanobacteria bloom formation observed by Paerl (1982, 1983, 1984) in various N.C. estuaries. Ambient bacterial abundances increased during both autumn and spring experiments when temperatures increased above 15 ^{o}C. Heteroflagellate peaks of greater than 2.0 x 10^3 cells ml^{-1} were short-lived (2 to 4 hr) and while bacteria concentrations remain elevated after 24 hours.

The plots of heteroflagellate (predator) and bacteria (prey) densities from in situ diffusion chambers revealed rapid heteroflagellate growth potential and an eventual grazing impact on bacteria. Rapid development of a heteroflagellate assemblage composed of larger forms during or following cyanobacteria bloom indicated the great potential for rapid growth, decline, and recovery on a time scale of 1 to 2 days. The rapid increase and decline in the achlorotic cryptomonad or "pointed body" densities also was typical of this ephemeral species. The

predator-prey cycles observed in autumn and spring diffusion chambers (Figs. 7-9) indicate that HNANO generally increase within 24 hours or even concurrently with the increase in bacteria densities. The growth response is faster and the cycles different than the predicted models of a 5 to 10 day (2 offset peaks - sinusoidal) cycle described by several investigators (Pomeroy 1978, Fenchel 1982d, Laake et al. 1983, Wright and Coffin 1984, Anderson and Fenchel 1985, Davis et al. 1985) or the 3 to 6 day cycle for nanoplankton assemblages growing on decomposing Spartina in laboratory experiments (Newell et. 1983). The predator-prey cycle of cyanobacterial bloom and rapid heteroflagellate growth, observed in November chambers, demonstrated an opportunistic response by heteroflagellates to optimum prey on the time scale of < 2 days under relatively stable conditions.

April bacterial assemblages, in contrast to those of fall, were dominated by the heterotrophic components which are more typical of the seasonal marsh assemblage. The intervals of heteroflagellate growth and peak densities were sustained for a longer period than in autumn chambers. The April chamber data supports previous seasonal data (Chapter 3) indicated that heteroflagellates grow in response to or may be coupled to bacterial growth rates rather than relative or absolute bacterial abundance. Bacterial and heteroflagellate growth occurred concurrently and concentrations were, as in seasonal experiments (Chapter 3), positively correlated at the point of 50% growth (Sherr et al. 1983) or midway along the growth curve. At a certain point during the incubation bacteria growth was no longer measurable due to grazing by increased numbers of heteroflagellates. However simulataneous

bacteria growth in corresponding bacterial control (1.0 μm) chambers indicated that actively growing populations could sustain relatively high densities of HNANO. Coupling of bacteria and HNANO growth rates may account for maintenance of high HNANO abundances in the 0.20 μm chambers during periods of relatively low bacteria abundances.

The decrease in bacteria densities in 0.20 μm chambers indicated that grazing impact occurred only when heteroflagellates increased significantly above maximum ambient concentrations. However, when grazing impact was evident, bacteria densities did not crash or decrease by an order of magnitude as predicted by Fenchel's (1982d) models. Decrease of heteroflagellates in 0.20 μm chambers may be due in part to autoinhibition, i.e., when densities exceed carrying capacity of enclosed system. Heteroflagellate populations in 1.0 μm chambers continued to increase after populations in 0.20 μm chambers declined, even when bacteria densities were less by comparison. Conditions in 1.0 μm chambers and bacterial assemblages and activity were more representative of ambient due to greater exchange rates typical of 1.0 μm chambers. Similar to bacteria, heteroflagellate populations declined slowly, returning to ambient or still elevated levels while bacteria densities increased. Bacteria densities quickly recovered within 24 hours to ambient levels after grazing impact even while heteroflagellate densities remain above ambient. In some chambers bacteria decreased without concurrent increase of heteroflagellates, but instead reflected the ambient pattern. Bacterial densities in chambers, then, as in the environment, frequently fluctuated independently of heteroflagellate abundances.

Grazing

Several factors may contribute to variation in grazing rates of marsh-mudflat heteroflagellates including environmental conditions, abundance, size and species diversity of available prey and predator species-specific grazing rates. Grazing, similar to growth rates, during both autumn and spring transition periods could be divided into two ranges of rates characteristic of seasonal in situ chamber activity. The lower range of grazing rates (35-70 bacteria h^{-1}) was observed most frequently during the first growth period of 13 - 19 April 1983. The higher range (75-120 bacteria h^{-1}) however, corresponded to specific heteroflagellate species assemblages or types of bacteria observed in individual chambers, rather than periods of increased growth. Comparison of heteroflagellate growth and ingestion rates in each chamber during both autumn and spring transitional periods indicated that clearance rates of chamber heteroflagellates assemblages varied independently of their respective growth rate or maximum growth periods ($p > 0.05$). Low grazing rates may typify the unstable tidal environment where feeding is less efficient; high rates may indicate the potential response in specialized environment, e.g., presence of cyanobacteria aggregates, or species-specific clearance rates. Large aggregates comprised of cyanobacteria and heteroflagellates are conducive to more efficient feeding in terms of spatial scales in which HNANO operate.

Heteroflagellate clearance and ingestion rates varied greatly among chambers in each experiment even when chamber bacteria abundance and growth patterns remained virtually identical. Fenchel (1982a), through an analysis of the two feeding strategies of heteroflagellates, filtering

and contact, was able to relate clearance rates to size and abundance of bacterial prey. Clearance rates of filter feeders, such as of choanoflagellates characteristic of the marsh-mudflat system during spring nanoplankton blooms (Chapter 5), were affected more by size of prey than by numbers. Smaller prey resulted in lower clearance rates. Contact feeders, such as actively swimming bodonids and pointed bodies characteristic of autumn nanoplankton, were affected more by bacterial densities, although larger sizes of bacteria resulted in higher clearance rates and more efficient feeding(Fenchel 1982a). Clearance rates for natural mixed HNANO assemblages, besides varying with the dominant feeding type, will be influenced by a suite of environmental factors.

The present study showed no consistent correlation of increased grazing rates with increased number of prey. However, heteroflagellate ingestion of cyanobacteria during autumn and flagellated bivalve gametes during spring in ambient samples and grazing of the larger sized bacteria in chambers indicates selective or preferential grazing of larger prey. Higher ingestion rates occurred most frequently during blooms of cyanobacteria or large rod-shaped bacteria which was particularly evident in autumn chambers. This agrees with the suggestion that type and size of bacteria may directly influence grazing rates.

Variation in individual chamber grazing rates also may be explained in part by differences specific to each chamber HNANO species assemblage. Fenchel (1982c) measured clearance rates of different heteroflagellates using a relatively uniformly sized bacteria (Pseudomonad) culture and was able to establish characteristic rates for various heteroflagellate forms. In this study, higher rates usually

corresponded to a dominant type or size of flagellate; chambers in autumn period containing larger forms, e.g., large bodonid and large Paraphysomonas-type capable of ingesting several cyanobacteria at a time, were characterized by higher rates whereas in April 1983, chambers with medium-sized (35 μm^3) choanoflagellates, which are voracious cyanobacteriovores (Chretiennot, 1974) yielded increased rates.

Diffusion chamber results for both transition periods indicate that heteroflagellates are capable of consuming approximately up to ten to seventeen times their volume in 24 hours. However, neither diffusion chamber nor environmental monitoring data showed evidence of heteroflagellate populations controlling bacteria fluctuations. Estimations of daily bacteria consumption by environmental heteroflagellates should take into account lower average concentrations and semi-starved conditions due to environmental instability in comparison to chamber populations. Accordingly, calculations should be based on the lower range of ingestion rates determined in chamber experiments. Calculations or extrapolations to account for percentage of bacterial carbon or daily bacterial productivity ingested by heteroflagellates may use average volumes of environmental heteroflagellate and bacteria populations, and an assumed carbon content (i.e., $10^{-7}\mu gC\ \mu m^{-3}$- Landry et al. 1984). Values of carbon per volume of microbe found in the literature and used to calculate biomass vary considerably and may not reflect specific environmental conditions or physiology of the heteroflagellate species (Newell and Christian 1981, Fenchel 1982c).

Indirect calculations to account for bacterial productivity consumed

by HNANO are based on rates of HNANO growth, a conversion of increase in HNANO concentrations or volume to biomass, and the use of an additional factor, the assumed growth efficiency, usually of 30% or 33% (Pomeroy 1979, Fenchel 1982b, Sherr and Sherr 1983), to convert the HNANO biomass increase to mg bacteria C $m^{-3}h^{-1}$ or ug bacteria C $l^{-1}h^{-1}$. These calculations then introduce two potentially inaccurate factors. In addition, HNANO growth rates reported in the literature, frequently were determined in vitro or using techniques involving disturbance of the natural community (Fenchel 1982d, Sherr et al. 1984, Wright and Coffin 1984a,b) which generally contribute to higher rates than occur in the original environment. The percentage of bacterial productivity accounted for by heteroflagellate grazing can be calculated more directly by using experimentally determined growth rates to estimate bacterial production, and clearance and ingestion rates to estimate bacteria consumed per hour. These calculations also involve a conversion to account for bacterial carbon using an assumed or estimated volume of bacteria and carbon content per volume. These assumptions may result in an estimate which is not specific to the type or nutritional state of the heteroflagellate assemblage and thus no longer account for the inherent variability possible in estuarine populations.

Values for ingestion rates bacterial consumption and corresponding percentages of bacterial carbon production consumed by heteroflagellates during autumn and spring, were calculated using the direct methods as described above. The volumes estimated for heteroflagellates ranged from 0.27 to 100 μm^3 and for bacteria ranged from 0.14 to 0.5 μm^3, and were converted to ugC using a conversion of 10^{-7} μgC μm^{-3}. The results of the

carbon flux calculations for heteroflagellate-bacteria trophodynamics presented in Table 3 indicate that heteroflagellates potentially consume 50 to 100% of bacterial standing crop or 1.5 to 6.0 x 10^6 bacteria cells per day. The experimentally determined grazing capacity of estuarine HNANO during fall and spring accounts for a large percentage of bacterial turnover in the marsh-mudflat system. In turn, the ambient bacterial production (85 - 317 $\mu gC\ l^{-1}\ d^{-1}$) will support several doublings or the estimated range of heteroflagellate production (22 - 98 $\mu gC\ l^{-1}\ d^{-1}$) based on growth and the experimentally determined heteroflagellate assimilation efficiency of 32%. The heteroflagellate ingestion rates, using bacterial growth rates and average volumes to estimate production of autumn and spring populations, account for 50 to 80% of daily bacterial carbon production (Table 3), or using the range of values of bacterial specific activity reported for estuarine environments (100 to 400 $\mu gC/l/d$ - Newell and Christian 1981, Ducklow 1983, Wright and Coffin 1984b, Kator et al. unpubl. man.), account for 30 to 100% of estimated bacterial productivity.

Calculations of carbon flux from bacteria to heteroflagellates based on carbon uptake determinations of bacterial productivity may lead to inaccurate estimates due to the large variation of bacterial productivity in a tidal system. For example, Newell and Christian (1981) found an order of magnitude difference in rates in a tidal marsh system on high and low tides. Values reported in the literature for cycling of bacterial productivity by heteroflagellates, then, may vary tremendously depending on several extrapolations and assumptions necessary for calculations involving standard (assumed) values for bacterial volumes,

Table 3. Bacteria and heteroflagellate trophodynamics (growth, production and grazing parameters) and calculations for carbon flux in heteroflagellate-bacteria food web. (* - cyanobacteria; ** - heteroflagellate assimilation efficiency = 32%)

	Date			
	28 Oct 82	3 Nov 82	16 Apr 83	22 Apr 83
I. Bacteria				
Population x 10^6 cells ml^{-1}	3.87	5.33 (0.5*)	4.53	4.19
Growth: uh^{-1}	0.027	0.095	0.035	0.055
Dt (h)	25.7	7.3	19.8	12.6
Production ug C l^{-1} d^{-1}	85	317	116	136
II. Heteroflagellates				
Population x 10^3 cells ml^{-1}	1.20	4.16	2.23	2.12
Growth: uh^{-1}	0.040	0.063	0.032	0.063
Dt (h)	14.1	10.7	21.7	11.0
Production ug C l^{-1} d^{-1}	12	31	7.5	7.1
Ingestion Rate bacteria d^{-1} flagellate^{-1}	1776	1680	1344	2280
Population Grazing Rate x 10^6 bacteria ml^{-1} d^{-1}	2.13	5.31 (1.0*)	3.00	4.83
III. Carbon Flux				
% Bacteria Standing Crop Consumed	55	99	57	>100
Bacterial Carbon Consumed: ug C l^{-1} d^{-1}	47	166	66	106
Bacterial Productivity Needed to Support Heteroflagellate Production ug C l^{-1} d^{-1} **	37.5	97.5	23.3	22.2
% Bacterial Productivity Accounted via Grazing by Heteroflagellates	53.3	52.4	56.9	77.9

carbon content, and rates of growth or productivity. Nevertheless, researchers using both indirect and direct methods to estimate grazing and production and carbon flux (Fenchel 1985, Heinbokel 1985, Landry et al.1984, Sherr and Sherr 1985, Wright and Coffin 1984) agree that heterotrophic nanoplankton grazing activity approximately accounts for the daily bacterial turnover or atleast 25 to 75% of the bacterial productivity in a variety of environments including oceanic, coastal, estuarine (salt marsh), and fjord.

Results of diffusion chamber experiments together with daily environmental monitoring demonstrated that heteroflagellate grazers, when fluctuating within environmental densities, did not reduce bacteria abundances. However bacteria growth in chambers, without heteroflagellate grazing pressure, indicated that environmental conditions supported only one or two doublings before bacteria enter stationary phase. Grazer control of bacterial populations by heteroflagellates may prevent substrate limitation which occurs with unrestricted growth. Recent studies have also demonstrated both tight coupling of bacterial and heteroflagellate growth rates and heteroflagellate nutrient regeneration and bacterial uptake (Taylor et al. 1985, Van Wambeke and Bianchi 1986). Nutrient regeneration by heteroflagellates, during grazing and active growth, may also serve to stimulate bacteria growth. Activity or presence of heteroflagellates apparently maintains bacteria in youthful stage of growth as suggested by results of recent micro-zooplankton grazer studies (Christian et al. 1982, Stoecker et al. 1983, Wright and Coffin 1984, Turley and Lochte 1985, Taylor et al. 1985). Short-term sampling is necessary in order to

elucidate the role of HNANO in the dynamic estuarine system particularly to further document coupling of HNANO and bacteria growth rates.

During both transition periods, pulses of growth occurred most frequently during growth of larger forms of bacteria or presence of cyanobacteria, particularly as aggregates. Recent investigations of nanoplankton dynamics have involved discussions or speculations on the importance of microaggregates or bacteria-protozoan associations for rapid cycling and enhanced production of bacteria and grazing nanoplankton (Azam et al. 1983, Ammerman et al. 1984, Sherr and Sherr, 1985). Epifluorescence analysis of the autumn diffusion chambers revealed the development of HNANO-protozoan-cyanobacteria aggregates and demonstrated that growth, grazing, and diversity of the HNANO assemblage was stimulated during their presence. The autumn experiments suggest that microaggregates play an important role in stimulating growth and grazing activity in nanoplankton trophodynamics. In situ diffusion chamber incubations using shorter sampling intervals should be an ideal methodology for observing the formation of microaggregates and resolving their importance in nanoplankton trophodynamics.

CHAPTER V

CHARACTERIZATION OF SPRING NANOPLANKTON ASSEMBLAGES USING ELECTRON AND EPIFLUORESCENCE MICROSCOPY

INTRODUCTION

Heterotrophic nanoflagellates (HNANO) are a dominant component of estuarine microzooplankton (Pomeroy and Johannes 1968; Sieburth et al. 1978; Sorokin 1979; Beers et al. 1980, 1982; Davis and Sieburth 1982) and are voracious grazers of bacteria (Haas and Webb 1979; King et al. 1980; Burney et al. 1981, 1982; Fenchel 1982 a,b,c,d; Sherr et al. 1982, 1983). The hypothesis advanced by Pomeroy (1974) that the major pathway of dissolved organic matter (DOM) through the aquatic food web is via DOM ---> bacteria ---> phagotrophic protozoans (HNANO) ---> ciliates or higher trophic levels is well accepted in subsequent literature (Sorokin 1978, 1981; Haas and Webb 1979; King et al. 1980; Fenchel 1982d; Sherr et al. 1982). However, there are few in situ studies characterizing seasonal assemblages of HNANO (Lackey and Lackey 1963; Beers et al. 1980; Davis 1982; Fenchel 1982 a,d) or their phagotrophic activity on actively growing bacterial populations in coastal and estuarine ecosystems.

The identification and quantitative analysis of the HNANO component of the total nanoplankton have been made more feasible recently by the development of electron photomicroscopy and epifluorescence direct count microscopy techniques (Leadbeater 1972a,b,c, 1974, 1975, 1981;

Thomsen 1973, 1979; Sieburth 1979; Davis 1982; Fenchel 1982a; Haas 1982). Most of the nanoplankton surveys focus on description and identification of scale-bearing flagellates (usually autotrophic nanoplankton, PNANO) and heterotrophic loricate choanoflagellates, the latter which can be diagnosed for the most part by siliceous surface structures easily observed under TEM, or SEM. There are however, little abundance and distribution data available for the areas most commonly surveyed, i.e. coastal waters of northern Europe, the Mediterranean, and boreal areas, because EM studies are unlikely to directly produce these kinds of data (Leadbeater and Manton 1976, 1981; Thomsen 1973, 1979, 1982; Hallegraeff 1983) and EM taxonomic studies have not generally been combined with other methods to produce numerical and distributional data.

Recent research implementing epifluorescence direct count microscopy, coupled with flourochrome dyes to distinguish between PNANO and HNANO components of the nanoplankton, have provided more accurate estimations of standing stock, biomass, and distributions of nanoflagellates in a few environments (Beers et al. 1982; Davis 1982, Fenchel 1982 a,b,c,d; Sherr et al. 1982, 1983). Except for a study involving cultured isolates from Narragansett Bay and Sargasso Sea nanoplankton (Davis and Sieburth 1984), these studies generally do not include both seasonal species identifications and standing stock information. Epifluorescence direct count and photomicroscopy techniques can be used only to document and differentiate among the basic types (not species) of HNANO and PNANO. Electron photomicroscopy provides the finer visual detail for identification but has not been

used in combination with epifluorescence techniques except for investigations of free-living and attached bacteria (Bowden 1977; Watson et al. 1977; Zimmerman 1977; Fuhrman and Azam 1980; Wilson and Stevenson 1980; Fuhrman 1981) and for cultured HNANO (Fenchel 1982a, Davis 1982).

In the present study, in situ chambers incubated in the marsh-mudflat system were utilized during spring bloom periods. Comparative epifluorescence and SEM photomicroscopic methods were employed to characterize the observed HNANO assemblages in terms of species composition and growth and grazing rates. Eleven species of Acanthoecidae choanoflagellates from these assemblages are described as new records for Chesapeake Bay and the presence of one Bicoecid is reported.

METHODS AND MATERIALS

Field Sampling

The marsh-mudflat site of the HNANO community dynamics study was located in a small, brackish (10 -22 ppt) tidal embayment (300 x 100 m) at Carmines Island, Virginia (37°17'N, 76°32'W) (Fig. 1). The embayment is connected to the York River by a narrow channel at one end, is bordered on both sides by a fringing Spartina alterniflora marsh and is fed by a tidal creek at the other end. Sampling station one (marsh) was located where the tidal creek enters the embayment forming a small marsh tidal pool at low water. Station two (mudflat) was located in the middle of a large shallow tidal pool formed in the embayment during low water. Diffusion chambers were suspended at the respective marsh and mudflat stations in shallow water reservoirs sunk into substrate; this arrangement simulated protected tidal pools typical of this cove marsh. A support structure consisted of a float mechanism that housed the chambers in open cages equipped with flow-through plexiglass baffles (Fig. 2). This structure allowed chambers to move vertically through the water column with tidal fluctuations, yet remain submerged during spring low tide. Diffusion chamber samples (2 ml) were taken daily at low tide (or more frequently) from sampling ports with syringes equipped with 22 gauge needles. Samples were preserved immediately in the field with a final concentration of 0.3% gluteraldehyde for epifluorescence direct count enumeration. Both chamber and concurrent environmental samples for analyses of ambient nanoplankton community and various physical parameters (temperature, salinity, nutrients) were taken at low water

Figure 1. Study site and station locations.

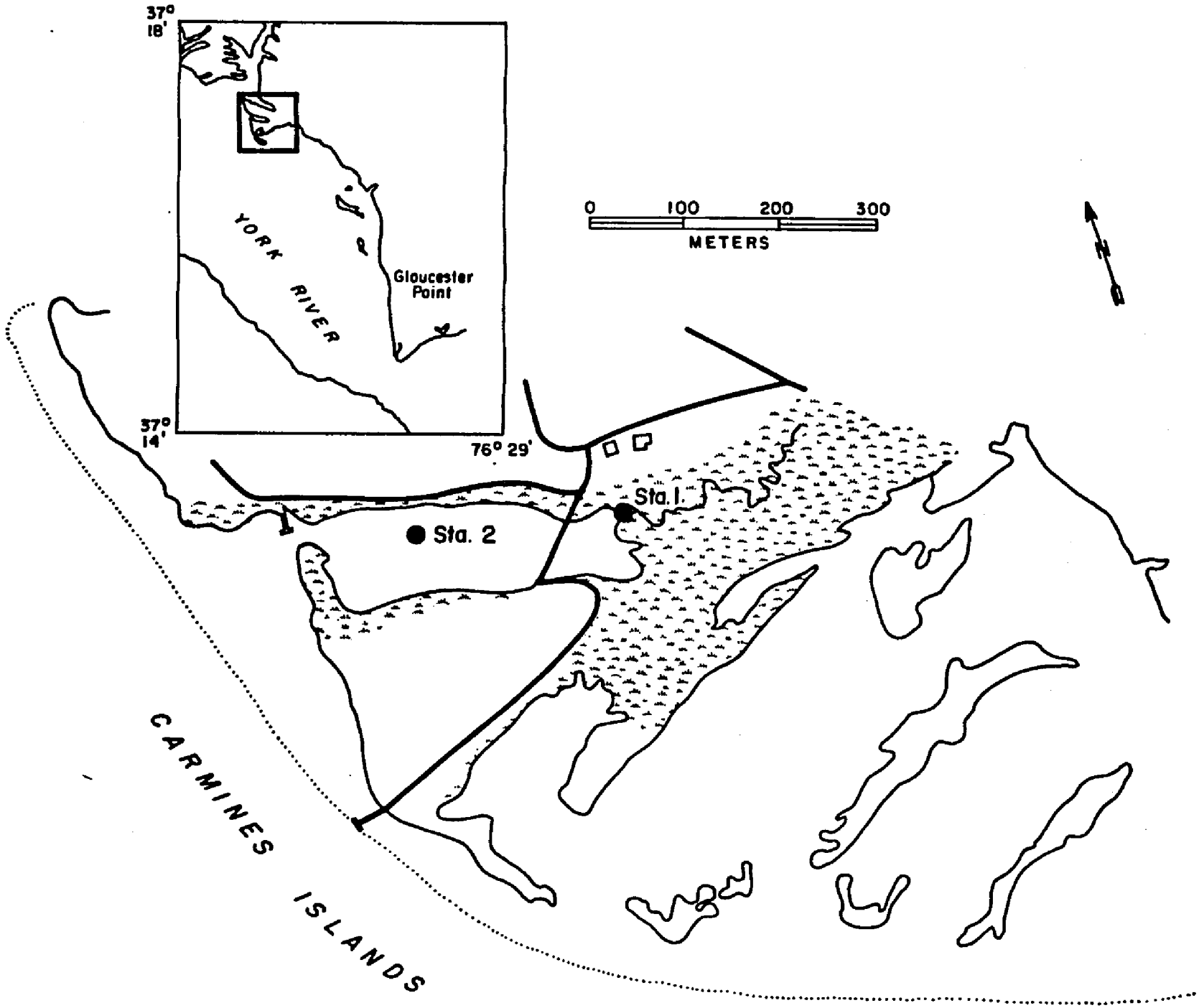
37° 18'
YORK RIVER
Gloucester Point
37° 14'
76° 29'
0 100 200 300
METERS
N
Sta. 1
Sta. 2
CARMINES ISLANDS

Figure 2. Diagram of diffusion chamber and support structure.

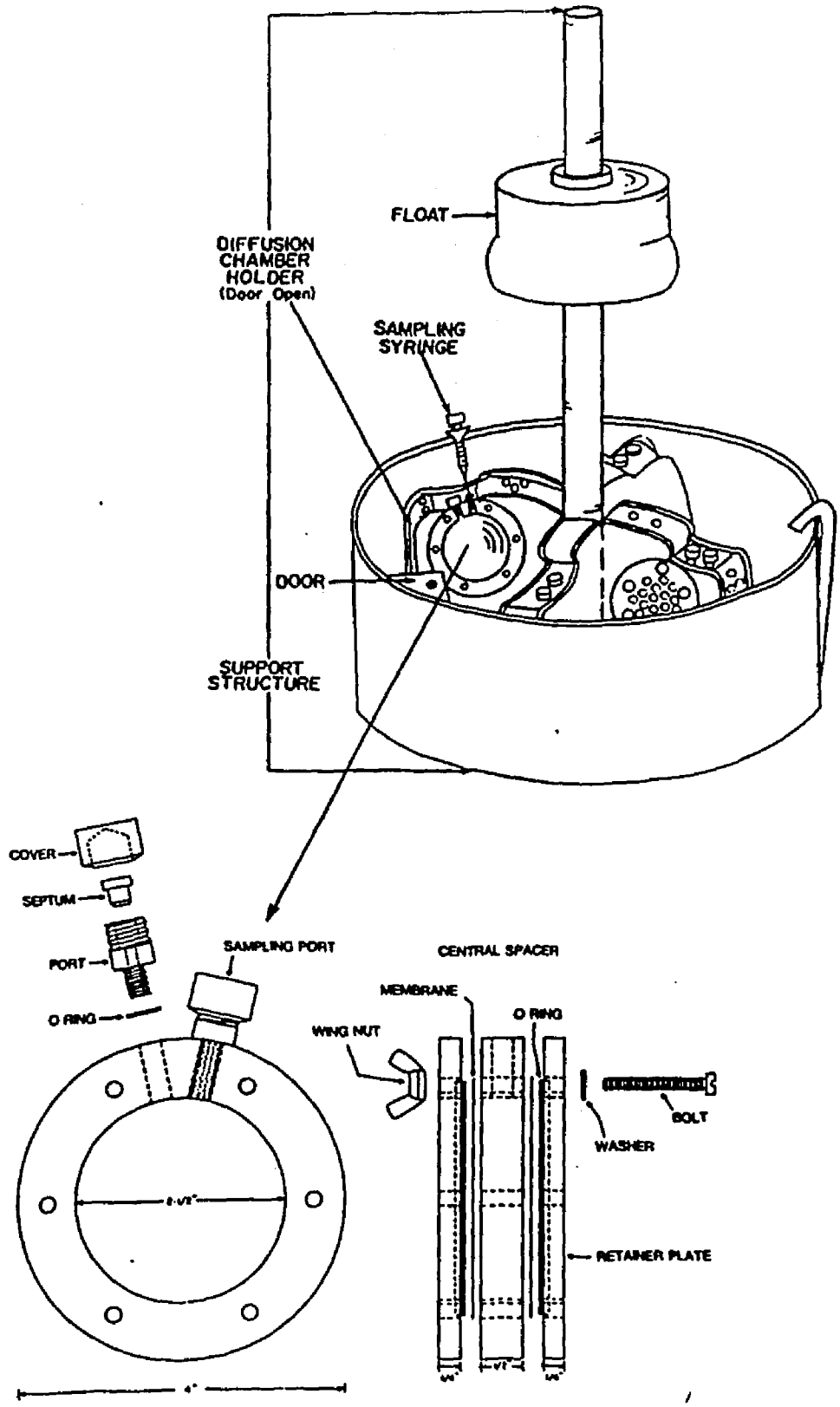

DIFFUSION CHAMBER

over a 7 to 10 day period (Chapter 3). Grazing rates of HNANO phagocytizing bacteria were determined using two different experimental approaches based on data from two different pore size series of chambers (Fenchel 1982b; Landry et al. 1984; Chapter 3). In situ diffusion chamber and daily environmental sampling at low water made possible evaluation of short term cycles in predator-prey interactions and correlation between bacteria and HNANO abundances.

Epifluorescence Microscopy

The method used is very similar to that outlined by Haas (1982). It is a modification of the acridine orange direct count technique (AODC) where proflavin is used rather than acridine orange as the fluorescent stain. The proflavin stain makes differentiation of heterotrophic and autotrophic species possible. Two ml samples, preserved with a final concentration of 0.3% glutaraldehyde, were stored at 4°C and later stained with proflavin. After staining, the sample is drawn onto an irgalen black prestained 0.20 µm Nuclepore membrane filter. The filter is then placed between thin films of low fluorescence immersion oil and between a glass slide and cover slip. Slides are observed with a Zeiss standard microscope equipped with a 12 volt, 100 watt tungsten-halogen lamp for epifluorescence, using a band pass 450-490 exciter filter, a FT 510 chromatic beam splitter and a long pass 528 barrier filter. The Planapochromat 100X, 1:4 NA oil immersion objective was used for counts of HNANO and bacteria.

Scanning Electron Microscopy (SEM)

A fixation technique involving a filter apparatus with Nuclepore filters, and a combined fixative (gluteraldehyde, acrolein, tannic acid) resulted in successful preparation of HANO, particularly loricate choanoflagellates. The final fixative concentrations were similar to those recommended by Van der Veer (1982) to fix small and delicate marine plankton and retain flagella for light microscopy. The method, derived from electron microscopic fixations, involved using centrifugation for rinsing and concentrating cells. The SEM fixation schedule presented here includes modifications of SEM and TEM methodology which incorporate the use of combinations of fixatives. It also involved gentle filtration onto large pore size Nuclepore filters (0.4 and 1.0 μm) to minimize cell disruption and yet obtain concentrations comparable to those observed with epifluorescence microscopy. At the end of the incubation, contents of the chamber were poured gently into sterilized glass screw-top test tubes and preserved. Samples prefixed with 0.5% glutaraldehyde for replicate epifluorescence counts and photographs may be stored at 4°C before SEM preparation. The prefix with glutaraldehyde was necessary before fixation with mixed 2% glutaraldehyde and tannic acid solutions (Murakami and Jones 1980). Prolonged prefixation for several hours with low concentrations of gluteraldehyde also helped eliminate the possibility of continued osmotic activity as well as provided replicate samples for epifluorescence microscopy.

Fixations were done at room temperature at pH 7.2. Combination of 4% glutaraldehyde with 8% acrolein, and 4% tannic acid (modified to

yield final fixation concentrations of 1.5%:2%:1% or 2%:2%:1%) for aldehyde fixation resulted in well-preserved flagella and other delicate structures. Acrolein penetrates cells and stops enzymatic activity quickly, rendering cells osmotically inactive and stabilizing glycoprotein. Tannic acid or tannin, an organic molecule (galloylglucose), is a mordant which enhances reactivity of molecules, especially for better staining with metals such as osmium. Not only does tannic acid facilitate osmium impregnation, but it helps prevent shrinkage during the critical point drying (CPD) step. Tannic acid will form precipitates in solutions, particularly in natural sea water where it complexes with peptides and polypeptides. Consequently cells and filters were rinsed thoroughly with buffer and distilled water before addition of (buffered) post-fixative 1% OsO_4 in 0.1M sodium cacodylate buffer and 0.2 μm filtered distilled water. Osmium is a good fixative for highly motile systems; it preserves most of the lipids and phospholipids which might otherwise be extracted during the alcohol dehydration. The osmium fix improves fixation of surface associated bacteria and yeasts and also prepares the specimen for TEM observation. The added advantage of the OsO_4 post-fix is that it imparts some conductivity to fixed specimens.

Specimens were dehydrated in a graded series of ethyl alcohol to 100% EtOH, encapsulated in BEEM capsules, and run through three changes of acetone. Samples in 100% acetone were critically point dried with liquid CO_2 in a model E300 Polaron C.P.D. and mounted on aluminum stubs with carbon paint (Dag 154). Stubs were coated with Au-Pd (150Å) in a vacuum evaporator at a vacuum of $5x10^{-7}$ torr. SEM photomicrographs were

taken with an AMR 1000 scanning electron microscope operated at an accelerating voltage of 20KV with a 200 um final aperture at 20^{o} to 45^{o} tilt.

Transmission Electron Microscopy (TEM)

Pellets of cells from diffusion chambers were obtained for whole mounts by centrifuging at 800 X g for 20 minutes. Pelleted cells were vapor-fixed in 2.5% glutaraldehyde with 0.1 M sodium cacodylate buffer for 90 minutes, followed by rinsing two times in buffer with 0.15 M NaCl after glutaraldehyde fixation (P. Mason, pers. comm.).

RESULTS

Choanoflagellates, particularly the family Acanthoecidae, and Paraphysomonas vestita are important components of Chesapeake Bay estuarine nanoplankton, and comprise a relatively large percentage of spring bloom heteroflagellate assemblages. Heteroflagellate blooms (concentrations > 4.5×10^3 cells ml^{-1}) dominated by choanoflagellates occurred in the marsh-mudflat tidal pool system at various times of the year. These blooms were observed frequently during mid to late spring (1981 and 1982) in low water tidal pool assemblages and occasionally during summer months, usually in association with diatoms in both seasons. The following figures and text present results of concurrent environmental monitoring and in situ diffusion chamber experiments of HNANO assemblages during three spring bloom periods from 1982 through 1984. Plots of epifluorescence direct counts (Figures 3, 7, 10, 14) show variation in abundances of ambient HNANO and bacteria for comparison with in situ chamber heteroflagellate versus bacteria growth curves (patterns). These plots demonstrate the high growth and yield potential of each chamber experiment spring bloom assemblage and the corresponding EM micrographs (Figs. 3-6, 8, 9, 11-13, 15-17) demonstrate the species diversity and associations within the nanoplankton community. The following paragraphs and choanoflagellate species descriptions (with corresponding SEM and TEM micrographs) represent results of combined epifluorescence direct count and EM photomicroscopy analysis of heteroflagellate species assemblages for each of the five

spring in situ diffusion chamber experiments of March, April, and May 1982; April 1983; and May-June 1984.

Marsh-mudflat system temperatures and salinities ranged from 4°to 35°C and from 10 to 22 ppt, respectively, during the 1982-1984 seasonal study. HNANO assemblages of March 1982, sampled when temperatures ranged from 11 to 13°C were dominated by Diaphanoeca species (Fig. 3). Diaphanoeca, reported most frequently in boreal environments (Leadbeater 1972a,b; Manton et al. 1981), may be typical of cold-water (late spring) heteroflagellate assemblages.

Heteroflagellate abundances monitored at the marsh station tidal pool in April 1982, when temperatures increased to a range between 14 and 20°C, were the highest recorded during the three year sampling period. Extended blooms of HNANO ranging from 5 to 24.7 x 10^3 cells^{-1} were observed during extended periods of low water concurrent with increased cyanobacteria densities. Blooms were sustained for several days, an unusually long period (Fig. 3 and compare to April 1983, Fig. 10) for this tidal environment. Average HNANO densities at the mudflat station, by contrast, remained close to the seasonal average of approximately 2.3 x 10^3 cells ml^{-1}. Heteroflagellates in diffusion chambers at both stations (Fig. 2) reached high densities (1 x 10^4 cells ml^{-1}). SEM investigation revealed a highly diverse heteroflagellate population dominated by Acanthoecidae choanoflagellates (Figs. 4-6). Ten Acanthoecidae species comprised nearly 75% of the total heteroflagellate assemblage. The dominant choanoflagellate genus, Stephanoeca, included in order of relative abundance, Stephanoeca elegans, S. urnula, S. constricta, S. complexa, S. diplocostata. var paucicostata. Savillea

Figure 3. Temperature, salinity, and heteroflagellate densities versus bacteria densities for in situ diffusion chamber experiment and ambient spring assemblages at the marsh station during 17-28 March 1982. SEM micrograph is of ambient assemblage including Diaphanoeca sp. in March 1982 at marsh station. Similar plots are presented for both the marsh and mudflat station during 17-28 April 1982. (Scale bar = 10 μm).

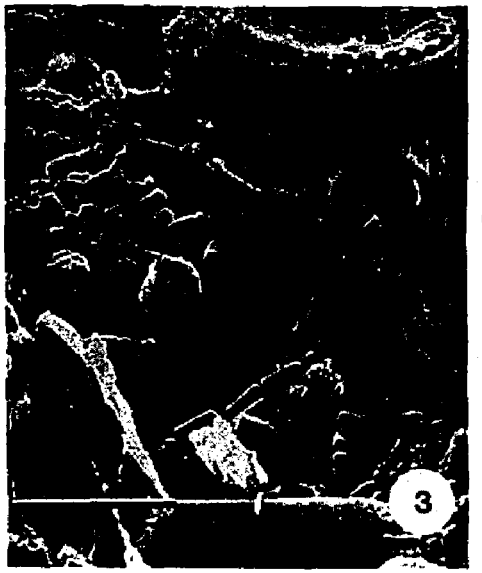
3

March 1982 Marsh
TEMP/SAL
AMBIENT
CHAMBER
Heteroflagellates x 10³ per ml
Bacteria x 10⁶ per ml
°C, ppt
HOURS
Date
April 1982 Marsh
TEMP/SAL
AMBIENT
CHAMBER
HETEROFLAGELLATES
BACTERIA
TEMPERATURE
SALINITY
April 1982 Mudflat
TEMP/SAL
AMBIENT
CHAMBER
TIME IN HOURS
Date

Figure 4. SEM micrograph of spring bloom assemblage of nanoplankton from the April 1982 in situ chamber experiment showing two Stephanoeca specimens in association with a cryptomonad and diatom, and an unidentified monad. Scale bar = 5 μm.

Figure 5. SEM micrograph of biflagellated heterotrophic monad from April 1982 chamber experiment. Scale bar = 2 μm.

Figure 6. SEM micrograph of a spring bloom assemblage of nanoplankton from the April 1982 in situ chamber experiment showing the direct attachment of Stephanoeca elegans and a pedicellate S. constricta. Scale bar = 5 μm.

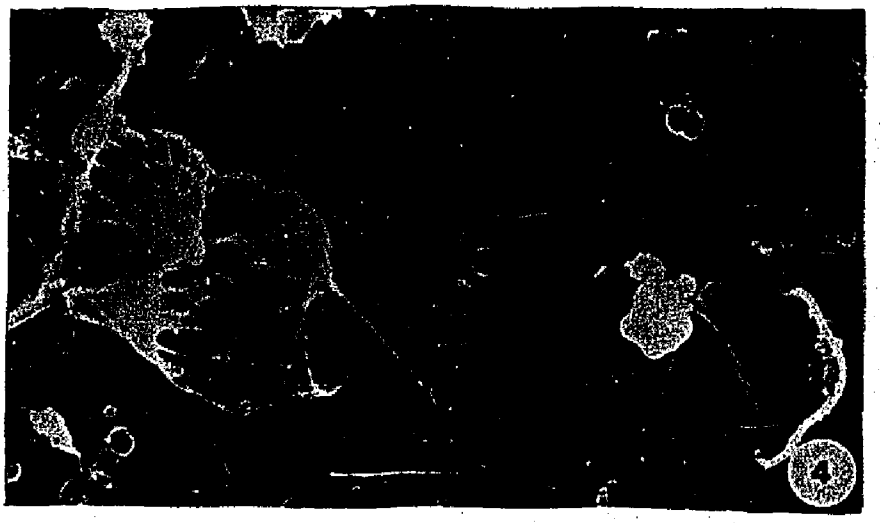

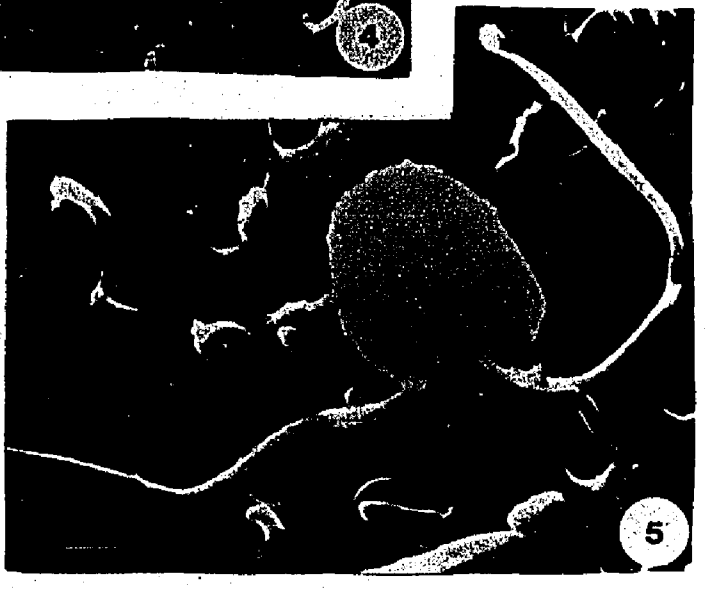

parva and Saepicula pulchra were also relatively abundant although observed less frequently than the most abundant species. Acanthoecopsis apoda, A. unguiculata, and A. spiculifera, were also represented although by considerably fewer numbers. HNANO blooms in the May 1982 tidal pool environment (3-5.4 x 10^3 cells ml^{-1}), when temperatures and salinities increased, were not as pronounced nor prolonged (Fig. 7) as those monitored in tidal pools during April. However assemblages in May chambers were similar and diversity remained high with a slight increase in SEM observations of A. apoda (Figs. 8 and 9).

April 1983 sampling period was characterized by large fluctuations in temperature (7 - 20°C) and salinity (10 - 15.5 ppt) (Fig. 10) due to increased winter and early spring rains and an anomalous snowstorm. Tidal pools of the marsh-mudflat system demonstrated transient (4-6 h) blooms of lowtide assemblages of HNANO with maximum concentrations of 4.64 x 10^3 cells ml^{-1} in marsh and 5.53 x 10^3 cells ml^{-1} in the mudflat samples. The increase in marsh station heteroflagellates also coincided with an increase in numbers of large rod-shaped bacteria and cyanobacteria. However, April 1983 chambers contained fewer Acanthoecidae choanoflagellate than those of April and May 1982 (Figs. 11-13). Choanoflagellates composed approximately 25 - 50% of heteroflagellate assemblage. Most common species were A. apoda and S. d. var. paucicostata and Pleurosiga sp. Assemblages were dominated instead by Paraphysomonas and bodonid forms.

The May - early June 1984 experiment was characterized by low salinities (11- 12.5 ppt) and comparable but less variable temperature (15- 22°C) than preceding experiments. Although no pulses of greater

Figure 7. Temperature, salinity, and heteroflagellate abundance versus bacteria densities for in situ diffusion chamber experiments and ambient assemblages during 19-26 May 1982 at the marsh and mudflat stations.

Figure 8. Two naked heteroflagellates with long sinuous flagella from the May 1982 in situ chamber experiment. Scale bar = 1 μm.

Figure 9. Pedicellate Stephanoeca constricta in association with diatoms in the May 1982 in situ chamber experiment. Scale bar = 1 μm.

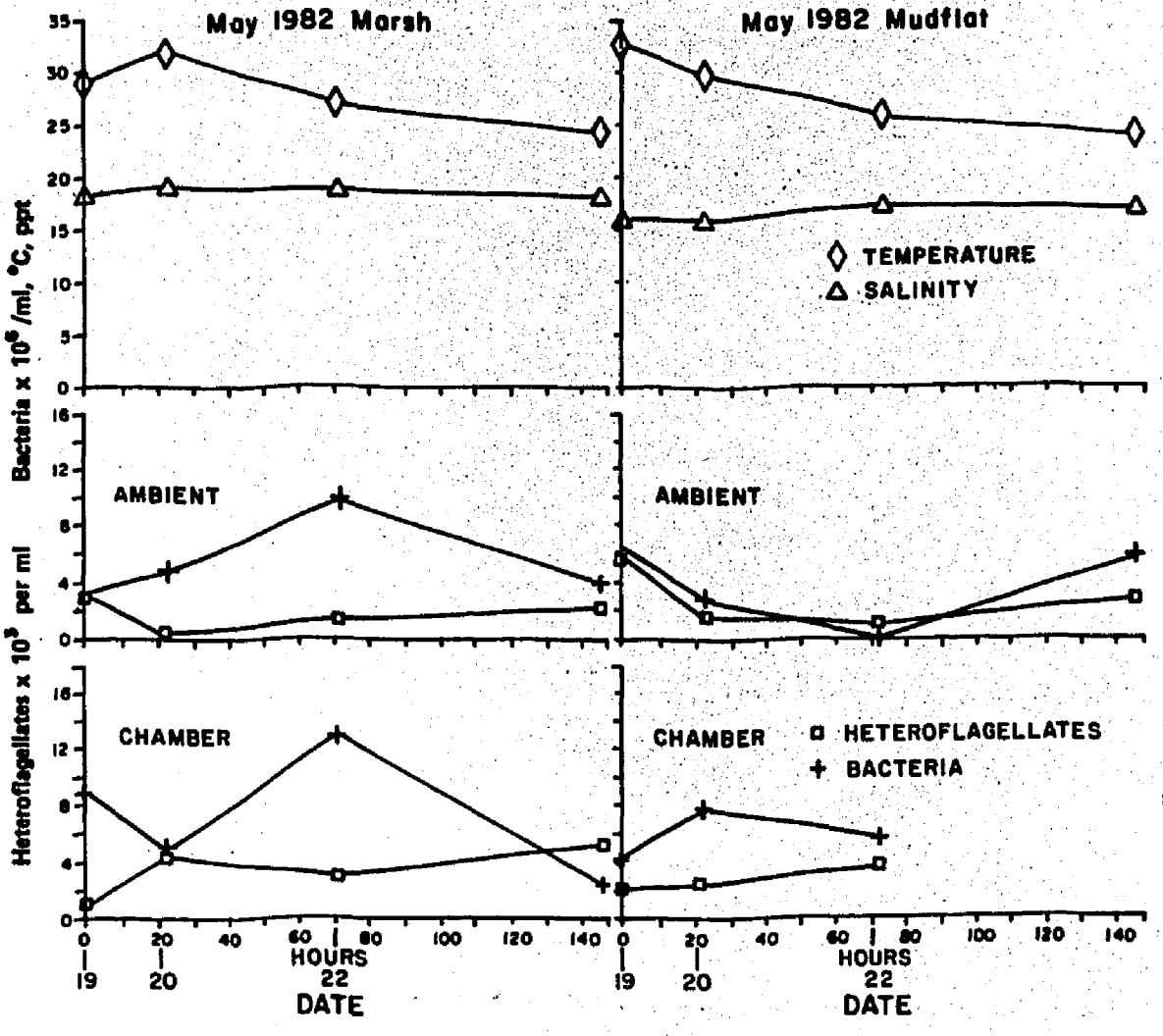
May 1982 Marsh
May 1982 Mudflat
TEMPERATURE
SALINITY
Bacteria x 10⁶ /ml, °C, ppt
AMBIENT
AMBIENT
CHAMBER
CHAMBER
HETEROFLAGELLATES
BACTERIA
Heteroflagellates x 10³ per ml
HOURS
DATE
19
20
22

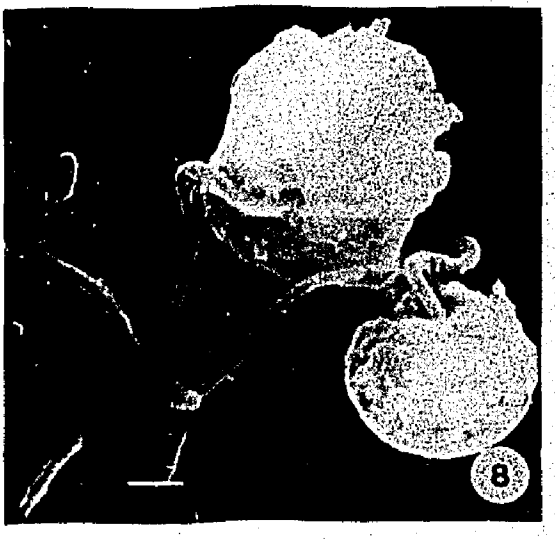
8

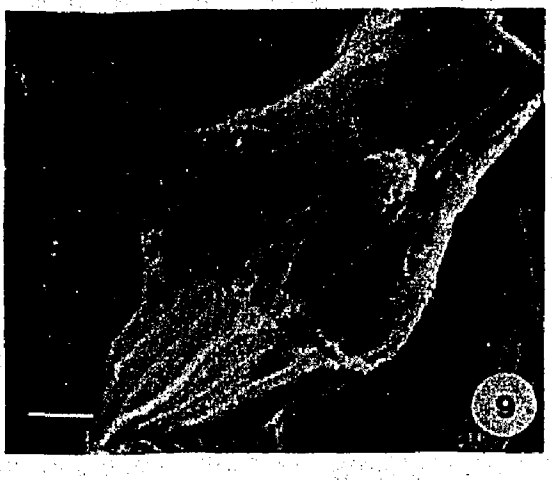
9

Figure 10. Temperature, salinity, and heteroflagellate densities versus bacteria abundances for in situ diffusion chamber experiments and ambient assemblages during 13-23 April 1983 at the marsh and mudflat stations.

Figure 11. SEM photomicrograph of small heteroflagellate in association with Nitzschia sp. from April 1983 in situ chamber experiment. Scale bar = 1 μm.

Figure 12. SEM micrograph of small bodonid form from April 1983 in situ diffusion chamber experiment. Scale bar = 1 μm.

Figure 13. SEM micrograph of a loricate choanoflagellate and naked monad from April 1983 experiment. Scale bar = 1 μm.

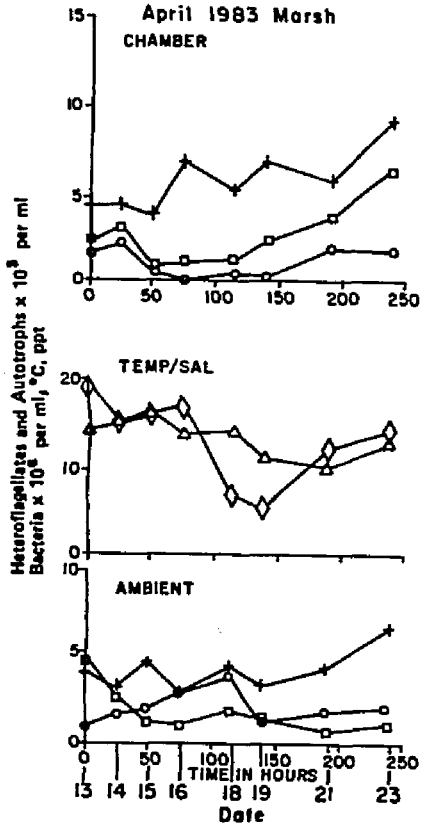
April 1983 Marsh
CHAMBER
TEMP/SAL
AMBIENT
Heteroflagellates and Autotrophs x 10³ per ml
Bacteria x 10⁶ per ml, °C, ppt
TIME IN HOURS
13 14 15 16 18 19 21 23
Date

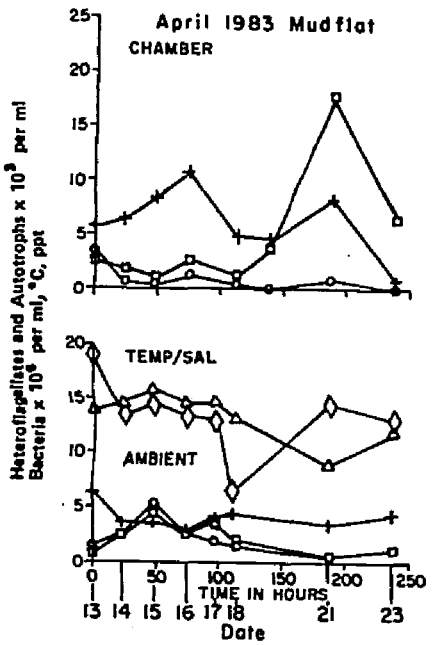
April 1983 Mudflat
CHAMBER
TEMP/SAL
AMBIENT
Heteroflagellates and Autotrophs x 10³ per ml
Bacteria x 10⁶ per ml, °C, ppt
TIME IN HOURS
13 14 15 16 17 18 21 23
Date

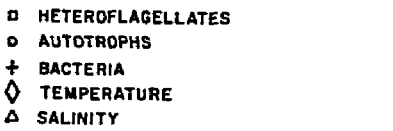
HETEROFLAGELLATES
AUTOTROPHS
BACTERIA
TEMPERATURE
SALINITY


11


12

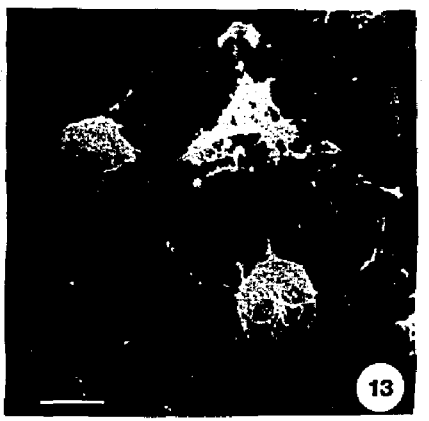
13

than 4.5×10^3 heteroflagellates ml^{-1} were observed, relatively high ambient concentrations, averaging 3.0×10^3 cells ml^{-1}, remained above annual averages (May 1981 - May 1982 - 2.3×10^3 and July - Dec 1982 - 1.7×10^3 cells ml^{-1}) for an unusually long period during the experiment. Ambient heteroflagellate abundances demonstrated less daily variability than previous spring bloom assemblages (Fig. 14).

Heteroflagellate assemblages of the May-June chambers, examined under TEM photomicroscopy, were comprised of approximately 40% choanoflagellates, dominated by Stephanoeca diplocostata. var. paucicostata and Acanthoecopsis sp., and 60% mixed assemblage of Paraphysomonas vestita, bodonids, and bicoecids (Figs. 15-17).

Detailed descriptions and corresponding SEM micrographs of the eleven Acanthoecidae choanoflagellate species observed in diffusion chambers are presented below. None of these species have previously been reported in Chesapeake Bay estuarine systems. A prototype (Fig. 18) of an Acanthoecidae choanoflagellate, illustrating diagnostic features referred to in the descriptions and micrographs, is included as part of Table 1 which summarizes diagnostic characters and ranges of dimensions of the eleven described species. HNANO populations from the chambers were dominated by large Paraphysomonas and Acanthoecidae choanoflagellate species. Chamber samples analyzed with TEM photomicroscopy in order to identify Paraphysomonas vestita using scale morphology, revealed Acanthoecidae species constituted nearly 25 to 50% of the HNANO (Figs. 15, 19). Positive identification of bicoecids was possible for the first time for the Chesapeake Bay area. These monad-like (two flagella) phagotrophs, are a significant component of this

Figure 14. Temperature, salinity, and heteroflagellate densities versus bacteria densities during 31 May - 5 June 1984 in situ chamber experiment at the mudflat station.

Figure 15. TEM photomicrograph of Acanthoecidae choanoflagellate from May-June 1984 in situ diffusion chamber experiment. Scale bar = 1 μm.

Figure 16. TEM photomicrograph of Paraphysomonas vestita from May-June 1984 in situ diffusion chamber experiment. Scale bar = 2 μm.

Figure 17. TEM photomicrograph of a haptophyte showing a hair-point flagella with mastigonemes from the May-June 1984 in situ diffusion chamber experiment. Scale bar = 2 μm.

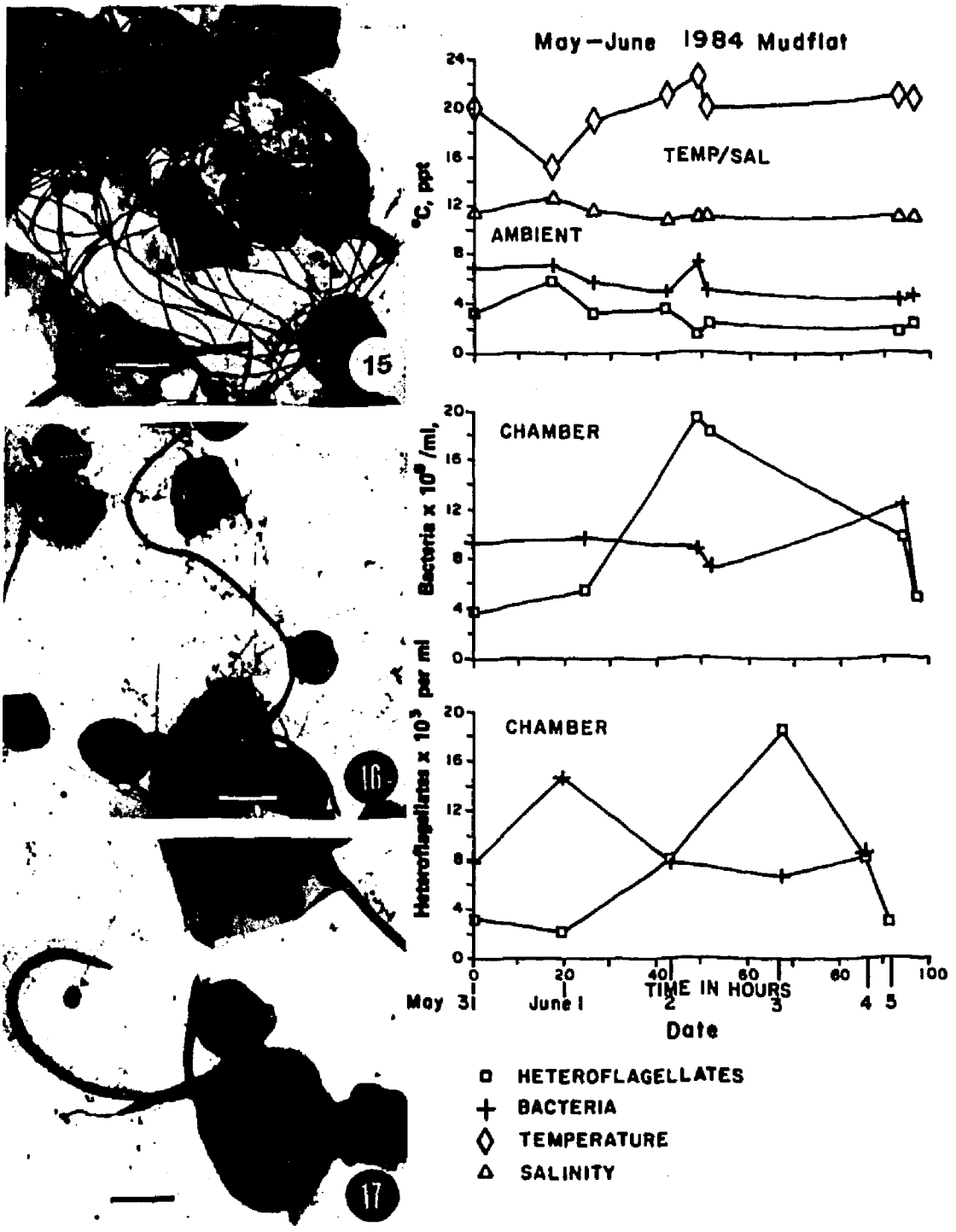
May–June 1984 Mudflat
TEMP/SAL
AMBIENT
°C, ppt
CHAMBER
Bacteria x 10⁸ /ml
CHAMBER
Heteroflagellates x 10³ per ml
TIME IN HOURS
May 31
June 1
Date
HETEROFLAGELLATES
BACTERIA
TEMPERATURE
SALINITY
15
16
17

Figure 18. Prototype of a choanoflagellate depicting diagnostic features of the lorica.

Table 1. Dimensions of species described in text.

	Diaphanoeca	Stephanoeca				
	grandis	diplocostata var. paucicostata	elegans	constricta	urnula	complexa
Lorica Ht (μm)	23.0-25.0	9.5-12.0	10.5-12.5	10.0-12.5	7.5-9.5	10.0-12.0
Cell (w x l)	3.3x4.0	2.5x3.5	2.5x3.0	2.5x3.0	2.0x2.5	2.5x3.2
Flagella Length (μm)	4-5	5			4.0-5.0	4.5-5.0
Posterior Chamber (μm)	NA	3-4	3.5-5.0	3.5-5.0	3.5	4.3-5.0
Anterior Chamber (μm)	NA	6.5-7.8 w	7.0-8.5 l	7.0-8.5 l	4.5-6.0 l	6.5-7.5 l
Longitudinal Costae #	11-12	12-13	18-21	16-19	14-15	10-14
Transverse Costae #	4	4-5	3,4	3,4	5-9	<4
Anterior Orifice (μm)	<3	3	4.5-6.0	3.5-4.5	2.0-2.5	3.5-4.0
Stalk		YES	YES			
Number of Cells Observed	3	5	>15	>14	10	5

w - width in μm
l - length in μm

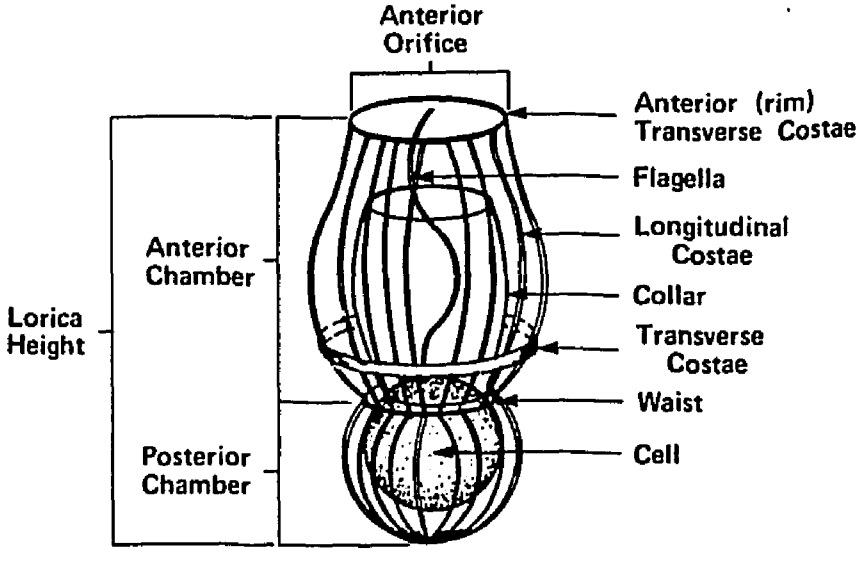

CHOANOFLAGELLATE
LORICA PROTOTYPE

Table 1. (continued)

	Acanthoecopsis			Saepicula	Savillea
	apoda	unquiculata	spiculifera	pulchra	parva
Lorica Ht (µm)	10.5-12.0	10.0-12.5	14.8-15.3	7.5-9.0	4.5-6.5
Cell (w x l)	2.5x3.5	3.3x5.0	2.5x4.5	2.0x3.0	2.5x3.5
Flagella Length (µm)			4.0	4.0	
Posterior Chamber (µm)	8-9	5.6x5.9 w x l	6.3	4.0-4.5 w	
Anterior Chamber (µm)	3.5-4.5 l	7.0x7.5 w x l	7.5x8.5 w x l		
Longitudinal Costae #	12-14	13-14	13-14	10	
Transverse Costae #	4	variable	variable		
Anterior Orifice (µm)	NA	NA	-	6.0-7.0	1.0-2.0
Stalk			YES		
Number of Cells Observed	>10	<5	<5	>5	>10

Figure 19. TEM photomicrograph of an Acanthoecopsis sp. from the May-June 1984 in situ diffusion chamber experiment. Scale bar = 1 μm.

Figure 20. TEM photomicrograph of a bodonid heteroflagellate from the May-June 1984 in situ diffusion chamber experiment. Scale bar = 1 μm.

Figure 21. TEM photomicrograph of a bicoecid heteroflagellate from the May-June 1984 in situ diffusion chamber experiment. Micrograph reveals the characteristic hyaline lorica and long sinuous flagella. Scale bar = 1 μm.

Figure 22. TEM photomicrograph of Paraphysomonas vestita from the May-June 1984 in situ diffusion chamber experiment. Micrograph reveals species-specific spined scales. Scale bar = 1 μm.

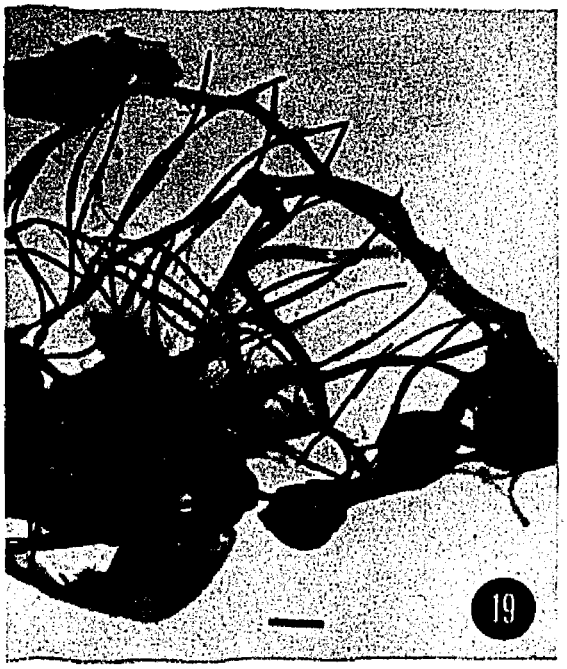
19

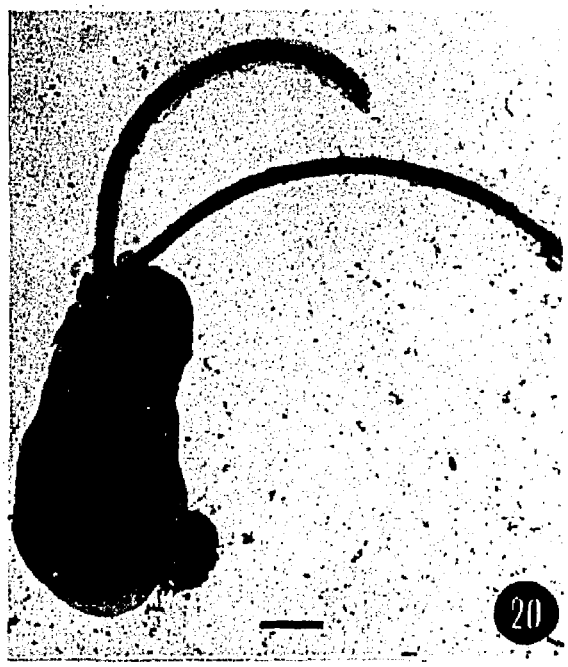
20

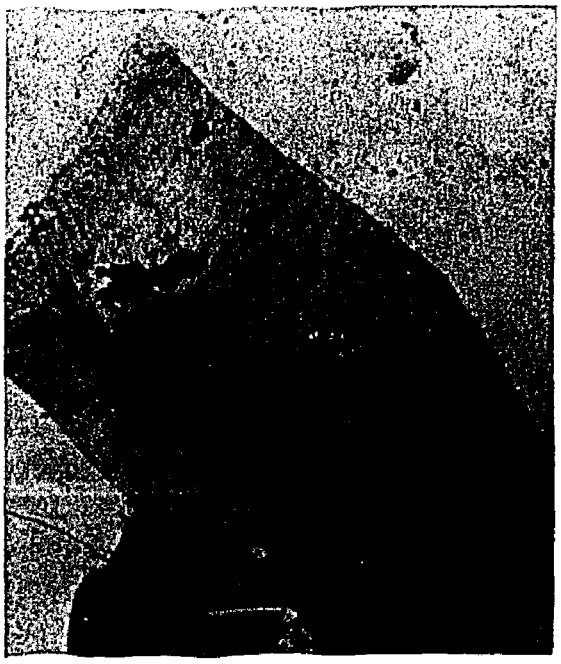


22

(May 1984 - Figs. 16, 20) HNANO assemblage and may have been underestimated in previous SEM preparations where characteristic hyaline sheaths, necessary for positive identification, are not as well preserved. However identification of Acanthoecidae was greatly limited by distortion of loricas in typical TEM preparations (Figs. 15, 19). Photomicroscopic analysis of all of these spring blooms demonstrate the necessity of combined analysis of epifluorescence, SEM, and TEM for complete evaluation of species assemblages. SEM is particularly valuable for choanoflagellates, showing details of lorica; TEM for showing choanoflagellate collars and the hyaline lorica of bicoecids and species specific scales of Paraphysomonas species (Fig. 22); and epifluorescence for enumeration.

Diaphanoeca grandis (Fig. 23)

This species was present in March 1982 in 5 to 8°C York River waters and in a culture of this water incubated at 5°C. The species was also found growing in diffusion chambers at the marsh pool stations where temperatures and salinities ranged between 7 to 13°C and 14.5 to 15.5 ppt.

The protoplast is ovoid (subspherical) with approximate dimensions of 4.0 µm x 3.3 µm when measured in dried preparations. The cell is suspended freely at the mid-section of the conical-shaped lorica, with the flagella extending towards the anterior orifice. The collar is hidden from observation with SEM micrography by a thin subtending membrane which completely lines the chamber from the anterior convergence to the second transverse costae. This characteristic

feature, described using light and TEM microscopy by Leadbeater (1973, 1981) and Thomsen (1982) for Stephanoeca and Diaphanoeca species, was clearly evident as a thin shroud-like investment in the present SEM preparations (Fig. 23). Total height (with stalk) of the delicate undulating lorica ranged from 33.5 to 36.0 µm. The large tear-drop shaped chamber was approximately 23.0 to 25.0 µm long and 16.0 to 18.5 µm wide at the widest diameter.

The lorica is formed by a series of overlapping costal strips (slightly curved rods) arranged in a distinct pattern of 11 to 12 longitudinal costae encircled by 4 to 5 transverse costae, a numerical arrangement also characteristic of the arctic D. multiannulata n.sp. (Buck 1981) and D. pedicellata and D. grandis of Jugoslavia (Leadbeater 1973). The longitudinal costae, each consisting of 6 or 7 costal strips of about 4 to 5 µm in length, radiate out along the length of the chamber. These costae are nearly equidistantly spaced (at approximate 2.2 µm intervals) where they meet the small anterior transverse costae (7.0 - 8.0 µm wide). The longitudinal costae extend past the anteriormost transverse costae and connecting membrane, as free anterior spines. The costal strips of longitudinal costae overlap to a certain degree, usually about 10 to 20% at the posterior end and 40 to 50% between the anterior transverse costae. This results in a close, nearly equidistant (2.0 - 2.5 µm) arrangement of the posterior transverse costae. The Virginia specimens described here occasionally have one more posterior transverse costae than the boreal (Thomsen 1982) specimens.

The posterior transverse costae are composed of a constant number (11 - 12) of slightly curved costal strips of approximately equal length (3.5 - 4.0 μm). One end of the costal strip attaches to the adjacent, either end to end or with a small degreee of linear overlap (5 to 15%) and the other end attaches directly to the longitudinal costal strip. Two or three different types of anterior - longitudinal costae attachments exist, which resemble those depicted for D. grandis and D. undulata by Thomsen (1982). The bottom transverse costae attaches near or at the junction of the first anterior spine and second longitudinal costal strip at the point of simple end to end joins. The next posterior costae crosses anterior to the overlap junctions between second and third longitudinal costal strips. One end of the costal strip connects directly to the longitudinal costae at the second and third strip overlap and the other attaches on a diagonal with 15 to 20% overlap to the adjacent costal strip. The mid-transverse costal strips, where the subtending membrane terminates, are slightly more curved. Transverse costal strips connect end to end (slight overlap) usually at the termination of a 40 to 50% overlap of third and fourth costal strips.

The small circular anterior transverse costae appears to be composed of a double layer of costal strips superimposed (with greater than 50% overlap) to form the small but thickened anterior ring. Figure 3 shows clearly the convergence and successive reduction of longitudinal costae beyond the anterior ring to form pairs of wider costae which then all merge to form narrow opening.

Figure 23. Diaphanoeca grandis - Collapsed lorica with cell, flagella, and fibrillar membrane extending from posterior costae. The eleven longitudinal costae and the five costal strips per costae are easily discerned. Transverse costae clearly show imbricate arrangement. Scale bar = 5 μm.

Figure 24. Stephanoeca diplocostata var. paucicostata. View of anterior end of lorica containing cell and coiled flagella. Irregularly spaced attachments of longitudinal costae at anterior rim are obvious. Scale bar = 2 μm.

Figure 25a. S. d. var. paucicostata. Two specimens among an assemblage of microplankton collected in April 1982. Anterior transverse costae and rimmed orifice obvious in specimen parallel to Skeletonema. Scale bar = 10 μm.

Figure 25b. Detail of Fig. 25a. Shows posterior chamber, suspended cell and costal junctions of anterior chamber. Scale bar = 2 μm.


23

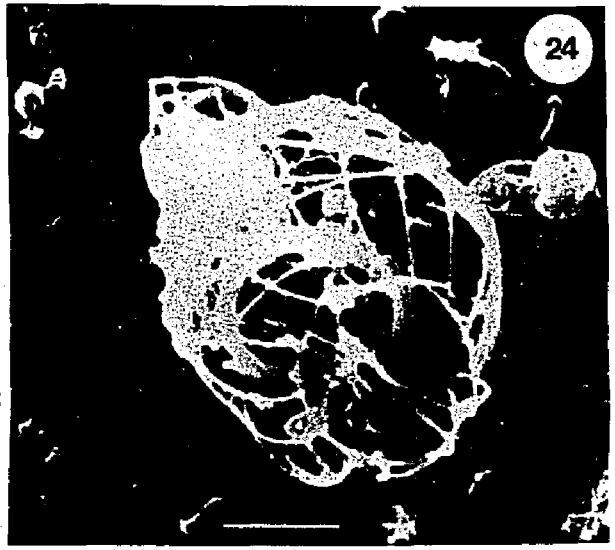
24

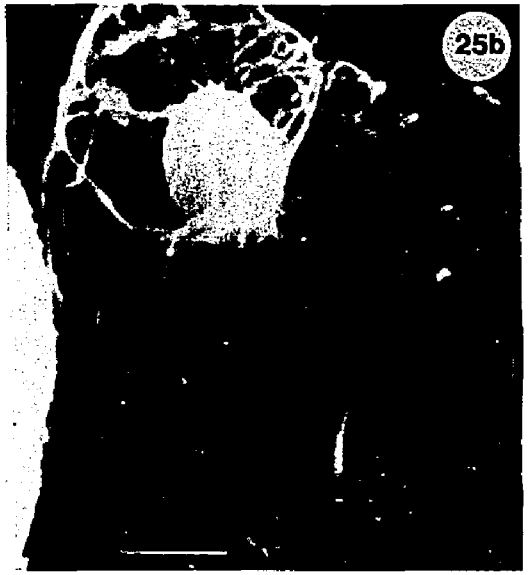
25b

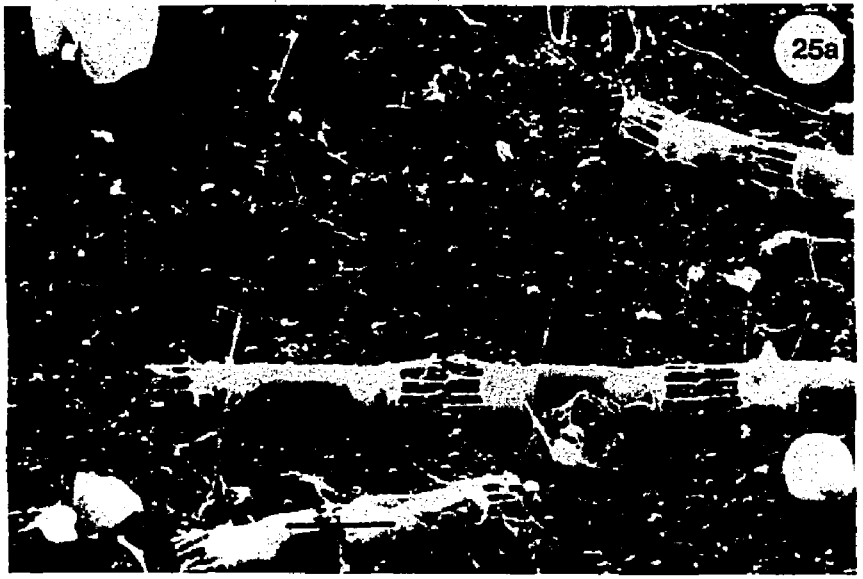
25a

Stephanoeca

Species of Stephanoeca genus dominated spring bloom heteroflagellate assemblages. Five species occurred in each of April and May 1982 chambers: S. elegans and S. diplocostata paucicostata were abundant in May 1984. The distinguishing characteristic common to all (Ellis 1930; Leadbeater 1981) is a divided lorica composed of relatively thick costal strips which completely surrounds the cell, collar, and flagellum. A waist-line constriction divides the small posterior chamber which is lined by a diaphanous membrane and contains the protoplast from the large anterior chamber which encloses the collar flagellum. A circular or oval anterior rim (orifice), formed by a thickened costae, is also a distinguishing feature. Species are frequently pedicellate, but the stalk is not species-specific nor necessary for attachment.

Stephanoeca diplocostata Ellis var. paucicostata Throndsen (Figs. 24-25)

Several basket-shaped loricate cells composed of two chambers were found growing in incubation chambers at the marsh tidal pool station during late April 1982 when temperatures and salinities ranged from 17-24°C and 15-18 ppt, respectively. Loricas ranged in height from 9.5 to 12.0 µm and in maximum width from 6.5 to 7.8 µm. S. d. paucicostata, is a less complex variety of S. diplocostata Ellis, possessing fewer transverse and total costae (less than 150 costal strips). A paired

transverse costae occurs only at maximum diameter of the lorica. The lorica is characterized by simpler and more regular costal strip arrangement than S. diplocostata which results in a smaller size and few pedicellate forms. Both S. diplocostata and S. d. paucicostata have been reported in a wide range of coastal environments ranging from Greenland, Scandinavia, Great Britain and Denmark (Throndsen 1970; Thomsen 1973; 1982; Leadbeater 1972 a,b) to Yugoslavia and Australia (Leadbeater 1973; Hallegraeff 1983). S. d. paucicostata has not been found as frequently as S. diplocostata and is more common in temperate and quiescent inland waters rather than in the open ocean nanoplankton. The relatively small size of the York River specimens described here is similar to those of the warmer, temperate waters of Yugoslavia and Australia.

Lorica of Virginia species are composed of 12-13 longitudinal costae and 4 or 5 transverse costae including the anterior rim, paired anterior transverse costae, and a variable number encircling the posterior chamber. Costae are composed of curved costal strips of approximately equal length (about 3 µm) and two lower (posterior) transverse costae may contain more than one ring of costal strips. Longitudinal costae are characteristically equally spaced in the anterior chamber (6-9 µm height) and become somewhat spirally deflected or less organized in the posterior chamber (3-4 µm height). The small posterior chamber contains most of the protoplast - an ovoid cell with approximate dimension of 2.5 X 3.5 µm and a curled flagella (approx. 5 µm in length). The inner surface, according to Leadbeater (1979b,c), is lined with a diaphanous membrane which extends into the anterior chamber

and joins with the protoplast at the waist between the chambers. About fifteen collar tentacles also extend into the anterior chamber.

Micrographs presented (Figs. 24-25) here demonstrate the different aspects of lorica construction upon which identification is based: the characteristic shape, double transverse costae, and regularly spaced longitudinal costae. Although curled flagella (Fig. 24) were frequently evident in Virginia specimens, membrane or periplast and collar were not. Leadbeater (1981) reported S. diplocostata and S. d. paucicostata associated with Enteromorpha, common in April and November tidal pool samples. Micrographs here also reveal or confirmed this species close association and/or attachment with various diatoms (Skeletonema spp.) as indicated by previous epifluorescence analysis.

Stephanoeca elegans (Norris) Throndsen (Figs. 26-34, 37)

Several specimens of Stephanoeca elegans were found within in situ chambers throughout April 1982. Loricas resemble beautiful bird cage patterns of regularly spaced longitudinal and transverse costae which form the well-defined small posterior chamber and the large barrel or bulb-shaped anterior chamber. The lorica contains two series of 18 to 21 longitudinal costae (usually 18 or 20), three transverse costae and an anterior rim, each composed of relatively few long, curved costal strips. The lorica heights range from 10.5 to 12.5 µm and posterior chamber heights range between 3.5 to 5.0 um (most are 4.0 µm). A series of costae, consisting of single (approx. 4.0 µm long) costal strips, form the posterior chamber and radiate out from the base enclosing most of the protoplast. The spherical to ovoid protoplast (approx. 2.5 x 3.0 µm) is

Figures 26 and 27.

Stephanoeca elegans. Specimens or organisms shown here were collected during April 1982 experiments Photomicrographs demonstrate the three-dimensional quality possible with SEM preparation and the preservation of the natural configuration of lorica. Scale bars = 1 μm.

Figure 26. Cell is evident but obscured by imperforate membrane of the posterior chamber. Lorica with 21 longitudinal costae and 3 transverse costae. Note costal strip morphology, particularly the spatulate and imbricate system of connections of longitudinal costal strips with the thickened costal strips of the anterior rim.

Figure 27. Lorica with a conical posterior chamber (perhaps due to shrinkage of imperforate membrane) containing a clearly visible coiled flagella. Two transverse costae encircle the 20-21 longitudinal costae at the waist.


26


27

firmly lodged in a periplast and is usually hidden by an imperforate sheath-like investment lining the posterior chamber. A transverse costae encircles the waist between chambers and also appears to be the terminal attachment point of the chamber investment. The longitudinal costae attach with spatulate ends to the outside of the transverse costae, where they interdigitate with the wedge-shaped spatulate attachments of anterior chamber costae. Posterior chambers, observed under SEM, containing cells or sheath appear cone-shaped (Figs. 27, 31, 37) and costae may be gently spiralled, while the empty chamber is hemispherical (Figs. 29, 30, 33, 37) as it appears live (Ellis 1930; Norris 1965; Throndsen 1974). Perhaps shrinkage of cell or sheath during SEM drying processes may exert different degrees of torque on the costae to produce the different, slightly spiralled morphology.

The anterior longitudinal costae radiate out at the waist region forming a broad chamber 7.0 to 8.5 µm long with maximum diameter ranging between 6.75 and 8.0 µm. Near the waist, paired transverse costae encircle the anterior chamber inside the longitudinal costae (Figs. 26, 27, 33). The chamber narrows towards the anterior end where the tansverse costal rim forms outside the longitudinal costae. The circular or oval orifice measures 4.5 to 5.5 µm at the widest point. Each anterior longitudinal costae is composed of two thick and slightly curved (usually convex out) costal strips. The second posterior series of strips are relatively wide at their posterior ends or where they attach to the posterior transverse costae and narrow gradually as they extend (convex out) to overlap the first anterior series of costal strips (Figs. 26, 27). Occasionally the second posterior series

consists of paired costal strips (Figs. 29, 33), where the additional one overlays the other and projects out, attached only at the waist. The posterior series attaches linearly, with a relatively large (approx. 0.5 μm) overlap, to the narrower and longer anterior costal strips (Figs. 26, 27, 30). These strips, which may appear under SEM as either convex or concave, attach anteriorly with spatulate ends at and between the joins of the costal strips forming the anterior rim. This anterior transverse costae is composed of 4 to 6 costal strips which overlap with varying lengths of > 1 μm to form a thickened anterior rim.

The shape of the large anterior chamber observed in the SEM micrographs presented here may vary from the barrel shape, similar to that of S. ampulla, to the less rounded urn (bulb) shape drawn by Norris (1965) and Throndsen (1974). The lorica shape depends on the configuration (degree of curve) and spacing between first anterior series of costal strips. The barrel lorica (Figs. 26, 29) occurs when costal strips remain curved gently outwards (convex out) and the spacing narrows gradually from the widest point of the chamber. The slightly indented urn shape (Figs. 27, 30) occurs when the costal strips straighten or turn concave in and the spacing narrows immediately beyond the widest point in the chamber. Many TEM or SEM micrographs of S. elegans lorica presented in literature also reveal deviations from the barrel or urn shape and spiralling (mentioned above) of the longitudinal costae. These varieties of lorica shapes do not appear to be diagnostic features but perhaps a function of stress during EM preparation or due to specimen age.

SEM micrographs of S. elegans from the York River reveal that

Figures 28 - 33.

Stephanoeca elegans. Specimens collected during April and May 1982 experiments each showing characteristic features. Scale bars = 1 μm.

Figure 28. Posterior view of lorica containing cell and imperforate membrane. Demonstrates that posterior costal strips may not all fuse posteriorly, but are encased in membrane.

Figure 29. Empty undistorted (symmetrical) lorica with eighteen longitudinal costae. Demonstrates hemispherical posterior chamber and barrel-shaped anterior chamber characteristic of natural configuration more commonly observed under light microscopy.

Figure 30. Spherical cell and hair-point flagella evident through partial imperforate membrane (with less distortion of posterior chamber). Note fibrillar webbing and large rod-shaped bacteria entrapped in the anterior chamber.

Figure 31. Lorica attached to diatom with a short pedicel.

Figure 32. Anterior view showing overlapping transverse costae of anterior rim and cell, flagella, and partial collar.

Figure 33. Complete lorica without imperforate membrane and dislodged cell with flagella. Evidence of double or paired anterior chamber costal strips.


28

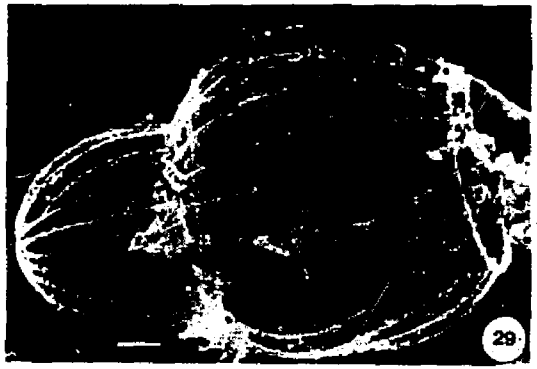
29


30


31


32


33

species attach frequently to diatoms with (Figs. 27, 30) or without a pedicel (Fig. 30), a very short projection, from the posterior chamber. The posterior chamber costal strips do not all connect when they converge to form a pedicel nor does the thick attachment appear to be a direct extension of these strips. These species may attach directly as juveniles as does S. diplocostata (Leadbeater 1979c). SEM pictures also clearly show a delicate fibrillar membrane (Figs. 23, 25, 33) enveloping the lower half to two thirds of the anterior chamber which contains small coccoid bacteria. These may be the symbiotic bacteria sometimes associated with choanoflagellates (Sieburth 1979). Larger coccoid and rod-shaped bacteria are frequently obvious inside the anterior chambers of these specimens. Prey are apparently trapped near the collar and flagella region of these specimens. The functional morphology of these loricate choanoflagellates is particularly evident in these micrographs.

Stephanoeca constricta Ellis (Figs. 9, 34-36b)

S. constricta species, although virtually identical in size (10.0 to 12.5 μm - chamber height), lorica construction (costal strip and costae arrangement), and posterior chamber and investment membrane configuration to S. elegans, is easily recognized by its constricted anterior chamber shape and stalked attachment to diatoms. S. constricta, then, can be distinguished definitively from S. elegans by two diagnostic features: 1) its characteristic kerosene bulb shaped anterior chamber formed by a marked constriction of longitudinal costae in the region of costal strip connections to create the smaller tubular orifice (3.5 to 4.3 μm); and 2) the presence of a relatively long stalk

Figure 34. Stephanoeaca elegans (Stephanoeca constricta). Two complete loricas with intact imperforate membrane and conical posterior chamber. Cell and hair-point flagella extend into distorted or constricted anterior chamber. One lorica is attached directly to Nitzchia by a short pedicel and the other possesses a relatively long sinuous stalk which is an extension of the imperforate membrane. The stalked lorica may be characteristic of S. constricta but constricted shape here may be due to EM preparation. Scale bar = 5 μm.

Figure 35. Stephanoeca constricta. Constricted lorica and flared tubular opening of mid-anterior chamber evident in these pictures. Constriction appears as a characteristic feature, rather than distortion. Lorica with less than 18 longitudinal costae. Long sinuous stalk obvious as continuation of posterior chamber membrane. Scale bar = 10 μm.

Figure 36a. Cell attached directly to diatom. Lorica demonstrates symmetrically constricted posterior chamber and tubular opening. Scale bar = 2 μm.

Figure 36b. Detail of Fig. 36a showing complex fibrillar attachment webbing between approximately 16 or 17 longitudinal costae and associated bacteria typical of S. constricta loricas. Scale bar = 1 μm.


34


36a


35

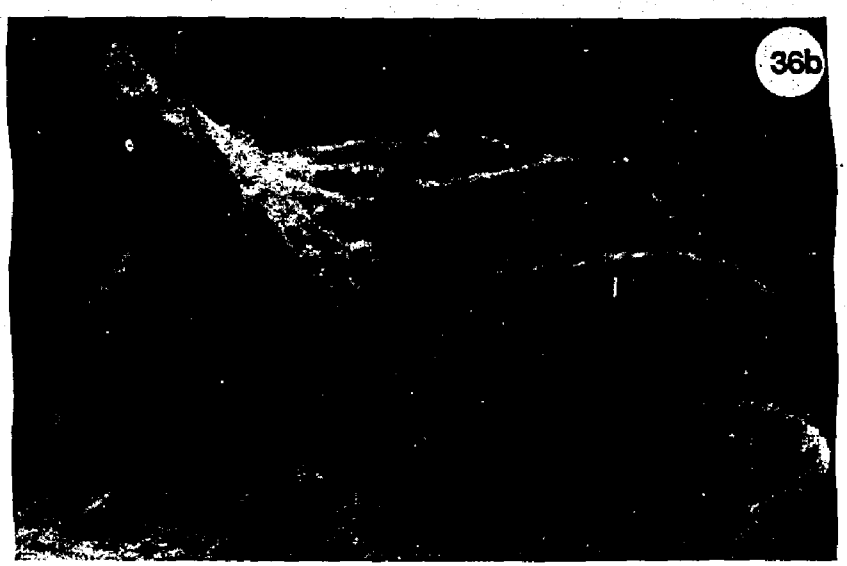
36b

(approx. 10.0 μm) which appears to be formed by an extension and merging of a few posterior longitudinal costal strips encased in membranous material (Figs. 34, 35). S. constricta also appears to have a smaller range in longitudinal costae number of 16 to 19 rather than 18 to 21 costae of S. elegans (Figs. 9, 36). Occasionally, lorica may possess one or two less costae in both chambers, but this is not necessarily a distinguishing feature. The fibrillar membrane, observed lining the anterior chamber of the two species, also seems to be more prominent and to envelop more of the S. constricta chamber. This observation using SEM microscopy should be confirmed with further sampling, SEM preparations and light microscopy.

Stephanoeca urnula (Figs. 37-40)

Stephanoeca urnula, typical of brackish inshore water (Thomsen 1973) was observed frequently in April and May 1982 chambers when salinities ranged between 15.5 and 18.5 ppt. Thomsen (1973) first described species from a brackish (19 ppt) inner bay (Tempelkrogen) of Iseford, Denmark and later observed large numbers at other brackish water localities (4 to 11‰) in Denmark and Finland. Lorica construction, particularly of anterior chamber, varied with salinity; less complicated lorica, containing fewer oblique transverse costae near the orifice, appear in lower salinity (<11‰) environments (Thomsen 1979). S. urnula species pictured here (Figs. 38-40) demonstrated some variability in shape and number of costae, however, lorica construction corresponded most closely to Danish species from similar salinity regimes (Iseford- 19‰), lending support to Thomsen's (1979) positive

Figure 37. Assemblages of Stephanoeca elegans (constricta) and S. urnula typical of those observed in April and May 1982. Two loricas without cells but with membranes show varying degrees of distortion of chamber in presence of a fibrillar membrane. Upper left specimen is attached to coccoid diatom (out of view) by a membranous stalk, perhaps characteristic of S. constricta. Lorica of complete specimen of S. urnula exemplifies increased complexity and spiralled structure of estuarine specimens. Scale bar = 2 μm.

Figures 38-40.

Stephanoeca urnula. Organisms were abundant in April 1982 samples, and demonstrate different numbers of spiralled costae and resulting variations of the 'urn' shape Scale bars = 1 μm.

Figure 38. Magnification of S. urnula from assemblage photo, reveals spiralled pattern of anterior chamber.

Figure 39. Complete and most complex lorica with twenty-six spiralling costae. Posterior chamber and cell size reduced but a thick flagellum is obvious.

Figure 40. Anterior view of complete lorica demonstrates junctions of anterior rim costae with longitudinal and spiralled costae. Hair point flagellum is evident.


37

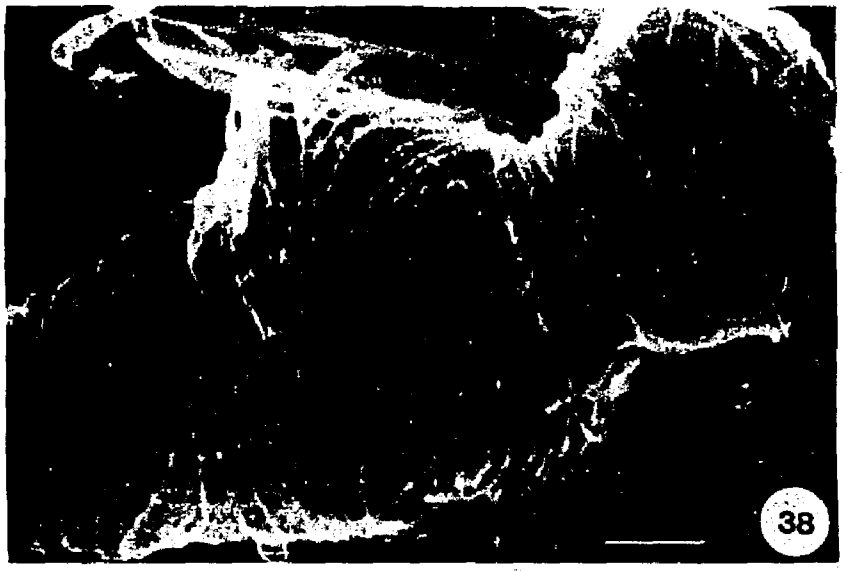
38

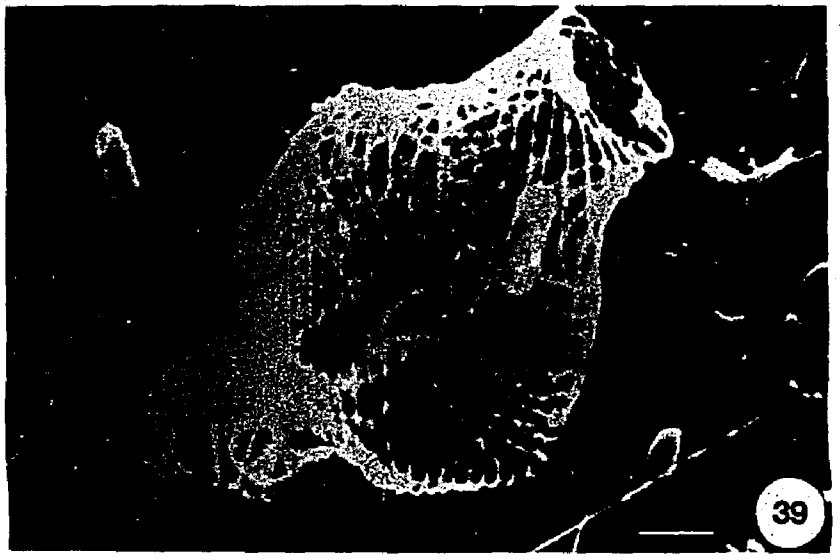
39

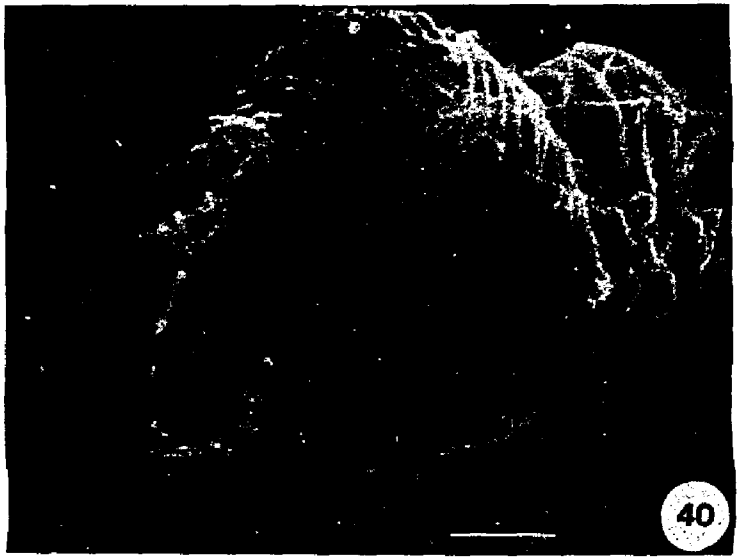
40

correlation of salinity and lorica complexity.

Total height of the Virginia specimen chamber ranges between 7.5 and 9.1 µm and approximate posterior and anterior chamber dimensions are 2.2 x 3.05 and 4.8 - 5.3 x 5.5 - 5.9 µm, respectively. The posterior chamber contains a spherical protoplast and is lined by an imperforate membrane extending to the waist (similar to S. elegans) which is encircled by multiple transverse costae. However, in contrast to S. elegans, the pattern of posterior chamber costae is irregular. It is composed of a series of obliquely arranged costae longitudinal (10-15) and transverse costae near the waist. The larger urn-shaped anterior chamber contains collar and hair point flagella (approximately 4.0 µm in length). The complex chamber is composed of 14 to 15 longitudinal costae each composed of two curved costal strips. Characteristic spiral basket weave construction of the basal chamber is formed by a large number ranging from 19 - 25 of obliquely oriented costal strips which join together anteriorly and attach at each end to first series of longitudinal costal strips. A relatively large number of transverse costae (4 to 7) encircle the chamber near its widest point forming a complicated series of attachments with the longitudinal costal strips. These subapical and interconnecting attachments, described by Thomsen (1979) are obvious in Figures 38 and 40. The lower part of the anterior chamber is characterized by a compact imbricated (spiralled) arrangement of obliquely oriented costal strips (16-17) joined together at the orifice and interconnecting with posterior ends of the longitudinal costal strips. A few Virginia specimens (Fig. 39) contain more anterior oblique costae than previously reported specimens (Thomsen

1973, 1979). Slight differences in lorica construction and shape of these specimens (Fig. 39, 40) is due in part to variation in numbers of transverse costae and oblique costae of the top and bottom spirals. However, despite variations, the three characteristic patterns of anterior chamber costae described by Thomsen (1979) are clearly evident in each SEM micrograph.

Stephanoeca complexa (Figures 41-43)

S. complexa cells were found in April and May 1982 chamber material and, like other Stephanoeca species observed in Virginia, the lorica sizes fell in lower range of those previously reported (Throndsen 1974). The ovoid cell (2.5 x 3.2 µm) and thick hair-point flagella (approx. 4.5 - 5.0 µm) are fairly well preserved in these specimens. The lorica dimensions (height 10.0 - 12.0 µm) and shape are very similar to those of barrel-shaped S. elegans. However, loricas are composed of fewer longitudinal costae (10 - 14, mean=12) arranged in a less regular pattern. Several obliquely aligned costal strips are evident, particularly in the posterior chamber. Posterior chamber dimensions fall in the range of 4.3 to 5.0 µm (for length) x 4.3 to 5.0 µm (for width) at maximum diameter; anterior chamber dimensions range from 6.5 - 7.5 µm (length) and 6.0 - 7.0 µm (width). Basal part of posterior chamber appears more flattened than S. elegans (Fig. 42) and the cone shape of some S. elegans was not evident. SEM photographs reveal a distinquishing feature (unique to S. complexa): the extension of the opaque (imperforate) (Figs. 43a,b) membrane of posterior chamber (characteristic of Stephanoeca) beyond the waist into the anterior

Figures 41-43a,b *Stephanoeca complexa*

Figure 41. Lorica shape is similar to *S. elegans* but has a more complex (less organized) arrangement of costae. Specimen also shows a characteristic posterior chamber membrane (solid) which extends beyond the waist to the prominent anterior transverse costae. Scale bar = 2 μm.

Figure 42. Detail of a posterior chamber showing random arrangement of longitudinal costae. Scale bar = 1 μm.

Figure 43a. Lorica, although covered with detritus, shows similarity to *S. elegans*. Scale bar = 2 μm.

Figure 43b. Detail shows extended membrane between posterior waist and anterio-transverse costae and random cross-linkages of diagonal costae. Scale bar = 1 μm.


41


43a

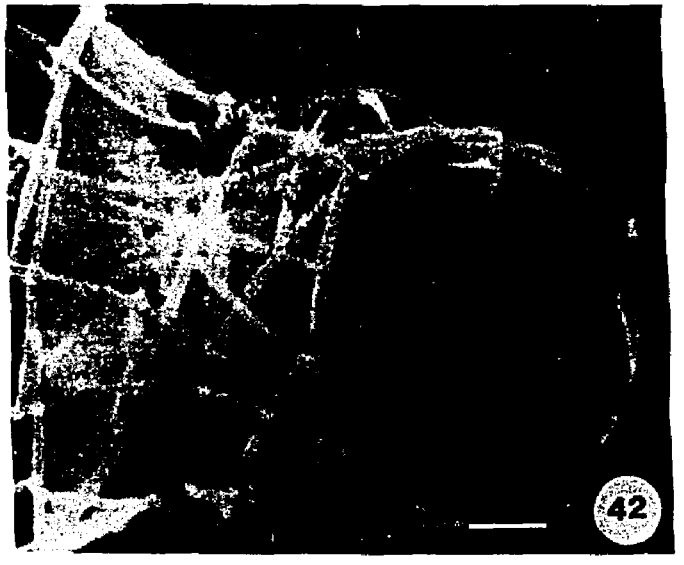
42

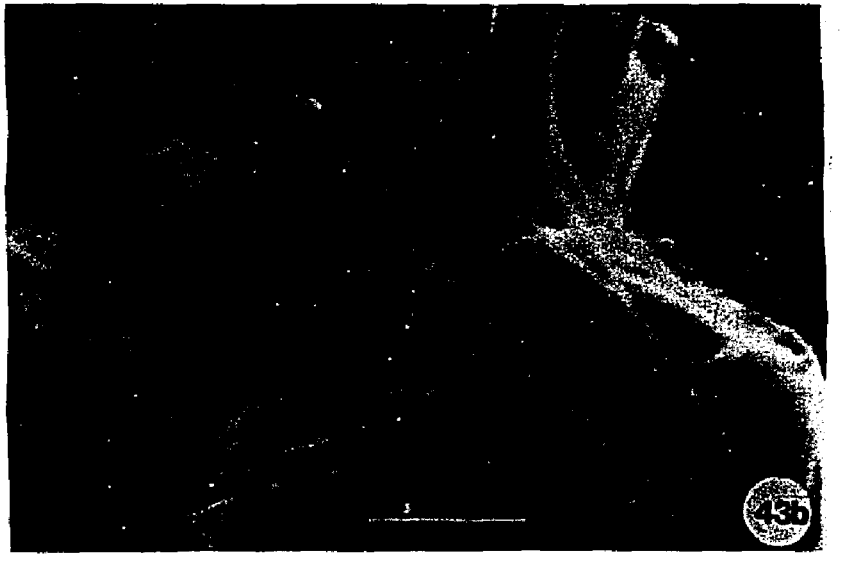
43b

chamber where it terminates at a well-defined thick transverse costae formed by wide overlapping costal strips. The posterior chamber consists of: 1) 10 to 12 longitudinal costae embedded in the imperforate membrane, 2) two to four, usually three, transverse costae, and 3) a variable number of diagonally oriented costae which crisscross between posterior end of chamber and mid-posterior and/or transverse costae located at waist. Occasionally oblique costae extend to anterior chamber transverse costae where chamber lining terminates (Fig. 42). Most lorica have aggregations of fine transverse costae or costal strips near the waist, however costae are only occasionally paired as in S. elegans.

Posterior chamber longitudinal costal strips overlap, forming linear connections easily observed under SEM (Figs. 43a,b), with anterior longitudinal costae composed of two curved costal strips. Costae are evenly spaced but characteristically transverse and obliquely oriented costal strips (diagonal pieces) crisscross (forming an irregular lattice work) external to the longitudinal array. Longitudinal costae terminate with spatulate connections (Figs. 41, 43) at oval anterior rim which ranges from 3.5 to 3.8 um at widest point. Various specimens demonstrate great variability in complexity of oblique costal strip arrangement of both lorica chambers (particularly in comparison to S. elegans). Although Norris (1965) reported some pedicellate specimens in NE Pacific (west coast U.S.A.) tidal areas, none were observed in these samples.

Acanthoecopsis

Three of four Acanthoecopsis species occurred in April and May 1982 and April 1983 samples. Blooms of A. apoda and A. unguiculata have been reported frequently in brackish surface inshore waters (Thomsen 1973, Leadbeater 1981). The genus is characterized by two well-defined chambers composed of 12 to 14 longitudinal costae, an open neck with long free anterior spines and the absence of transverse costae near the end of the lorica. The genus also lacks a membrane lining the posterior chamber, more typical of Stephanoeca genus, and the spherical to ovoid protoplast appears to be free floating in some species. Acanthoecopsis cells divide before complete assembly of lorica, unlike S. diplocostata (Leadbeater 1979a), which accounts for variability observed in lorica, particularly of anterior chambers.

Acanthoecopsis apoda (Fig. 44a,b)

A. apoda is reported in many aquatic environments over a wide range of temperature (0 - 32°C) and salinity (2 - 33 ppt) (Leadbeater 1972a,b; Thomsen 1973, 1979, 1982). This species was commonly observed in spring samples where temperature and salinities ranged from 7 to 32°C and 10 to 21 ‰. A characteristic feature of A. apoda, as the name suggests is the absence of a stalk, although the species is closely related to A. assymetrica (Thomsen 1979) which possesses a short asymmetrically placed stalk. The protoplast appears larger and more spherical (and flattened) (2.5 x 3.5 µm) than that of other species observed under SEM and

Figure 44a. Acanthoecopsis apoda with spherical protoplast and flagellum prominent. Scale bar = 2 μm.

Figure 44b. Higher magnification of Fig. 44a. shows overlapping connections and complexity of paired transverse costae. Scale bar = 1 μm.

Figure 45. Acanthoecopsis spiculifera. Two epibiont specimens attached to diatoms. Specimen laying on side attached by stalk to cocconeid diatom transverse costae. Second specimen standing on anterior end; transverse costae and ornamentation obvious. Scale bar = 5 μm.

Figure 46. Acanthoecopsis unguiculata. Diagonal costae form complex, organized post chamber. Collar and tentacles are evident. Scale bar = 10 μm.


44a

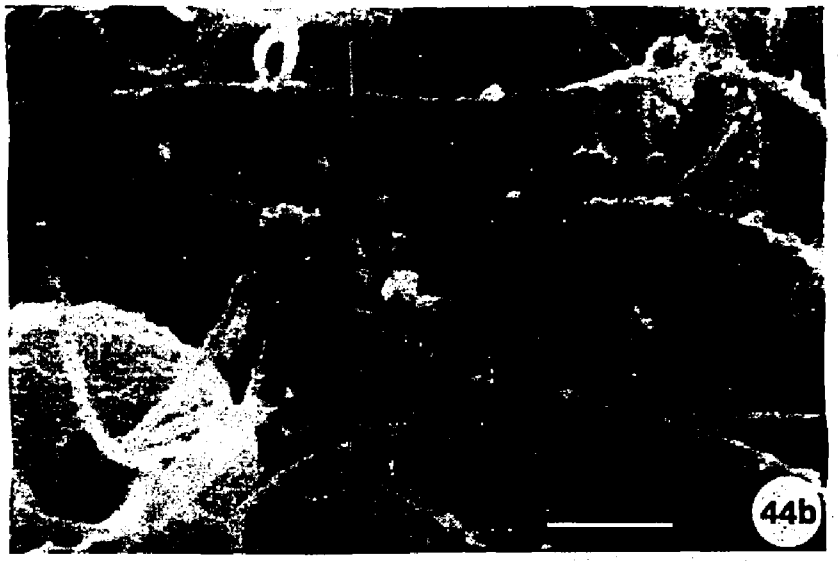
44b

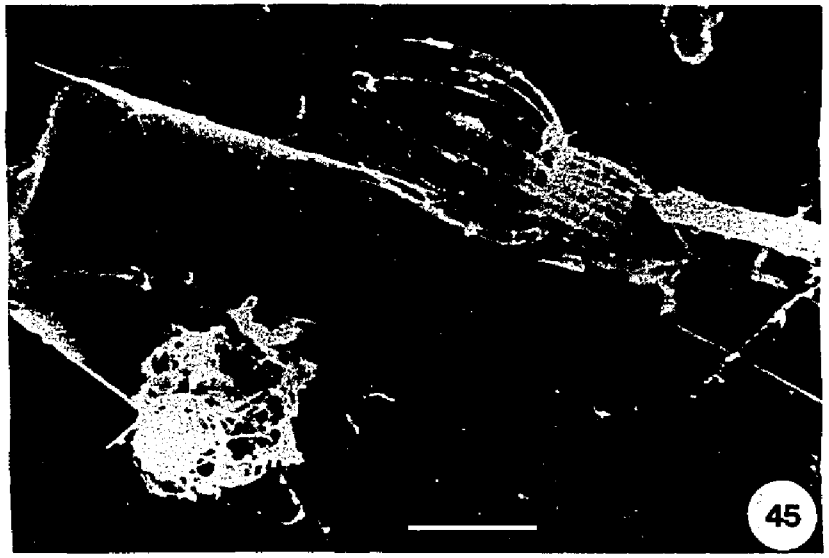
45

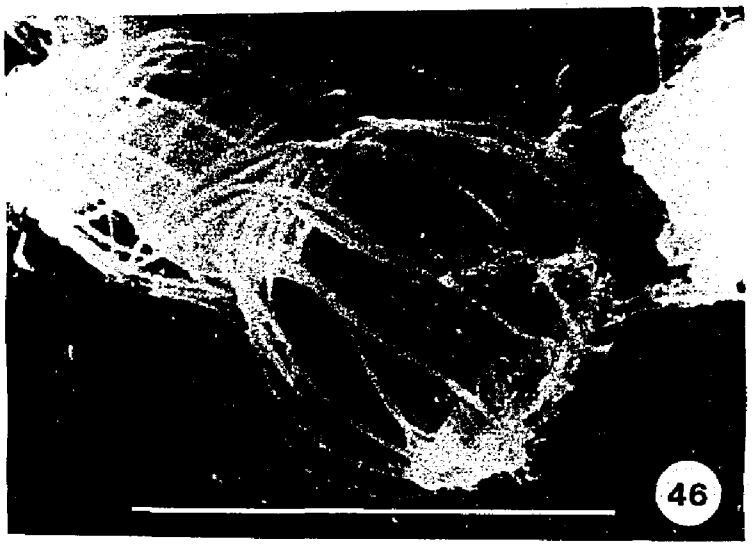
46

occasionally it extends into the posterior chamber. Lorica, with thinner and less elaborate arrangement of costal strips, appears more delicate than other Acanthoecopsis or Stephanoeca species. Approximately 12 to 14 longitudinal costae traverse the length of the lorica (10.5 - 12.0 µm) and posterior chamber (6.0 - 8.5 µm in length) is terminated at the waist by paired tranverse costae. The barrel-shaped anterior chamber forms a short broad open neck whose spines are composed 1 to 2 costal strips. The short spines of the pictured (Fig. 44a) specimen may indicate a youthful (juvenile) stage of assembly. The anterior chamber is characteristically encircled at the basal end by two closely appressed transverse costae and longitudinal costae beyond this point were usually distorted (wavy in SEM preparation). Lorica of this species and Diaphanoeca were among the few that did not maintain natural (ambient) shape for SEM photomicroscopy.

Acanthoecopsis spiculifera (Fig. 45)

This species is found in tide pools where other Acanthoecopsis species occur but are more frequently observed as epibionts in stagnant waters (Thomsen 1978, 1979, 1982). Only two Virginia specimens were observed during the marsh-mudflat experimental period. Both occurred in an April 1982 chamber and were attached to diatoms (Fig. 45), (one by its stalk to coccoid diatom (Thalassiosira) and the other attached at its anterior end to a diatom frustule). Lorica, characterized by two well-defined barrel-shaped chambers, are composed of several (~14) longitudinal costae each of four costal strips. The relatively narrow orifice is formed by free-end or spicules. The protoplast in the

posterior chamber is closely enveloped by narrowly spaced longitudinal costae and transverse rings (2-3) which encircle the ovoid cell at oblique angles. Placement of oblique costal strips of the posterior chambers vary in different specimens (Thomsen 1977); basal oblique costal strips of these specimens appear arranged more regularly forming tranverse costae, than in previously reported TEM micrographs (Thomsen 1977, Leadbeater 1981). Two to three transverse costae (more perpendicular to longitudinal costae) encircling the end of the cell near the waist, appear to be the most constant feature of the posterior chamber. Longitudinal costae spread slightly at the collar forming a broad anterior chamber where widely spaced costae consist of two overlapping curved costae. Reported number and placement of anterior transverse costae has differed (Norris 1965, Thomsen 1977) although spacing between costae is always typically greater than occurs in A. apoda. Norris (1965) observed no anterior transverse costae but Thomsen (1977) later reported two anterior transverse costae; one was fixed to the second longitudinal costal strip and the other crossed the junction between the second and third longitudinal costal strip. Each cell pictured (Fig. 45) corresponds to each of these descriptions and perhaps the top lorica (length-wise) represents a less developed stage of lorica assembly.

Acanthoecopsis unguiculata (Fig. 46)

Acanthoecopsis unguiculata is frequently found in quiescent stagnant tidal pools and marine habitats (Thomsen 1973, 1979, 1982, Leadbeater 1981). The species was first described (Thomsen 1973) from

samples in a sheltered brackish lagoon where the salinity range (16.4 - 21.4 ‰) was very similar to that of the present study. However only two specimens were observed in material (chamber incubations) from the York River marsh-mudflat system. Protoplasts were large, flattened ovoid cells (5.0 μm in length) with thick hair-point flagella extending into the anterior chamber (Fig. 46). The lorica is divided into two well-defined chambers composed of 12 -14 longitudinal costae. It is distinguished from other Acanthoecopsis species by the lack of anterior transverse costae and more complex irregularly arranged costae of the posterior chamber.

The lorica (approximately 10 um total height) is composed of two series of costal strips with different morphologies. Longitudinal costae parallel to long axis are narrower than second set which are arranged in an irregular pattern of diagonals criss-crossing exterior longitudinal costae (forming two sets of loose spirals). The anterior chamber is formed by free ends of longitudinal costae with apiculate tips and by an additional number of diagonally oriented costal strips extending from posterior chambers which connect to series of variable number of transverse costal rings near the waist.

Savillea parva (Figs. 47-50)

Savillea parva is also commonly found in tidal pools; previous records demonstrate a world-wide distribution (Ellis 1930, Norris 1965, Boucoud-Camou 1967, Leadbeater 1972b, and Thomsen 1973). This relatively small species was abundant in April and May 1982 chambers (Fig. 50). S. parva is easily recognized by its distinctive single

Figures 47 and 48

Savillea parva. Two specimens from April 1982 demonstrating characteristic tubular opening, small cell, straight flagella and fibrillar membrane. Fig. 47: scale bar = 5 um. Fig. 48: scale bar = 1 μm.

Figure 49. Four flagella of large autotroph surrounding Savillea parva specimen, demonstrating the species' small size. Scale bar = 5 μm.

Figure 50. Posterior view of cell of Savillea parva showing convergence of costae. Scale bar = 1 μm.

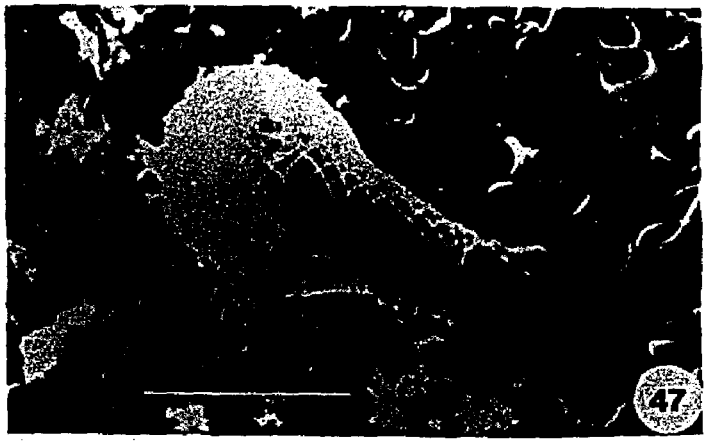
47


48

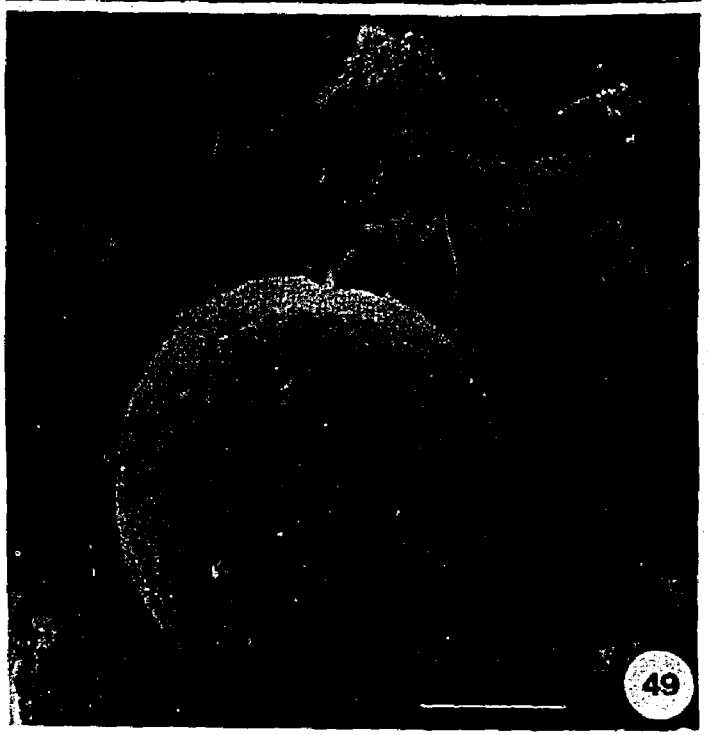
49

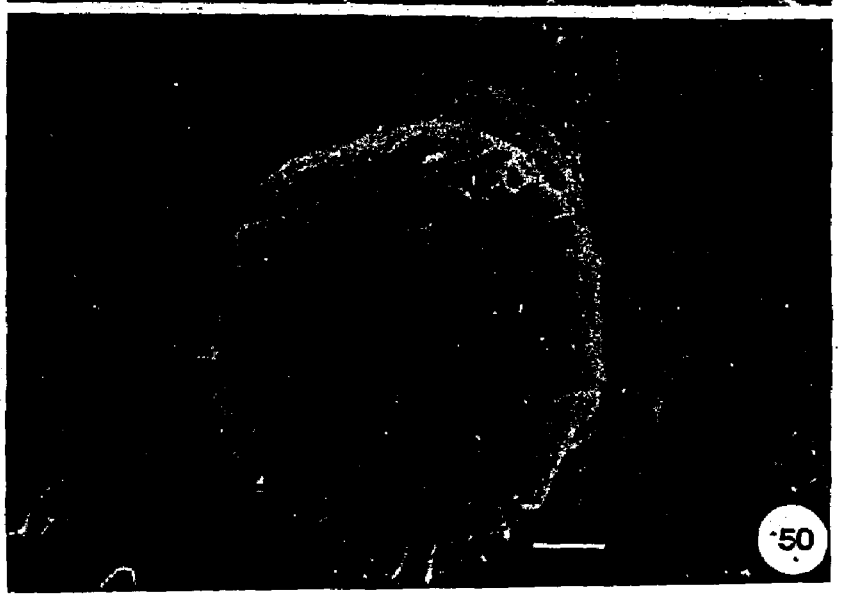
50

chamber lorica and the numerous compactly spiralled costae (basket-weave) which form the characteristic open-ended light bulb shape (Total height 6-11 µm). The posterior end, the larger bulb part contains a freely suspended spherical protoplast (2-3 µm). The lorica is composed of two groups of spirally arranged costae; the steeper spiralled costae are outermost and end abrubtly at the anterior ring. The anterior ring is formed by flattening of inner spirals of costae composed of crescentic strips. Difference in width and length of cyclindrical neck constituted the most obvious variation in loricas observed during this study (Figs. 47-50).

Saepicula pulchra (Figs. 51-53)

Saepicula pulchra were observed in April and May 1982 samples as solitary specimens and never in association with other heteroflagellates or diatoms as were Stephanoeca species. The lorica consists of two chambers separated by an ill-defined wide waist (Leadbeater 1980) which contains a freely suspended cell (mean 2.1 (width) x 3.0 (length)). SEM preparation revealed that the hair-point flagella (~ 4.0 µm) extend to the anterior ring unlike other choanoflagellates and frequently extend beyond the end of the lorica. Although this species is easily identified by characteristic bell-shaped lorica and very wide orifice rimmed by thick anterior ring, the lorica construction was quite variable, particularly in number and orientation of extended diagonal costae. Two series of costae, arranged more or less regularly, form the lorica; longitudinal series (approx. 10) are almost parallel to long axis and a second series of variable number of almost perpendicular costae

Figures 51-53a,b

Saepicula pulchra. Three specimens which demonstrate similar shape but different costal arrangements. Scale bars = 1 μm.

Figure 51. Cell is free-floating with flagella extending to the anterior tranverse costae.

Figure 52. This specimen is less-organized than that in Fig. 51. Flagellum extends beyond anterior ring. Note the large rod bacterium near or on the rims.

Figure 53a. Lorica without cell demonstrates costae of varying thickness.

Figure 53b. Detail of Fig. 53a. showing diagonal arrangement of costae at posterior end.

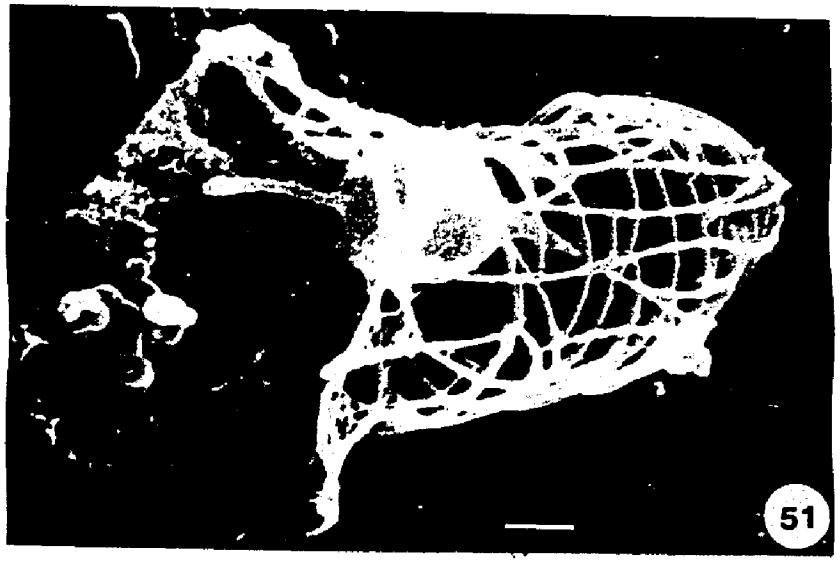
51

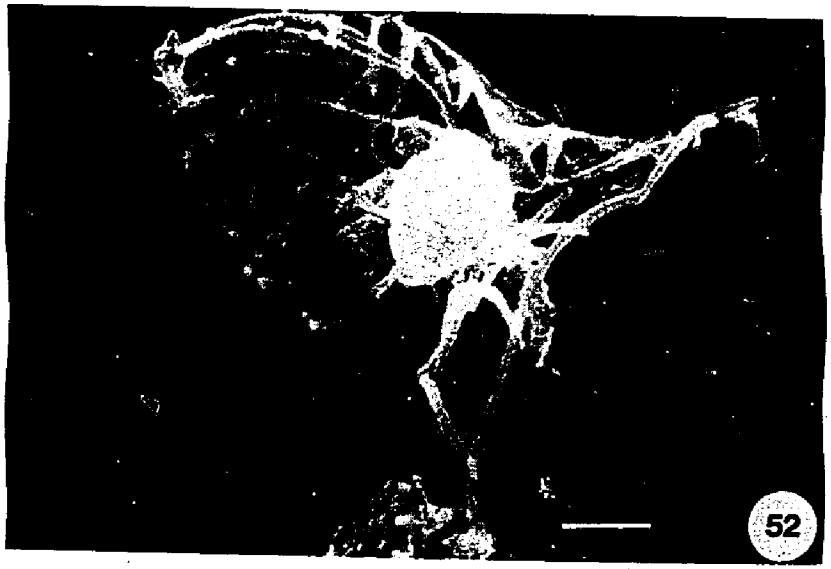
52

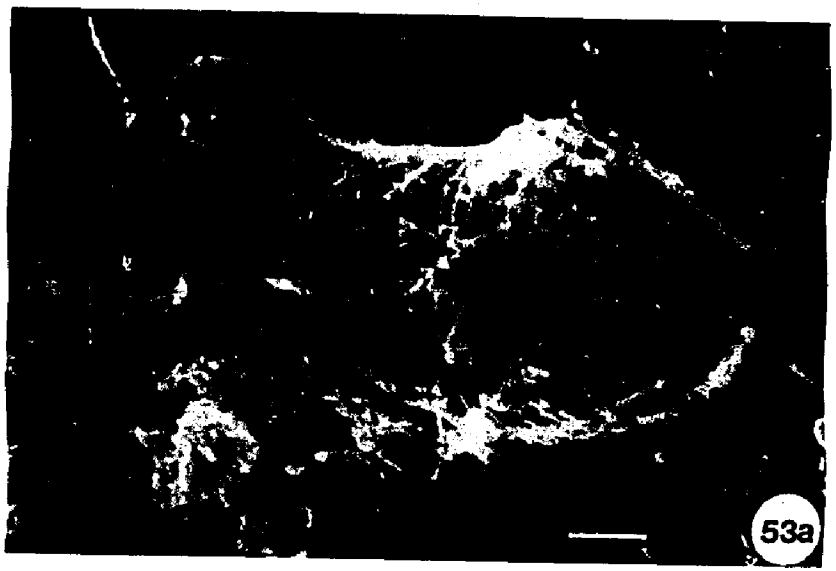
53a

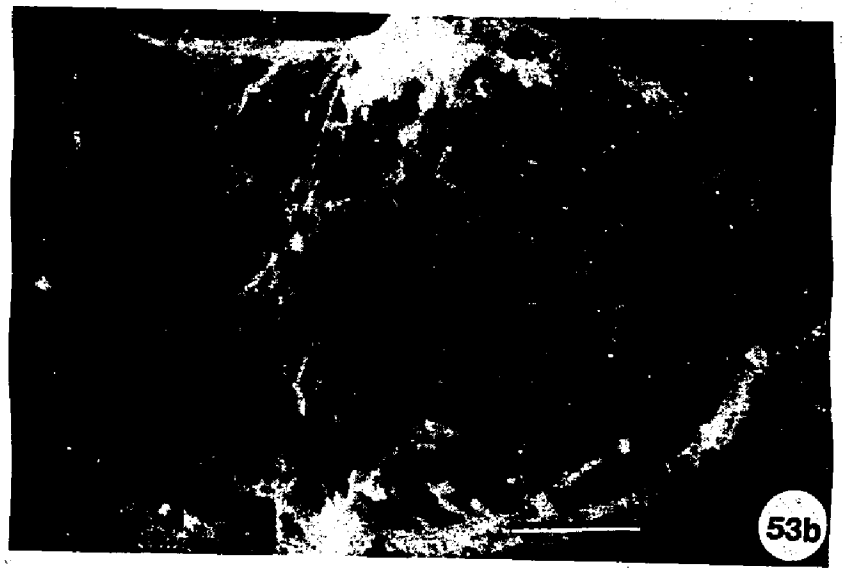
53b

form transverse costae at the waist. Diagonal costal strips are also usually attached to longitudinal costal strips midway along its length (Figs. 51 - 53a,b). The posterior chamber arrangement is most variable, composed of longitudinal and numerous transverse and diagonal costae. The three-dimensional SEM preparations, where bell lorica occasionally oriented vertical and rest on the anterior ring, also reveals that posterior lorica do not always converge completely (Fig. 53b) but have a small open basal ring. The widening anterior chamber is formed by divergent longitudinal costae, each consisting of one thick (concave) curved costal strip with apiculate (blunt) anterior tips. These blunt tips form t-joints, obvious in SEM (Figs. 51, 52), with costal strips of anterior ring.

Growth and Grazing Activity

Average growth and grazing rate parameters for each chamber incubation determined at both marsh and mudflat stations for each monthly experiment are presented in Table 2. Figures 2 - 6 demonstrate the variability in growth patterns and possible grazing effects. For example, the length of the growth period and the peak number of HNANO observed is very similar in all the April 1982 chambers where growth occurred without a lag and peak HNANO abundances were all > 15 x 10^3 cells ml^{-1} within 72 hours. However, all other chamber incubations showed great variability in length of the lag period and periods of maximum growth and peak heteroflagellate densities. These variable patterns are particularly evident in April 1983 and May 1984 chamber plots where growth periods are offset within each month, or replicate chambers show different growth patterns and are more typical of seasonal variability observed in situ chamber growth experiments throughout the 1981 -1984 study period. Chambers throughout the spring periods demonstrated grazing or at least a decrease in bacteria concentrations but usually not until HNANO conentrations peaked at concentrations much greater than ambient.

Growth and grazing rates of March chambers containing Diaphanoeca were relatively low (μ= 0.021h^{-1}, Dt 32.3h), possibly because of low temperatures (< 15°C) since bacteria concentrations, 5.28 x 10^6 cells ml^{-1} were not limiting. By contrast, abundances and growth and grazing rates of April and May 1982 chamber assemblages were considerably higher

Table 2. Growth and grazing rates of spring heteroflagellate assemblages at the marsh and mudflat stations. Growth, clearance, and ingestion rates are mean values of in situ diffusion chamber experiments.

Site	Date	Growth Rate μh^{-1} Mean	Range	CV	Generation Dt (h)	B	Clearance $\mu l\ d^{-1}$	Ingestion B h^{-1}	CV
MARSH	1982								
	March 17-22	0.018	0.015-0.020	32%	32.30	5.28	0.113	33.0	23%
	April 17-18	0.090	0.070-0.120	20%	7.70	5.62	0.398	115.5	
	18-21	0.030	0.025-0.040	27%	23.26	9.27	0.422	124.8	
	17-21	0.072	0.025-0.120	49%	9.63	7.87	0.422	120.2	34%
	May 19-22	0.043	0.024-0.074	4%	16.20	8.01	0.424	115.3	32%
	1983								
	April 13-21	0.032	0.014-0.068	44%	21.70	5.27	0.265	56.5	36%
	18-23	0.070	0.031-0.105	41%	9.86	5.65	0.265	95.0	33%
MUDFLAT	1982								
	March 17-22	0.026	0.020-0.037	30%	26.97	5.23		31.7	27%
	April 17-18	0.028	0.019-0.036	21%	24.80	6.02	0.504	149.0	
	18-21	0.031	0.026-0.033	10%	22.40	5.92	0.288	70.0	
	17-21	0.030	0.019-0.036	17%	23.80	5.99	0.432	123.0	29%
	May 19-22	0.024			29.10	3.50	0.516	112.0	16%
	1983								
	April 19-22	0.038	0.021-0.062	37%	18.50	7.70	0.266	80.0	38%
	1984								
	June 1-3	0.038	0.018-0.056	41%	18.07	9.07	0.288	96.0	30%

μ - heteroflagellate growth rate (h - hour); CV - coefficient of variation
Dt - doubling time (h - hours)
B - bacteria density (x 10^6 cells ml^{-1}) during heteroflagellate growth
Clearance - volume of water cleared per heteroflagellate per day
Ingestion - Bacteria consumed per heteroflagellate per hour

than March 1982. April 1982 chambers contained greatest abundances and diversity of choanoflagellates observed during the series of spring bloom experiments which corresponded to the unusual extended marsh tidal pool bloom of heteroflagellates (ave. 9.27 x 10^3 cells ml^{-1}) (Fig.3) and increased densities of cyanobacteria. Choanoflagellate growth rates with generation times as low as 7.7 h were measured over a short period early during the incubation. Growth rates ranged from 0.025 to 0.118 h^{-1} with a mean of 0.072 $h^{-1} \pm$ 0.035, Dt 9.6 h) or at least two doublings per day. These growth rates resulted in very high concentrations of HNANO ranging from 5.89 to 36.9 x 10^3 cells ml^{-1} (Fig.3), second only to values reported for two chambers in May 1981 and April 1983. High concentrations and diverse assemblages of choanoflagellate remained in the chambers for periods of several days concurrent with high ambient HNANO concentrations. Chamber bacteria concentrations were higher than in March, ranging from 3.17 to 16.9 x 10^6 cells ml^{-1} with a mean of 7.81 x 10^6 cells ml^{-1} during periods of growth. Higher than normal bacterial concentrations indicate active growth which could help support high abundance of HNANO in chambers; subsequently grazing reduced bacterial concentrations to ambient. Cyanobacteria and large rod-shaped bacteria decrease most quickly and, as evident in SEM micrographs, are consumed by choanoflagellates. Clearance (0.422±0.096 ul d^{-1} CV 22.7%) and grazing (90 - 120 bacteria h^{-1}, mean 120 h^{-1}± 41 CV 34.4% or 2883 bacteria d^{-1}) rates were less variable than growth rates.

Although ambient concentrations during May 1982 (1.96 x 10^3 heteroflagellates ml^{-1}, 5.82 x 10^6 bacteria ml^{-1}; Fig. 4) were much

lower than during April 1982, the chamber innoculum contained above average numbers of heteroflagellates (3.5-6.0 x 10^3 cells ml^{-1}). The innoculum apparently included a concentrated patch of choanoflagellates bloom because a diverse assemblage of choanoflagellates with relatively high growth rates developed in the chambers. The assemblage were very similar to April although Acanthoecopsis species were observed more frequently. Growth rates averaging 0.064 h^{-1} ± 0.01 were similar to April rates, again indicating at least 2 divisions per day or generation times of less than 12 hours. High numbers of bacteria (8.81 x 10^6 and 15.3 x 10^6 cells ml^{-1}), including cyanobacteria, were growing in the chamber (μ = 0.025 - 0.095 h^{-1}) at the end of the lag period for HNANO. Average bacteria abundance during HNANO growth periods were again relatively high (9.32 and 6.7 x 10^6 cells ml^{-1}) and after several days decreased to below ambient levels again indicating grazing impact (Fig. 4). Clearance rates and grazing rates were quite variable but mean rates (F= 0.40 μl d^{-1} ± 0.01; I = 115 bacteria h^{-1} (65 - 165)) were very similar to April 1982 chamber assemblages.

The April 1983 experiment was conducted during a similar period of the lunar month as during April 1982. However the April 1983 period was characterized by anomalous weather conditions and greater ranges in temperature and salinity. A snowstorm resulted in a short-term (48 hour) decrease to below normal temperatures and salinities (<10°C and 9 - 11‰, respectively). Average growth rate (μ= 0.038 h^{-1}) of the first April 1983 series (4/13 - 21, was lower than April, May 1982 averages, however a few individual rates were comparable to those of previous year. The second series, initiated at onset of lower temperatures and

incubated through a period of increasing temperatures and low tide assemblages, demonstrated a wide range in growth rates (μ= 0.031 - 0.105 h^{-1}). Average rates (μ=0.07 h^{-1},Dt=9.9h) were similar in magnitude to April, May 1982 chambers. The second series, under epifluorescence analysis, appeared to contain a higher percentage of cyanobacteria and choanoflagellates. Although measured growth rates were lower, maximum heteroflagellate densities (11.0 - 42.0 x 10^3 cells ml^{-1}) achieved after several days were comparable to April 1982, and in some cases, higher. Grazing rates and clearance rates were, as in previous experiments, extremely variable. Average clearance rates F=0.27 $\pm$ 0.08 μl d^{-1} and grazing rates 80 $\pm$ 30.2 bacteria h^{-1} (1920 bacteria d^{-1}) were significantly lower than April-May 1982 rates (where percentages of choanoflagellates abundances were also greater). Heteroflagellate growth rates of June 1984 chambers (Ave. μ = 0.038 $\pm$0.016 (0.018-0.056 h^{-1}) and maximum abundances (~20.0 x 10^3 cells ml^{-1}) in chambers were comparable to April 1983 when salinities were also comparable. Average bacteria concentrations were also similar (5.67 x 10^6 cells ml^{-1}), although much more variable than previous year. Range in grazing and clearance rates were similar both in range and variability, although grazing rates were slightly higher.

DISCUSSION

Choanoflagellates and Bicoecids have been reported in coastal waters, estuaries, and littoral tide pools (Leadbeater 1972a, Thomsen 1973, Leadbeater 1981). To date, only one published ecological study of heterotrophic nanoplankton includes description of choanoflagellates and various other HNANO species (Davis 1982). TEM and SEM descriptive and ecological studies of HNANO species are lacking for Atlantic coastal waters. The eleven Acanthoecidae species described here expands their range through the mid-Atlantic coast. Their seasonal abundance and sporadic blooms in marsh-mudflat systems are to be expected since they are cosmopolitan in nature. Multispecies HNANO blooms dominated by choanoflagellates occurred frequently in Virginia salt marsh tidal pools at concentrations considered as "mass occurrence" in France ($5 - 20 \times 10^3$ cells ml^{-1}) in a tide pool environment (Chretiennot 1974). Choanoflagellate blooms reported here confirm their potential numerical importance as grazers of cyano- and other bacteria in the estuarine environment (Caron et al. 1982, Sieburth 1984).

In situ diffusion chambers, which in effect mimic quiescent tidal pool niches, proved to be ideal for simultaneous identification and for growth and grazing activity experimentation with ambient populations of choanoflagellate, either free-swimming or epibionts. Specific choanoflagellate species (i.e. S. urnula), observed through wide salinity ranges, maintained the same lorica characters but demonstrated some morphological differences (Thomsen 1973, Leadbeater 1981). Most

frequently the morphological variation involves variation in numbers of costae in the anterior chamber. Lorica of S. urnula from this study most closely corresponded to those described from similar salinities (17 - 19 ppt; Thomsen 1973). This observation supports the speculation that annual differences in species composition where species are characterized by less complex lorica construction, e.g. fewer costal strips, may be attributed to long term decrease in seasonal salinities due to above average rainfall. However further studies are needed to confirm this salinity correlation. Chamber incubations and SEM photodocumentation of lorica morphology from a series of different environmental salinities would be an appropriate method for assessing effects of salinity fluctuation on lorica complexity.

Diffusion chamber experiments illustrate high potential growth and grazing rates during each spring period. Growth and grazing rates of consecutive years of spring periods were not affected directly by large differences in temperature and salinity ranges. Although experiments were conducted on nearly identical dates in consecutive years, salinities and temperature ranges differed considerably. Marked differences between environmental conditions of April and May 1982 and the following April 1983 reflected increased winter and spring rainfall and below normal temperatures during the April 1983 snowstorm. However, although initial April 1982 rates during pronounced ambient bloom were the highest measured, rates and HNANO abundances in diffusion chambers during 1982 were very similar to April 1983 and May 1984 averages. Increase in temperatures from April to May 1982 did not result in increased rates or abundances nor did decreased temperatures from March to April 1983 result

in lower growth rates.

Assemblages dominated by large percentage ($\leq$ 50%) of choanoflagellates yielded highest growth rates although each chamber experiment was characterized by high concentrations ($\geq 1 \times 10^4$ cells ml^{-1}) which except for April 1982 bloom exceeded ambient levels. This study demonstrates that choanoflagellates may grow rapidly in marsh tidal pools and blooms may be observed at successive low tides. Except for the unusual April bloom, most blooms are short-lived and were not sustained through a tidal stage. It is thus possible that spring periods of increased temperatures and extended low tides favor bacteria and cyanobacteria growth which provide ideal prey for rapid HNANO growth in marsh surface tidal pools, and cyanobacteria growth in stratified York River waters. Maximum in situ growth rates indicate generation times, approximately 6 to 10 hours, which are longer than the duration of low tide in the large ambient marsh pool where HNANO blooms were observed. Thus blooms are most likely a result of aggregation rather than rapid growth alone. Such aggregation may occur from tidal concentration effects of HNANO imported from ebbing marsh creek waters; during the spring, increased heteroflagellate abundances most frequently occurred after ebbing tide.

Average grazing rates, determined at peak HNANO growth, ranging from 60 -120 bacteria h^{-1} (mean ~100) indicate that spring HNANO assemblages, frequently dominated by choanoflagellates, may consume bacterial numbers which account for approximately all of the daily bacterial production, i.e. one doubling per day. HNANO species composition differences may be responsible for the lower grazing rates by the March 1982 chamber

populations compared to those of April 1982 and April 1983 which were some of the highest (Table 2). March 1982 HNANO assemblages were dominated by D. grandis, which according to Manton et al. (1981) may feed relatively inefficiently due to its lorica construction and sluggish flagellar activity. April 1982 and some April 1983 diffusion chambers were dominated by Acanthoecidae Stephanoeca choanoflagellates which characteristically demonstrate high clearance and grazing rates (Fenchel 1982b). The SEM micrographs (Figs. 26-32) help illustrate how functional morphology of these species would facilitate efficient feeding and clearance rates. Entrapped large rod-shaped and cyano-bacteria are evident in the lorica of choanoflagellates of April and May 1982 chambers. Higher grazing and clearance rates observed in chamber experiments at relatively high heteroflagellate concentrations also may be stimulated by the presence of optimum prey such as these cyanobacteria.

Results of these spring experiments demonstrate that HNANO, particularly choanoflagellates, play an important role in estuarine microbial trophodynamics as abundant and voracious bacteriovores. However in contrast to in situ chamber concentrations, average ambient spring HNANO concentrations are not elevated compared to the annual ambient average of $2.3 - 2.7 \times 10^3$ cells ml^{-1}. The environmental abundances, in combination with lower range of grazing rates (50 - 80 bacteria h^{-1}), perhaps more typical of ambient populations, indicate choanoflagellates may consume 40 to 110% of bacterial carbon production. This activity would thus prevent substrate limitation and maintain the bacteria in log phase of growth. The study of growth and grazing rates

using in situ diffusion chamber incubations combined with EM photomicroscopic identifications may provide an excellent opportunity for testing differences between grazing rates and predator and prey types.

CHAPTER VI

SUMMARY AND CONCLUSIONS

Heterotrophic nanoplankton (HNANO) play an important role in the microbial trophodynamic paradigm (Pomeroy 1974) by transferring secondary production to higher trophic levels through their consumption of bacteria. The bactivorous nanoplankton, primarily the heterotrophic nanoflagellates or heteroflagellates, ranging from 2 to 12 μm in size, are numerically and functionally important component of estuarine salt marsh systems of the Chesapeake Bay. However until recently little quantitative information was available for in situ growth and grazing rates of heteroflagellates under natural conditions. The study of trophodynamics of estuarine heteroflagellates was conducted in a salt marsh-mudflat system where short time scale sampling was required to resolve the variability in nanoplankton dynamics and interactions of heteroflagellates and bacteria as predator and prey, respectively.

The objectives of the study were: 1) to obtain information for the seasonal distribution, abundances, and types of heteroflagellates in the marsh-mudflat system; 2) to determine the temporal scales necessary to resolve the degree of variability and seasonal pattern of predator-prey interactions; 3) to develop a field methodology to obtain in situ growth and grazing rates of heteroflagellates; 4) to describe predator-prey interactions or cycles; and 5) to determine if heteroflagellate activity affects bacterial population dynamics.

1. Heteroflagellates in the estuarine system are euryhaline and eurythermal, and assemblages are dominated by four types including choanoflagellates, Paraphysomonas sp., bodonids, and small monads. Annual average heteroflagellate density is approximately are 2.0×10^3 cells ml^{-1} and concentrations of 4.5×10^3 cells ml^{-1} indicate a bloom in the tidal environment. Environmental abundances fluctuate between approximately 1.0 and 5.0×10^3 cells ml^{-1} throughout the year but unlike bacterial populations, heteroflagellate fluctuations do not follow a seasonal pattern. Annual heteroflagellate population patterns in shallow estuarine environments were not correlated to seasonal variations in bacterial abundance or temperature. Heteroflagellate numbers were slightly elevated above the annual averages during the fall and spring transition periods. However sampling over short time scales revealed that hourly and daily fluctuations in heteroflagellate abundances were frequently of the same magnitude as or greater than those observed over weekly or monthly time scales. These short-term peaks of diverse heteroflagellate and bacteria populations were observed in tide pool environments formed at low water in the marsh-mudflat system, particularly during periods of extended low tide. The variation in nanoplankton populations and concentrations during the tidal cycles, demonstrated the necessity of monitoring abundances at short intervals in order to determine the frequency of formation of low tide heteroflagellate assemblages.

2. Diffusion chambers represent specialized conditions of the quiescent (low turbulence) tidal pools at low water where advection effects are

removed and microniches are more stable. Rapid divisions of heteroflagellates in chambers may indicate an adaptation to a more favorable environment where prey concentration is no longer limiting. Chamber experiments indicate the potential for high rates of heteroflagellate growth and grazing under various environmental conditions. High growth rates and high densities of heteroflagellates in in situ diffusion chamber experiments generally corresponded to periods of increased abundance in ambient heteroflagellate populations. Periods of HNANO growth in chambers were concurrent with increased growth or change in species composition of bacteria in the chambers. Frequently growth of heteroflagellates in chambers demonstrated two different ranges of rates or two different phases of growth. The initial lag phase or slower rates with doubling times of approximately 24 hours or greater are perhaps typical of populations from unstable tidal environments while the second phase of accelerated growth rates with doubling times of 7 to 14 hours usually occur when larger and/or actively growing bacterial prey are available. A lag phase in heteroflagellate growth may result from handling disturbance of innoculation or may indicate food-limitation. Divisions may not occur until after several hours of active grazing. Blooms or growth pulses may occur rapidly (within hours) particularly as an opportunistic response to optimum or diverse food sources which are grazed more efficiently, i.e., larger bacteria (>0.20 μm^3), cyanobacteria, or gametes. The second phase of growth in chambers is also characterized by increased diversity and size of heteroflagellates similar to that observed in situ during periods of extended low water.

3. Environmental variability, rapidly shifting ambient nanoplankton

populations, and variation in growth of heteroflagellates in chambers suggest in situ rates may change quickly. Growth rates may be underestimated for example, if the sampling interval does not account for a synchronous division following the feeding phase. Further in situ growth and grazing determinations should involve short sampling intervals (2 to 4 hours) to determine accelerated growth rates more accurately and to detect possible synchronous divisions or diel patterns in growth and grazing.

4. The first year (1981-1982) of in situ chamber experiments revealed the dynamic nature of nanoplankton in the marsh-mudflat system during early autumn (1982) and spring (1983) transition periods. Nanoplankton assemblages in late October and early November were characterized by a greater relative abundance of larger bodonid forms, and colorless and orange fluorescing cryptomonads, and orange flourescing cyanobacteria. April 1982 was characterized by choanoflagellate blooms and rapid growth and grazing rates. The second year of experiments involving more intensive sampling confirmed that the transition periods were optimum for rapid blooms of these nanoplankton assemblages, particularly during extended periods of low tide. Heteroflagellate densities and accelerated growth rates during these periods were as great as that of summer, demonstrating that the annual pattern in heteroflagellates growth rates does not follow a seasonal pattern which can be resolved on a monthly scale.

The lack of a consistent seasonal pattern in monthly mean growth rates of heteroflagellates in the marsh-mudflat system; the large range

in growth responses among individual chambers during a period of a week; the variability in the seasonal pattern of environmental heteroflagellate densities and the opportunistic nature of the heteroflagellate growth response to specific conditions (i.e., suitable prey) all indicate the necessity to investigate microbial dynamics in a marsh-mudflat system should by intensively sampling several parameters over short periods (i.e., hourly intervals over several tidal cycles) rather than by monthly or bimonthly seasonal experiments.

5. During both transition periods, pulses of heteroflagellate growth occurred most frequently during growth of larger forms of bacteria or presence of cyanobacteria, particularly as aggregates. An unusually dense bloom of cyanobacteria occurred in tide pools and chambers during the autumn 1982 experiment. Large bodonid forms and Paraphysomonas grew rapidly in association with the cyanobacteria aggregates, demonstrating an opportunistic response to optimum prey. The autumn experiments suggest that microaggregates play an important role in stimulating growth and grazing activity in nanoplankton trophodynamics. In situ diffusion chamber incubations using shorter sampling intervals (<2 hours) should be an ideal methodology for observing the formation of microaggregates and resolving their importance in HNANO trophodynamics.

6. The spring bloom assemblages of 1982 through 1984 were further characterized using in situ diffusion chamber experiments and a combination of epifluorescence direct counts and scanning and transmission electron microscopy (SEM and TEM) to enumerate and describe the heteroflagellates. Photomicroscopic analysis of the spring

assemblages demonstrated the necessity of combined analysis for identification of the heteroflagellate species assemblage. SEM, shows details of loricas with a minimum of distortion which is particularly valuable for choanoflagellate identification. TEM is valuable for identification of the hyaline sheaths of bicoecids and species-specific scales of Paraphysomonas species. The SEM preparation, modified specifically for preservation of heteroflagellates, revealed that the dominant component of the spring blooms was composed of several members of the loricate choanoflagellate family, Acanthoecidae. Eleven Acanthoecidae choanoflagellate species, identified from the spring chamber experiments were described for the first time in the Chesapeake Bay area.

Results of the more intensive spring experiments and combined methodologies documents the important role of heteroflagellates, particularly choanoflagellates, as abundant and voracious bacteriovores in estuarine microbial trophodynamics. In situ growth and grazing rates determined for the spring chamber populations, ranged from 0.023 to 0.196 h^{-1} and 40 to 210 bacteria h^{-1} per heteroflagellate, respectively. These high rates represent an opportunistic response to optimum conditions and expression of maximum grazing potential. The SEM micrographs illustrate how the functional morphology of the lorica of the Acanthoecidae species facilitates efficient feeding and clearance rates. The study of growth and grazing rates using in situ diffusion chamber incubations combined with EM photomicroscopic identifications may provide an excellent opportunity for testing differences between grazing rates and predator and prey types.

7. Ambient heteroflagellates fluctuated independently of bacteria densities and growth in chambers was not correlated with bacteria density. The lack of positive correlation of initial bacteria concentrations with heteroflagellate growth supports the idea that bacteria abundance (above a threshold) does not determine growth rates nor density of heteroflagellates. However, limiting or controlling factors of HNANO populations in the natural environment (i.e., marsh-mudflat system) may include turbulent instability, food-limitation, and predation pressure. Instability of the water column may increase food-limitation or require elevated bacteria numbers for efficient feeding and subsequent growth. Bacterial concentrations seldom decreased below grazing threshold concentrations in chambers, however in the unconfined environment, physical agitation from water movement and decreased availability of microniches, e.g., microaggregates, may decrease heteroflagellate feeding efficiencies. Ambient threshold bacterial concentrations for grazing may actually be higher than for chamber populations or may be dependent on presence of optimum prey, e.g., larger bacteria or a diversity of food sources, to yield increased grazing and growth. Although rates measured in diffusion chamber may be more representative of ambient rates than rates from incubations carried out in glass bottles, caution must be exercised in extrapolating directly to ambient conditions.

8. Predator-prey interactions evident in diffusion chambers experiments demonstrate the short-term opportunistic response of heteroflagellates to stable conditions. The classic 5 to 7 day sinusoidal predator-prey cycle

consisting of a bacteria peak followed by a heteroflagellate peak, usually after 2 to 3 days, was not typical of the marsh-mudflat system. Instead the growth response of the bacteria (prey) and heteroflagellate (predator) populations in diffusion chambers was more closely coupled within less than 2 days. Frequently the two populations increased concurrently rather than out of phase, confirming a close coupling of bacteria and heteroflagellate growth rates.

9. Several factors may contribute to variation in grazing rates of marsh-mudflat heteroflagellates including environmental conditions, abundance, size and species diversity of available prey, and predator species-specific grazing rates. Clearance and grazing rates for natural mixed HNANO assemblages, besides varying with the size or density of bacteria and with the dominant feeding type, will be influenced by a suite of environmental factors. There was no correlation between grazing rates and bacteria densities determined in chambers, perhaps because grazing aproaches saturation near concentrations (4.0 to 8.0 x 10^6 cells ml^{-1}) found in the marsh-mudflat system. However epifluorescence microscopy indicated that heteroflagellates preferentially grazed the larger sized bacteria and higher ingestion rates occurred frequently during blooms of cyanobacteria or large rod-shaped bacteria. The size and type of bacteria and type of predator (i.e., choanoflagellates) influenced grazing rates.

10. During any season, ambient densities of heteroflagellates are capable of grazing 30 to 100% of the standing crop of bacteria, i.e, 1.0 to 6.0 x 10^6 cells per day. Grazing activity by the ambient

heteroflagellate population usually accounts for nearly half the estimated daily bacterial carbon production for the marsh-mudflat system, with the seasonal range of estimates ranging from 20 to 100% of the daily bacteria turnover. The bacterial carbon production, in turn will support 1 to 3 doublings of heteroflagellates. However, these numbers are only rough estimations based on one of a variety of assumed values for carbon content of bacteria and heteroflagellates found in the literature and rough estimates of the volumes of the two mixed populations. The percentages reported in the literature of bacterial carbon production consumed by heteroflagellates are also compared to estimates of bacterial productivity which generally are not specific to the study area and do not take into account environmental variability. These estimates could be greatly improved by using a combination of chamber experiments and CHN analysis to determine the volumes and carbon content of the specific HNANO assemblages and by determining specific activity of bacteria with tidal stage.

11. Both environmental patterns of HNANO and in situ experiments demonstrated that heteroflagellates (at ambient densities) do not control the fluctuations in bacteria concentrations nor do estuarine bacterial concentrations regulate or control the number of heteroflagellates found in the shallow tidal environment. However, growth rates in chambers did indicate that peak growth of heteroflagellate and bacteria were closely coupled. Bacteria growing without heteroflagellate grazing pressure enter a stationary phase after only one or two doublings which may be due in part to substrate limitation. Heteroflagellate grazing activity may regulate the standing stocks of bacteria to the extent that it prevents

substrate limitation. Heteroflagellate grazing pressure may maintain bacteria in a youthful phase so bacteria may flourish when optimum conditions for growth occur such as in the summer when substrate and temperatures are not limiting. Heteroflagellates also may affect microbial productivity through increased grazing and remineralization (nutrient regeneration) activities as short-term responses to increased bacterial populations, thus sustaining both bacterial growth and cycling of bacterial carbon in estuarine trophodynamics. The potential for high growth and grazing rates demonstrated by in situ chamber experiments under nearly all environmental conditions and the lack of seasonal patterns in fluctuating densities indicate heteroflagellates may serve as a relatively constant pathway of bacterial carbon into the estuarine food chain.

REFERENCES

Ammerman, J. W., J. A. Fuhrman, A. Hagstrom, and F. Azam. 1984. Bacterioplankton growth in seawater: I. Growth kinetics and cellular characteristics in seawater cultures. Mar. Ecol. Prog. Ser. 18: 31-39.

Andersen, P., and T. Fenchel. 1985. Bacteriovory by microheterotrophic flagellates in seawater samples. Limnol. Oceanogr. 30: 198-202.

Anderson, I. C., M. W. Rhodes, and H. I. Kator. 1983. Seasonal variation in survival of Escherichia coli exposed in situ in membrane diffusion chambers containing filtered and nonfiltered estuarine water. Appl. Environ. Microbiol. 45: 1877-1883.

Andrews, P., and P. J. L. Williams. 1971. Heterotrophic utilization of dissolved organic compounds in the sea. III. Measurement of the oxidation rates and concentrations of glucose and amino acids in sea water. J. mar. biol. Ass. U.K. 51: 111-125.

Azam, F., T. Fenchel, J. G. Field, J. S. Gray, L. A. Meyer-Reil, and F. Thingstad. 1983. The ecological role of water-column microbes in the sea. Mar. Ecol. Prog. Ser. 10: 257-263.

Azam, F., and R. E. Hodson. 1977. Size distribution and activity of marine heterotrophs. Limnol. Oceanogr. 22: 492-501.

Azam, F., and R. E. Hodson. 1981. Multiphasic kinetics for d-glucose uptake by assemblages of natural marine bacteria. Mar. Ecol. Prog. Ser. 6: 213-222.

Beers, J. R., F. M. H. Reid, and G. L. Stewart. 1980. Microplankton population structure in Southern California near-shore waters in late spring. Mar. Biol. 60: 209-226.

Boucaud-Camou, E. 1967. Les Choanoflagelles des cotes de la Manche: I. Systematique. Bull. Soc. linn. Normandie. 10, 7:191-209.

Bowden, W. B. 1977. Comparison of two direct count techniques for enumerating aquatic bacteria. Appl. environ. Microbiol. 33: 1229-1232.

Buck, K. 1981. A study of Choanoflagellates (Acanthoecidae) from the Weddell Sea, including a description of Diaphanoeca multiannulata n. sp. J. Protozool. 28: 47-54.

Burney, C. M., P. G. Davis, K. M. Johnson, and J. M. Sieburth. 1981. Dependence of dissolved carbohydrate concentration upon small scale nanoplankton and bacterioplankton distributions in the western Sargasso Sea. Mar. Biol. 65: 289-296.

Burney, C. M., P. G. Davis, K. M. Johnson, and J. M. Sieburth. 1982. Diel relationships of microbial trophic groups and in-situ dissolved carbohydrate dynamics in the Caribbean Sea. Mar. Biol. 67: 311-322.

Burney, C. M., K. M. Johnson, and J. M. Sieburth. 1981. Diel flux of dissolved carbohydrate in a salt marsh and a simulated estuarine ecosystem. Mar. Biol. 63: 175-187.

Burney, C. M., and J. M. Sieburth. 1977. Dissolved carbohydrates in seawater. II, A specrtophotometric procedure for total carbohydrate analysis and polysaccharide estimation. Mar. Chem. 5: 15-28.

Caperon, J., and J. Meyer. 1972. Nitrogen-limited growth of marine phytoplankton - II. Uptake kinetics and their role in nutrient limited growth of phytoplankton. Deep-Sea Res. 19: 619-632.

Caron, D. A. 1983. Technique for enumeration of heterotrophic and phototrophic nanoplankton, using epifluorescence microscopy, and comparison with other procedures. Appl. Environ. Microbiol. 46: 491-498.

Caron, D. A., P. G. Davis, L. P. Madin, and J. M. Sieburth. 1982. Enrichment of heterotrophic bacteria and bacterivorous protozoa in oceanic macroaggregates. Science, N.Y. 218: 795-797.

Chalmers, A. G., R. G. Wiegert, and P. L. Wolf. 1985. Carbon balance in a salt marsh: interactions of diffusive export, tidal deposition and rainfall-caused erosion. Est. Coast. Shelf Sci. 21: 757-771.

Chretiennot, M-J. 1974. Nanoplancton de Flaques supralittorales de la region de Marseilles. II. Etude quantitative. Protistologica. 10: 477-88.

Christian, R. R., R. B. Hanson, and S. Y. Newell. 1982. Comparison of methods for measurement of bacterial growth rates in mixed batch cultures. Appl. environ. Microbiol. 43: 1160-1165.

Crawford, C. C., J. E. Hobbie, and K. L. Webb. 1973. Utilization of dissolved organic compounds by microorganisms in an estuary. In: Estuarine microbial ecology, eds. L. H. Stevenson and R. R. Cowell, Univ. of South Carolina Press, Columbia. pp. 169-180.

Davis, P. G. 1982. Bacterivorous flagellates in marine waters. Doctoral dissertation, University of Rhode Island, Kingston.

Davis, P. G., D. A. Caron, P. W. Johnson, and J. M. Sieburth. 1985. Phototrophic and apochlorotic components of picoplankton and nanoplankton in the North Atlantic: geographic, vertical, seasonal, and diel distributions. Mar. Ecol. Prog. Ser. 21: 15-26.

Davis, P. G., and J. M. Sieburth. 1982. Differentiation of the phototrophic and heterotrophic nanoplankton populations in marine waters by epifluorescence microscopy. Annls Inst. oceanogr., Monaco. 58: 249-260.

Davis, P. G., and J. M. Sieburth. 1983. Comparison of cultured and natural populations of heterotrophic microflagellates from estuarine and oceanic waters. J. Protozool. 30: 22a.

Davis, P. G., and J. M. Sieburth. 1984. Estuarine and oceanic microflagellate production of actively growing bacteria. Estimation by frequency of dividing-divided bacteria. Mar. Ecol. Prog. Ser. 19: 237-246.

Dietz, A. S., L. J. Albright, and T. Tuominen. 1976. Heterotrophic activities of bacterioneuston and bacterioplankton. Can. J. Microbiol. 22: 1699-1709.

Eberlein, K., U. H. Brockmann, K. D. Hammer, G. Kattner, and M. Laake. 1983. Total dissolved carbohydrates in an enclosure experiment with unialgal Skeletonema costatum culture. Mar. Ecol. Prog. Ser. 14: 45-58.

Ellis, W. N. 1930. Recent researches on the Choanoflagellata (Craspedomanadines). Annls. Soc. r. zool. Belg. 60: 49-88.

Fenchel, T. 1980. Suspension feeding in ciliated protozoa: functional response and particle size selection. Microb. Ecol. 6: 1-11.

Fenchel, T. 1982a. Ecology of heterotrophic microflagellates. I. Some important forms and their functional morphology. Mar. Ecol. Prog. Ser. 8: 211-223.

Fenchel, T. 1982b. Ecology of heterotrophic microflagellates. II. Bioenergetics and growth. Mar. Ecol. Prog. Ser. 8: 225-231.

Fenchel, T. 1982c. Ecology of heterotrophic microflagellates. III. Adaptations to heterogeneous environments. Mar. Ecol. Prog. Ser. 9: 25-33.

Fenchel, T. 1982d. Ecology of heterotrophic microflagellates. IV. Quantitative occurrence and importance as consumers of bacteria. Mar. Ecol. Prog. Ser. 9: 35-42.

Ferguson, R. L., E. N. Buckley, and A. V. Palumbo. 1984. Response of marine bacterioplankton to differential filtration and confinement. Appl. Environ. Microbiol. 47: 49-55.

Ferguson, R. L., and A. V. Palumbo. 1979. Distribution of suspended bacteria in neritic waters south of Long Island during stratified conditions. Limnol. Oceanogr. 24 (4): 697-705.

Ferguson, R. L., and P. Rublee. 1976. Contribution of bacteria to the standing crop of coastal plankton. Limnol. Oceanogr. 21: 141-145.

Frost, B. W. 1972. Effects of size and concentration of food particles on the feeding behavior of the marine planktonic copepod Calanus pacificus. Limnol. Oceanogr. 17: 805-815.

Fuhrman, J. A. 1981. Influence of method on the apparent size distribution of bacterioplankton cells: epifluorescence microscopy compared to scanning electron microscopy. Mar. Ecol. Prog. Ser. 5: 103-106.

Fuhrman, J. A., J. W. Ammerman, and F. Azam. 1980. Bacterioplankton in the coastal euphotic zone: distribution, activity and possible relationships with phytoplankton. Mar. Biol. 60: 201-207.

Fuhrman, J. A., and F. Azam. 1980. Bacterioplankton secondary production estimates for coastal waters of British Columbia, Antarctica and California. Appl. environ. Microbiol. 39: 1085-1095.

Fuhrman, J. A., and F. Azam. 1982. Thymidine incorporation as a measure of heterotrophic bacterioplankton production in marine surface waters: evaluation and field results. Mar. Biol. 66: 109-120.

Furnas, M. J. 1982a. An evaluation of two diffusion culture techniques for estimating phytoplankton growth rates in situ. Mar. Biol. 70: 63-72.

Furnas, M. J. 1982b. Growth rates of summer nanoplankton (< 10um) populations in lower Narragansett Bay, Rhode Island, USA. Mar. Biol. 70: 105-115.

Galvao, H. M. 1984. Nanoplankton dynamics in a saltmarsh - mudflat ecosystem. MSc. Thesis, College of William and Mary. 83 pp.

Gast, V. 1985. Bacteria as a food source for microzooplankton in the Schlei Fjord and Baltic Sea with special reference to ciliates. Mar. Ecol. Prog. Ser. 22: 107-120.

Gast, V., and U. Horstmann. 1983. N-remineralization of phyto- and bacterioplankton by the marine ciliate Euplotes vannus. Mar. Ecol. Prog. Ser. 13: 55-60.

Gershey, R., M. D. Mackinnon, R. M. Moore, and P. J. L. Williams. 1979. Comparison of three oxidation methods for the analysis of the dissolved organic carbon in seawater. Mar. Chem. 7: 289-306.

Gocke, K., R. Dawson, and G. Liebezeit. 1981. Availability of dissolved free glucose to heterotrophic microorganisms. Mar. Biol. 62: 209-216.

Goldman, J. C. 1984. Oceanic nutrient cycles. In: Flows of energy and materials in marine ecosystems. ed. J. J. R. Fasham. Plenum Press, New York. Pp. 137-170.

Haas, L. W. 1982. Improved epifluorescence microscopy for observing planktonic microorganisms. Annls Inst. oceanogr., Paris. 58: 261-266.

Haas, L. W., and K. L. Webb. 1979. Nutritional mode of several non-pigmented microflagellates from the York River estuary, Virginia. J. exp. mar. Biol. Ecol. 39: 125-134.

Hagstrom, A., J. W. Ammerman, S. Henrichs, and F. Azam. 1984. Bacterioplankton growth in seawater: II. Organic matter utilization during steady-state growth in seawater cultures. Mar. Ecol. Prog. Ser. 18: 41-48.

Hagstrom, A., U. Larsson, P. Horstedt, and S. Normark. 1979. Frequency of dividing cells, a new approach to the determination of bacterial growth rates in aquatic environments. Appl. environ. Microbiol. 37: 805-812.

Hallegraeff, G. M. 1983. Scale-bearing and loricate nanoplankton from east Australian current. Bot. Mar. 26: 493-515.

Hanson, R. B., D. Shafer, T. Ryan, D. H. Pope, and H. K. Lowery. 1983. Bacterioplankton in Antarctic ocean waters during late austral winter: abundance, frequency of dividing cells, and estimates of production. Appl. environ. Microbiol. 45: 1622-1632.

Hanson, R. B., and W. J. Wiebe. 1977. Heterotrophic activity associated with particulate size fractions in a Spartina alterniflora salt marsh estuary, Sapelo Island, Georgia, USA and the continental shelf waters. Mar.Biol. 42: 321-330.

Heinbokel, J. F. 1978. Studies on the functional role of tintinnids in the Southern Californian Bight. I. Grazing and growth rates in laboratory cultures. Mar. Biol. 47: 177-189.

Hicks, S. E., and F. C. Carey. 1968. Glucose determinations in natural waters. Limnol. Oceanogr. 13: 361-336.

Hobbie, J. E., R. J. Daley, and S. Jasper. 1977. Use of Nuclepore filters for counting bacteria by fluorescence microscopy. Appl. environ. Microbiol. 33 (5): 1225-1228.

Hobbie, J. E., and P. Rublee. 1977. Radioisotoope studies of heterotrophic bacteria in aquatic ecosystems. In: Cairns, J. (ed.) Aquatic microbial communities. Garland Pub. Co., New York. 441-476.

Iturriaga, R. 1981. Phytoplankton photoassimilated extracellular products: heterotrophic utilization in marine environment. Kieler Meeresforsch. 5: 318-324.

Johnson, K. M., P. G. Davis, and J. M. Sieburth. 1983. Diel variation of TCO_2 in the upper layer of oceanic waters reflects microbial composition, variation, and possibly methane cycling. Mar. Biol. 77: 1-10.

Johnson, K. M., and J. M. Sieburth. 1977. Dissolved carbohydrates in seawater. I, A precise spectrophotometric analysis for monosaccharides. Mar. Chem. 5: 1-13.

Johnson, P. W., and J. M. Sieburth. 1979. Chroococcoid cyanobacteria in the sea: a ubiquitous and diverse phototrophic biomass. Limnol. Oceanogr. 24: 928--935.

King, K. R., J. T. Hollibaugh, and F. Azam. 1980. Predator-prey interactions between a larvacean Oikopleura dioica and bacterioplankton in enclosed water columns. Mar. Biol. 56: 49-57.

Kopp, J. F., and G. D. McKee. 1979. Methods for chemical analysis of water and waste. U. S. E. P. A. Publication EPA-600/4-79-020 pp.460

Kopylov, A. I., T. I. Mamayeva, and S. F. Batsanin. 1980. Energy balance of the colorless flagellate Parabodo attenuatus (Zoomastigophora, Protozoa). Oceanology. 20: 705-708.

Kopylov, A. I., and E. S. Moiseyev. 1980. Effect of colorless flagellates on the determination of bacterial production in seawater. Dokl. Akad. Nauk SSSR Biol. Sci. 252: 272-274.

Laake, M., A. B. Dahle, K. Eberlein, and K. Rein. 1983. A modelling approach to the interplay of carbohydrates, bacteria, and non-pigmented flagellates in a controlled ecosystem experiment with Skeletonema costatum. Mar. Ecol. Prog. Ser. 14: 71-79.

Lackey, J. B., and E. W. Lackey. 1963. Microscopic algae and protozoa in the waters near Plymouth in August 1962. J. mar. biol. Assoc. U. K. 43: 797-805.

Landry, M. R., L. W. Haas, and V. L. Fagerness. 1984. Dynamics of microbial plankton communities: experiments in Kaneohe Bay, Hawaii. Mar.Ecol. Prog. Ser. 16: 127-133.

Landry, M. R., and R. P. Hassett. 1982. Estimating the grazing impact of marine micro-zooplankton. Mar. Biol. 67: 283-288.

Leadbeater, B. S. C. 1972a. Fine-structural observations on some marine choanoflagellates from the coast of Norway. J. mar. biol.Ass. U.K. 52: 67-79.

Leadbeater, B. S. C. 1972b. Ultrastructural observations on some marine choanoflagellates from the coast of Denmark. Br. phycol. Jour. 7: 195-211.

Leadbeater, B. S. C. 1972c. Identification, by means of electron microscopy, of flagellate nanoplankton from the coast of Norway. Sarsia. 49: 107-124.

Leadbeater, B. S. C. 1973. External morphology of some marine choanoflagellates from the coast of Jugoslavia. Arch. Protistenk. 115: 234-252.

Leadbeater, B. S. C. 1974. Ultrastructural observations on nanoplankton collected from the coast of Jugoslavia and the Bay of Algiers. J. mar. biol. Ass. U.K. 54: 179-196.

Leadbeater, B. S. C. 1975. A microscopical study of the marine choanoflagellate Savillea micropora (Norris) comb. nov., and preliminary observations in lorica development in S. micropora and Stephanoeca diplocostata Ellis. Protoplasma. 83: 111-29.

Leadbeater, B. S. C. 1978. Renaming of Salpingoeca sensu Grontved. J. mar. biol. Ass. U.K. 58: 511-515.

Leadbeater, B. S. C. 1979a. Developmental and ultrastructural observations on two stalked marine choanoflagellates, Acanthoecopsis spiculifera Norris and Acanthoeca spectabilis. Ellis. Proc. R. Soc., B,. 204: 57-66.

Leadbeater, B. S. C. 1979b. Developmental studies on the loricate choanoflagellate Stephanoeca diplocostata Ellis.I. Ultrastructure of the non-dividing cell and costal strip production. Protoplasma. 98: 241-262.

Leadbeater, B. S. C. 1979c. Development studies on the loricate choanoflagellate Stephanoeca diplocostata Ellis. II. Cell division and lorica assembly. Protoplasma. 98: 311-328.

Leadbeater, B. S. C. 1980. Four new species of loricate choanoflagellates from South Brittany, Franch. Cahiers Biol Mar. 21: 345-353.

Leadbeater, B. S. C. 1981. Ultrastructure and deposition of silica in loricate choanoflagellates. In :Silicon and siliceous structures in biological systems (ed. T. L. Simpson & B. E. Volcani), Springer-Verlag, Berlin. Pages 295-322.

Linley, E. A. S., and R. C. Newell. 1981. Microheterotrophic communities associated with the degradation of kelp debris. Kieler Meeresforsch. 5: 344-355.

Linley, E. A. S., R. C. Newell, and S. A. Bosma. 1981. Heterotrophic utilisation of mucilage released during fragmentation of kelp (Ecklonia maxima and Laminaria pallida). 1. Development of microbial communities associated with the degradation of kelp mucilage. Mar. Ecol. Prog. Ser. 4: 31-41.

Linley, E. A. S., R. C. Newell, and M. I. Lucas. 1983. Quantitative relationships between phytoplankton, bacteria and heterotrophic microflagellates in shelf waters. Mar. Ecol. Prog. Ser. 12: 77-89.

Manton, I., G. Bremer, and K. Oates. 1981. Problems of structure and biology in a large collared flagellate (Diaphanoeca grandis Ellis) from arctic seas. Proc. R. Soc. London. 213: 15-26.

McFeters, G. A., and D. G. Stuart. 1981. In situ studies using membrane filter chambers. In: (B. J. Dutka, ed.) Membrane filtration. Marcel Dekker, Inc., New York. pp. 481-512.

Meyer-Reil, L.-A. 1977. Bacterial growth rates and biomass production. In: Rheinheimer, G. (ed.) Microbial ecology of a brackish water environment. Springer-Verlag, New York. 223-236.

Meyer-Reil, L.-A. 1978. Uptake of glucose by bacteria in the sediment. Mar. Biol. 44: 293-298.

Meyer-Reil, L.-A., M. Bolter, G. Liebezeit, and W. Schramm. 1979. Short-term variations in microbiological and chemical parameters. Mar. Ecol. Prog. Ser. 1: 1-6.

Meyer-Reil, L.-A., R. Dawson, G. Liebezeit, and H. Tiedge. 1978. Fluctuations and interactions of bacterial activity in sandy beach sediments and overlying waters. Mar. Biol. 48: 161-171.

Meyer-Reil, L.-A., R. Dawson, G. Liebezeit, and H. Tiedge. 1979. Short term variation in microbiological and chemical parameters. Mar. Ecol. Prog. Ser. 1: 1-6.

Moestrup, O., and H. A. Thomsen. 1976. Fine structural studies on the flagellate genus Bicoeca: 1. Bicoeca maris with particular emphasis on the flagellar apparatus. Protistologica. 7: 101-120.

Murakami, T., and A. L. Jones. 1980. Conductive staining of biological specimens for non-coated scanning electron microscopy: double staining by tannin-osmium and osmium-thiocarbohyrazine-osmium methods. In: Scanning Electron Microscopy. eds. O. Johari, M. Ohtsuki, and I. C. Pontarelli. SOM, Inc. Chicago. Pp. 221-226.

Newell, R. C., E. A. S. Linley, and M. I. Lucas. 1983. Bacterial production and carbon conversion based on saltmarsh plant debris. Estuar. coast. Shelf Sci. in press.

Newell, R. C., M. I. Lucas, and E. A. S. Linley. 1981. Rate of degradation and efficiency of conversion of phytoplankton debris by marine micro-organisms. Mar. Ecol. Prog. Ser. 6: 123-136.

Newell, S. Y., and R. R. Christian. 1981. Frequency of dividing cells as an estimator of bacterial productivity. Appl. environ. Microbiol. 42: 23-31.

Nissen, H., P. Nissen, and F. Azam. 1984. Multiphasic uptake of D-glucose by an oligotrophic marine bacterium. Mar. Ecol. Prog. Ser. 16: 155-160.

Norris, R. E. 1965. Neustonic marine Craspedomonadales (Choanoflagellates) from Washington and California. J. Protozool. 12: 589-602.

Paerl, H. W. 1982. Environmental factors promoting and regulating N2 fixing blue-green algal blooms in the Chowan River, N. C. Univ. North Carolina Water Resour. Res. Instr Publ. No. 176. Pp. 69.

Paerl, H. W. 1985. Microzone formation: its role in the enhancement of aquatic N2 fixation. Limnol. Oceanogr. 30: 1246-1252.

Paerl, H. W., and J. F. Ustach. 1982. Blue-green algal scums: an explanation for their occurrence during freshwater blooms. Limnol. Oceanogr. 27: 212-217.

Pomeroy, L. R. 1974. The ocean's food web, a changing paradigm. Bioscience. 24: 499-504.

Pomeroy, L. R. 1979. Secondary production mechanisms of continental shelf communities. In: Ecological processes in coastal and marine systems. Eds. R. J. Livingston. Plenum Publishing, New York. Pp. 163-186.

Pomeroy, L. R. 1984. Microbial processes in the sea: diversity in nature and science. In: Heterotrophic activity in the sea. eds. J. E. Hobbie, and P. J. LeB. Williams, Plenum Publishing Co. New York. pp. 1-23.

Pomeroy, L. R., and R. E. Johannes. 1968. Occurrences and respiration of ultraplankton in the upper 500 meters of the ocean. Deep Sea Res. 51: 381-391.

Rhodes, M. W., I. C. Anderson, and H. I. Kator. 1983. In situ development of sublethal stress in Escherichia coli: effects on enumeration. Appl. Environ. Microbiol. 45: 1870-1876.

Rublee, P. A., S. M. Merkel, and M. A. Faust. 1983. Nutrient flux in the Rhode River: Tidal transport of microorganisms in brackish marshes. Estuar. cstl. Shelf Sci. 17: 669-680.

Sherr, B., and E. Sherr. 1983. Enumeration of heterotrophic microprotozoa by epifluorescence microscopy. Est. Coast. Shelf Sci. 16: 1-7.

Sherr, B., E. Sherr, and S. Y. Newell. 1984. Abundance and productivity of heterotrophic nanoplankton in Georgia coastal waters. J. Plankton Res. 6: 195-202.

Sherr, B. F., E. B. Sherr, and T. Berman. 1982. Decomposition of organic detritus: a selective role for microflagellate protozoa. Limnol. Oceanogr. 27: 765-769.

Sherr, B. F., E. B. Sherr, and T. Berman. 1983. Growth, grazing, and ammonia excretion rates of a heterotrophic microflagellate fed with four species of bacteria. Appl. environ. Microbiol. 45: 1196-1201.

Sherr, E. B., and B. F. Sherr. 1983. Double-staining epifluorescence technique to assess frequency of dividing cells and bacteriovory in natural populations of heterotrophic microprotozoa. Appl. environ. Microbiol. 46: 1388-1393.

Sherr, E. B., B. F. Sherr, R. D. Fallon, and S. Y. Newell. 1986. Small, aloricate ciliates as a major component of the marine heterotrophic nanoplankton. Limnol. Oceanogr. 31: 177-183.

Sieburth, J. M. 1979. Sea microbes. Oxford University Press, New York.

Sieburth, J. M., and P. G. Davis. 1982. The role of heterotrophic nanoplankton in the grazing and nurturing of planktonic bacteria in the Sargasso and Caribbean Seas. Annls Inst. oceanogr., Monaco. 58S: 285-296.

Sieburth, J. M., V. Smetacek, and J. Lenz. 1978. Pelagic ecosystem structure: heterotrophic compartments of the plankton and their relationship to plankton size fractions. Limnol. Oceanogr. 23: 1256-1263.

Sorokin, Y. I. 1971. Bacterial populations as components of oceanic ecosystems. Mar. Biol. 11: 101-105.

Sorokin, Y. I. 1975. Heterotrophic microplankton as a component of marine ecosystems. J. Obschei. biologii. M. 36: 716-730.

Sorokin, Y. I. 1977. The heterotrophic phase of plankton succession in the Japan Sea. Mar. Biol. 41: 107-117.

Sorokin, Y. I. 1978. Decomposition of organic matter and nutrient regeneration. In: Kinne, O. (ed.) Marine ecology, Vol. IV, Dynamics. Wiley, Chichester. p. 501-616.

Sorokin, Y. I. 1979. Zooflagellates as a component of the community of eutrophic and oligotrophic waters in the Pacific Ocean. Oceanology. 19: 316-319.

Sorokin, Y. I. 1981. Microheterotrophic organisms in marine ecosystems. In: Longhurst, A. R. (ed.) Analysis of marine ecosystems. Academic Press, New York. p. 293-342.

Stoecker, D., L. H. Davis, and A. Provan. 1983. Growth of Favella sp. (Ciliata: Tintinnina) and other microzooplankters in cages incubated in situ and comparison to growth in vitro. Mar. Biol. 75: 293-302.

Taylor, G. T., R. Iturriaga, and C. W. Sullivan. 1985. Interactions of bactivorous grazers and heterotrophic bacteria with dissolved organic matter. Mar. Ecol. Prog. Ser. 23: 129-141.

Thomsen, H. A. 1973. Studies on marine choanoflagellates. I. Silicified choanoflagellates of the Isefjord (Denmark). Ophelia. 12: 1-26.

Thomsen, H. A. 1976. Studies on marine choanoflagellates. II. Fine-structural observations on some silicified choanoflagellates from the Isefjord (Denmark), including the description of two new species. Norw. J. Bot. 23: 33-51.

Thomsen, H. A. 1977. Studies on marine choanoflagellates III. An electron microscopial survey of genus Acanthoecopsis. Arch Protistenk. 119: 86-99.

Thomsen, H. A. 1978. Nanoplankton from the Gulf of Elat (Gulf of Aqaba) with particular emphasis on choanoflagellates. Israel J. Zool. 27:33-44.

Thomsen, H. A. 1979. Electron microscopical observations on brackish water nanoplankton from the Tvarminne area, S. W. Coast of Finland. Acta Bot. Fennica. 110: 11-37.

Thomsen, H. A. 1982. Planktonic choanoflagellates from Disko Bugt, West Greenland, with a survey of the marine nanoplankton of the area. Meddr Gronland (Biosci.). 8: 1-35.

Throndsen, J. 1970. Marine planktonic Acanthoecaceans Craspedophyceae) from Arctic waters. Nytt Mag. Bot. 17: 103-111.

Throndsen, J. 1974. Planktonic choanoflagellates from North Atlantic Waters. Sarsia. 56: 95-122.

Turley, C. M., and K. Lochte. 1985. Direct measurement of a bacterial productivity in stratified waters close to a front in the Irish Sea. Mar. Ecol. Prog. Ser. 23: 209-219.

Van Der Veer, J. 1982. Simple and reliable methods for the fixation, mounting and staining of small and delicate marine plankton for light microscopic identification. Mar. Biol. 66: 9-14.

Van Wambeke, F., and M. A. Bianchi. 1985. Bacterial biomass production and ammonium regeneration in Mediterranean sea water supplemented with amino acids. 2. Nitrogen flux through heterotrophic microplankton food chain. Mar. Ecol. Prog. Ser. 23: 117-128.

Watson, S. W., T. J. Novitsky, H. L. Quinby, and F. W. Valois. 1977. Determination of bacterial number and biomass in the marine environment. Appl. Environ. Microbiol. 33: 940-946.

Wiebe, W. J., and L. P. Pomeroy. 1972. Micro-organisms and their association with aggregates and detritus in the sea: a microscopic study. Memorie Ist. ital. Idrobiol. 29 (Suppl): 325-352.

Wiebe, W. J., and D. F. Smith. 1977. Direct measurement of dissolved organic carbon release by phytoplankton and incorporation by microheterotrophs. Mar. Biol. 42: 213-223.

Williams, P. J. Leb. 1981. Incorporation of microheterotrophic processes into the classical paradigm of the planktonic food web. Kieler Meeresforsch. 5: 1-28.

Wilson, C. A., and L. H. Stevenson. 1980. The dynamics of the bacterial population associated with a salt marsh. J. exp. mar. Biol. Evol. 48: 123-138.

Wright, R. T., and B. K. Burnison. 1979. Heterotrophic activity measured with radiolabelled organic substrates. In: (Costerton, J. W., Colwell, R. R., eds.) Native aquatic bacteria: enumeration, activity, and ecology. American Society for Testing and Materials, Special Technical Publication 695. pp. 140-155.

Wright, R. T., and R. B. Coffin. 1983. Planktonic bacteria in estuaries and coastal waters of northern Massachusetts: spatial and temporal distribution. Mar. Ecol. Prog. Ser. 11: 205-216.

Wright, R. T., and R. B. Coffin. 1984a. Factors affecting bacterioplankton density and productivity in salt marsh estuaries. In: Reddy, C. A., Klug, M. J. (eds.) Current perspectives in microbial ecology. Am. Soc. for Microbiol., Washington, D. C.

Wright, R. T., and R. B. Coffin. 1984b. Measuring Microzooplankton grazing on planktonic marine bacteria by its impact on bacterial production. Microb. Ecol. 137-149.

Zimmerman, R. 1977. Estimation of bacterial numbers and biomass by epifluorescence microscopy and scanning electron microscopy. In: Rheinheimer, G. (ed.) Microbial ecology of a brackish water environment. Springer-Verlag, Berlin. p. 103-120.

VITA

Alyce Thomson Fritz

Born in Poughkeepsie, New York, August 6, 1951. Graduated from Maine-Endwell High School, Endwell, New York, June 1969. Received B.S. in Biology with Honors from Bucknell University, Lewisburg, Pennsylvania, June 1973 and M.A. in Marine Science from University of Virginia, Charlottesville, Virginia, August 1977. Enrolled as a graduate student in the School of Marine Science, College of William and Mary in Virginia to pursue a Ph.D. in September 1977. Received graduate assistantships in the Divisions of Biological Oceanography from September 1977 until December 1981 and beginning January 1981 received a graduate assistantship from the Division of Marine Resource Management until June 1984.

Accepted a position as Research Associate at the University of Maryland Eastern Shore in July 1984. In November 1984, accepted a position as biological oceanographer with Minerals Management Service. Presently employed, beginning in November 1985, as the Coastal Resource Coordinator for the National Oceanic and Atmospheric Administration (NOAA) HAZMAT Branch, assigned to the U. S. Environmental Protection Agency, Region III.